

**Submerged Anaerobic Membrane Bioreactors for
Wastewater Treatment and Membrane Fouling
Characterization and Control**

A Thesis

Presented to

The Faculty of Graduate Studies

of

Lakehead University

by

Weijue Gao

In partial fulfillment of requirements

for the degree of

Doctor of Philosophy

September 20, 2011

© Weijue Gao, 2011

Abstract

This thesis focused on effects of transient conditions (pH shocks, temperature variation and temperature shocks) on the performance and membrane fouling characterization and control of submerged anaerobic membrane bioreactors (SAnMBR) for pulp and paper effluent treatment (thermomechanical whitewater and pressate). A comprehensive characterization of cake layer formed on membrane surfaces was conducted using various techniques.

Results show that a pH 8.0 shock had a minor impact, while pH 9.1 and 10.0 shocks exerted significant long-lasting negative impacts on performance of the SAnMBR. The SAnMBR system was highly resilient and could successfully tolerate the 5 °C/10 °C temperatures shocks at 37 °C and the temperature variations from 37 to 45 °C. The temperature shock of 5 °C and 10 °C at 45 °C led to slight disturbance and significant disturbance of the performance, respectively.

A new insight was achieved on fundamental understanding of membrane fouling with regard to cake layer structure that changes significantly from the top layer to the bottom layer. Additionally, the freshly formed cake layers (2 days) were thinner, higher in EPS concentration, high in porosity, but much lower in particle size distributions (PSDs), as compared to the cake layers of 25 days at 55 °C.

The elevated pH shocks, high operating temperatures and temperature shocks induced dispersion and breakage of large sludge flocs. Smaller flocs had a higher tendency to accumulate on membrane surfaces. PSDs act as a key factor to generate high fouling resistance.

EPS, SMP, and colloidal particles contents in supernatant were increased with an increase in operating temperature and were positively correlated to the membrane filtration resistance that increased with an increase in operating temperature.

PCR-DGGE study showed that there were significant differences in microbial community population density along the cake layer depth. Temperature not only affected the richness of the microbial populations but also the diversity of the microbial community.

The results suggest that SAnMBR is a promising technology for pulp and paper effluent treatment and for system closure. However, membrane fouling, particularly cake layer formation, should be minimized. Operating SAnMBR at mesophilic temperatures is more attractive than that at thermophilic temperature, from a membrane fouling point of view.

Keywords: Submerged anaerobic membrane bioreactor; pH shock; Sludge properties; Biogas production; Micro-tome slicing; Cake layer; Porosity; EPS; SMP; Microbial community; Membrane fouling; temperature; temperature shock; pulp and paper effluent

Acknowledgements

It is a pleasure to thank the many people who made this thesis possible. Looking back, I am surprised and at the same time very grateful for all I have received throughout these years. It has certainly shaped me as a person and has led me where I am now.

I want to first express my deep gratitude to my Ph.D. supervisor Dr. Baoqiang Liao for the guidance and support enlightened me through his wide knowledge with his enthusiasm, his inspiration, and his great efforts during my studies. The valuable support of my co-supervisor Dr. Kam Tin Leung is highly appreciated for his patient teaching, kind guidance, and wise advice. Many thanks also go to my Supervisory Committee member Dr. Heidi Schraft for her valuable advice and guidance.

I would like to thank my family, especially my parents and my husband (Ming Gao), who have always supported my choices, helped me get through the difficult times, and provided me with all the unconditional understanding, caring, and encouragement.

I must acknowledge the Lakehead University for providing me this opportunity, as well as Natural Sciences and Engineering Research Council of Canada (NSERC) for funding this research. Thank the support of Abitibi-Bowater Inc. (Thunder Bay, Ontario) and Tembec Inc. (Temiscaming, Quebec) for providing thermo-mechanical pulping wastewater and anaerobic seed sludge, respectively.

The author thanks Dr. D. Chapman for his help in micro-tome slicing technique and Grzegorz Kepka for his training with confocal laser scanning microscopy (CLSM). Special thanks to my team members and friends who provided me with valuable work experience at Lakehead University.

Table of Contents

Acknowledgements.....	i
Table of Contents.....	ii
List of Tables.....	ix
List of Figures.....	x
Chapter 1 Introduction.....	1
1.1 Current problems associated with pulp and paper wastewater treatment.....	1
1.2 A rational approach to improving the treatment of pulp and paper wastewater treatment.....	3
1.3 Motivation of the present study.....	5
1.4 Objectives.....	6
1.5 Scope of this thesis.....	6
1.6 References.....	7
Chapter 2 Literature review.....	10
2.1 Thermo-mechanical pulping pressate and whitewater.....	10
2.2 Treatment technologies for pulp and paper mills effluent.....	12
2.3 Membrane bioreactors for pulp and paper wastewater treatment.....	15
2.3.1 Aerobic membrane bioreactors.....	16
2.3.2 Anaerobic membrane bioreactors (AnMBRs).....	18
2.3.2.1 Overview of anaerobic digestion.....	18
2.3.2.2 AnMBRs for pulp and paper wastewater treatment.....	19
2.4 Membrane fouling and control in membrane bioreactors.....	21

2.4.1 Mechanisms of membrane fouling	22
2.4.2 Characterization of membrane foulants.....	24
2.4.2.1 Physical characterization	24
2.4.2.2 Chemical characterization.....	25
2.4.2.3 Microbiological characterization	26
2.4.3 Factors affecting membrane fouling.....	27
2.4.3.1 Membrane	28
2.4.3.2 Sludge characteristics.....	30
2.4.4 Strategies for membrane fouling control	34
2.4.4.1 Reducing the fouling rate.....	34
2.4.4.2 Membrane cleaning.....	38
2.5 References	38
Chapter 3 Influence of elevated pH shocks on the performance of a submerged anaerobic membrane bioreactor	60
3.1 Introduction	61
3.2 Materials and methods	63
3.2.1 Experimental setup and operation	63
3.2.2 Analytical methods	65
3.2.2.1 Membrane fouling determination	65
3.2.2.2 EPS extraction and measurement.....	66
3.2.2.3 Particle size distribution.....	66

3.2.2.4	Characterization of cake layer	67
3.2.2.5	Water quality measurements.....	68
3.2.2.6	Statistical analysis.....	68
3.3	Results and discussion.....	69
3.3.1	Effect on COD removal and biogas production	69
3.3.2	Effect on membrane fouling.....	72
3.3.3	Sludge properties and their effects on membrane fouling.....	74
3.3.4	Effect on cake layer properties	78
3.3.4.1	FTIR analysis of membrane foulants.....	78
3.3.4.2	Effect on particle size, porosity and specific resistance	79
3.4	Conclusions	82
3.5	References	83
Chapter 4	Structure of cake layer in a submerged anaerobic membrane bioreactor ...	89
4.1	Introduction	90
4.2	Materials and methods	92
4.2.1	Experimental system.....	92
4.2.2	Cake layer cryosectioning and collection.....	94
4.2.3	Analytical techniques used for cake characterization.....	96
4.2.3.1	Physical structure characterization of cake layer.....	96
4.2.3.2	Chemical structure characterization of cake layer	97
4.2.3.3	Microbial community.....	98

4.3 Results and discussion.....	98
4.3.1. Process performance.....	98
4.3.2 Physical structure of cake layer	100
4.3.2.1 Thickness of cake layer.....	100
4.3.2.2 Porosity	101
4.3.2.3 Particle size distribution.....	102
4.3.2.4 EPS matrix morphology.....	104
4.3.3 Chemical structure.....	106
4.3.3.1 FTIR analysis.....	106
4.3.3.2 Extracted EPS content.....	107
4.3.3.3 EDX analysis	110
4.3.4 Microbial community	111
4.3.5 Relation to membrane fouling	113
4.4 Conclusions	114
4.5 References	115
 Chapter 5 Effects of temperature and temperature shock on the performance and microbial community structure of a submerged anaerobic membrane bioreactor.....	 121
5.1 Introduction	121
5.2 Materials and methods	124
5.2.1 Experimental set up	124
5.2.2 Temperature variations.....	125

5.2.3 Particle size distribution	126
5.2.4 Analytical methods	126
5.2.5 Microbial community analysis	126
5.3 Results and discussion.....	127
5.3.1 Effect on COD removal	127
5.3.2 Effect on gas production.....	131
5.3.3 Effect on particle size distributions	133
5.3.4 Microbial community	135
5.4 Conclusions	137
5.5 References	138
 Chapter 6 Effects of extracellular polymeric substances and soluble microbial products on membrane fouling in a submerged anaerobic membrane bioreactor	 142
6.1 Introduction	142
6.2 Materials and methods	144
6.2.1 Experimental set up	144
6.2.2 Operating conditions.....	145
6.2.3 Total fouling resistance	147
6.2.4 Mixed liquor fractions sampling.....	147
6.2.5 Analytical methods	148
6.2.6 Statistical analysis.....	148
6.3 Results and discussion.....	149

6.3.1 Total fouling resistance	149
6.3.2 Effect of operating temperatures on bound EPS and SMP	151
6.3.3 Effect of temperature shocks on bound EPS and SMP	153
6.3.4 Relationships of bound EPS to membrane fouling	155
6.3.5 Relationships of mixed liquor fractions to membrane fouling	157
6.4 Conclusions	159
6.5 References	159
Chapter 7 Influence of temperature and temperature shock on cake layer structure and membrane fouling from a submerged anaerobic membrane bioreactor	165
7.1 Introduction	165
7.2 Materials and methods	167
7.2.1 Laboratory-scale SAnMBR	167
7.2.2 Experimental plan	167
7.2.3 Fouling resistance	169
7.2.4 Cake layer sampling	170
7.2.5 Analytical methods for cake layer characterization	171
7.2.5.1 Cake porosity	171
7.2.5.2 Particle size distribution analysis	171
7.2.5.3 EPS extraction and measurement	172
7.2.5.4 Microbial community	172
7.3 Results and discussion	173

7.3.1 Performance of the SAnMBR.....	173
7.3.2 Cake layer thickness	175
7.3.3 Effect on PSDs.....	176
7.3.4 Effect on cake layer porosity	178
7.3.5 Effect on EPS content in cake layer	179
7.3.6 Microbial community	183
7.3.7 Development of membrane fouling at the initial stage of filtration	186
7.4 Conclusions:	189
7.5 References	190
Chapter 8 Conclusions and recommendations	194
8.1 Conclusions	195
8.1.1 Feasibility of SAnMBR system for treatment of thermomechanical pulping whitewater / pressate	195
8.1.2 Cake layer investigation and parameter variations with cake depth	195
8.1.3 Impact of transient conditions on the performance of the SAnMBR and membrane fouling.....	196
8.1.3.1 pH shock	196
8.1.3.2 Temperature	197
8.2 Recommendations for future research.....	198
Nomenclature and abbreviations.....	201
Publication list	204

List of Tables

Table 2-1	Typical wastewater generation and pollution load from thermo-mechanical pulping mills.....	11
Table 2-2	Aerobic MBR performance for treatment of pulp and paper industry wastewater.....	17
Table 2-3	Anaerobic MBR performance for treatment of pulp and paper industry wastewater.....	20
Table 3-1	Sampling frame for the comparisons of parameters between before and after each pH shock (average value was compared).....	65
Table 3-2	MLSS concentration in each phase.....	74
Table 4-1	Characteristics of influent.....	94
Table 4-2	Structural parameters of the cake layers.....	106
Table 7-1	Temperature variations in detail.....	168
Table 7-2	Cake layer porosity.....	178

List of Figures

Figure 1-1	Two main configurations: (a) external /side-stream AnMBR and (b) submerged/immersed AnMBR.....	4
Figure 2-1	Membrane fouling mechanisms.....	23
Figure 2-2	Factors affecting membrane fouling.....	28
Figure 2-3	Classification of membranes based on pore size.....	29
Figure 3-1	Schematic of the anaerobic submerged membrane bioreactor and experimental setup.....	64
Figure 3-2	Microscopy image of cake layer (a) Initial true color image and (b) binary image.....	68
Figure 3-3	Variation of (a) organic loading rate and membrane flux during operation, and (b) the COD.....	70
Figure 3-4	Variation of (a) biogas production rate and (b) CH ₄ /CO ₂ ratio in produced biogas.....	72
Figure 3-5	Effect of the elevated pH shocks on membrane fouling rates. Results are expressed as average ± one standard deviation (n = 3) (flux = 5.1±0.4, 4.8±0.5 and 4.4 ± 0.5 L/m ² h, MLSS = 8.6 ± 0.4, 10.0 ± 0.7, 9.6 ± 0.6 g/L for pH 8.0, 9.1 and 10.0 shock, respectively; biogas sparging rate = 0.75 LPM).....	73
Figure 3-6	Effect of the elevated pH shock on BPC content in the sludge suspension.....	75
Figure 3-7	Particle size distribution of sludge suspension before and after (a) pH 8.0 shock, (b) pH 9.1 shock and (c) pH 10.0 shock.....	76
Figure 3-8	Variation of (a) protein, (b) polysaccharide content and (c) PN/PC ratio in EPS with operational time.....	77
Figure 3-9	FTIR spectra of the membrane foulants in cake layer (cake layer formed after 6 days filtration, 5-8 pieces of membrane with cake layer were used for analysis).....	79
Figure 3-10	Particle size distribution of cake layer before and after pH 10.0	

	shock (cake layer formed after 6 days filtration, 5-8 pieces of membrane with cake layer were used for analysis).....	80
Figure 3-11	(a) Cake porosity, and (b) cake specific resistance before and after pH 10.0 shock (cake layer formed after 6 days filtration, 5-8 pieces of membrane with cake layer were used for analysis).....	82
Figure 4-1	Cake layer cryosectioning.....	95
Figure 4-2	Typical TMP profiles plotted with operational time (Flux = 4.57 ± 0.20 L/m ² h; MLSS = 8.5 ± 0.20 g/L; biogas sparging rate = 1.5 L/min).....	99
Figure 4-3	Cross section of cake layer observed by COM: (a) after one day of operation, and (b) after 5 days of operation.....	100
Figure 4-4	COM images of cryosectioned slices of: (a) top cake layer, (b) middle cake layer, (c) bottom cake layer.....	101
Figure 4-5	Cake layer area porosity distribution with thickness under different TMP.....	102
Figure 4-6	Particle size distributions of cake layers at different depths.....	103
Figure 4-7	CLSM images of cake layer at different depths with 3D reconstruction images on the right accordingly (TMP=43.5kPa): (a) cake layer outer surface; (b) 1200 μ m away from the cake outer surface; (c)1900 μ m away from the cake outer surface. Proteins were stained with Sypro Orange (green) and polysaccharides were stained with ConA (red). The white parts of the 3D reconstruction images correspond to the area covered by EPS, and the black parts correspond to other area of the cake layer (area covered by cells and vacancy).....	105
Figure 4-8	FTIR spectrum of top, middle and bottom cake layers.....	107
Figure 4-9	Extracted EPS content in the top, middle and bottom cake layers: (a) calculated as EPS weight per unit cake layer dry weight and (b) calculated as EPS weight per unit volume of wet cake layer.....	109
Figure 4-10	The correlation between the content of EPS (calculated as EPS	

	weight per unit wet weight of the cake layers) and the substratum coverage of: (a) protein ($r_p=0.891$; $p=0.001$) and (b) polysaccharides ($r_p=0.950$; $p=0.000$).....	110
Figure 4-11	EDX analysis for: (a) gel layer and (b) cake layer.....	111
Figure 4-12	PCR-DGGE fingerprints of 16S rDNA gene fragments amplified from DNA extracted from bulk sludge and cake sludge at different depths.....	112
Figure 5-1	Variation of organic loading rate and membrane flux during operation.....	128
Figure 5-2	Variation of the influent, supernatant and permeate COD	128
Figure 5-3	Biogas production. (A) variation of biogas production rate (B) biogas composition and concentration.....	132
Figure 5-4	Particle size distribution of sludge suspension (A) before and after 5°C shocks at 37°C (B) before and after 10°C shocks at 37°C (C) before and after 5°C shocks at 45°C (D) before and after 10°C shocks at 45°C (E) at 37°C, 45°C and 55°C steady state based on volume (F) at 37°C, 45°C and 55°C steady state based on number....	134
Figure 5-5	PCR-DGGE fingerprints of 16S rDNA gene fragments amplified from DNA extracted from bulk sludge (A) and cluster analysis of the DGGE band patterns (B). (a) 37°C steady state (day 53); (b) 37°C steady state (day 68); (c) 5°C shock at 37°C; (d) 10°C shock at 37°C; (e) 45°C steady state (day 207); (f) 45°C steady state (day 245); (g) 5°C shock at 45°C; (h) 10°C shock at 45°C; (i) 55°C steady state (day 400); (j) 55°C steady state (day 412); (k) 55°C steady state (day 416).....	136
Figure 6-1	Temperature variations (a) three phases throughout the operating time (b) detailed temperature rises during the shocks at 37°C.....	146
Figure 6-2	Development of total fouling resistance at different temperatures (steady state) (Flux = 6.65 ± 0.44 L/m ² •h (37 °C); Flux = 6.46 ± 0.33 L/m ² •h (45 °C); Flux = 5.49 ± 0.26 L/m ² •h (55 °C)).....	150

Figure 6-3	Bound EPS contents at different operating temperatures (steady state).....	151
Figure 6-4	SMP concentrations at different operating temperatures (steady state).....	152
Figure 6-5	Colloidal particles contents at different operating temperatures (ANOVA, $p < 0.05$).....	153
Figure 6-6	Bound EPS contents: (a) 5 and 10 °C shocks at 37 °C; (b) 5 and 10 °C shocks at 45 °C.....	154
Figure 6-7	SMP concentrations: (a) 5 and 10 °C shocks at 37 °C; (b) 5 and 10 °C shocks at 45 °C.....	155
Figure 6-8	Correlation between total fouling resistance and bound EPS.....	156
Figure 6-9	Correlation between total fouling resistance and SMP.....	158
Figure 7-1	Schematic diagram of a stirred filtration cell.....	170
Figure 7-2	Comparison of total fouling resistance between steady state and temperature shocks: (a) 5 °C and 10 °C shocks at 37 °C; (b) 5 °C and 10 °C shocks at 45 °C. (In each black cycle, the 1 st and 2 nd data point indicates the fouling resistance just before and after temperature shock, respectively).....	174
Figure 7-3	R_i and R_p at 37°C (6d), 45°C (6d) and 55°C (12d) steady state	175
Figure 7-4	Cross sections of cake layers observed by COM: (a) at 37°C steady state (25d) (b) at 45°C steady state (25d) (c) at 55°C steady state (25d) (d) at 55°C steady state (2 d).....	176
Figure 7-5	Particle size distributions of (a) cake layers at 37, 45 and 55 °C steady state (cake layer age, 25d) (b) cake layers at 55 °C steady state with different cake layer ages (c) 5 and 10 °C shocks at 37 °C (cake layer age, 6d) (d) 5 and 10 °C shocks at 45 °C (cake layer age, 6d).....	177
Figure 7-6	Protein concentrations in bound EPS of cake layers (6d): (a) 5 and 10 °C shocks at 37 °C; (b) 5 and 10 °C shocks at 45 °C.....	179
Figure 7-7	EPS content in the cake sludge at 37, 45 and 55°C steady	

	state with different cake ages.....	180
Figure 7-8	Profile of EPS and SMP transporting through cake layer and Membrane.....	182
Figure 7-9	PCR-DGGE fingerprints of 16S rDNA gene fragments amplified from DNA extracted from cake sludge. (a') 37 °C steady state (day 53, cake layer age: 25d); (b') 37 °C steady state (day 68, cake layer age: 6d); (c') 5 °C shock at 37 °C (day 83, cake layer age: 6d); (d') 10 °C shock at 37 °C (day 107, cake layer age: 6d); (e') 45 °C steady state (day 207, cake layer age: 25d); (f') 45 °C steady state (day 245, cake layer age: 6d); (g') 5 °C shock at 45 °C (day 250, cake layer age: 6d); (h')10 °C shock at 45 °C (day 264, cake layer age: 6d); (i') 55 °C steady state (day 400, cake layer age: 25d); (j') 55 °C steady state (day 412, cake layer age: 12d); (k') 55 °C steady state (day 416, cake layer age: 2d).....	183
Figure 7-10	Cluster analysis of the DGGE band patterns.....	184
Figure 7-11	Relation between fouling resistance and cake layer quantity.....	187
Figure 7-12	Cake layers observed by COM: (a) at 55°C steady state after 25 days of operation (bottom layer) (b) at 55°C steady state after 2 days of operation (surface).....	188

Chapter 1 Introduction

1.1 Current problems associated with pulp and paper wastewater treatment

The pulp and paper industry, the third largest industrial polluter to air, water, and land in both Canada and the United States, releases well over a hundred million kg of pollutants each year (1996). It accounts for four percent of the world's energy use and uses more fresh water to produce a ton of product than any other industry.

The sources of different wastewaters in the pulp and paper industry are from wood preparation, pulping, pulp washing, screening, washing, bleaching, and paper machine and coating operations (Pokhrel and Viraraghavan, 2004). The significant environmental impacts of pulp and paper manufacturing mainly result from the pulping and bleaching processes. Generally speaking, these wastewaters are high in biochemical oxygen demand (BOD), chemical oxygen demand (COD), total suspended solids (TSS), toxicity and color. They contain wood debris and a lot of organic material such as lignin and other organic material from the trees (including chlorinated organic material). They also contain alcohols, chelating agents and inorganic materials like chlorates and transition metal compounds. The main source of nutrients, phosphorus and nitrogen, are also released into wastewaters. The consumption of fresh water can seriously harm habitat near mills, reduce water levels, alter water temperature, and change pH value and colour of the waterbody (Munkittrick et al., 1997; Bosker, 2007). Therefore, in order to reduce the pollution output and to meet stringent new regulations, treatment of wastewaters from this industry receives special attention.

The treatability of the pulp and paper mill wastewater and performance of available treatment processes are reviewed by Pokhrel and Viraraghavan (2004). A number of treatment technologies, such as physical processes (steam stripping) and conventional biological treatment (activated sludge or aerated lagoon systems), have been used to treat and reutilize pulp and paper mill effluents (Pokhrel and Viraraghavan, 2004). However, in a steam stripper system, low fuel value of the stream causes frequent flameout problems at the incinerator. This problem can result in permit violations due to

the emission of unburned gases (Burgess et al., 2002). On the other hand, since the operational costs of a steam stripper are proportional to the volume of liquid to be treated, they are more cost effective when treating low volume, high-strength streams (Milet and Duff, 1998). In contrast to steam stripping, the operating cost of biological treatment is proportional to the strength of the stream to be treated, due to the costs associated with nutrients, aeration, and sludge handling. The biological oxidation of condensate contaminants may be a more cost-effective technology than steam stripping, especially if large volume, low-strength condensate streams are to be treated. Nevertheless, the operation is accomplished in two separate basins, thereby occupying a substantial amount of real estate. In addition, biomass separation is a challenge.

Aerobic wastewater treatment processes are commonly used in the Canadian pulp and paper industry. Only a few installations of anaerobic treatment have been employed for the pulp and paper effluent treatment (Elliott and Mahmood, 2007). Even though both aerobic and anaerobic treatment processes have been successfully used for wastewater treatment in the pulp and paper industry (Barton et al., 1998), there are a number of drawbacks associated with the conventional aerobic and anaerobic treatments. High energy costs associated with aeration (10-20% in the activated sludge processes), large amount of excess sludge, and the potential stripping of volatile organic compounds (VOCs) by aeration are the major concerns of aerobic treatment. Anaerobic processes offer several widely known advantages over conventional aerobic processes (Liao et al., 2006). First, no oxygen is required, so the expense and energy required to dissolve oxygen into water are eliminated. Second, methane is produced and serves as a renewable energy source. Where the economics are favourable, this methane may be combusted to produce electricity and heat. Finally, less biomass is produced. In the absence of oxygen as an electron acceptor, anaerobic microbial systems discard the electrons onto methane instead of using them to grow more microorganisms. These advantages are offset by the slow growth rates of the methanogenic organisms and the microbial complexity of the systems. Biomass retention is critical to provide sufficient solids retention time (SRT) for the methanogens, which has historically deterred its application in the pulp and paper industry. Elliott and Mahmood (2007) summarized the developments in sludge

preconditioning technologies that have substantially reduced the SRT with higher methane recovery, but even so the low effluent COD concentrations achieved by aerobic processes are difficult to achieve by anaerobic processes. Additionally, both aerobic and anaerobic treatment may suffer from biomass separation problems, including sludge bulking and deflocculation (Thompson et al., 2001).

Therefore, the low treatment efficiencies and high costs associated with these systems provide the pulp and paper industry a significant incentive to investigate and develop better treatment technologies for water treatment and reuse (Rintala and Puhakka, 1994).

1.2 A rational approach to improving the treatment of pulp and paper wastewater treatment

In recent years, considerable attention has been paid to the use of membranes technologies in conjunction with anaerobic reactors, namely anaerobic membrane bioreactors (AnMBRs). In anaerobic processes, membranes could be used as filtration unit so that biomass can be fully retained within the reactor, thoroughly decoupling the hydraulic retention time (HRT) and SRT. With the incorporation of membrane technologies, complete biomass retention eliminates the impact of biomass separation problems. Methanogenic organisms or sulfate-reducing bacteria (Vallero et al., 2005) with slow-growth rate can be retained to achieve high biogas production and sulfate reduction rate. AnMBR also provides very low suspended solids concentrations in the treated effluent and improves the effluent quality, as well as greatly extends and further increases system productivity (Liao et al., 2006). It allows the concentration of biomass to increase in the reactor, thus facilitating relatively smaller reactors and higher organic loading rates (OLRs). These are attractive for treating effluents that contain relatively high level of organic materials, and produce good quality permeates that can be reused.

AnMBR systems are implemented based on two main configurations: external/side-stream AnMBR (Fig.1-1 a) and submerged/immersed AnMBR (Fig.1-1 b). For the external configuration, the membrane modules are placed outside the bioreactor and a pump is required to push bioreactor effluent into the membrane unit and permeate

through the membrane. To date, most of reported AnMBRs studies (Table 1-1) focused side-stream AnMBRs. However, this configuration needs high cross-flow velocity to alleviate membrane fouling, which may result in breakage of sludge flocs, reduction in sludge activity, high energy cost, and consequently reduced economic feasibility of this technology (Hu and Stuckey, 2006). Modified external MBRs have been developed by applying gas scouring in the separated membrane tank with the advantages of creating a shear force to scour membrane surface to control the membrane fouling and the low energy consuming.

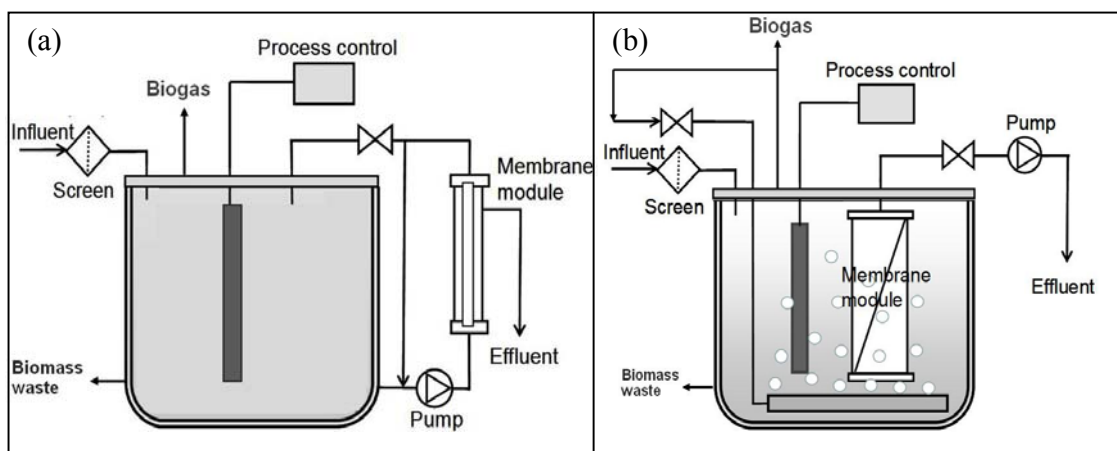


Figure 1-1 Two main configurations: (a) external /side-stream AnMBR and (b) submerged/immersed AnMBR

One interesting alternative to the conventional side-stream process is the submerged anaerobic membrane bioreactor (SAnMBR), which employs membranes submerged into the liquid. Also, the membrane is operated under a vacuum, instead of direct pressure. The operating conditions are much milder than in external membrane bioreactor (MBR) systems because of the lower tangential velocities. Indeed, the energy demand of this configuration can be up to two orders of magnitude lower than that of external systems (Chang et al., 2002), and the biomass stress associated with recirculation can be reduced. In addition, such a configuration allows for the self cleaning of the membrane surface by recirculating the biogas produced (Liao et al., 2006).

1.3 Motivation of the present study

The Canadian pulp and paper industry has been expected to achieve closed cycle operation and subsequent reuse of treated effluent. Considering the disadvantages and problems associated with current treatment technologies mentioned above, there is an urgent need to investigate and develop better technologies for industrial effluents. It is expected that SAnMBR which combines the advantages of both anaerobic digestion and submerged membrane bioreactor will achieve lower energy consumption, higher process efficiency and stability, and superior quality of treated effluent that are not achievable with current technologies.

Although anaerobic digestion is a process frequently applied for the treatment of various industrial wastewaters. It is not used as widely as the aerobic biological treatment process for the pulp and paper industry. A few studies for thermo-mechanical pulping whitewater or pressate treatment were conducted using activated sludge process (Slade et al., 2003), aerobic treatment process (Jahren et al., 2002) and anaerobic treatment process (Rintala and Lepistö, 1992), however, the submerged AnMBRs have not been used. The optimal SAnMBR design and operational parameters for treating pulp and paper mill effluent have not yet been identified. Although such configuration is expected to offer advantages in terms of low energy requirements, high COD removal performance and process stability, as compared to external side-stream AnMBRs, the studies of SAnMBRs appear to be very limited.

Membrane fouling has been considered as the major obstacle of the wide application of MBRs. Because of the great complexity and variability of the operational and the environmental conditions, current understanding of membrane fouling is still insufficient. Further investigation on fouling mechanisms will be helpful to develop effective control strategies.

Additionally, biological treatment, especially anaerobic treatment, is often challenged by operation under transient states with respect to operational conditions, pollutants, and physical characteristics. In anaerobic digestion, difficulties encountered in real industrial wastewater treatment are often brought by unstable factors (Sipma et al., 2010), including influent characteristics, HRT, OLR, pH, temperature, salinity and

presence of inhibitory compounds, etc (Chen et al., 2008). It is of importance to investigate the effects of these transient conditions on the performance of the SAnMBRs. The uniqueness of membrane fouling associated with these transient conditions has not been addressed.

1.4 Objectives

The long-term goal of this study is to investigate and develop the next generation of technologies (i.e., SAnMBR technology) for energy recovery from pulp and paper mill effluents and subsequent reuse of treated effluent and ultimately system closure. For this purpose, it is of concern to study the feasibility of the SAnMBRs, to investigate the development of membrane fouling, and to identify the viability of the SAnMBR systems under transient conditions (e.g. pH, temperature). The specific research objectives are as follows:

- (1) Develop SAnMBR technology for in-mill treatment of thermo-mechanical pulping whitewater / pressate and closed cycle operation;
- (2) Investigate the properties and structure of sludge cake layers formed on membrane surfaces;
- (3) Investigate the impact of pH shock on the performance of the SAnMBR and membrane fouling; and
- (4) Study the effects of temperature variations and temperature shocks on the performance of the system and membrane fouling in the SAnMBR.

1.5 Scope of this thesis

This thesis studied the application of SAnMBRs for wastewater treatment as well as membrane fouling characterization and control. The feasibility of a SAnMBR system for in-mill treatment of thermo-mechanical pulping whitewater and pressate was investigated. In attempt to study the phenomenon of cake formation, the cake layer structure was physically, chemically and microbiologically characterized in detail. The influence of transient conditions (pH shock, temperature variation and temperature shocks) on the performance of a SAnMBR was studied with the emphasis set to membrane fouling. The thesis is written and organized in a manuscript format.

In Chapter 1, the research background and study objectives are presented.

Chapter 2 covers a literature review with a brief introduction of the sources and characteristics of thermo-mechanical pulping pressate and whitewater, followed by current treatment technologies for pulp and paper mills effluent, including MBR technology. Available information on current understanding of MBR fouling and strategies for membrane fouling control is included.

In Chapter 3 and 4, a laboratory-scale submerged anaerobic membrane bioreactor (SAnMBR) was used for thermo-mechanical pulping whitewater treatment. Chapter 3 evaluates the influence of pH shocks on the performance of the SAnMBR. Changes in COD removal, biogas production, sludge and cake layer properties, and their correlations to membrane fouling – before and after pH shocks – were systematically studied.

Sludge cake formation on membrane surfaces was identified as the dominant mechanism of membrane fouling (Meng et al., 2009). Therefore, in Chapter 4, various analytical techniques were used to develop an improved fundamental understanding of the spatial distribution of physical, chemical and microbiological structure of cake layer formed on membrane surfaces.

Chapter 5, 6 and 7 deal with the application of a SAnMBR treating thermo-mechanical pulping pressate at different temperatures (37, 45 and 55°C) and temperature shocks (5 and 10°C) at each tested temperature. Effect of temperature and temperature shocks on the performance and microbial community structure of the SAnMBR is presented in Chapter 5. Chapter 6 focuses on effects of extracellular polymeric substances (EPS) and soluble microbial products (SMP) on membrane fouling. Influence of temperature and temperature shock on cake layer structure and membrane fouling is discussed in Chapter 7.

Finally, Chapter 8 summarizes and concludes the thesis. Recommendations for future research are provided based on the general discussion.

1.6 References

National Pollutant Release Inventory, Environment Canada, 1996.

- Barton, D. A., Hickman, G. T., Matthews, K. O., Tielbaard, M. H. (1998). Stand-alone biological treatment of Kraft mill condensates-pilot plant studies. *International Environ. Conference and Exhibition*: 521-537.
- Bosker, T. (2007). Thermo-mechanical pulp mill effluent effects on fish reproduction: an investigation of cause. *Biology*, University of New Brunswick. Ph.D.
- Burgess, T. L., Gibson, A. G., Furstein, S. J., Wachs, I. E., 2002. Converting waste gases from pulp mills into value-added chemicals. *Environmental Progress* 21, 137-141.
- Chang, I.-S., Le Clech, P., Jefferson, B., Judd, S., 2002. Membrane Fouling in Membrane Bioreactors for Wastewater Treatment. *Journal of Environmental Engineering* 128, 1018.
- Chen, Y., Cheng, J. J., Creamer, K. S., 2008. Inhibition of anaerobic digestion process: A review. *Bioresource Technology* 99, 4044-4064.
- Elliott, A., Mahmood, T., 2007. Pretreatment technologies for advancing anaerobic digestion of pulp and paper biotreatment residues. *Water Research* 41, 4273-4286.
- Hu, A. Y., Stuckey, D. C., 2006. Treatment of Dilute Wastewaters Using a Novel Submerged Anaerobic Membrane Bioreactor. *Journal of Environmental Engineering* 132, 190-198.
- Jahren, S. J., Rintala, J. A., Odegaard, H., 2002. Aerobic moving bed biofilm reactor treating thermomechanical pulping whitewater under thermophilic conditions. *Water Research* 36, 1067-1075.
- Liao, B.-Q., Kraemer, J. T., Bagley, D. M., 2006. Anaerobic Membrane Bioreactors: Applications and Research Directions. *Critical Reviews in Environmental Science and Technology* 36, 489 - 530.
- Meng, F., Chae, S.-R., Drews, A., Kraume, M., Shin, H.-S., Yang, F., 2009. Recent advances in membrane bioreactors (MBRs): Membrane fouling and membrane material. *Water Research* 43, 1489-1512.
- Milet, G. M. D., Duff, S. J. B., 1998. Treatment of kraft condensates in a feedback-controlled sequencing batch reactor. *Water Science and Technology* 38, 263-271.

- Munkittrick, K. R., Servos, M. R., Carey, J. H., Van Der Kraak, G. J., 1997. Environmental impacts of pulp and paper wastewater: Evidence for a reduction in environmental effects at North American pulp mills since 1992. *Water Science and Technology* 35, 329-338.
- Pokhrel, D., Viraraghavan, T., 2004. Treatment of pulp and paper mill wastewater--a review. *Science of The Total Environment* 333, 37-58.
- Rintala, J. A., Lepistö, S. S., 1992. Anaerobic treatment of thermomechanical pulping whitewater at 35-70°C. *Water Research* 26, 1297-1305.
- Rintala, J. A., Puhakka, J. A., 1994. Anaerobic treatment in pulp- and paper-mill waste management: A review. *Bioresource Technology* 47, 1-18.
- Sipma, J., Osuna, M. B., Emanuelsson, M. A. E., Castro, P. M. L., 2010. Biotreatment of Industrial Wastewaters under Transient-State Conditions: Process Stability with Fluctuations of Organic Load, Substrates, Toxicants, and Environmental Parameters *Critical Reviews in Environmental Science and Technology* 40, 147-197.
- Slade, A. H., Anderson, S. M., Evans, B. G., 2003. Nitrogen fixation in the activated sludge treatment of thermomechanical pulping wastewater: effect of dissolved oxygen. *Water Science and Technology* 48, 1-8.
- Thompson, G., Swain, J., Kay, M., Forster, C. F., 2001. The treatment of pulp and paper mill effluent: a review. *Bioresource Technology* 77, 275-286.
- Vallero, M. V. G., Lettinga, G., Lens, P. N. L., 2005. High rate sulfate reduction in a submerged anaerobic membrane bioreactor (SAMBaR) at high salinity. *Journal of Membrane Science* 253, 217-232.

Chapter 2 Literature review

2.1 Thermo-mechanical pulping pressate and whitewater

The pulp and Paper Industry is normally considered as two kinds of separated industries, the pulp (raw material for paper industry) and the paper industry; each of them produces different types of wastewater. There is also a third related industry, the paper recycling industry. This industry has historically been considered a major consumer of natural resources (e.g., wood, water, and energy) and a significant contributor of pollutants discharged into the environment.

There is a considerable incompatibility for the compositions and the concentrations of substances in process wastewaters in the pulp and paper industry, depending on the kind of raw material as well as the pulping procedures. Wood is the most common raw material in this industry. The goal of pulping is to separate cellulose fibres from hemicelluloses and lignins. Several pulping processes, including mechanical pulping, chemical pulping (kraft process and sulphite process), chemo-mechanical pulping and thermo-mechanical pulping, have been used in this industry to break down the wood, followed by paper making operations. The details of these processes and the wastewater characteristics are discussed in a previous review by Pokhrel and Viraraghavan (2004).

The thermo-mechanical pulping process is primarily used for newsprint production. It is precisely named by the process which involves steaming the raw materials at temperatures above 100 °C (thus thermo) and mechanically separating the fibres in a pressurized refiner (thus mechanical). The thermo-mechanical pulping process produces wood pulp by two stages (Wikipedia, 2011b). The logs are first converted into small wood chips after stripping off their bark. After an atmospheric pre-steaming has taken place, these wood chips have a moisture content of around 25-30 %. A pressurized steaming is then part of the process which generates heat and water vapour in order to weaken and soften the lignin which acts as an adhesive substance for the cellulose fibres (Thompson et al., 2001), so that the chips can be refined into pulp by crushing or grinding. The separated individual fibres are hard and rigid because the lignin has not

been removed. The mechanical processes use fewer chemicals than either kraft or sulfite mills. The yield of the thermo-mechanical pulping process is as high as 93–97% based on dry wood (Sjöström, 1993). The thermo-mechanical pulping process is further modified using chemicals during the steaming stage, and the process is called chemi-thermomechanical pulping (CTMP).

The wastewater pollution load from the thermo-mechanical pulping process is given in Table 2-1. The substances in the process waters of the thermo-mechanical pulping system originate from several sources (Sundbolm, 1999). During the debarking and defiberization processes, some of the wood components (hemicelluloses, carbohydrates, pectins, extractives, and inorganic salts) will be dissolved and dispersed in the water. Residuals of processing chemicals applied in mechanical pulping, bleaching and papermaking will be circulated backward to pulping. In addition, organic and inorganic substances may come in with fresh water or leakages from sealing and lubrication.

A concentrated pressate stream is generated from the plug screw feeders which are designed to extract the undesirable portion surrounding the wood fibres between atmospheric pre-steaming and refining. The thermo-mechanical pulping pressate is rich in wood extractives (e.g., lipophilic extractives) and contains most of the chemical oxygen demand (COD) generated in the thermo-mechanical pulping plant.

Table 2-1

Typical wastewater generation and pollution load from thermo-mechanical pulping mills (Rintala and Puhakka, 1994).

Process	Wastewater (m ³ /adt pulp or paper)	SS ^a (kg/adt pulp)	COD (kg/adt ^b pulp)
thermo-mechanical pulping - unbleached	10-30	10-40	40-60
thermo-mechanical pulping - bleached	10-30	10-40	50-120
CTMP - unbleached	10-15	20-50	70-120
CTMP - bleached	10-15	20-50	100-180

^a SS = suspended solids

^b adt = air dry ton (100 percent air dry is the same as 90 percent fibers and 10 percent moisture)

The thermo-mechanical pulping whitewater is used throughout the pulping process (including the Recycled pulp mill) as well as the paper-making machine. This commonly shared water is continually sewerred and replaced with heated make-up water. The thermo-mechanical pulping whitewater can be described as heated process water containing pulp cellulose “fines” and other soluble materials. The main contaminants in it are lignins, resin and fatty acid, chemical additives and other wood extractives (sterols, lignans, steryl esters, etc.). They are dissolved, colloidal, or suspended. Although thermo-mechanical pulping whitewater contains readily biodegradable organic compounds and a moderately high strength of COD of 1000–5600 mg/L (Jahren et al., 2002), it is characterized by a low biodegradability ratio of BOD₅/COD with a temperature range from 50 °C to 80 °C. The high concentration of COD in the whitewater is due to the lignin fraction (40 %) that still remains after bleaching as well as carbohydrates (40 %) and extractives (20 %) (Jahren et al., 2002).

2.2 Treatment technologies for pulp and paper mills effluent

The treatment of pulp and paper mill effluent generally consists of pre-treatment, primary treatment, and secondary treatment (1996).

Pre-treatment is necessary to remove pieces of wood or dirt that can be present in the effluents. As the thermo-mechanical pulping wastewaters are acidic, neutralization of effluents is conducted in order to avoid system corrosion and acidic pollution of the water bodies

Primary treatment is achieved by sedimentation or flotation in a clarifier to remove suspended solids from effluents. The efficiency of sedimentation (50-90 %) is increased if chemicals are added. Dissolved air flotation is an accepted process to clarify the newsprint wastewater prior to secondary biological treatment (Horan and Chen, 1998). However, primary treatment cannot efficiently remove organic material (e.g., BOD and COD).

Biological treatment commonly acts as a secondary treatment where organic pollution and oxygen demand are reduced. Biological treatment processes, including aerobic and anaerobic processes, are based on the activity of a wide range of microorganisms, converting the biodegradable organics and other contaminants present in

the wastewater into innocuous and simple end products such as carbon dioxide, water, and excess biomass (sludge). Aerobic treatments are currently preferred for most of pulp and paper mills due to their high BOD and COD removal efficiency. Several aerobic processes like aerated lagoons (Welander et al., 1997), activated sludge (AS) (Clauss et al., 1999), trickling filters, sequencing batch reactors (Tardif and Hall, 1997), are available in the treatment of pulp and paper mill wastewaters. Thermo-mechanical pulping wastewater was claimed to be readily degradable by the activated sludge process (Shere and Daly, 1982). Integrated thermo-mechanical pulping mill effluents treated by a pilot scale aerobic biofilter under average loading of $3.5 \text{ kg BOD d}^{-1}\text{m}^{-3}$ met the regulation limits for BOD, TSS as well as for toxicity (Kantardjieff and Jones, 1997). Substantial removal of COD, total organic carbon (TOC), BOD, lignin and resin acids of thermo-mechanical pulping wastewater using high rate compact reactors at a retention time of 1.5 h has been reported (Magnus et al., 2000a; Magnus et al., 2000b). Slade et al. (2003) achieved 94–96 % BOD removal, 82–87 % total COD removal, 79–87 % soluble COD removal, and > 99 % total extractives removal for thermo-mechanical pulping whitewater treatment by employing N-ViroTech, a novel technology, which selects nitrogen-fixing bacteria as the bacteria primarily responsible for carbon removal in a aerobic biological system. Nevertheless, sludge management problems have been raised in pulp and paper mills by the wide application of the AS process. Landfill, incineration, composting and animal feeding, and other beneficial uses are employed depending on what further usage the sludge is destined for. However, conventional management methods suffer from shrinking landfill space, leachate related issues, high supplemental fuel costs, and air pollution concerns (Mahmood and Elliott, 2006). On the other hand, sludge bulking will result in severely reduced mixed liquor suspended solids (MLSS) concentration and excessive concentrations of solids being discharged in the final effluent. Although sludge bulking can be controlled by the addition of chemicals (e.g. chlorine, hydrogen peroxide, ferrous salts, lime) (Saaymant et al., 1996), it still seems to be inevitable in pulp and paper mills (Thompson et al., 2001). The employment of membrane separation technology has proven to be a promising method to eliminate sludge bulking problem (Laitinen et al., 2006) and to enhance the system stability under

the varied experimental conditions (Tardif and Hall, 1997) by solid-liquid separation. The application of membrane bioreactors for pulp and paper wastewater treatment will be reviewed in detail in the following section.

Anaerobic process performances have been extensively used for treating pulp and paper wastewaters (Pokhrel and Viraraghavan, 2004). Completely stirred tank reactor (CSTR) is a common reactor type widely applied in anaerobic digestion. In completely mixed reactors, the average SRT is equal to the HRT, resulting in biomass separation problems which could deteriorate the performance of conventional biological treatment (Liao et al., 2006). There are also several anaerobic reactor designs that provide biomass retention, such as upflow anaerobic sludge blanket (UASB) (Buzzini and Pires, 2007), anaerobic contact reactor, anaerobic filter (Ahn and Forster, 2002), and fluidized bed (Fahmy et al., 1994). Among them anaerobic lagoons were the first anaerobic systems in the pulp and paper industries, and UASB reactor was introduced as the first high-rate anaerobic process in 1983 (Rintala and Lepistö, 1992). Although pulp and paper mill effluents tend to be biodegradable, they still require very large, expensive biological secondary treatment systems to achieve high effluent quality. Removal efficiencies ranging from 40-85 % have been reported for anaerobic treatability of pulp and paper wastewater, so that some form of additional treatment is required for residual COD reduction (Thompson et al., 2001).

The wastewaters from mechanical and chemical pulping are typically non-toxic to methanogenic degradation and contain degradable organic compounds. Consequently, anaerobic digestion is an attractive treatment for these effluents (Lee et al., 1989). Anaerobic and aerobic treatments of thermo-mechanical pulping mill effluents were compared with the achieved COD removal of 84 % and 86 %, respectively (Jahren et al., 1999). Thermo-mechanical pulping wastewaters are toxic to water organisms due to the presence of wood extractives such as resin acids and unsaturated fatty acids (Kostamo et al., 2004). Most of the toxicity of mechanical pulping effluents can be significantly reduced by well-operated biological treatment. Normally, these secondary treated effluents become non-toxic to fish at full concentration and can be discharged into water bodies with all due precaution (Cabral et al., 1998).

In the case of specific problems (e.g. residual COD, toxicity, colour), tertiary processes can take place to avoid water quality disturbance and to further improve the effluent quality (Thompson et al., 2001), such as ozonation (Helble et al., 1999), chemical coagulation (Chen and Horan, 1998), flotation, flocculation, activated carbon absorption, membrane filtration (Bhattacharjee et al., 2007), massive lime treatment, and foam separation. For instance, coagulants and adsorption are useful for removing turbidity and color from the wastewater (Pokhrel and Viraraghavan, 2004). The necessary ozone (100-800 mg/L) dose can help to remove 50-90 % of the lipophilic wood extractives from thermo-mechanical pulping wastewater (Laari et al., 1999; Laari et al., 2000).

2.3 Membrane bioreactors for pulp and paper wastewater treatment

The pulp and paper industry is one of the most important industries of the North American economy and ranks as the fifth largest in the U.S. economy, and it is responsible for 50 % of all wastes being dumped into Canada's waters. It has been obliged to substantially reduce the amount of fresh water used and the volume of effluent discharged to the environment due to the implementation of stringent regulations. The concept of "zero effluent" technology was developed by Canadian market pulp mills (Sundbolm, 1999). It means that the wastewater is treated to such an extent within the mill that no process effluent is discharged, thus promoting recirculation of the process waters. Therefore, in-mill treatment of pulp and paper mill effluent would maintain a stable operation in general, a good heat balance, promote "zero effluent" technology, thus reducing the final environmental impact. In order to reduce the consumption of freshwater and maximize water reuse, the system should be able to occupy minimal space and be capable of producing an effluent of high quality consistently. For these requirements, membrane bioreactor (MBR) presents a promising technology adopted in the treatment of pulp and paper wastewater to meet stringent discharge limit or for sustainable reclamation and reuse.

The MBR technology is relatively new for the pulp and paper industry. It is a system that combines biological treatment with membrane filtration into a single process.

The membrane separations system replaces the traditional gravity sedimentation unit (clarifier), and simplifies multi-unit operations to a single unit operation. In 1969, the first application of MBR was reported to perform the function of separating the final effluent from the activated sludge by an ultrafiltration membrane (Ng and Kim, 2007). In North America, full-scale MBR application for treating industrial wastewater dated back to 1991 (Yang et al., 2006). Since then, MBRs have been increasingly employed for industrial (Nelson et al., 2008), municipal (Simmons et al., 2011), and agricultural (Cicek, 2003) wastewater treatment, where a small footprint, water reuse, or stringent discharge standards were required. Based on our recent review (Lin et al., 2010), a large number of publications have explored MBRs for industrial wastewater treatment in the last 5 years. There are four major manufacturers of MBRs: Kubota Corp. (Tokyo, Japan), Mitsubishi Rayon Corp., Ltd. (Tokyo, Japan), GE Water and Process Technologies (Oakville, Ontario, Canada) and U.S. Filter Corp. For MBR commercial application, the North America installations account for 11 % of worldwide installations, and Zenon (now part of GE Power & Water) occupies the majority of this MBR market (Yang et al., 2006).

2.3.1 Aerobic membrane bioreactors

Table 2-2 summarizes several literature reports regarding the typical applications of aerobic MBRs for treatment of pulp and paper industry wastewaters. Aerobic MBR systems were found superior to the conventional activated sludge (CAS) system, sequencing batch reactor (SBR), ultrafiltration (UF), and SBR+UF processes in COD, suspended solids, and toxicity removal (Tardif and Hall, 1997; Dufresne et al., 1998). It can efficiently eliminate 100 % of suspended solids with no need for further treatment. A COD reduction of 48-99 % with at a HRT of 0.12 to 2 days is observed in Table 2-2. Even in some treatment processes, anaerobic digester was firstly responsible for primary decomposition of complex organic materials. Afterwards, aerobic treatment of the obtained effluent in a MBR was still required to meet current regulations (Galil et al., 2003).

Table 2-2

Aerobic MBR performance for treatment of pulp and paper industry wastewater (Lin et al., 2010)

Wastewater	Configuration, Scale ^a and volume	Characteristics of membrane ^b	Type of reactor ^c	Temp (°C)	HRT (d)	SRT (d)	OLR (kg COD/m ³ d)	MLSS (g/L)	Feed COD (mg/L)	COD removal
Chemico-thermomechanical pulping effluent (Dufresne et al., 1998)	Submerged, L (0.09 m ³)	Hollow fiber, pore size: 0.1 μm	Aerobic CSTR	35	2.0	15	6.0	13.0	12000	82%
Mechanical newsprint mill whitewater (Ragona and Hall, 1998)	External, L (0.01 m ³)	Ceramic tubular UF membrane, pore size: 0.05 μm	Aerobic CSTR	55	- ^d	-	-	-	5520	48-58%
Synthetic kraft pulp mill condensate (Berube and Hall, 2000)	External, L (0.008 m ³)	Ceramic tubular UF membrane, pore size: 0.05 μm	Aerobic CSTR	55-70	0.12	-	-	10.0	1014 ^g	>99% ^e
Paper mill wastewater from the anaerobic process (Galil et al., 2003)	External, P	Zenon membrane	Anaerobic -Aerobic CSTR	-	-	-	-	11.2	960	86%
Kraft pulp mill foul condensates (Dias et al., 2005)	Submerged, L (0.004 m ³)	Pore size: 0.03 μm	Aerobic CSTR	33.45, 55	0.79	-	6.45	<3.0	5120 ±11	87-97%
Paper mill wastewater after treated anaerobically (Gommers et al., 2007)	External, P	-	Anaerobic -Aerobic CSTR	-	-	-	-	-	2900	91.7%
Effluent from an UASB reactor treating paper mill wastewater (Lerner et al., 2007)	Submerged, P (9 m ³)	PO, pore size: 0.1-0.4 μm	Anaerobic -Aerobic CSTR	-	0.79	24	10.35	15.0	910 ± 320	89%
The black liquor, pulp bleaching effluent and white water (Zhang et al., 2009c)	Submerged, P (10 m ³)	Hydrophilic PSf, pore size: 0.1 μm	Aerobic CSTR	25-34	0.75	20	-	8.0	600	92.1%

^a L = laboratory/bench scale, P = pilot scale. ^b PO = polyolefin, PSf = Polysulfone, UF = ultrafiltration.^c CSTR = completely stirred tank reactor. ^d - indicates value not reported.^e Units are methanol concentration.

Additionally, pulp and paper wastewaters have a high temperature (50-70 °C). Thermophilic aerobic processes provide treatment of the high-temperature effluents from pulp and paper mills at their discharged temperature, saving operational costs on pre-cooling and post-heating process water prior to and after biological treatment. There was a distinct advantage in considering the performance of the thermophilic aerobic digester based on COD removal and the specific methane production rates. Although COD removal efficiency decreased as the temperature increased at three temperatures (35, 45, and 55 °C) (Dias et al., 2005), it was still as high as almost 90 %. Compare to an steam stripping system, the capital and operation costs was much less for thermophilic aerobic MBR (60 °C) (Hall and Berube, 2000).

2.3.2 Anaerobic membrane bioreactors (AnMBRs)

An AnMBR can be simply defined as a biological treatment process operated without oxygen and using a membrane to provide complete solid-liquid separation.

2.3.2.1 Overview of anaerobic digestion

Anaerobic digestion is a complex biochemical reaction carried out by several types of microorganisms. During the anaerobic process, a gas that is mainly composed of methane and carbon dioxide, also referred to as biogas, is produced. Anaerobic digestion occurs in four steps:

- Hydrolysis : A chemical and biological reaction where complex and large organic polymers (e.g., proteins, cellulose, lignin, and lipids) are decomposed into simpler and soluble monomers (e.g., amino acids, glucose, fatty acids, and glycerol) by water and hydrolytic bacteria to split the chemical bonds between the substances. Hydrolysis of the complex molecules is catalyzed by extracellular enzymes such as cellulases, proteases, and lipases.
- Fermentation or Acidogenesis: A biological reaction where simple monomers are converted into organic acids (e.g., acetic, propionic, formic, lactic, butyric, or succinic acids), alcohols and ketones (e.g., ethanol, methanol, glycerol, acetone), acetate, CO₂, and H₂ by acidogenic bacteria in the absence of oxygen.

- Acetogenesis: A biological reaction where the fermentation products are converted into acetate (the main product of carbohydrate fermentation) by what are known as acetogenic bacteria.
- Methanogenesis: A biological reaction where acetates are converted into methane and carbon dioxide, while hydrogen is consumed by methanogenic bacteria (organisms capable of producing methane have been identified only from the Archaea).

In anaerobic digestion, the stages of hydrolysis and acidogenesis are more robust than acetogenesis and methanogenesis. Because of the complicated metabolic pathway of anaerobic processes, the symbiotic relationship among all these microorganisms is vital to achieve process stability. Any disturbances in the balance between acid forming and methane forming microorganisms will cause reactor instability. The two groups have different sensitivity to environmental conditions and diverse physiology, nutritional needs, growth kinetics. For example, the optimal pH range for methanogens is 6.8-7.2 while a more acid pH is desirable for acid forming microorganisms (Rajeshwari et al., 2000). Adjustment of pH value is usually necessary to maintain a proper acidic/basic environment to protect biological metabolism and to prevent inorganic fouling induced by mineral precipitation to some extent.

2.3.2.2 AnMBRs for pulp and paper wastewater treatment

Although both aerobic and anaerobic treatment systems are feasible to treat wastewater from all types of pulp and paper mills, anaerobic processes are considered more suitable to treat high strength organic effluents with energy production (Wijekoon et al., 2011). In the meantime, membrane separation technique is capable of removing absorbable organic halides (AOX), COD, and color from pulp and paper mills. Table 2-3 shows the selected AnMBRs performances for pulp and paper wastewaters treatment.

Table 2-3

Anaerobic MBR performance for treatment of pulp and paper industry wastewater (Lin et al., 2010)

Type of wastewater	Configuration, Scale ^a and volume	Characteristics of membrane ^b	Type of reactor ^c	Temp (°C)	HRT (d)	SRT (d)	OLR (kg COD/m ³ d)	MLSS (g/L)	Feed COD (mg /L)	Effluent COD (mgL ⁻¹)	COD removal
Kraft bleach plant effluent (Hall et al., 1995)	External, L (0.015 m ³)	Tubular UF memberane, MWCO: 10000 Da	Anaerobic, CSTR	35	1.0	- ^d	0.04 ^c	7.6-15.7	40 ^e	~16 ^e	61% ^e
Evaporator condensate (Minami et al., 1991; Minami, 1994)	External, P (5 m ³)	MF membrane, pore size :0.2 µm.	Anaerobic, UFAF	53	0.5	-	35.5 ^f	7.6	17800 ^f	1200 ^f	93 ^f
Thermo-mechanical pulping whitewater (Gao et al., 2010)	Submerged, L (0.01 m ³)	PVDF, UF membrane, MWCO: 70000 Da	Anaerobic, CSTR	37	~2.5	280	2.4 ± 0.4	5.7-10.0	2600,5500, 10000	112 ± 35	> 95 %
Kraft evaporator condensate (Lin et al., 2009)	Submerged, L (0.01 m ³)	PVDF UF membrane, MWCO: 70000 Da	Anaerobic, CSTR	37, 55	-	~230	-	10.0	10000	-	97-99 %

^a L = laboratory/bench scale, P = pilot scale. ^b MF = microfiltration, PVDF=polyvinylidene fluoride, UF = ultrafiltration.^c CSTR = completely stirred tank reactor, UFAF = upflow anaerobic filter. ^d - indicates value not reported.^e Units are AOX (absorbable organic halogen). ^f Units are BOD instead of COD.

The application of external AnMBRs for the effluent from this industry was investigated in the 1990s (Minami et al., 1991; Minami, 1994). Recently, Liao's group developed a submerged AnMBR system for pulp and paper wastewaters treatment (Lin et al., 2009; Gao et al., 2010; Liao et al., 2010; Xie et al., 2010). This relatively new system provided an equal or superior permeate quality and simultaneously eliminated the sludge deflocculation and separation issues associated with external configuration. Also, the produced biogas could be recirculated to minimize membrane fouling by scouring the membrane surface. Compared to the performances of mesophilic SAnMBR, thermophilic treatment can provide comparable permeate quality while facing the more serious challenge of membrane fouling (Lin et al., 2009). Therefore, a SAnMBR which combines the advantages of both anaerobic digestion and membrane separation can be anticipated to be a promising technology for the pulp and paper industry to achieve in-mill treatment, energy recovery, subsequent reuse of treated effluent and ultimately system closure, namely "zero effluent".

2.4 Membrane fouling and control in membrane bioreactors

As a reliable and efficient technology, MBRs have become an option for many domestic and industrial wastewater treatments. However, membrane fouling is considered to be one of the most challenging issues that restricts their widespread applications. It results in loss of membrane performance, a reduction of permeate flux or an increase of trans-membrane pressure (TMP), reduced productivity and increased operating costs (e.g., added energy consumption, increased membrane cleaning and replacement cost). According to different wastewater characteristics and operational conditions summarized by Lin et al. (2010), it is concluded that more attention should be paid to membrane fouling control in MBRs when applied to treat industrial wastewaters. However, unified and well-structured theories on membrane fouling are not currently available because of the inherent complexity of the system (Chang et al., 2002). As a result, considerable efforts have been made to explore the mechanisms of membrane fouling and the control strategies.

2.4.1 Mechanisms of membrane fouling

According to removability of the foulants, membrane fouling can be classified into removable, irremovable and irreversible fouling (Meng et al., 2009). For removable fouling, foulants can be readily removed from the membrane surface by appropriate physical cleaning (e.g., backwashing). Irremovable fouling caused by stronger interactions between foulants and membrane materials needs chemical cleaning to remove. The irreversible fouling (or permanent fouling) represents fouling remaining on the membrane surface or within the membrane pores even after intensive chemical cleaning.

In terms of fouling forms, the membrane fouling can be divided into internal fouling (pore clogging/narrowing) and external fouling (cake/gel layer formation) coupled with concentration polarization. The external foulants were found to have much broader distributions of molecular weight (M_w) than the internal foulants (Zhu et al., 2011). Generally, irremovable fouling and irreversible fouling are attributed to pore blocking, and cake layer formation makes main contribution to removable fouling.

Membrane fouling also can be classified into biofouling, organic fouling and inorganic fouling according to the components of foulants (Liao et al., 2006). Biofouling refers to the deposition of cell debris and colloidal particles, growth and metabolism of bacteria cells or flocs on the membranes, as well as adsorption and rejection of extracellular polymeric substances (EPS) and soluble microbial products (SMP) (Liao et al., 2006; Meng et al., 2009). Organic fouling is defined as the accumulation and adsorption of organic constituents on membranes. Inorganic fouling is due to the chemical or biological precipitation of a great number of metal ions due to the presence of a great number of cations (i.e., Ca^{2+} , Mg^{2+} , Al^{3+} and Fe^{3+}), anions and ionisable groups of biopolymers (i.e., CO_3^{2-} , SO_4^{2-} , PO_4^{3-} , OH^- , COO^-) (Meng et al., 2009).

From the aspect of time, MBR fouling is divided into short-term and long-term fouling. Challenges still remain to predict long-term fouling by using short-term experimental data (Le-Clech et al., 2006). It was found that short-term and long-term fouling undergo different fouling mechanisms (Ognier et al., 2002; Geng and Hall, 2007). Based on their analysis, short-term fouling is mostly reversible due to sludge deposition

and superficial pore blocking. Long-term fouling is comprised of reversible and irreversible fouling caused by the long contact time of deposited compounds with the membrane surface.

Membrane fouling mechanisms are usually observed as shown in Fig. 2-1. At the initial stage of filtration, membrane fouling is caused by the accumulation and adsorption of solutes or colloids on membrane surface and pore surfaces, because their sizes are comparable or smaller than the membrane pores. At the same time, sludge flocs will deposit onto the membrane surface, while the shear force causes the detachment of foulants. If the shear force at the membrane surface is not adequate to remove the foulants, cake formation occurs. Of course, spatial and temporal changes of the foulants composition during long-term operation are anticipated (Meng et al., 2009). As the dominant mechanism of membrane fouling (Shin et al., 2005; Chu and Li, 2006; Jeison and van Lier, 2007; Meng and Yang, 2007; Ramesh et al., 2007; Wang et al., 2007), the process of cake formation on membrane surfaces and its structure are of importance.

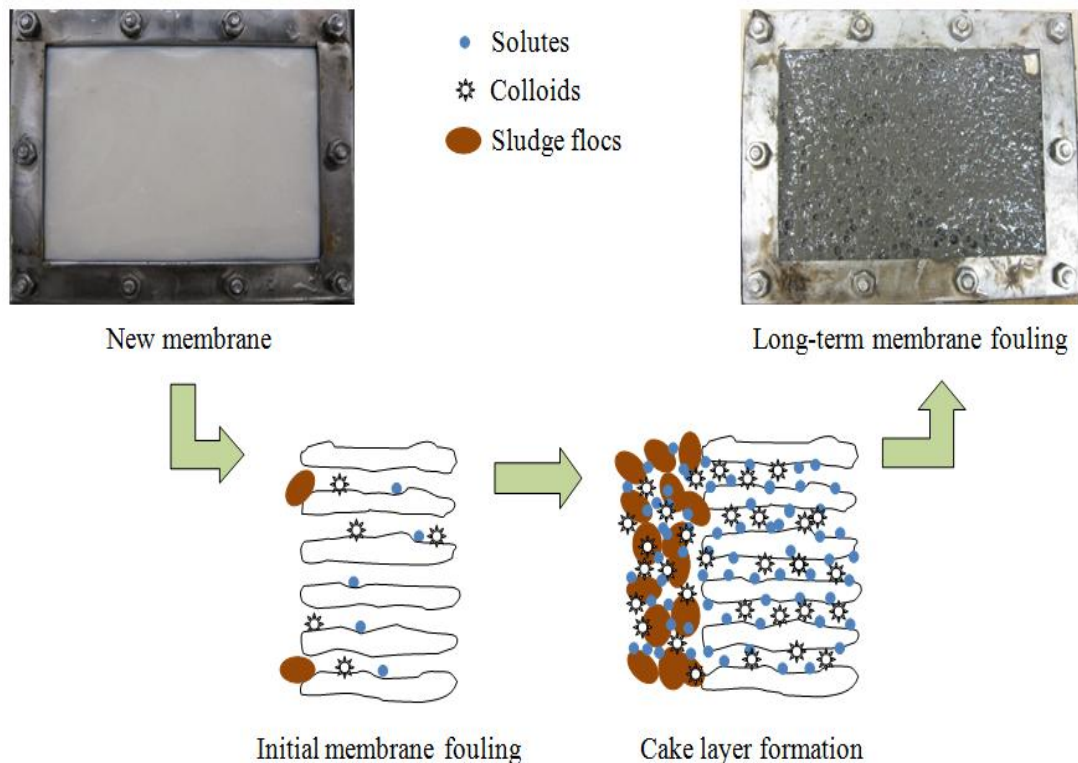


Figure 2-1 Membrane fouling mechanisms

2.4.2 Characterization of membrane foulants

2.4.2.1 Physical characterization

A number of techniques such as scanning electron microscopy (SEM), confocal laser scanning microscopy (CLSM) (Ng et al., 2006c; Lee et al., 2008), atomic force microscopy (AFM), direct observation (Li et al., 2003; Zhang et al., 2006; Subramani et al., 2009), have been used for physical characterization of membrane fouling. SEM is one of the most common instruments providing high resolution images at nano/micro-meter scale. SEM was utilized to observe the fouling layer directly and evaluate the effectiveness of fouling control methods (Zhang et al., 2009a). Rod-shape bacterial clusters were one of the contributors to cake layer by SEM images (Pendashteh et al., 2011). However, SEM fails to keep the natural state of the fouling layer due to the pretreatment protocols of SEM samples including sample dehydration and gold coating. There has been improvement by environmental SEM which allows the observation of wet samples with a relatively low lateral resolution (10-20 nm) (Choi et al., 2005; Le-Clech et al., 2007). Special specimen pretreatment is not needed for AFM which measures forces between the tip and the sample, leading to a deflection of the cantilever according to Hooke's law. AFM can provide information of cake surface morphology with three-dimensional (3D) images. By observations using SEM and AFM, the "gel layer" caused by soluble microbial products (SMPs) and "cake layer" by flocs showed great differences in morphology (Yu et al.). CLSM has become a powerful approach for characterisation of membrane fouling (see section 4.1). In a CLSM, a laser beam passes through a light source aperture and then is focused by an objective lens onto the surface of a fluorescent specimen. Scattered and reflected laser light as well as any fluorescent light from the illuminated spot is then re-collected by the objective lens. A beam splitter separates off some portion of the light into the detection apparatus, before which specific filters selectively pass the fluorescent wavelengths while blocking the original excitation wavelength. After passing a pinhole, the light intensity is detected by a photodetection device (usually a photomultiplier tube (PMT)), transforming the light signal into an electrical one that is recorded by a computer (Wikipedia, 2011a). The key feature of CLSM, optical sectioning, allows 3D reconstructions of complex objects. The

combination of CLSM and image analysis can not only visualize the 3D structure of the fouling layer, but also quantify its architecture (Yun et al., 2006).

2.4.2.2 Chemical characterization

The chemical components of membrane foulants have been extensively characterized by energy-dispersive X-ray spectroscopy (EDX) (An et al., 2009), Fourier transform infrared (FTIR) spectroscopy (Zhou et al., 2007), X-ray photoelectron spectroscopy (XPS) (Choo and Lee, 1996a; Howe and Clark, 2002), three-dimensional excitation-emission matrix (EEM) fluorescence spectroscopy (Sheng and Yu, 2006), solid state ^{13}C -nuclear magnetic resonance (NMR) spectroscopy (Kimura et al., 2005), size exclusion chromatography (SEC), and inductively coupled plasma (ICP) (Lee and Kim, 2009). The foulants were rich in proteins and polysaccharides according to FTIR spectra and NMR analysis. EEM fluorescence spectroscopy is a sensitive technique which has been successfully utilized to obtain the structural information of organic substances by capture of their specific fluorescence features (Liu et al., 2011). Protein-like substances (polypeptides) were identified as an important role in organic fouling EEM fluorescence analyses (Teychene et al., 2008; Zhu et al., 2011). SEC can separate organic foulants on the basis of size exclusion to understand the molecular weight distribution or size of EPS/SMP compounds. Based on SEC analysis, the SMPs in the supernatant of the mixed liquor of the full-scale MBR mainly consists of macromolecules (9900 - 277,000 Da), humic substance (1000 - 4000 Da), and the organic acids (< 1000 Da) (Chang). The foulants comprised not only organic substances but also inorganic elements. Based on SEM-EDX analysis, inorganic precipitates in an AnMBR consist of struvite (e.g., $\text{MgNH}_4\text{PO}_4 \cdot 6\text{H}_2\text{O}$), calcite, and clay (Berube et al., 2006), which can be attributed to the production of ammonium and phosphate ions during anaerobic decomposition of organics. ICP and EDX are usually used for inorganic fouling characterization with the limitation of deliquescent samples and surface detection, respectively. An et al. (2009) suggested that bridging between deposited biopolymers and inorganic foulants (Mg, Ca, Na, Fe, Al, K, and Si) could enhance the compactness of fouling layer.

2.4.2.3 Microbiological characterization

The microbial community structures have been investigated to explore the biodiversity and population dynamics of microorganism in MBRs using microbiology methods such as polymerase chain reaction-denaturing gradient gel electrophoresis (PCR-DGGE) (Wan et al., 2011; Wiszniowski et al., 2011) and Fluorescence In Situ Hybridization (FISH) (Wilen et al., 2008). PCR-DGGE is a useful DNA fingerprinting procedure tool in studying complex microbial communities. Specialized 16s PCR primers amplify a portion of the gene (~400 base pairs) and include a high “G+C clamp” that anchors one end of the double stranded DNA to itself. These PCR-amplified 16s rRNA gene fragments are all the same size, but they move to different locations in a denaturing gradient gel because different sequences are immobilized (via denaturation) at different locations in the gel. The separated individual DNA fragments (bands) can be isolated and sequenced (Madsen, 2008). In a full-scale anaerobic bioreactor treating paper mill wastewater, the majority of prominent bands from the archaeal DGGE profile as well as a major proportion of the archaeal clone library matched with sequences from *Methanosaeta* spp (Roest et al., 2005). Some bacterial members, such as the family *Cellulomonadaceae* (*Cellulomonas*, *Oerskovia*) capable of hydrolysing cellulose and carbohydrates, the genus *Propionibacterium* which produce propionate, sulphate-reducing bacteria, and syntrophic fatty acid-oxidising microorganisms, can be affiliated with all steps along the anaerobic degradation pathway. A recent study based on PCR-DGGE analysis observed an obvious microbial community succession from the subphylum of *Betaproteobacteria* to *Deltaproteobacteria* was in the cake layer in an anoxic/aerobic MBR (Gao et al., 2011). FISH applies microscopic detection of cells whose biomarkers (e.g., deoxyribonucleic acid (DNA), ribosomal ribonucleic acid (rRNA)) hybridize to fluorescently tagged probe molecules of known binding specificity, showing the composition and spatial structure of the microbial community in the reactor (Yang et al., 2010). FISH and 16S rRNA gene sequence analyses revealed that the *Betaproteobacteria* probably played a major role in the development of the mature fouling layers (Miura et al., 2007).

The state-of-the-art approaches used for membrane fouling studies are critically reviewed by Meng et al. (2010). The visualisation, identification and characterisation of foulants using these techniques are helpful for the fundamental understanding of the development membrane fouling process.

2.4.3 Factors affecting membrane fouling

A number of factors affecting membrane fouling are shown in Fig. 2-2. Five main categories of factors strongly influence the nature and extent of membrane fouling: membrane properties, sludge characteristics, hydrodynamic conditions, operating conditions, and environmental conditions. In addition, the fouling effects of the influent properties are generally attributed to wastewater composition, types and characteristics of contaminant, nutrients, and temperature (Arabi, 2009). For instance, heavy metals present in wastewater of several industries (e.g., metal finishing, hydrometallurgical, refining, petrochemical, tanneries and battery manufacturing companies) are considered as a toxicant group which strongly reduces the activity of microorganisms, changes the sludge culture, and hence induces alterations in EPS, floc size and membrane fouling (Amiri et al., 2010). The complex interactions of membrane material, sludge properties and operational conditions are still not fully understood.

In a MBR, the fouling behaviour is considered to be directly determined by sludge characteristics, membrane properties and their interactions. Hydrodynamic conditions (i.e. permeate flux, TMP, aeration intensity (Menniti and Morgenroth, 2010)) exert direct shear stress on the fouling layer and sludge itself. The biological system design and operation parameters e.g., SRT, HRT or OLR (Zhang et al., 2010), F/M ratio, nutrient conditions, etc., play significant roles in the membrane filtration performance. Although the operating and environmental conditions have no direct effect on membrane fouling, the control of them can modify the biological process and consequently change physicochemical properties of the sludge. The membrane properties and sludge characteristics that influence membrane fouling are briefly reviewed here, while the effect of hydrodynamic conditions on membrane fouling is discussed in a later section (section 2. 4. 4).

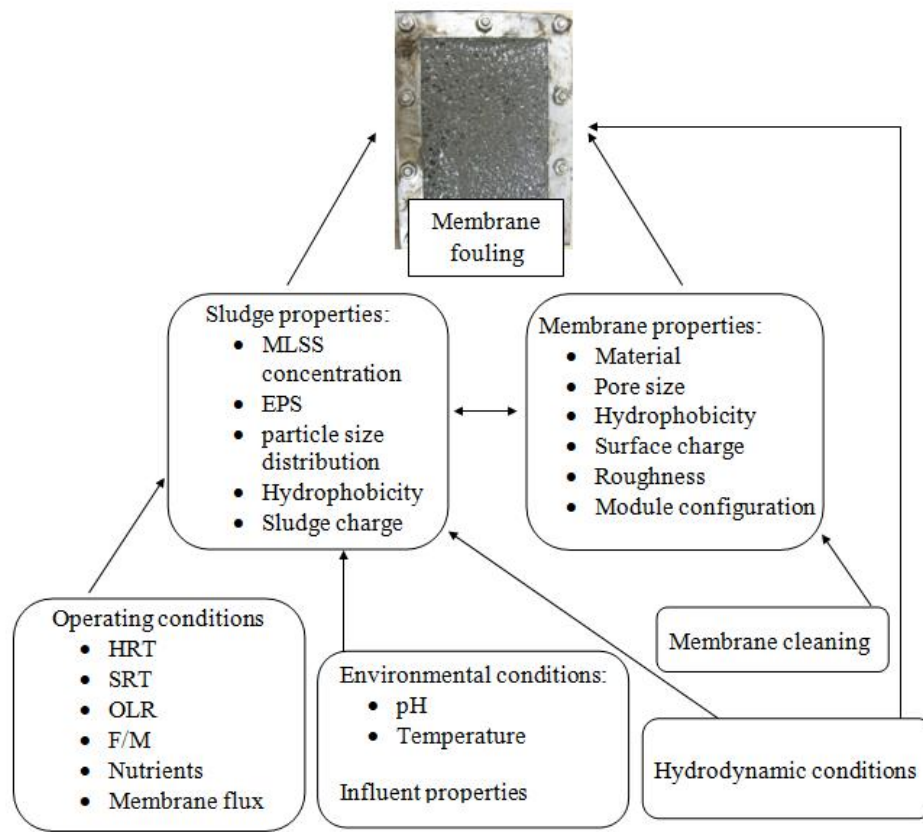


Figure 2-2 Factors affecting membrane fouling

2.4.3.1 Membrane

Membrane characteristics such as materials, pore size (Bilad et al., 2011), porosity, surface charge, roughness, and hydrophilicity/hydrophobicity, etc., have a direct impact on membrane fouling. In the order of descending pore size (or molecular weight cut-off (MWCO)), membranes are generally classified as microfiltration (MF), ultrafiltration (UF), nanofiltration (NF), and reverse osmosis (RO) membranes (Fig. 2-3). The membranes for the current commercial submerged MBR processes are MF and UF membranes in the form of flat sheet or hollow fibre. Hong et al. (2002) showed that the initial fouling extent for MF membranes was higher than that for UF, presumably due to pore blocking. Comparing the UF membranes ranging from 20,000 to 70,000 Da, the one with the small MWCO and smooth surface tends to exhibit a serious initial flux decline (He et al., 2005). It was suggested that highly porous membranes with even pore size

distribution that have as little overlap as possible with the size distribution of the particles to be filtered can limit fouling due to pore blocking and enhance filtration efficiency. The suitable membrane pore sizes used in wastewater treatments are in the range of 0.02-0.5 μm (Stephenson et al., 2000).

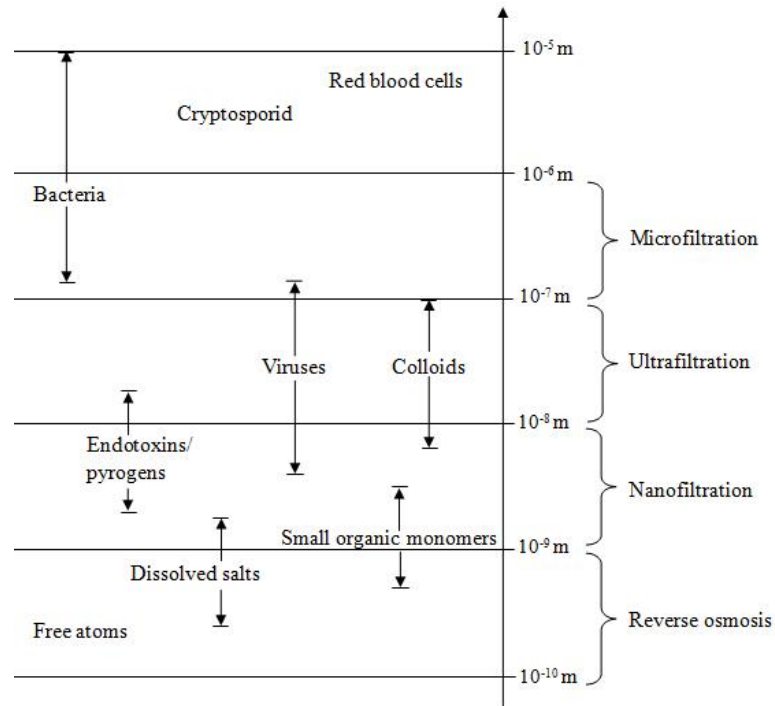


Figure 2-3 Classification of membranes based on pore size (Judd, 2006)

According to the nature of the membrane material, membranes can be categorized as polymeric (e.g. polyamide, polysulfone, polypropylene, polyethylene (PE), polyethersulfone (PES), polyvinylidene fluoride (PVDF), and polyvinyl chloride (PVC)), inorganic (e.g. ceramic, metallic, and porous glass), and modified materials. Polymeric membranes have been used in MBRs for wastewater treatment due to their low costs. Even cloth-media (Acrylate, Polyester, and Nylon) filters have been used to reduce manufacturing and operating cost of the MBR (Zahid and El-Shafai, 2011). In general, hydrophobic membranes tend to favour the strong attachment of hydrophobic molecules (i.e., lipids, protein), thus reducing the applicable fluxes. Extensive studies focus on the surface modification of hydrophobic polymeric membranes by grafting hydrophilic groups (Sainbayar et al., 2001). On the other hand, negatively and neutrally charged

membranes have lower fouling potential than positively charged membranes, as most bacterial flocs are negatively charged with a zeta potential from -10 mV to -30 mV (Kraemer, 2002). Kang et al. (2006) also agreed that the membrane with a hydrophilic, more negatively charged, and smooth surface would be more effective in reducing the initial adhesion of microorganisms. However, the membranes will not be in direct contact with the suspension anymore when cake layer or gel layer form to act as a secondary membrane affecting the filtration performance.

2.4.3.2 Sludge characteristics

A complex system like AnMBR is basically an enclosed system that concentrates organic foulants in the sludge suspension. Membrane fouling can be determined by the components in the mixed liquor (i.e., cells, cell debris, microbial metabolites, and substrate components). Not only suspended solids, but also many other fractions like colloids (Wang and Tarabara, 2008), soluble organic matter (Min et al., 2008), inorganic precipitates (Demadis et al., 2005) and extracellular polymers (Wang et al., 2009) can contribute to the overall performance. The relative contributions of suspended solids, colloids, and dissolved molecules (DM) to the membrane fouling resistance were found to be 65 %, 30 %, and 5 %, respectively by Defrance et al. (2000) and 24 %, 50 %, and 26 % by Bouhabila et al. (2001), respectively. The resistance-in-series (RIS) model (see section 7.2.3) has been used frequently to analyze the membrane fouling phenomenon (Khalili-Garakani et al., 2011) and to characterize the relative significance of each resistance component in heterogeneous membrane bioreactors (MBRs). It should be noted that when the RIS model is used to analyze the individual resistances of the sludge components, additivity of individual resistances is questionable (Chang et al., 2009).

Membrane filtration performance in MBRs was proven to depend on the concentration of mixed liquor suspended solids (MLSS), and membrane fouling took place more rapidly at higher MLSS concentration (Chang and Kim, 2005). MLSS concentration is considered to directly cause the increase of cake layer resistance (R_c) which is often expressed by the following equation (Chang et al., 2001).

$$R_c = \alpha \cdot V \cdot C_b \quad (2-1)$$

where α is specific cake resistance (m^2/kg); V is permeate volume per unit area (m^3/m^2); and C_b is bulk MLSS concentration (kg/m^3). On the other hand, it was reported that MLSS concentration (3.6-8.4 g/L) didn't affect permeate flux (air flow rate of 6 L/min) (Hong et al., 2002) and the fouling rates in the MBRs were closely related to the dissolved matter (Arabi and Nakhla, 2008a). Lee et al. (2001) even suggested improvement of membrane permeability with increasing in MLSS concentrations. Rosenberger et al. (2005) organized the complex interaction between MLSS and membrane fouling in more detail with regard to experimental set-ups and showed that for low MLSS concentrations (< 6 g/L), membrane fouling decreased with the increase in MLSS concentrations. At medium MLSS concentrations (8-12 g/L), no impact was found. A very high MLSS concentrations (> 15 g/L) resulted in an increase in fouling. On the other hand, MLSS concentration is closely related to viscosity of biomass suspension, and an increase in sludge viscosity will weaken the hydrodynamic conditions close to the membranes to yield a substantial TMP increase (Ueda et al., 1996). For each MBR system, a critical MLSS concentration (10-17 g/L) exists under which the viscosity remains low and rises only slowly with the MLSS concentration and above which viscosity tends to increase exponentially with the solids concentration (Le-Clech et al., 2006).

In terms of particle size distribution, Carmen-Kozeny equation (see section 7.2.5.1, equation 7-5) establishes its impact on the cake layer resistance: the smaller the floc sizes are, the greater the cake resistance is. The magnitude of back-transport mechanisms is strongly related to particle size as the shear-induced hydrodynamic diffusivity is positively proportional to the square of the particle diameter multiplied by the shear rate (Tardieu et al., 1998). Consequently, a particle with a larger size on the membrane surface can be detached much more easily at the same shear conditions. A higher hydraulic resistance was associated with smaller floc particles experiencing a higher tendency to deposit over the membrane surface (Altmann and Ripperger, 1997). Kromkamp et al. (2006) found that the smallest particles in the suspension can determine the filtration rate.

As described in section 6.1, extracellular polymeric substances (EPS) and soluble microbial products (SMPs) (Tian et al., 2011) have received considerable attention in recent years with many reports indicating that they are one of the most significant factors affecting fouling in MBRs. Due to presence of the membrane in the MBR process, although the EPS production is not affected, the large macromolecules (polysaccharides, proteins (including enzymes), DNA, lipids, nucleic acids, and humic substances) are retained in the sludge suspension by the membrane. The accumulation of EPS can cause an increase of viscosity of the mixed liquor and an increase in the filtration resistance (Nagaoka et al., 1996). The attachment of sludge flocs to a membrane is often mediated and strengthened by these macromolecules.

EPS are high molecular weight (M_w) secretions biosynthesized and released by microbial cells due to cell metabolism and auto-lysis. The EPS extracted from the membrane foulants exhibited broader distributions of M_w compared with the EPS in the influent and the effluent (An et al., 2009). Most of its components are either tightly bound to cells or loosely associated with cells. According to (Li and Yang, 2007), EPS can be further classified into loosely bound EPS (LB-EPS) and tightly bound EPS (TB-EPS), and a modified heat extraction method separated the LB-EPS from TB-EPS by extraction temperature of 50 °C. The functions of the EPS matrix are multiple. Since EPS are adhesive and viscous, the integrity and stability of flocs or biofilm are reinforced remarkably. Floc breakage leads to the release of EPS present inside the floc structure, decreasing settleability, a loss of biological activity, and change in microorganism population (Chang et al., 2002). Furthermore, EPS enhances the survival and robustness of the biofilm microorganisms by retention of water and accumulation of enzymatic activities, such as digestion of exogenous macromolecules for nutrient acquisition. Nutrients can be adsorbed and stored in the hydrated matrix for microbial growth and metabolism. EPS also serves as a protective barrier that cushions microorganism against harmful environmental effects such as desiccation, extreme pHs, salt exposure, biocides and hydraulic shears. Methods of bound EPS extraction include chemical methods (Ethylenediaminetetraacetic acid (EDTA), formaldehyde + NaOH, glutaraldehyde), physical methods (heating, sonication, cation exchange resin, sonication+ cation

exchange resin, and centrifugation alone) (Comte et al., 2006). Chemical extraction was the more effective in extracting the largest amount of bound EPS (Liu and Fang, 2003; Comte et al., 2006), whereas the cation exchange resin and heating are preferred methods because of their simplicity (Le-Clech et al., 2006). It is reported that both quantity and composition of bound EPS in sludge suspension or on the membrane surface influenced membrane fouling (Ji and Zhou, 2006). Except for protein and carbohydrates that are typically characterized in the solution containing EPS, humic substances were identified as the major components of EPS in the activated sludge (more than 34 %) (Dvorák et al., 2011). Thus, the occurrence of other contents requires more attention in future research (Le-Clech et al., 2006).

SMP, namely soluble EPS, are defined as the pool of organic compounds that are released into solution from substrate metabolism (substrate-utilisation-associated products (UAP)) and biomass decay (biomass-associated products (BAP)) (Barker and Stuckey, 1999; Laspidou and Rittmann, 2002). In MBR systems, they can also originate from the influent feed substrate. There are mainly three methods of separating the water phase from the biomass: filtration through a filter paper, centrifugation and sedimentation. The first method was found to be the most effective and the simple compared to the two other methods in the literature. It is suggested to filter the solution through, at least, a 1.2 µm filter paper in order to remove colloids (Le-Clech et al., 2006). The measurement of SMP was similar with EPS. Lyko et al. (2008) suggested that dissolved organic carbon (DOC) was an alternative to complex and costly measurements of SMP components. Fouling propensity was directly correlated with the concentration and composition of SMP (Wu and Lee, 2011). Accumulated SMP in the mixed liquor were inhibitory to the metabolic activity of the activated sludge and had a negative influence to the membrane permeability (Harada et al., 1994; Huang et al., 2000). SMP can block membrane pores, absorb on the membrane surface, form a gel layer, and/or build up on cake layers through physical and chemical adsorption, leading to smaller filtration areas, greater hydraulic resistance (Rosenberger et al., 2005) and finally a decrease in membrane permeability (Liao et al., 2004).

Some researchers further characterized the microbial communities, especially those involved in cake layer formation and fouling evolution. The microbial community shifted in different ways at the different SRTs (Duan et al., 2009; Wu et al., 2011). At lower fluxes, fouling layer community composition was quite similar and independent of sludge ages, while distinct microbial communities developed on membrane surfaces at high fluxes (Huang et al., 2008). The selective enrichments of certain species on membrane surface were observed (Miura et al., 2007; Huang et al., 2008; Calderón et al., 2011). The structures of microbial communities in the suspended solids and on the membrane surface were distinctly different. Higher cell surface hydrophobicities, higher EPS concentrations, and higher ratios of protein to carbohydrate within the EPSs were found in membrane isolates than those in the isolates from suspended solids (Jinhua et al., 2006). Identifying the determinant of selective cell deposition and the dominant species in cake layers are of interest to develop strategies for membrane fouling control.

2.4.4 Strategies for membrane fouling control

2.4.4.1 Reducing the fouling rate

Several common strategies used to reduce the fouling rate have been reported: membrane modification by plasma treatment (Yu et al., 2005) or nanocoating (Bae et al., 2006), sustainable flux operation (sub-critical flux operation), flux stoppage (relaxation), gas sparging, SRT control, and activated carbon/coagulant/flocculent addition.

The fouling rate can be reduced by operating a membrane below the critical flux. The critical flux was introduced over 15 years ago (Field et al., 1995) and was originally defined as the flux below which no fouling occurs. However, in complex systems fouling is inevitable, even at no flux conditions, because fouling occurs as soon as the membranes touch the bulk sludge. Consequently, the definition of the critical flux is modified as the flux above which the relation between flux and TMP becomes non-linear (Jeison, 2007). Among the several proposed critical flux determination methods (Tiranuntakul et al., 2011), a flux-step method can be easily applied in any type of membrane process, both at lab and full scale (Le Clech et al., 2003). In order to refer to a

certain flux for long term operation, the concept of sub-critical flux or sustainable flux, the flux below critical flux with acceptable value $dTMP/dt$, is considered for gaining tolerable levels of fouling to operate MBRs for extended periods of time. The sustainable operation periods can be prolonged by other methods such as membrane relaxation and the ultraviolet (UV) inactivation (Phattaranawik and Leiknes, 2011). UV irradiation of biomass is proposed to control biofouling by reducing the activities and productions of EPS/SMP without cell breakage. However, the penetration of the UV irradiation will be limited when the biomass concentration is high. In a high MLSS environment, membrane relaxation (flux stoppage) is typically applied to encourage diffusive back transport of foulants away from the membrane surface under a concentration gradient. The effect of back transport can be enhanced by shear force created by gas scouring.

It is feasible to control membrane fouling by selecting suitable operational parameters since they govern biomass growth and decay (Meng et al., 2009). Organic loading rate (OLR) is determined by the influent organic concentration and hydraulic retention time (HRT). Long-term starvation will cause serious membrane fouling due to total loss of cell activity releasing large amounts of BAPs (humic-acid substances) (Wu and Lee, 2011). On the contrary, a low HRT or high OLR as food-to-microorganism (F/M) ratio increased membrane fouling rates (Salazar-Peláez et al.; Trussell et al., 2006). In addition, a shorter HRT or higher OLR provides more nutrients to the biomass, leading to a greater biological growth and a higher MLSS (Dufresne et al., 1998). Therefore, the increase of OLR will induce the production of more EPS because bound EPS is growth related and is produced in direct proportion to substrate utilization (Laspidou and Rittmann, 2002). Of course, the influent composition (i.e., the substrate type (Li and Yang, 2007; McAdam et al., 2007) and the protein/polysaccharides ratio (PN/PC) (Arabi and Nakhla, 2008b)) strongly correlated with bound EPS and SMP production as well as the formation of colloids. SRT variations directly alter sludge composition and MLSS concentration (Patsios and Karabelas, 2011). Either a too short SRT (Ng et al., 2006b; Huang et al., 2008) or a too long SRT (Han et al., 2005) was found to result in extensive membrane fouling. Infinite SRT in SANMBR accelerated cake layer development as a result of the highest MLSS and SMP concentrations (Huang et al., 2011). According to

Meng et al. (2009), there is an optimum SRT determined by different operating conditions for each MBR.

Gas sparging and its intensity (hydrodynamic conditions) have a complex influence as a way to control membrane fouling in submerged MBRs. Air sparging is widely used in aerobic MBRs, where it carries out a triple function: provide oxygen transfer to the biomass, maintain the solids in suspension and promote scouring of the membrane surface (Bouhabila et al., 1998; Cui et al., 2003). As mentioned, in SAnMBRs biogas can be recirculated in order to achieve a similar effect. The size (Fane et al., 2005; Prieske et al., 2008) and motion (Jirachote Phattaranawik, 2007; Zhang et al., 2009b) of bubbles have effects on generation of secondary liquid flows that enhance the liquid-membrane surface mass transfer. Better hydrodynamic conditions can be achieved by increasing the aeration intensity in submerged MBRs. In most cases, intensity of aeration or biogas scouring was just simply described as gas flow rate. Besides, superficial gas velocity (U_G) values and the ratio of gas volume to permeate water volume (Dai et al., 2010) appear to be adopted. However, increasing aeration intensity or flow velocity could increase energy cost and disrupt sludge flocs, producing small size particles and releasing more EPS which negatively impact membrane fouling (Khan and Visvanathan, 2008; Meng et al., 2008). There exists a practical limit above which only a minor benefit for membrane fouling control is provided (Han et al., 2005). Furthermore, some researchers observed a decrease in biological performance that was interpreted as the negative effect of high shear conditions over microbial activity (Choo and Lee, 1996b; Kim et al., 2001).

The modification of suspension properties has been tested in order to control membrane fouling and enhance membrane filtration. The addition of powdered activated carbon (PAC), granular activated carbon (GAC) (Insel et al., 2011) or zeolite (Damayanti et al., 2011) to a MBR will adsorb colloids and soluble compounds (Satyawali and Balakrishnan, 2009). The PAC can also provide solid support for biomass growth to form strong and dense biologically activated carbon which enhances flocculation ability and prevent accumulation on membranes (Ng et al., 2006a; Hu and Stuckey, 2007). Akram and Stuckey (2008) found that when applied at very low dosages, PAC addition can

improve membrane performance in terms of cost, flux and soluble COD removal. The addition of 3.4 g/L PAC reduced the flux as a result of the increased sludge viscosity. Additionally, membrane fouling reducer (MFR) (the modified cationic polyelectrolyte and FeCl_3) or membrane flux enhancer (MFE) was reported to be able to lead to the flocculation of activated sludge and reduce membrane fouling in MBRs (Iversen et al., 2009; Koseoglu-Imer et al., 2011). With the addition of MFR, soluble foulants in the bulk sludge were entrapped by the microbial flocs during flocculation, leading to an increase in the concentration of bound EPS. A more porous cake layer substantially enhanced membrane filterability (Hwang et al., 2007; Lee et al., 2007). More recently, Teychene et al. (2011) proposed the formation of a non-compressible fouling layer by fine particles addition to avoid or to delay TMP jump.

Coagulants are generally applied in water and wastewater treatment for removing colloidal and soluble organic fractions (Wu et al., 2006). The use of coagulants (alum (Song et al., 2008), $\text{Al}_2(\text{SO}_4)_3$, FeCl_3 (Koseoglu et al., 2008; Zhang et al., 2008), chitosan (Iversen et al., 2008), filter acids (Ji et al., 2008), cationic polyelectrolytes (Dizge et al.), polymeric aluminum chloride (Tian et al., 2008) and polymeric ferric sulphate have been tested in MBRs with positive results. Once dissolved in water, alum forms hydroxide aggregates of larger flocs by charge neutralisation and bridging. Polymeric coagulants had a better effect on filterability enhancement of mixed liquor than monomeric coagulants (Wu et al., 2006; Koseoglu et al., 2008).

In recent studies, a number of new methods have been applied to mitigate membrane fouling. Ultrasound has been proved to be effective to enhance membrane permeability due to cavitation effect and acoustic streaming (Xu et al., 2011). However, ultrasonic irradiation may have slightly negative effect on the anaerobic bacterial activity (Sui et al., 2008). In addition, ozonation of bulk sludge has been tested as a means of membrane fouling control during continuous MBR operation (Huang and Wu, 2008; Mascolo et al., 2010). Ozonation modified the surface properties and provided a beneficial condition for re-flocculation among flocs, resulting in an increase in the decreased zeta-potential, enhanced hydrophobicity of the flocs' surface and a decrease in the liquid viscosity (Huang and Wu, 2008; Sun et al., 2011). There is also electric field

proposed to effectively move the sludge away from the membrane by an electric repulsive force, because the surface of the activated sludge is negatively charged (Akamatsu et al., 2011).

2.4.4.2 Membrane cleaning

Reducing the rate of fouling can prolong the length of time between cleanings. However, at some point, when further filtration is no longer sustainable due to elevated TMP or low flux, the membrane must be cleaned. Physical cleaning is normally achieved by permeate backwashing (Yigit et al., 2009), that is reversing permeate through the membrane whilst continuing to scour the membrane with bubbling. Backwashing has been found to successfully remove most of the removable fouling. Chemical cleaning has been widely applied for cleaning membranes in MBRs either in situ (Wei et al., 2011) or ex situ. The chemical agents include NaOCl, NaOH, H₂O₂, Cl₂, etc. For example, Alkaline cleaning (NaOH) has been used to remove biological fouling. Tian et al. (2010) indicated that NaOH and ethanol were able to eliminate inner pore fouling, and ethanol could also restore the hydrophilicity of the polyvinyl chloride (PVC) membrane. The prevalent cleaning agents are sodium hypochlorite (for organic foulants) and citric acid (for inorganic foulants). Alternatively, a low concentration of chemical agents can be added to the backflush water to produce “chemically enhanced backflush”.

2.5 References

- Food and Agriculture Organization of the United Nations, Environmental impact assessment and environmental auditing in the pulp and paper industry. 1996. Available from <http://www.fao.org/docrep/005/v9933e/V9933E00.HTM>.
- Wikipedia, Confocal laser scanning microscopy. 2011a. Available from http://en.wikipedia.org/wiki/Confocal_laser_scanning_microscopy.
- Wikipedia, Pulp (paper). 2011b. Available from [http://en.wikipedia.org/wiki/Pulp_\(paper\)](http://en.wikipedia.org/wiki/Pulp_(paper)).
- Ahn, J. H., Forster, C. F., 2002. A comparison of mesophilic and thermophilic anaerobic upflow filters treating paper-pulp-liquors. *Process Biochemistry* 38, 256-261.

- Akamatsu, K., Lu, W., Sugawara, T., Nakao, S.-i., Development of a novel fouling suppression system in membrane bioreactors using an intermittent electric field. *Water Research In Press, Corrected Proof*,
- Akram, A., Stuckey, D. C., 2008. Flux and performance improvement in a submerged anaerobic membrane bioreactor (SAMBR) using powdered activated carbon (PAC). *Process Biochemistry* 43, 93-102.
- Altmann, J., Ripperger, S., 1997. Particle deposition and layer formation at the crossflow microfiltration. *Journal of Membrane Science* 124, 119-128.
- Amiri, S., Mehrnia, M. R., Azami, H., Barzegari, D., Shavandi, M., Sarrafzadeh, M. H., 2010. Effect of heavy metals on fouling behaviour in membrane reactors. *Iran. J. Environ. Health. Sci. Eng.* 7, 337-384.
- An, Y., Wang, Z., Wu, Z., Yang, D., Zhou, Q., 2009. Characterization of membrane foulants in an anaerobic non-woven fabric membrane bioreactor for municipal wastewater treatment. *Chemical Engineering Journal* 155, 709-715.
- Arabi, S. (2009). *Impact of Influent Feed and Mixed Liquor Characteristics on Fouling in Submerged Membrane Bioreactors for Wastewater Treatment*. Department of Chemical and Biochemical Engineering. London, Canada, The University of Western Ontario. Ph.D.
- Arabi, S., Nakhla, G., 2008a. Impact of calcium on the membrane fouling in membrane bioreactors. *Journal of Membrane Science* 314, 134-142.
- Arabi, S., Nakhla, G., 2008b. Impact of protein/carbohydrate ratio in the feed wastewater on the membrane fouling in membrane bioreactors. *Journal of Membrane Science* 324, 142-150.
- Bae, T.-H., Kim, I.-C., Tak, T.-M., 2006. Preparation and characterization of fouling-resistant TiO₂ self-assembled nanocomposite membranes. *Journal of Membrane Science* 275, 1-5.
- Barker, D. J., Stuckey, D. C., 1999. A review of soluble microbial products (SMP) in wastewater treatment systems. *Water Research* 33, 3063-3082.

- Berube, P. R., Hall, E. R., 2000. Effects of elevated operating temperatures on methanol removal kinetics from synthetic kraft pulp mill condensate using a membrane bioreactor. *Water Research* 34, 4359-4366.
- Berube, P. R., Hall, E. R., Sutton, P. M., 2006. Parameters governing permeate flux in an anaerobic membrane bioreactor treating low-strength municipal wastewaters: a literature review. *Water Environment Research* 78, 887-896.
- Bhattacharjee, S., Datta, S., Bhattacharjee, C., 2007. Improvement of wastewater quality parameters by sedimentation followed by tertiary treatments. *Desalination* 212, 92-102.
- Bilad, M. R., Declerck, P., Piasecka, A., Vanysacker, L., Yan, X., Vankelecom, I. F. J., 2011. Treatment of molasses wastewater in a membrane bioreactor: Influence of membrane pore size. *Separation and Purification Technology* 78, 105-112.
- Bouhabila, E. H., Ben Aim, R., Buisson, H., 1998. Microfiltration of activated sludge using submerged membrane with air bubbling (application to wastewater treatment). *Desalination* 118, 315-322.
- Bouhabila, E. H., Ben Aim, R., Buisson, H., 2001. Fouling characterisation in membrane bioreactors. *Separation and Purification Technology* 22-23, 123-132.
- Buzzini, A. P., Pires, E. C., 2007. Evaluation of a upflow anaerobic sludge blanket reactor with partial recirculation of effluent used to treat wastewaters from pulp and paper plants. *Bioresource Technology* 98, 1838-1848.
- Cabral, F., Vasconcelos, E., Goss, M. J., Cordovil, C. M. d. S., 1998. The value, use, and environmental impacts of pulp-mill sludge additions to forest and agricultural lands in Europe. *Environmental Reviews* 6, 55-64.
- Calderón, K., Rodelas, B., Cabirol, N., González-López, J., Noyola, A., 2011. Analysis of microbial communities developed on the fouling layers of a membrane-coupled anaerobic bioreactor applied to wastewater treatment. *Bioresource Technology* 102, 4618-4627.
- Chang, I.-S., Bag, S.-O., Lee, C.-H., 2001. Effects of membrane fouling on solute rejection during membrane filtration of activated sludge. *Process Biochemistry* 36, 855-860.

- Chang, I.-S., Kim, S.-N., 2005. Wastewater treatment using membrane filtration--effect of biosolids concentration on cake resistance. *Process Biochemistry* 40, 1307-1314.
- Chang, I.-S., Le Clech, P., Jefferson, B., Judd, S., 2002. Membrane Fouling in Membrane Bioreactors for Wastewater Treatment. *Journal of Environmental Engineering* 128, 1018.
- Chang, I. S., Fieldb, R., Cuib, Z., 2009. Limitations of resistance-in-series model for fouling analysis in membrane bioreactors: A cautionary note. *Desalination and Water Treatment* 8, 31-36.
- Chang, S., Application of submerged hollow fiber membrane in membrane bioreactors: Filtration principles, operation, and membrane fouling. *Desalination In Press*, Corrected Proof,
- Chen, W., Horan, N. J., 1998. The Treatment of a High Strength Pulp and Paper Mill Effluent for Wastewater Re-Use -- III) Tertiary Treatment Options for Pulp and Paper Mill Wastewater to Achieve Effluent Recycle. *Environmental Technology* 19, 173 - 182.
- Choi, H., Zhang, K., Dionysiou, D. D., Oerther, D. B., Sorial, G. A., 2005. Effect of permeate flux and tangential flow on membrane fouling for wastewater treatment. *Separation and Purification Technology* 45, 68-78.
- Choo, K.-H., Lee, C.-H., 1996a. Membrane fouling mechanisms in the membrane-coupled anaerobic bioreactor. *Water Research* 30, 1771-1780.
- Choo, K. H., Lee, C. H., 1996b. Effect of anaerobic digestion broth composition on membrane permeability. *Water Science and Technology* 34, 173-179.
- Chu, L., Li, S., 2006. Filtration capability and operational characteristics of dynamic membrane bioreactor for municipal wastewater treatment. *Separation and Purification Technology* 51, 173-179.
- Cicek, N., 2003. A review of membrane bioreactors and their potential application in the treatment of agricultural wastewater. *CANADIAN BIOSYSTEMS ENGINEERING* 45, 37-49.

- Clauss, F., Balavoine, C., Hélaïne, D., Martin, G., 1999. Controlling the settling of activated sludge in pulp and paper wastewater treatment plants. *Water Science and Technology* 40, 223-229.
- Comte, S., Guibaud, G., Baudu, M., 2006. Relations between extraction protocols for activated sludge extracellular polymeric substances (EPS) and EPS complexation properties: Part I. Comparison of the efficiency of eight EPS extraction methods. *Enzyme and Microbial Technology* 38, 237-245.
- Cui, Z. F., Chang, S., Fane, A. G., 2003. The use of gas bubbling to enhance membrane processes. *Journal of Membrane Science* 221, 1-35.
- Dai, H., Yang, X., Dong, T., Ke, Y., Wang, T., 2010. Engineering application of MBR process to the treatment of beer brewing wastewater. *Modern Applied Science* 4, 103-109.
- Damayanti, A., Ujang, Z., Salim, M. R., 2011. The influenced of PAC, zeolite, and *Moringa oleifera* as biofouling reducer (BFR) on hybrid membrane bioreactor of palm oil mill effluent (POME). *Bioresource Technology* 102, 4341-4346.
- Defrance, L., Jaffrin, M. Y., Gupta, B., Paullier, P., Geaugey, V., 2000. Contribution of various constituents of activated sludge to membrane bioreactor fouling. *Bioresource Technology* 73, 105-112.
- Demadis, K. D., Neofotistou, E., Mavredaki, E., Tsiknakis, M., Sarigiannidou, E.-M., Katarachia, S. D., 2005. Inorganic foulants in membrane systems: chemical control strategies and the contribution of "green chemistry". *Desalination* 179, 281-295.
- Dias, J. C. T., Rezende, R. P., Silva, C. M., Linardi, V. R., 2005. Biological treatment of kraft pulp mill foul condensates at high temperatures using a membrane bioreactor. *Process Biochemistry* 40, 1125-1129.
- Dizge, N., Koseoglu-Imer, D. Y., Karagunduz, A., Keskinler, B., Effects of cationic polyelectrolyte on filterability and fouling reduction of submerged membrane bioreactor (MBR). *Journal of Membrane Science* In Press, Corrected Proof,

- Duan, L., Moreno-Andrade, I., Huang, C.-l., Xia, S., Hermanowicz, S. W., 2009. Effects of short solids retention time on microbial community in a membrane bioreactor. *Bioresource Technology* 100, 3489-3496.
- Dufresne, R., Lavallee, H.-C., Lebun, R.-E., Lo, S.-N., 1998. Comparison of performance between membrane bioreactor and activated sludge system for the treatment of pulping process wastewaters, TAPPI, Norcross, GA, ETATS-UNIS.
- Dvorák, L., Gómez, M., Dvoráková, M., Ruzicková, I., Wanner, J., 2011. The impact of different operating conditions on membrane fouling and EPS production. *Bioresource Technology* 102, 6870-6875.
- Fahmy, M., Kut, O. M., Heinzle, E., 1994. Anaerobic-aerobic fluidized bed biotreatment of sulphite pulp bleaching effluents--II. Fate of individual chlorophenolic compounds. *Water Research* 28, 1997-2010.
- Fane, A. G., Yeo, A., Law, A., Parameshwaran, K., Wicaksana, F., Chen, V., 2005. Low pressure membrane processes ~ doing more with less energy. *Desalination* 185, 159-165.
- Field, R. W., Wu, D., Howell, J. A., Gupta, B. B., 1995. Critical flux concept for microfiltration fouling. *Journal of Membrane Science* 100, 259-272.
- Galil, N. I., Sheindorf, C., Stahl, N., Tenenbaum, A., Levinsky, Y., 2003. Membrane bioreactors for final treatment of wastewater. *Water Science and Technology* 48, 103-110.
- Gao, D.-w., Fu, Y., Tao, Y., Li, X.-x., Xing, M., Gao, X.-h., Ren, N.-q., 2011. Linking microbial community structure to membrane biofouling associated with varying dissolved oxygen concentrations. *Bioresource Technology* 102, 5626-5633.
- Gao, W. J. J., Lin, H. J., Leung, K. T., Liao, B. Q., 2010. Influence of elevated pH shocks on the performance of a submerged anaerobic membrane bioreactor. *Process Biochemistry* 45, 1279-1287.
- Geng, Z., Hall, E. R., 2007. A comparative study of fouling-related properties of sludge from conventional and membrane enhanced biological phosphorus removal processes. *Water Research* 41, 4329-4338.

- Gommers, K., De Wever, H., Brauns, E., Peys, K., 2007. Recalcitrant COD degradation by an integrated system of ozonation and membrane bioreactor. *Water Science and Technology* 55, 245-251.
- Hall, E. R., Berube, P. R., 2000. Removal of methanol from evaporator condensate using a high temperature membrane bioreactor: determination of optimal operating temperature and system costs. *Pulp & Paper Canada* 101, 54.
- Hall, E. R., Onysko, K. A., Parker, W. J., 1995. Enhancement of Bleached Kraft Organochlorine Removal by Coupling Membrane Filtration and Anaerobic Treatment. *Environmental Technology* 16, 115 - 126.
- Han, S.-S., Bae, T.-H., Jang, G.-G., Tak, T.-M., 2005. Influence of sludge retention time on membrane fouling and bioactivities in membrane bioreactor system. *Process Biochemistry* 40, 2393-2400.
- Harada, H., Momonoi, K., Yamazaki, S., Takizawa, S., 1994. Application of anaerobic UF membrane reactor for treatment of a wastewater containing high strength particulate organics. *Water Science and Technology* 30, 307-319.
- He, Y., Xu, P., Li, C., Zhang, B., 2005. High-concentration food wastewater treatment by an anaerobic membrane bioreactor. *Water Research* 39, 4110-4118.
- Helble, A., Schlayer, W., Liechti, P.-A., Jenny, R., Möbiust, C. H., 1999. Advanced effluent treatment in the pulp and paper industry with a combined process of ozonation and fixed bed biofilm reactors. *Water Science and Technology* 40, 343-350.
- Hong, S. P., Bae, T. H., Tak, T. M., Hong, S., Randall, A., 2002. Fouling control in activated sludge submerged hollow fiber membrane bioreactors. *Desalination* 143, 219-228.
- Horan, N. J., Chen, W., 1998. The Treatment of a High Strength Pulp and Paper Mill Effluent for Waste Water Re-Use -- I) The Use of Modelling to Optimise Effluent Quality from the Existing Wastewater Treatment Plant. *Environmental Technology* 19, 153 - 161.

- Howe, K. J., Clark, M. M., 2002. Fouling of Microfiltration and Ultrafiltration Membranes by Natural Waters. *Environmental Science & Technology* 36, 3571-3576.
- Hu, A. Y., Stuckey, D. C., 2007. Activated Carbon Addition to a Submerged Anaerobic Membrane Bioreactor: Effect on Performance, Transmembrane Pressure, and Flux. *Journal of Environmental Engineering* 133, 73-80.
- Huang, L.-N., De Wever, H., Diels, L., 2008. Diverse and Distinct Bacterial Communities Induced Biofilm Fouling in Membrane Bioreactors Operated under Different Conditions. *Environmental Science & Technology* 42, 8360-8366.
- Huang, X., Liu, R., Qian, Y., 2000. Behaviour of soluble microbial products in a membrane bioreactor. *Process Biochemistry* 36, 401-406.
- Huang, X., Wu, J., 2008. Improvement of membrane filterability of the mixed liquor in a membrane bioreactor by ozonation. *Journal of Membrane Science* 318, 210-216.
- Huang, Z., Ong, S. L., Ng, H. Y., 2011. Submerged anaerobic membrane bioreactor for low-strength wastewater treatment: Effect of HRT and SRT on treatment performance and membrane fouling. *Water Research* 45, 705-713.
- Hwang, B.-K., Lee, W.-N., Park, P.-K., Lee, C.-H., Chang, I.-S., 2007. Effect of membrane fouling reducer on cake structure and membrane permeability in membrane bioreactor. *Journal of Membrane Science* 288, 149-156.
- Insel, G., Hocaoglu, S. M., Cokgor, E. U., Orhon, D., 2011. Modelling the effect of biomass induced oxygen transfer limitations on the nitrogen removal performance of membrane bioreactor. *Journal of Membrane Science* 368, 54-63.
- Iversen, V., Koseoglu, H., Yigit, N. O., Drews, A., Kitis, M., Lesjean, B., Kraume, M., 2009. Impacts of membrane flux enhancers on activated sludge respiration and nutrient removal in MBRs. *Water Research* In Press, Corrected Proof,
- Iversen, V., Mohaupt, J., Drews, A., Lesjean, B., Kraume, M., 2008. Side effects of flux enhancing chemicals in membrane bioreactors (MBRs): study on their biological toxicity and their residual fouling propensity. *Water Science and Technology* 57, 117-123.

- Jahren, S. J., Rintala, J. A., Odegaard, H., 2002. Aerobic moving bed biofilm reactor treating thermomechanical pulping whitewater under thermophilic conditions. *Water Res* 36, 1067-1075.
- Jahren, S. J., Rintala, J. A., Odegaard, H., 1999. Anaerobic thermophilic (55 ° C) treatment of TMP whitewater in reactors based on biomass attachment and entrapment. *Water Science and Technology* 40, 67-75.
- Jeison, D. (2007). Anaerobic membrane bioreactors for wastewater treatment Wageningen, The Netherlands, Wageningen University. Ph.D.
- Jeison, D., van Lier, J. B., 2007. Cake formation and consolidation: Main factors governing the applicable flux in anaerobic submerged membrane bioreactors (AnSMBR) treating acidified wastewaters. *Separation and Purification Technology* 56, 71-78.
- Ji, J., Qiu, J., Wong, F.-s., Li, Y., 2008. Enhancement of filterability in MBR achieved by improvement of supernatant and floc characteristics via filter aids addition. *Water Research* 42, 3611-3622.
- Ji, L., Zhou, J., 2006. Influence of aeration on microbial polymers and membrane fouling in submerged membrane bioreactors. *Journal of Membrane Science* 276, 168-177.
- Jinhua, P., Fukushi, K., Yamamoto, K., 2006. Bacterial Community Structure on Membrane Surface and Characteristics of Strains Isolated from Membrane Surface in Submerged Membrane Bioreactor. *Separation Science and Technology* 41, 1527 - 1549.
- Jirachote Phattaranawik, A. G. F., Audrey C. S. Pasquier, Wu Bing,, 2007. Membrane bioreactor with bubble-size transformer: Design and fouling control. *Environmental and Energy Engineering* 53, 243-248.
- Judd, S., 2006. *The MBR book: principles and applications of membrane bioreactors in water and wastewater treatment*, Elsevier Ltd.,
- Kang, S., Hoek, E. M. V., Choi, H., Shin, H., 2006. Effect of Membrane Surface Properties During the Fast Evaluation of Cell Attachment. *Separation Science and Technology* 41, 1475 - 1487.

- Kantardjieff, A., Jones, J. P., 1997. Practical experiences with aerobic biofilters in TMP (thermomechanical pulping), sulfite and fine paper mills in Canada. *Water Science and Technology* 35, 227-234.
- Khalili-Garakani, A., Mehrnia, M. R., Mostoufi, N., Sarrafzadeh, M. H., 2011. Analyze and control fouling in an airlift membrane bioreactor: CFD simulation and experimental studies. *Process Biochemistry* 46, 1138-1145.
- Khan, S. J., Visvanathan, C., 2008. Influence of mechanical mixing intensity on a biofilm structure and permeability in a membrane bioreactor. *Desalination* 231, 253-267.
- Kim, J.-S., Lee, C.-H., Chang, I.-S., 2001. Effect of pump shear on the performance of a crossflow membrane bioreactor. *Water Research* 35, 2137-2144.
- Kimura, K., Yamato, N., Yamamura, H., Watanabe, Y., 2005. Membrane Fouling in Pilot-Scale Membrane Bioreactors (MBRs) Treating Municipal Wastewater. *Environmental science and technology* 39, 6293-6299.
- Koseoglu-Imer, D. Y., Dizge, N., Karagunduz, A., Keskinler, B., 2011. Influence of membrane fouling reducers (MFRs) on filterability of disperse mixed liquor of Jet Loop Bioreactors. *Bioresource Technology* 102, 6843-6849.
- Koseoglu, H., Yigit, N. O., Iversen, V., Drews, A., Kitis, M., Lesjean, B., Kraume, M., 2008. Effects of several different flux enhancing chemicals on filterability and fouling reduction of membrane bioreactor (MBR) mixed liquors. *Journal of Membrane Science* 320, 57-64.
- Kostamo, A., Holmbom, B., Kukkonen, J. V. K., 2004. Fate of wood extractives in wastewater treatment plants at kraft pulp mills and mechanical pulp mills. *Water Research* 38, 972-982.
- Kraemer, H. E. (2002). Characterization of microbial aggregates in relation to membrane biofouling in submerged membrane bioreactors. Toronto, Canada, Ryerson University. MSc Thesis.
- Kromkamp, J., Faber, F., Schroen, K., Boom, R., 2006. Effects of particle size segregation on crossflow microfiltration performance: Control mechanism for concentration polarisation and particle fractionation. *Journal of Membrane Science* 268, 189-197.

- Laari, A., Korhonen, S., Kallas, J., Tuhkanen, T., 2000. Selective Removal of Lipophilic Wood Extractives from Paper Mill Water Circulations by Ozonation. *Ozone: Science & Engineering: The Journal of the International Ozone Association* 22, 585 - 605.
- Laari, A., Korhonen, S., Tuhkanen, T., Verenich, S., Kallas, J., 1999. Ozonation and wet oxidation in the treatment of thermomechanical pulp (TMP) circulation waters. *Water Science and Technology* 40, 51-58.
- Laitinen, N., Luonsi, A., Vilen, J., 2006. Landfill leachate treatment with sequencing batch reactor and membrane bioreactor. *Desalination* 191, 86-91.
- Laspidou, C. S., Rittmann, B. E., 2002. A unified theory for extracellular polymeric substances, soluble microbial products, and active and inert biomass. *Water Research* 36, 2711-2720.
- Le-Clech, P., Chen, V., Fane, T. A. G., 2006. Fouling in membrane bioreactors used in wastewater treatment. *Journal of Membrane Science* 284, 17-53.
- Le-Clech, P., Marselina, Y., Ye, Y., Stuetz, R. M., Chen, V., 2007. Visualisation of polysaccharide fouling on microporous membrane using different characterisation techniques. *Journal of Membrane Science* 290, 36-45.
- Le Clech, P., Jefferson, B., Chang, I. S., Judd, S. J., 2003. Critical flux determination by the flux-step method in a submerged membrane bioreactor. *Journal of Membrane Science* 227, 81-93.
- Lee, C. H., Park, P. K., Lee, W. N., Hwang, B. K., Hong, S. H., Yeon, K. M., Oh, H. S., Chang, I. S., 2008. Correlation of biofouling with the bio-cake architecture in an MBR. *Desalination* 231, 115-123.
- Lee, J., Ahn, W.-Y., Lee, C.-H., 2001. Comparison of the filtration characteristics between attached and suspended growth microorganisms in submerged membrane bioreactor. *Water Research* 35, 2435-2445.
- Lee, J. W., Peterson, D. L., Stickney, A. R., 1989. Anaerobic treatment of pulp and paper mill wastewaters. *Environmental Progress* 8, 73-87.

- Lee, M., Kim, J., 2009. Membrane autopsy to investigate CaCO₃ scale formation in pilot-scale, submerged membrane bioreactor treating calcium-rich wastewater. *Journal of Chemical Technology and Biotechnology* 84, 1397-1404.
- Lee, W.-N., Chang, I.-S., Hwang, B.-K., Park, P.-K., Lee, C.-H., Huang, X., 2007. Changes in biofilm architecture with addition of membrane fouling reducer in a membrane bioreactor. *Process Biochemistry* 42, 655-661.
- Lerner, M., Stahl, N., Galil, N. I., 2007. Comparative study of MBR and activated sludge in the treatment of paper mill wastewater. *Water Science and Technology* 55, 23-29.
- Li, H., Fane, A. G., Coster, H. G. L., Vigneswaran, S., 2003. Observation of deposition and removal behaviour of submicron bacteria on the membrane surface during crossflow microfiltration. *Journal of Membrane Science* 217, 29-41.
- Li, X. Y., Yang, S. F., 2007. Influence of loosely bound extracellular polymeric substances (EPS) on the flocculation, sedimentation and dewaterability of activated sludge. *Water Research* 41, 1022-1030.
- Liao, B.-Q., Kraemer, J. T., Bagley, D. M., 2006. Anaerobic Membrane Bioreactors: Applications and Research Directions. *Critical Reviews in Environmental Science and Technology* 36, 489 - 530.
- Liao, B. Q., Bagley, D. M., Kraemer, H. E., Leppard, G. G., Liss, S. N., 2004. A review of biofouling and its control in membrane separation bioreactors. *Water Environment Research* 76, 425-436.
- Liao, B. Q., Xie, K., Lin, H. J., Bertoldo, D., 2010. Treatment of kraft evaporator condensate using a thermophilic submerged anaerobic membrane bioreactor. *Water Science and Technology* 61, 2177-2183.
- Lin, H., Gao, W., Meng, F., Liao, B., Leung, K.-T., Zhao, L., Chen, J., Hong, H., 2010. Membrane Bioreactors for Industrial Wastewater Treatment: A Critical Review. *Critical Reviews in Environmental Science and Technology* Accept.
- Lin, H. J., Xie, K., Mahendran, B., Bagley, D. M., Leung, K. T., Liss, S. N., Liao, B. Q., 2009. Sludge properties and their effects on membrane fouling in submerged anaerobic membrane bioreactors (SAnMBRs). *Water Research* 43, 3827-3837.

- Liu, T., Chen, Z.-l., Yu, W.-z., You, S.-j., 2011. Characterization of organic membrane foulants in a submerged membrane bioreactor with pre-ozonation using three-dimensional excitation-emission matrix fluorescence spectroscopy. *Water Research* 45, 2111-2121.
- Liu, Y., Fang, H. H. P., 2003. Influences of Extracellular Polymeric Substances (EPS) on Flocculation, Settling, and Dewatering of Activated Sludge. *Critical Reviews in Environmental Science and Technology* 33, 237-273.
- Lyko, S., Wintgens, T., Al-Halbouni, D., Baumgarten, S., Tacke, D., Drensla, K., Janot, A., Dott, W., Pinnekamp, J., Melin, T., 2008. Long-term monitoring of a full-scale municipal membrane bioreactor--Characterisation of foulants and operational performance. *Journal of Membrane Science* 317, 78-87.
- Madsen, E. L., 2008. *Environmental microbiology: from genomes to biogeochemistry*, Blackwell publishing Ltd., Malden, USA.
- Magnus, E., Carlberg, G. E., Hoel, H., 2000a. TMP wastewater treatment, including a biological high-efficiency compact reactor: Removal and characterization of organic components. *NORD PULP PAP RES J.* 15, 29-36.
- Magnus, E., Carlberg, G. E., Norske, H. H., 2000b. TMP wastewater treatment, including a biological high-efficiency compact reactor: Toxicity reduction and removal of extractives. *NORD PULP PAP RES J.* 15, 37-45.
- Mahmood, T., Elliott, A., 2006. A review of secondary sludge reduction technologies for the pulp and paper industry. *Water Research* 40, 2093-2112.
- Mascolo, G., Laera, G., Pollice, A., Cassano, D., Pinto, A., Salerno, C., Lopez, A., 2010. Effective organics degradation from pharmaceutical wastewater by an integrated process including membrane bioreactor and ozonation. *Chemosphere* 78, 1100-1109.
- McAdam, E. J., Judd, S. J., Cartmell, E., Jefferson, B., 2007. Influence of substrate on fouling in anoxic immersed membrane bioreactors. *Water Research* 41, 3859-3867.

- Meng, F., Chae, S.-R., Drews, A., Kraume, M., Shin, H.-S., Yang, F., 2009. Recent advances in membrane bioreactors (MBRs): Membrane fouling and membrane material. *Water Research* 43, 1489-1512.
- Meng, F., Liao, B., Liang, S., Yang, F., Zhang, H., Song, L., 2010. Morphological visualization, componential characterization and microbiological identification of membrane fouling in membrane bioreactors (MBRs). *Journal of Membrane Science* 361, 1-14.
- Meng, F., Yang, F., 2007. Fouling mechanisms of deflocculated sludge, normal sludge, and bulking sludge in membrane bioreactor. *Journal of Membrane Science* 305, 48-56.
- Meng, F., Yang, F., Shi, B., Zhang, H., 2008. A comprehensive study on membrane fouling in submerged membrane bioreactors operated under different aeration intensities. *Separation and Purification Technology* 59, 91-100.
- Menniti, A., Morgenroth, E., 2010. The influence of aeration intensity on predation and EPS production in membrane bioreactors. *Water Research* 44, 2541-2553.
- Min, K. N., Ergas, S. J., Mermelstein, A., 2008. Impact of dissolved oxygen concentration on membrane filtering resistance and soluble organic matter characteristics in membrane bioreactors. *Water Science and Technology* 57, 161-165.
- Minami, K., 1994. A trial of high performance anaerobic treatment on wastewater from a kraft pulp mill. *Desalination* 98, 273-283.
- Minami, K., Okamura, K., Ogawa, S., Naritomi, T., 1991. Continuous anaerobic treatment of wastewater from a kraft pulp mill. *Journal of Fermentation and Bioengineering* 71, 270-274.
- Miura, Y., Watanabe, Y., Okabe, S., 2007. Membrane Biofouling in Pilot-Scale Membrane Bioreactors (MBRs) Treating Municipal Wastewater: Impact of Biofilm Formation. *Environmental science and technology* 41, 632-638.
- Nagaoka, H., Ueda, S., Miya, A., 1996. Influence of bacterial extracellular polymers on the membrane separation activated sludge process. *Water Science and Technology* 34, 165-172.

- Nelson, M. I., Chen, X. D., Sidhu, H. S. (2008). Reducing the Emission of Pollutants in Industrial Wastewater through the Use of Membrane Bioreactors: 95-107.
- Ng, A. N. L., Kim, A. S., 2007. A mini-review of modeling studies on membrane bioreactor (MBR) treatment for municipal wastewaters. *Desalination* 212, 261-281.
- Ng, C. A., Sun, D., Fane, A. G., 2006a. Operation of Membrane Bioreactor with Powdered Activated Carbon Addition. *Separation Science and Technology* 41, 1447 - 1466.
- Ng, H. Y., Tan, T. W., Ong, S. L., 2006b. Membrane fouling of submerged membrane bioreactors: impact of mean cell residence time and the contributing factors. *Environmental Science and Technology* 40, 2706-2713.
- Ng, H. Y., Tan, T. W., Ong, S. L., Toh, C. A., Loo, Z. P., 2006c. Effects of solid retention time on the performance of submerged anoxic/oxic membrane bioreactor. *Water Science and Technology* 53, 7-13.
- Ognier, S., Wisniewski, C., Grasmick, A., 2002. Membrane fouling during constant flux filtration in membrane bioreactors. *Membrane Technology* 2002, 6-10.
- Patsios, S. I., Karabelas, A. J., 2011. An investigation of the long-term filtration performance of a membrane bioreactor (MBR): The role of specific organic fractions. *Journal of Membrane Science* 372, 102-115.
- Pendashteh, A. R., Fakhru'l-Razi, A., Madaeni, S. S., Abdullah, L. C., Abidin, Z. Z., Biak, D. R. A., 2011. Membrane foulants characterization in a membrane bioreactor (MBR) treating hypersaline oily wastewater. *Chemical Engineering Journal* 168, 140-150.
- Phattaranawik, J., Leiknes, T., 2011. Extractive biofilm membrane bioreactor with energy recovery from excess aeration and new membrane fouling control. *Bioresource Technology* 102, 2301-2307.
- Pokhrel, D., Viraraghavan, T., 2004. Treatment of pulp and paper mill wastewater--a review. *Science of The Total Environment* 333, 37-58.
- Prieske, H., Drews, A., Kraume, M., 2008. Prediction of the circulation velocity in a membrane bioreactor. *Desalination* 231, 219-226.

- Ragona, C. S. F., Hall, E. R., 1998. Parallel operation of ultrafiltration and aerobic membrane bioreactor treatment systems for mechanical newsprint mill whitewater at 55 [deg]C. *Water Science and Technology* 38, 307-314.
- Rajeshwari, K. V., Balakrishnan, M., Kansal, A., Lata, K., Kishore, V. V. N., 2000. State-of-the-art of anaerobic digestion technology for industrial wastewater treatment. *Renewable and Sustainable Energy Reviews* 4, 135-156.
- Ramesh, A., Lee, D. J., Lai, J. Y., 2007. Membrane biofouling by extracellular polymeric substances or soluble microbial products from membrane bioreactor sludge. *Applied Microbiology and Biotechnology* 74, 699-707.
- Rintala, J. A., Lepistö, S. S., 1992. Anaerobic treatment of thermomechanical pulping whitewater at 35-70°C. *Water Research* 26, 1297-1305.
- Rintala, J. A., Puhakka, J. A., 1994. Anaerobic treatment in pulp- and paper-mill waste management: A review. *Bioresource Technology* 47, 1-18.
- Roest, K., Heilig, H. G. H. J., Smidt, H., de Vos, W. M., Stams, A. J. M., Akkermans, A. D. L., 2005. Community analysis of a full-scale anaerobic bioreactor treating paper mill wastewater. *Systematic and Applied Microbiology* 28, 175-185.
- Rosenberger, S., Evenblij, H., te Poele, S., Wintgens, T., Laabs, C., 2005. The importance of liquid phase analyses to understand fouling in membrane assisted activated sludge processes--six case studies of different European research groups. *Journal of Membrane Science* 263, 113-126.
- Saaymunt, G. B., Schutte, C. F., van Leeuwen, J., 1996. The effect of chemical bulking control on biological nutrient removal in a full scale activated sludge plant. *Water Science and Technology* 34, 275-282.
- Sainbayar, A., Kim, J. S., Jung, W. J., Lee, Y. S., Lee, C. H., 2001. Application of Surface Modified Polypropylene Membranes to an Anaerobic Membrane Bioreactor. *Environmental Technology* 22, 1035 - 1042.
- Salazar-Peláez, M. L., Morgan-Sagastume, J. M., Noyola, A., Influence of hydraulic retention time on fouling in a UASB coupled with an external ultrafiltration membrane treating synthetic municipal wastewater. *Desalination In Press, Corrected Proof*,

- Satyawali, Y., Balakrishnan, M., 2009. Effect of PAC addition on sludge properties in an MBR treating high strength wastewater. *Water Research* 43, 1577-1588.
- Sheng, G.-P., Yu, H.-Q., 2006. Characterization of extracellular polymeric substances of aerobic and anaerobic sludge using three-dimensional excitation and emission matrix fluorescence spectroscopy. *Water Research* 40, 1233-1239.
- Shere, S. M., Daly, P. G., 1982. High Rate Biological Treatment of TMP Effluent Pulp and Paper Canada 83, 62-66.
- Shin, J.-H., Lee, S.-M., Jung, J.-Y., Chung, Y.-C., Noh, S.-H., 2005. Enhanced COD and nitrogen removals for the treatment of swine wastewater by combining submerged membrane bioreactor (MBR) and anaerobic upflow bed filter (AUBF) reactor. *Process Biochemistry* 40, 3769-3776.
- Simmons, F. J., Kuo, D. H. W., Xagorarakis, I., 2011. Removal of human enteric viruses by a full-scale membrane bioreactor during municipal wastewater processing. *Water Research* 45, 2739-2750.
- Sjöström, E., 1993. *Wood chemistry, fundamentals and applications*, 2nd. Academic Press, New York.
- Slade, A. H., Anderson, S. M., Evans, B. G., 2003. Nitrogen fixation in the activated sludge treatment of thermomechanical pulping wastewater: effect of dissolved oxygen. *Water Science and Technology* 48, 1-8.
- Song, K.-G., Kim, Y., Ahn, K.-H., 2008. Effect of coagulant addition on membrane fouling and nutrient removal in a submerged membrane bioreactor. *Desalination* 221, 467-474.
- Stephenson, T., Judd, S., Jefferson, B., Brindle, K., 2000. *Membrane bioreactors for wastewater treatment*, IWA Publishing, London, UK.
- Subramani, A., Huang, X., Hoek, E. M. V., 2009. Direct observation of bacterial deposition onto clean and organic-fouled polyamide membranes. *Journal of Colloid and Interface Science* 336, 13-20.
- Sui, P., Wen, X., Huang, X., 2008. Feasibility of employing ultrasound for on-line membrane fouling control in an anaerobic membrane bioreactor. *Desalination* 219, 203-213.

- Sun, F.-y., Wang, X.-m., Li, X.-y., 2011. Effect of biopolymer clusters on the fouling property of sludge from a membrane bioreactor (MBR) and its control by ozonation. *Process Biochemistry* 46, 162-167.
- Sundholm, J., 1999. *Mechanical Pulping*. Papermaking Science and Technology, Fapet Oy Published,, Helsinki, Finland.
- Tardieu, E., Grasmick, A., Geaugey, V., Manem, J., 1998. Hydrodynamic control of bioparticle deposition in a MBR applied to wastewater treatment. *Journal of Membrane Science* 147, 1-12.
- Tardif, O., Hall, E. R., 1997. Alternatives for treating recirculated newsprint whitewater at high temperatures. *Water Science and Technology* 35, 57-65.
- Teychene, B., Guigui, C., Cabassud, C., 2011. Engineering of an MBR supernatant fouling layer by fine particles addition: A possible way to control cake compressibility. *Water Research* 45, 2060-2072.
- Teychene, B., Guigui, C., Cabassud, C., Amy, G., 2008. Toward a better identification of foulant species in MBR processes. *Desalination* 231, 27-34.
- Thompson, G., Swain, J., Kay, M., Forster, C. F., 2001. The treatment of pulp and paper mill effluent: a review. *Bioresource Technology* 77, 275-286.
- Tian, J.-y., Chen, Z.-l., Yang, Y.-l., Liang, H., Nan, J., Li, G.-b., 2010. Consecutive chemical cleaning of fouled PVC membrane using NaOH and ethanol during ultrafiltration of river water. *Water Research* 44, 59-68.
- Tian, J. Y., Liang, H., Li, X., You, S. J., Tian, S., Li, G. B., 2008. Membrane coagulation bioreactor (MCBR) for drinking water treatment. *Water Res*
- Tian, Y., Chen, L., Zhang, S., Zhang, S., 2011. A systematic study of soluble microbial products and their fouling impacts in membrane bioreactors. *Chemical Engineering Journal* 168, 1093-1102.
- Tiranuntakul, M., Schneider, P. A., Jegatheesan, V., 2011. Assessments of critical flux in a pilot-scale membrane bioreactor. *Bioresource Technology* 102, 5370-5374.
- Trussell, R. S., Merlo, R. P., Hermanowicz, S. W., Jenkins, D., 2006. The effect of organic loading on process performance and membrane fouling in a submerged

- membrane bioreactor treating municipal wastewater. *Water Research* 40, 2675-2683.
- Ueda, T., Hata, K., Kikuoka, Y., 1996. Treatment of domestic sewage from rural settlements by a membrane bioreactor. *Water Science and Technology* 34, 189-196.
- Wan, C.-Y., De Wever, H., Diels, L., Thoeye, C., Liang, J.-B., Huang, L.-N., 2011. Biodiversity and population dynamics of microorganisms in a full-scale membrane bioreactor for municipal wastewater treatment. *Water Research* 45, 1129-1138.
- Wang, F., Tarabara, V. V., 2008. Pore blocking mechanisms during early stages of membrane fouling by colloids. *Journal of Colloid and Interface Science* 328, 464-469.
- Wang, X.-M., Li, X.-Y., Huang, X., 2007. Membrane fouling in a submerged membrane bioreactor (SMBR): Characterisation of the sludge cake and its high filtration resistance. *Separation and Purification Technology* 52, 439-445.
- Wang, Z., Wu, Z., Tang, S., 2009. Extracellular polymeric substances (EPS) properties and their effects on membrane fouling in a submerged membrane bioreactor. *Water Research* 43, 2504-2512.
- Wei, C.-H., Huang, X., Ben Aim, R., Yamamoto, K., Amy, G., 2011. Critical flux and chemical cleaning-in-place during the long-term operation of a pilot-scale submerged membrane bioreactor for municipal wastewater treatment. *Water Research* 45, 863-871.
- Welander, T., Löfgvist, A., Selmer, A., 1997. Upgrading aerated lagoons at pulp and paper mills. *Water Science and Technology* 35, 117-122.
- Wijekoon, K. C., Visvanathan, C., Abeynayaka, A., 2011. Effect of organic loading rate on VFA production, organic matter removal and microbial activity of a two-stage thermophilic anaerobic membrane bioreactor. *Bioresource Technology* 102, 5353-5360.

- Wilén, B.-M., Onuki, M., Hermansson, M., Lumley, D., Mino, T., 2008. Microbial community structure in activated sludge floc analysed by fluorescence in situ hybridization and its relation to floc stability. *Water Research* 42, 2300-2308.
- Wiszniewski, J., Ziembinska, A., Ciesielski, S., 2011. Removal of petroleum pollutants and monitoring of bacterial community structure in a membrane bioreactor. *Chemosphere* 83, 49-56.
- Wu, B., Yi, S., Fane, A. G., 2011. Microbial behaviors involved in cake fouling in membrane bioreactors under different solids retention times. *Bioresource Technology* 102, 2511-2516.
- Wu, J., Chen, F., Huang, X., Geng, W., Wen, X., 2006. Using inorganic coagulants to control membrane fouling in a submerged membrane bioreactor. *Desalination* 197, 124-136.
- Wu, S. C., Lee, C. M., 2011. Correlation between fouling propensity of soluble extracellular polymeric substances and sludge metabolic activity altered by different starvation conditions. *Bioresource Technology* 102, 5375-5380.
- Xie, K., Lin, H. J., Mahendran, B., Bagley, D. M., Leung, K. T., Liss, S. N., Liao, B. Q., 2010. Performance and fouling characteristics of a submerged anaerobic membrane bioreactor for kraft evaporator condensate treatment. *Environmental Technology* 31, 511-521.
- Xu, M., Wen, X., Yu, Z., Li, Y., Huang, X., 2011. A hybrid anaerobic membrane bioreactor coupled with online ultrasonic equipment for digestion of waste activated sludge. *Bioresource Technology* 102, 5617-5625.
- Yang, S., Yang, F., Fu, Z., Wang, T., Lei, R., 2010. Simultaneous nitrogen and phosphorus removal by a novel sequencing batch moving bed membrane bioreactor for wastewater treatment. *Journal of Hazardous Materials* 175, 551-557.
- Yang, W., Cicek, N., Ilg, J., 2006. State-of-the-art of membrane bioreactors: Worldwide research and commercial applications in North America. *Journal of Membrane Science* 270, 201-211.

- Yigit, N. O., Civelekoglu, G., Harman, I., Koseoglu, H., Kitis, M., 2009. Effects of various backwash scenarios on membrane fouling in a membrane bioreactor. *Desalination* 237, 346-356.
- Yu, H.-Y., Xie, Y.-J., Hu, M.-X., Wang, J.-L., Wang, S.-Y., Xu, Z.-K., 2005. Surface modification of polypropylene microporous membrane to improve its antifouling property in MBR: CO₂ plasma treatment. *Journal of Membrane Science* 254, 219-227.
- Yu, S.-l., Zhao, F.-b., Zhang, X.-h., Jing, G.-l., Zhen, X.-h., Effect of components in activated sludge liquor on membrane fouling in a submerged membrane bioreactor. *Journal of Environmental Sciences* 18, 897-902.
- Yun, M.-A., Yeon, K.-M., Park, J.-S., Lee, C.-H., Chun, J., Lim, D. J., 2006. Characterization of biofilm structure and its effect on membrane permeability in MBR for dye wastewater treatment. *Water Research* 40, 45-52.
- Zahid, W. M., El-Shafai, S. A., 2011. Use of cloth-media filter for membrane bioreactor treating municipal wastewater. *Bioresource Technology* 102, 2193-2198.
- Zhang, H.-f., Sun, B.-s., Zhao, X.-h., Gao, Z.-h., 2008. Effect of ferric chloride on fouling in membrane bioreactor. *Separation and Purification Technology* 63, 341-347.
- Zhang, H., Xia, J., Yang, Y., Wang, Z., Yang, F., 2009a. Mechanism of calcium mitigating membrane fouling in submerged membrane bioreactors. *Journal of Environmental Sciences* 21, 1066-1073.
- Zhang, J., Chua, H. C., Zhou, J., Fane, A. G., 2006. Factors affecting the membrane performance in submerged membrane bioreactors. *Journal of Membrane Science* 284, 54-66.
- Zhang, J., Zhou, J., Liu, Y., Fane, A. G., 2010. A comparison of membrane fouling under constant and variable organic loadings in submerge membrane bioreactors. *Water Research* 44, 5407-5413.
- Zhang, K., Cui, Z., Field, R. W., 2009b. Effect of bubble size and frequency on mass transfer in flat sheet MBR. *Journal of Membrane Science* 332, 30-37.
- Zhang, Y., Ma, C., Ye, F., Kong, Y., Li, H., 2009c. The treatment of wastewater of paper mill with integrated membrane process. *Desalination* 236, 349-356.

- Zhou, J., Yang, F.-l., Meng, F.-g., An, P., Wang, D., 2007. Comparison of membrane fouling during short-term filtration of aerobic granular sludge and activated sludge. *Journal of Environmental Sciences* 19, 1281-1286.
- Zhu, X., Wang, Z., Wu, Z., 2011. Characterization of membrane foulants in a full-scale membrane bioreactor for supermarket wastewater treatment. *Process Biochemistry* 46, 1001-1009.

Chapter 3 Influence of elevated pH shocks on the performance of a submerged anaerobic membrane bioreactor

Adapted from the publication:

W.J. Gao, H.J. Lin, K.T. Leung and B.Q. Liao. Influence of elevated pH shocks on the performance of a submerged anaerobic membrane bioreactor. *Process Biochemistry*, 2010, 45(8):1279-1287.

Abstract:

The effects of elevated pH shocks on the performance and membrane fouling of a submerged anaerobic membrane bioreactor (SAnMBR) treating thermomechanical pulping whitewater was studied over a 120-day period. Changes in chemical oxygen demand (COD) removal, biogas production, sludge and cake layer properties, and their correlations to membrane fouling – before and after pH shocks – were systematically studied using various analytical tools. The results showed that a pH 8.0 shock had a minor impact, while pH 9.1 and 10.0 shocks exerted significant long-lasting negative impacts on COD removal, biogas production and membrane filtration performance of the SAnMBR. When the normal pH (7.0) was resumed, it took approximately 1, 6, and 30 days for the performance to recover for pH 8.0, 9.1 and 10.0 shocks, respectively. The elevated pH shocks induced the dispersion of sludge flocs and resulted in the accumulation of colloids and solutes or biopolymers in the sludge suspension, and thus deteriorated membrane performance. Statistical analysis showed that the ratio of proteins to polysaccharides (PN/PC) in extracellular polymeric substances (EPS) had a strongly negative effect on the membrane fouling rate. There were smaller size particles deposited on the membrane surface and a more compact and denser cake layer was formed after being exposed to an alkaline shock at pH 10, resulting in higher membrane fouling rates.

3.1 Introduction

In anaerobic bioreactors, biomass retention is of significant importance since it decouples solids retention time (SRT) from hydraulic retention time (HRT), making biomass concentration independent of the low-growth rates of methanogenic consortia. A complete retention of all microorganisms in the bioreactor, including slow-growing anaerobic microorganisms, can be achieved in anaerobic membrane bioreactors (AnMBRs) by the use of micro or ultra-filtration membrane modules. In recent years, considerable effort has been focused on the development of a submerged anaerobic membrane bioreactor (SAnMBR) that employs membranes submerged in an anaerobic reactor. The advantages of the SAnMBR system over conventional anaerobic digestion have been well-documented in the literature that indicates it has excellent effluent quality, low sludge production, high-treatment efficiency, a small footprint, net energy production, low energy consumption and gentle mixing (Wen et al., 1999; Liao et al., 2006; Jeison and van Lier, 2007; Akram and Stuckey, 2008; Lin et al., 2009).

Anaerobic digestion is a complex process and is greatly influenced by many factors. These factors include wastewater specificity, HRT, influent organic concentration, organic loading rate, pH, temperature and nutritional requirements, etc. Among these factors, pH variation has been reported to greatly influence the microbial metabolism including utilization of carbon and energy sources, efficiency of substrate degradation, synthesis of proteins and various types of storage materials, and release of metabolic products from cells (Baily and Ollis, 1986). Moreover, pH variation can also affect cell morphology and structure and, therefore, flocculation and adhesion phenomena (Gottschalk, 1986). The optimum pH for anaerobic digestion appears to be 6–8 (Ward et al., 2008). Some studies were carried out on the effect of acidic pH on the anaerobic digestion system (Yu and Fang, 2003), but little attention has been paid to the impact of alkaline conditions on the system's performance. In practice, a number of industrial wastewaters, including brewery effluent (Rao et al., 2007), fish condensate (Sandberg and Ahring, 1992), petroleum wastewater (Rajganesh et al., 1995) and kraft wood pulping effluent (Van Tran, 2008), are alkaline. The combination of various wastewater streams with different pH values and fluctuation in temperature in an integrated plant will

result in changes in pH with time and cause pH shocks in downstream biological treatment system (Sipma et al., 2010). In addition, incidental pH shocks may also occur, due to the failure of pH control systems. Therefore, it is highly desirable to understand the impact of elevated pH shocks on the performance of anaerobic bioreactors. However, fewer studies have dealt with the impact of alkaline conditions on the anaerobic digestion system performance.

For membrane bioreactor systems, membrane fouling remains the principal obstacle constraining their extensive applications (Huang et al., 2000; Lee et al., 2003; Han et al., 2005; Lin et al., 2009). Sludge properties, including particle size, extracellular polymeric substances (EPS) and soluble microbial products (SMPs), are identified to play an important role in controlling membrane fouling (Huang et al., 2000; Chang and Kim, 2005; Akram and Stuckey, 2008; Lin et al., 2009). It is well known that sludge properties are affected by operating and environmental conditions (Chang and Kim, 2005; Han et al., 2005; Lin et al., 2009). Therefore, a change in operating and/or environmental conditions in SAnMBRs may lead to changes in sludge properties and membrane fouling behaviour. Although effects of sludge properties on membrane fouling have been studied (Huang et al., 2000; Lee et al., 2003; Li et al., 2008; Lin et al., 2009), there is no report yet on the effect of the elevated pH shock on anaerobic sludge properties and thus membrane fouling. Furthermore, pH shocks may also affect membrane functions directly. A change in pH will affect membrane morphology, surface charge and the pore structure of membranes, and thus membrane filtration (Dong et al., 2006; Nanda et al., 2010; Tadkaew et al., 2010). Detailed knowledge of the influence of elevated pH shocks on anaerobic sludge properties, membrane performance, and membrane fouling will facilitate the development of membrane fouling control measures and optimize operational parameters in SAnMBRs.

The objective of this study was to investigate the impact of elevated pH shocks on chemical oxygen demand (COD) removal, biogas production, the behaviour of membrane fouling, sludge and cake layer properties, and their correlations to membrane fouling in a SAnMBR system.

3.2 Materials and methods

3.2.1 Experimental setup and operation

A schematic diagram of the experimental setup used for this study is shown in Fig. 3-1. The SAnMBR has a volume of 10 L and is composed of a bottom zone (3.5 L) and a top zone (6.5 L). A flat sheet microfiltration membrane module (0.03 m², 10 cm × 15 cm on each of the two sides of the module) was submerged in the top zone of the reactor. The bottom zone was used as the sludge blanket. All membranes used in this study were made of polyvinylidene fluoride (PVDF) materials using the phase inversion method. The molecular weight cut off (MWCO) was characterized as 70,000 Da. At the base of the membrane module, a stainless steel tube diffuser was located and headspace biogas was recirculated by a gas recycle pump (Masterflex Console Drive, Model 7520-40, Thermo Fisher Scientific, USA) (0.75 x 2 L/min) to provide mixing and to control solids deposition over the membrane surface. The gas sparging rate was maintained at 0.75 x 2 L/min (LPM). The seeded sludge was obtained from an upflow anaerobic sludge blanket (UASB) reactor treating pulping wastewater at Tembec Industries Inc. (Temiscaming, Quebec). A magnetic stirrer (Thermolyne Cimarec, Model S47030) was located at the bottom of the reactor to provide necessary mixing to the sludge liquor. The temperature was maintained constant at 37 ± 1 °C by circulating warm water through the water jacket of the reactor. The pH was automatically adjusted to 7.0 ± 0.2 by a pH regulation pump and a pH electrode (Thermo Scientific, Beverly, MA) using 0.1M NaOH solution. The biogas production was monitored with a water displacement gas collector.

Thermomechanical pulping whitewater from a local pulp and paper mill was pumped into the bottom of the bioreactor automatically by a feeding pump (Masterflex Model 7520-50, Barnant Co., USA), which is controlled by a level sensor (Madison Co., USA), and controller (Flowline, USA). Macro-nutrients, nitrogen (NH₄Cl) and phosphorus (KH₂PO₄) were fed in a proportion of COD:N:P of 100:2.6:0.4 to sustain the nutrient concentrations required for biomass growth in an anaerobic environment (Vogelaar et al., 2002). To prevent trace metal limitations of the methanogens, a trace element solution (Welandar et al., 1999) was supplemented to the influent. The filtrate

was intermittently obtained by using a peristaltic pump (Masterflex, C/L, Model 77120-70, Barnant Co., USA) operating in the mode of 4min on and 1min off. Membrane flux was controlled by adjusting the pump speed and two calibrations were made each day. When the trans-membrane pressure (TMP) reached 30 kPa, the reactor was shut down and a physical cleaning procedure was conducted. Physical cleaning was carried out by scraping off the cake layer on the membrane surface carefully by using a plastic sheet followed by wiping and rinsing the membrane surfaces with a soft sponge and tap water, respectively. Usually, physical cleaning was performed 15-20 times for each membrane until its performance was deteriorated and was then replaced by a new membrane. During the operation of the reactors, no sludge was discharged except for sludge sampling and sludge cake characterization. This corresponded to an SRT of approximately 280 days.

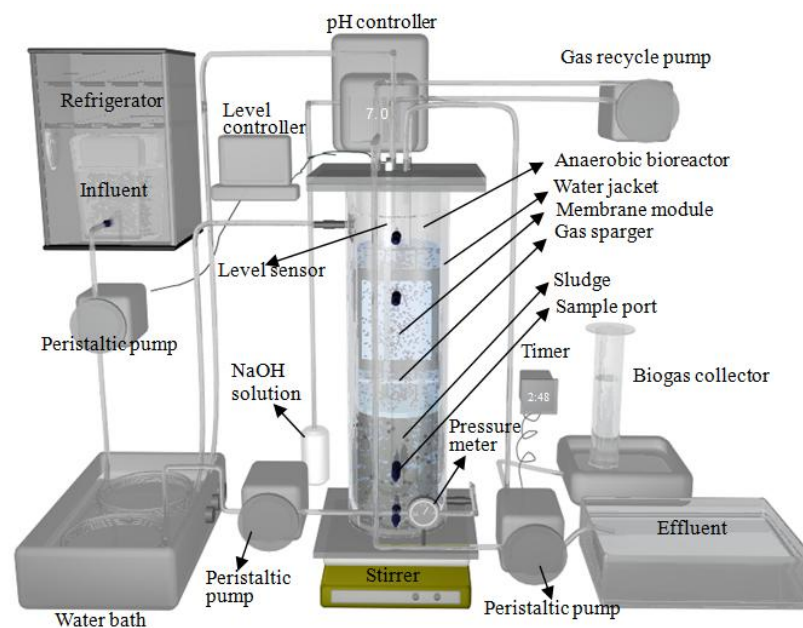


Figure 3-1 Schematic of the anaerobic submerged membrane bioreactor and experimental setup.

The operation of the reactor system was divided into five phases: Phase 1 (0–21st day) can be characterized as the start-up period; Phase 2 (22nd–33rd day) is the steady period; in Phase 3 (34th–42nd day), Phase 4 (43rd–63rd day) and Phase 5 (64th–120th day),

the reactor was exposed to pH 8.0, 9.1 and 10.0 shock, respectively. pH shocks were achieved by pumping excess amount of NaOH solution into the SAnMBR.

3.2.2 Analytical methods

COD removal efficiency, biogas production rate, sludge and cake properties and their correlations to membrane fouling - before and after pH shocks - were systematically characterized. The sampling time frame for the comparisons of sludge properties was within two weeks before and after each pH shock and was summarized in Table 3-1. Detailed methodology is given below.

Table 3-1

Sampling frame for the comparisons of parameters between before and after each pH shock (average value was compared).

Parameters for comparison	Sampling time for pH 8.0 shock (d)		Sampling time for pH 9.1 shock (d)		Sampling time for pH 10.0 shock (d)	
	before	after	before	after	before	after
Membrane fouling rate	3,5,9	2,3,4	1,2,3	4,5,7	2,3,6	4,8,10
BPC content	1,3,5,7,9	2,3,4	1,2,3	4,5,7	2,4,6,8	4,6,8,10,12
PSD	3,5	2,3	1,3	4,7	2,6,8	6,10,12
Cake sludge	-	-	-	-	2,8	8,14

3.2.2.1 Membrane fouling determination

Membrane resistance was analyzed using Darcy's law as indicated in Eq. (3-1)

$$R_t = \frac{\Delta p_T}{\eta \times J} \quad (3-1)$$

where, R_t is the total resistance (m^{-1}), Δp_T is the transmembrane pressure (kPa), η is the dynamic viscosity ($kPa \cdot s$) and J is the membrane flux ($m^3 \cdot m^{-2} \cdot s^{-1}$).

Membrane fouling rate (ΔR) of the mixed liquor was calculated as ΔR_{24} ($m^{-1} \cdot h^{-1}$), the change rate of R within 24 h of filtration, according to Equation (3-2):

$$\Delta R_{24} = \frac{R_{24} - R_0}{\Delta t} \quad (3-2)$$

where Δt is filtration time (h). R_0 and R_{24} are the R values (m^{-1}) at starting time and after a 24-hour filtration, respectively.

3.2.2.2 EPS extraction and measurement

The extraction of bound EPS was based on a cation exchange resin (CER) (Dowex® Marathon® C, Na⁺ form, Sigma–Aldrich, Bellefonte, PA) method (Frølund et al., 1996): 100mL sludge suspension was taken and centrifuged (IEC MultiRF, Thermo IEC, Needham Heights, MA, USA) at 18,700×g for 10 min at 4 °C. The sludge pellets were re-suspended to their original volume using a buffer consisting of 2mM Na₃PO₄, 4mM NaH₂PO₄, 9mM NaCl and 1mM KCl at pH 7. Then, the sludge was transferred to an extraction beaker with buffer solution and the CER (80 g/g-MLSS) added. The suspension was stirred (Corning 171 Scholar Stirrer, Corning, USA) for extraction of EPS for 2 h at 4 °C. The extracted EPS was recovered by centrifugation of the CER/sludge suspension for 20 min at 18,700×g at 4 °C in order to remove the CER and MLSS. The EPS was normalized as the sum of polysaccharides (PC) and proteins (PN), which were measured colorimetrically by the methods of DuBois et al. (1956) and Lowery et al. (1951), respectively. Bovine serum albumin (BSA) was used as a protein standard and glucose was used as a polysaccharide standard. The coefficients of variation (COV) of the proteins, carbohydrates and total EPS for four identical EPS extraction samples were 2.7 %, 2.8 % and 2.8 %, respectively.

3.2.2.3 Particle size distribution

The particle size distribution (PSD) of mixed liquor was determined by a Malvern Mastersizer 2000 instrument (Worcestershire, UK) with a detection range of 0.02-2000 μ m. The scattered light is detected by means of a detector that converts the signal to a size distribution based on volume or number. Each sample was measured 3 times with a standard deviation of 0.1-4.5%. The PSD measurements were conducted routinely 2 – 3 times each week.

Cake layers were carefully scraped off from membrane surfaces using a plastic sheet. The collected cake layer was rinsed with distilled water and then gently resuspended for PSD measurement.

3.2.2.4 Characterization of cake layer

The nature and functional groups of membrane foulants were studied using the Fourier transform infrared spectroscopy (FTIR) technique. The fouled membrane module was removed from the bioreactor when TMP was too high (>30 kPa) or required for sludge cake characterization. Several pieces (five-to-eight) of membrane with cake layer were cut from the membrane module after the end of each filtration. The samples were dehydrated in the oven (105 °C) for 24 h to obtain dry foulants. A Bruker Ten 37 FTIR Spectrometer (Bruker Co. Ltd.) was used to characterize the major functional groups of biopolymers in the membrane foulants.

The porosity of sludge cake layers formed on membrane surfaces was observed by conventional optical microscopy (Olympus, Japan), combined with the use of a micro-slicing technique. A series of membrane pieces (four-to-eight pieces) with cake layers was cut from the membrane sheet after the end of each filtration. The pieces of cake layer were fixed on to a sample stage using optimal cutting temperature compound (O.T.C.) compound (Sakura Finetechnical Co. Ltd. Tokyo, 103, Japan). In order to prevent the structure and thickness of cake layer from changing, the layer was saturated with 0.85% NaCl aqueous solution (Zhang and Bishop, 1994) and then frozen at -22 °C. The stage was then mounted on a cryostate microtome (Histostate Microtome, Model: 855, Reichert Scientific Instruments Division of Warner Lambert Technologies Inc., NY, USA). Cake layer samples were cut into horizontal slices. For each sample, a series of 100 µm-thick sections was made from the cake layer surface to the entire depth of the layer. The surface images were acquired and transferred to gray-scale formation (256 gray-scale levels) with Adobe Photoshop CS3 software (Fig. 3-2 (a)). Before analyzing an image, a threshold has to be determined in order to distinguish pores from the background, obtaining a binary image (Fig. 3-2 (b)). For each binary image, the threshold was estimated as the gray level value that corresponded to that maximum of the gray level histogram second derivation (Cenens et al., 2002). The pore area values can be determined by analyzing the binary images. The COV was 14.7 %. Four samples in all were analyzed and four-to-eight pieces of membrane with cake layer were cut from each membrane sheet for porosity determination.

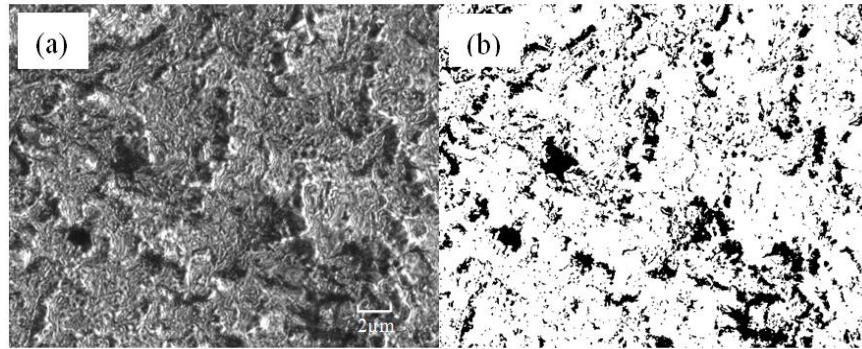


Figure 3-2 Microscopy image of cake layer (a) Initial true color image and (b) binary image.

3.2.2.5 Water quality measurements

Samples of influent and effluent were taken periodically from the system. Parameters, including COD and mixed liquor suspended solids (MLSS) were analyzed as defined in Standard Methods (APHA, 2005). Supernatant COD was determined after centrifuging the mixed liquor for 20 min at $18,700\times g$. Soluble microbial products (polysaccharides and proteins) in the supernatant and effluent were analyzed using the methods described above. MLSS, supernatant COD and permeate COD were routinely measured 2–3 times each week and duplicate measurements were performed for each parameter at each time.

The total volatile fatty acids (VFAs) concentration in the supernatant and permeate was analyzed using the distillation and titration method as described in the American Public Health Association Method 5560C (APHA, 2005). Ammonia was measured by ion chromatography using a Dionex 120 equipped with a CG16 guard column and CS16 analytical column. Anions nitrate and nitrite nitrogen were also measured by ion chromatography using the Dionex 120 equipped with an AG14 guard column and AS14 analytical column. Nine samples in total were analyzed for total VFAs and ammonia, nitrate and nitrite.

3.2.2.6 Statistical analysis

Statistical analysis was carried out using the Statistical Package for the Social Science (SPSS) V11.0 produced by SPSS Incorporation (America) with the aim to

characterize the influence of sludge properties on the membrane fouling rate and the comparison of changes in sludge and cake layer properties before and after pH shocks. An analysis of variance (ANOVA) was used to test for differences between treatment means when studying the influence of pH shocks on sludge properties. The Type I error rate was set at 0.05 for all statistical tests performed in this study. Pearson's product momentum correlation coefficient (r_p) was used to estimate the linear relationships between sludge properties and membrane fouling rate (ΔR_{24}).

3.3 Results and discussion

3.3.1 Effect on COD removal and biogas production

The SAnMBR was loaded at an average rate of 2.4 ± 0.4 kgCOD/m³ day throughout the 120 days of operation (Fig. 3-3 (a)). The membrane flux was maintained at a value of 5.2 ± 0.5 L/m² h before a pH 10 shock (days 0–63) and 4.3 ± 0.6 L/m² h after the pH 10 shock (days 64–120). The COD concentrations in the influent, supernatant and permeate during the whole operation period are shown in Fig. 3-3 (b). The influent COD value fluctuated from 2782 to 3350 mg/L, while the permeate COD value was lower than 800 mg/L at the initial start-up period and fell to less than 300 mg/L after 22 days of operation. The steady-state COD removal efficiency was about 90 %.

At day 35, an alkaline aqueous solution (NaOH) pumped into the reactor caused an increase in pH value from 7.0 to 8.0 for 12 h. The increase in pH resulted in a higher COD value in the supernatant and permeate, and thus a decrease in the COD removal efficiency (from 90 % to 83 %). It took about seven hours for the system to restore to pH 7.0. The reactor performance recovered, in terms of COD removal and the biogas production rate, on day 36.

At day 44, the reactor pH was increased from 7.0 to 9.1. This resulted in a rapid decrease in the COD removal efficiency from almost 90 % to less than 75 %. On day 46, the pH was restored to 7.0. The COD removal efficiency restored to values exceeding 90 % within 6 days. These results indicated that the system was tolerant of moderate alkali pH conditions.

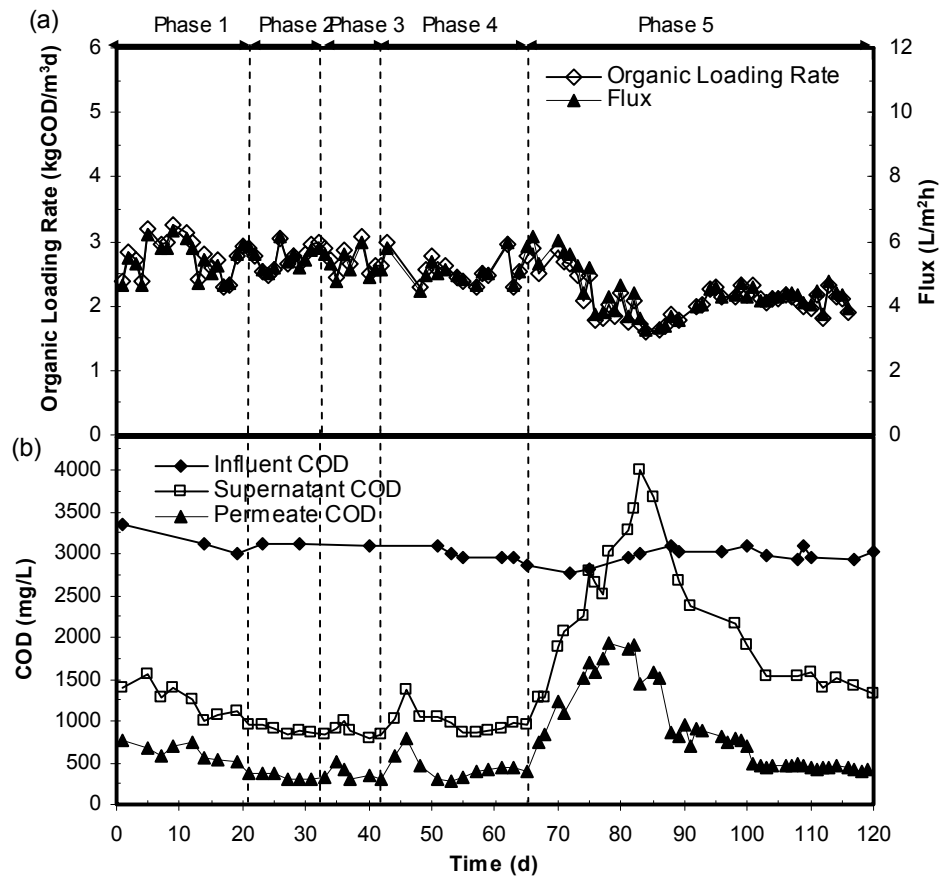


Figure 3-3 Variation of (a) organic loading rate and membrane flux during operation, and (b) the COD.

At day 65, the reactor pH was subsequently increased from 7.0 to 10.0. Although the pH was adjusted to 7.5 at day 66 using 0.01M HCl, it seems that COD degradation was largely deteriorated, and the COD removal efficiency decreased sharply from more than 90 % to less than 30 % in the following days. This pH change reduced COD removal for more than 30 days. The higher supernatant COD, as compared to the influent COD, from day 78 to day 90 strongly suggests the accumulation of soluble microbial products (SMPs) and volatile fatty acids in the SANMBR. Chemical analysis of the total VFA during pH 10.0 shock suggests that the total VFA concentration in supernatant (721 mg/L) was higher than that (608 mg/L) in the permeate, implying that some VFAs were retained in the bioreactor by the cake layer and membrane.

Fig. 3-4(a) shows the biogas production rate during the whole process. At Phases 2 and 3, the biogas production rates were 0.41 ± 0.04 and 0.38 ± 0.07 L/g COD removed, respectively, indicating a slight impact on biogas production rate with a pH 8.0 shock. At Phase 4, the biogas production rates were sharply decreased to almost 0 as a response to the pH 9.1 shock and it took 6 days to restore them to the normal level. With respect to Phase 5, a similar profile to Phase 4 was observed. However, it required a much-longer recovery period (30 days). Moreover, after the process ran stably, it showed a lower biogas yield (0.35 ± 0.02 vs 0.41 ± 0.01 L/g COD removed before the pH 10.0 shock). This could be related to the toxicity caused by pH shocks. Chemical analysis showed that the ammonia concentration in the mixed liquor (36.5 mg/L) was significantly higher than that (21.8 mg/L) in the feed, implying the accumulation of ammonia in the mixed liquor was caused by biomass death or decay after the pH 10.0 shock. The free form of ammonia (FA) has been suggested to be the actual toxic agent and an increase in pH would result in increased toxicity (Borja et al., 1996) because of the shift to a higher FA to ionized (NH_4^+) ammonia ratio at higher pH. Process instability due to ammonia often results in VFAs accumulation, as observed by an increase in the total VFA concentration from 15 to 30 mg/L under steady-state operation to 451 and 721 mg/L after pH 9.0 and 10.0 shocks, respectively, which again leads to a decrease in pH and thereby declining concentration of FA. The interaction between FA, VFAs and pH may lead to this phenomenon (Angelidaki et al., 1993; Borja et al., 1996).

The gas composition was also markedly influenced by pH shocks as shown in Fig. 3-4(b). At pH 7.0, the gas phase was composed of about 68 % methane and 25 % carbon dioxide. The remainder of the gas was mainly nitrogen. After the reactor received a pH 8.0 shock, the CH_4/CO_2 ratio was slightly reduced from 2.7 to 2.1, and recovered within 2 days. Further increased pH shocks resulted in a significant reduction of CH_4/CO_2 and a longer recovery period.

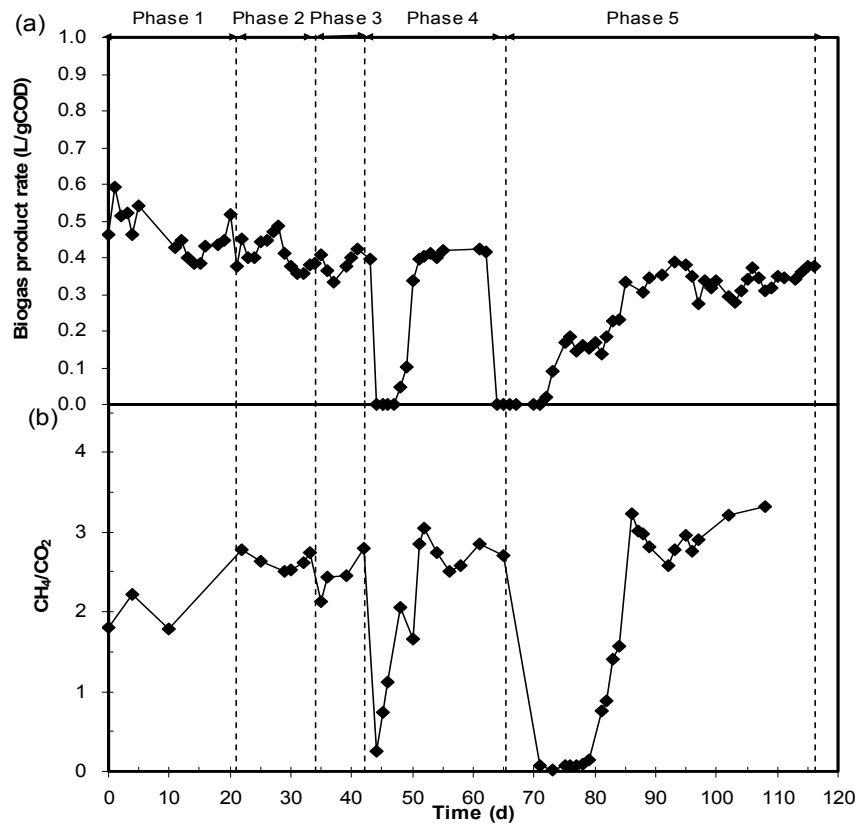


Figure 3-4 Variation of (a) biogas production rate and (b) CH_4/CO_2 ratio in produced biogas.

3.3.2 Effect on membrane fouling

Fig. 3-5 presents the comparison of membrane fouling rates (ΔR_{24}) which are before and after the various pH shocks. Membrane fouling rates were found to be slightly different before and after a pH 8.0 shock, indicating the pH 8.0 shock had some effect on the membrane fouling rate (ANOVA, $p < 0.05$). However, after pH increased to 9.1, a significant increase in the membrane fouling rate was observed (ANOVA, $p < 0.05$). The deterioration in membrane permeability was especially pronounced after pH 10.0 shock (ANOVA, $p < 0.05$).

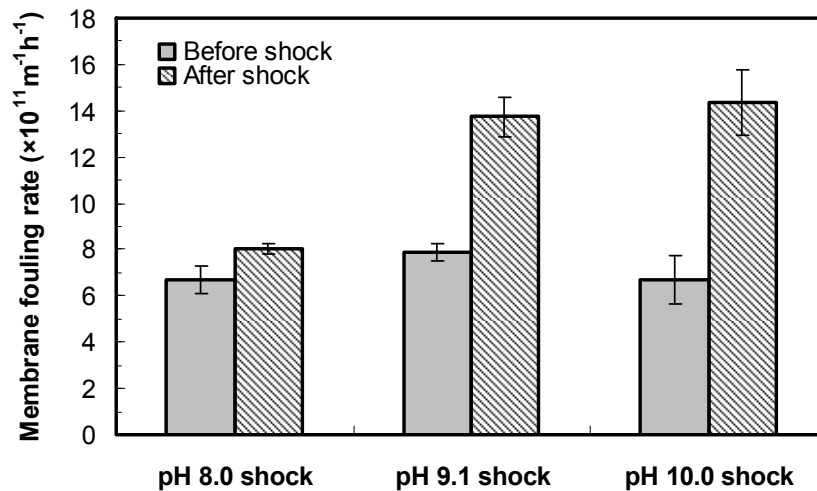


Figure 3-5 Effect of the elevated pH shocks on membrane fouling rates. Results are expressed as average \pm one standard deviation ($n = 3$) (flux = 5.1 ± 0.4 , 4.8 ± 0.5 and 4.4 ± 0.5 L/m² h, MLSS = 8.6 ± 0.4 , 10.0 ± 0.7 , 9.6 ± 0.6 g/L for pH 8.0, 9.1 and 10.0 shock, respectively; biogas sparging rate = 2 x 0.75 LPM).

Since each phase was conducted under the same feed and similar operation conditions, the different filtration performances at each phase should be mainly caused by the different characteristics of the bulk phase and cake layers on the membrane and membrane functions affected by pH value. Thus, a further study was performed to identify and characterize the bulk sludge and the components and formation mechanism of the cake layer on membrane surfaces. A change in pH value would affect membrane function directly. It is well known that changes in pH would result in changes in membrane morphology, surface charge and pore structure and ultimately membrane permeability (Dong et al., 2006; Nanda et al., 2010; Tadkaew et al., 2010). However, the observed changes in the membrane fouling rate was the result of a combined effect of pH shocks on sludge and cake layer properties as well as membrane function. The relative importance of changes in sludge and cake layer properties and membrane function on membrane fouling is unknown and needs further study.

3.3.3 Sludge properties and their effects on membrane fouling

The MLSS concentration in each phase is given in Table 3-2. MLSS concentration was initially 5.7 ± 0.8 g/L and then gradually increased to 10.0 ± 0.7 g/L during Phase 2 to Phase 4. The pH 8.0 shock had no significant impact on the sludge production rate while a pH 9.1 shock retarded sludge production and a pH 10.0 shock caused a slight decrease in MLSS concentration.

Table 3-2
MLSS concentration in each phase.

Phase	Phase 1	Phase 2	Phase 3	Phase 4	Phase 5
MLSS (g/L)	5.7 ± 0.8	6.8 ± 0.4	8.6 ± 0.4	10.0 ± 0.7	9.6 ± 0.6

Although MLSS concentrations varied over the investigated periods, it did not appear to influence membrane fouling rates (ΔR_{24}) ($r_p = -0.146$, $p = 0.527$, sample number $n = 20$). In addition, MLSS concentrations were kept almost the same before and after each shock. These results indicated MLSS concentration was not the main cause of the significantly different filtration behaviour shown in Fig. 3-5. Some studies reported that membrane fouling was independent of MLSS concentration until a very high value (e.g. 30-40 g/L) was reached (Yamamoto et al., 1989; Ross et al., 1990). No significant impacts of MLSS concentration on membrane fouling observed in this study might be due to the fact that the range of MLSS concentration tested here was much lower than critical values reported in the above literature. It is interesting to note that the supernatant COD was consistently higher than the effluent COD over the experimental time as shown in Fig. 3-3(b), indicating significant retention of organic matter by the membrane filtration and cake layer. Similar phenomenon of organic accumulation in the aerobic and anaerobic MBR suspensions have been reported previously (Wang and Li, 2008; Lin et al., 2009). The difference in organic content between the supernatant and the effluent was classified as biopolymer clusters (BPC) by Wang and Li (2008). The impact of pH shocks on the BPC content is shown in Fig. 3-6. Except for pH 8.0 shock (ANOVA, $p > 0.05$), the significantly higher BPC content after pH 9.0 and 10.0 shocks could be originated from biomass death and decay (ANOVA, $p < 0.05$). In addition, more SMPs could be

produced during unstable conditions (Parker et al., 1972). This higher BPC content (Fig. 3-6) after pH shocks corresponded to a higher membrane fouling rate (Fig. 3-5). It is therefore inferred that BPC played a key role in the membrane fouling rate. It is reasonable because BPC originates from organic polymers, such as SMP and colloidal organic substances in the suspension (Wang and Li, 2008), which were considered as major foulants affecting membrane filtration and cake layer formation (Lee et al., 2003; Li et al., 2008; Wang and Li, 2008).

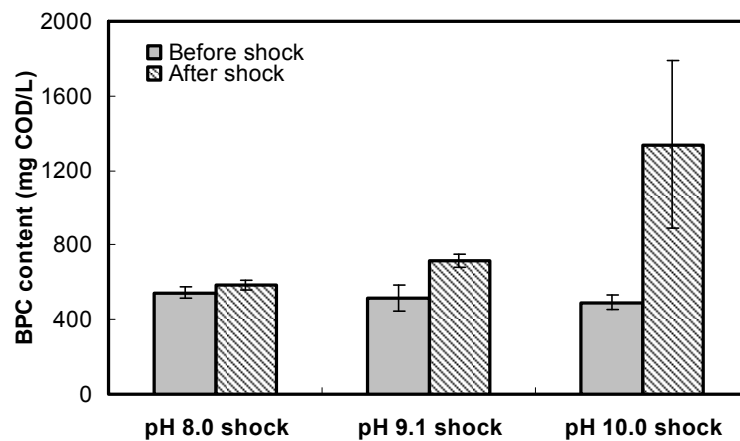


Figure 3-6 Effect of the elevated pH shock on BPC content in the sludge suspension.

The particle size distributions (PSDs) of sludge suspension in SAnMBR before and after each pH shock are presented in Fig. 3-7 (a)-(c). There is no obvious difference between the two curves in Fig. 3-7(a) indicating pH 8.0 shock had no significant impact on PSD. Fig. 3-7(b) and (c) shows that the flocs shifted to smaller sizes after the pH 9.1 and 10.0 shocks. These results indicate that pH 9.1 and 10.0 shocks induced the breakage of sludge flocs continuously. This is consistent with findings of Sandberg and Ahring (1992) that an excessively alkaline pH can lead to disintegration of microbial granules. The breakage of sludge flocs might be due to erosion of strengths or due to a rupture of the network of polysaccharide fibrils which is the support of the different compounds and particularly the cells (Parker et al., 1972).

Previous studies showed that small particles had a strong tendency to deposit on the membrane surface and form a cake layer (Bae and Tak, 2005; Lin et al., 2009). This

is because the back transport velocity of the particles decreased with their size (Bae and Tak, 2005). Therefore, the increased membrane fouling rate in Fig. 3-5 could be at least partially explained by flocs breakup induced by the pH shocks, which cause higher cake formation rates. This result is consistent with the findings of Wisniewski and Grasmick (1998) in that suspension produced after flocs breakup consists mainly of particles having a size of around 2 μm , which is responsible for flux decline.

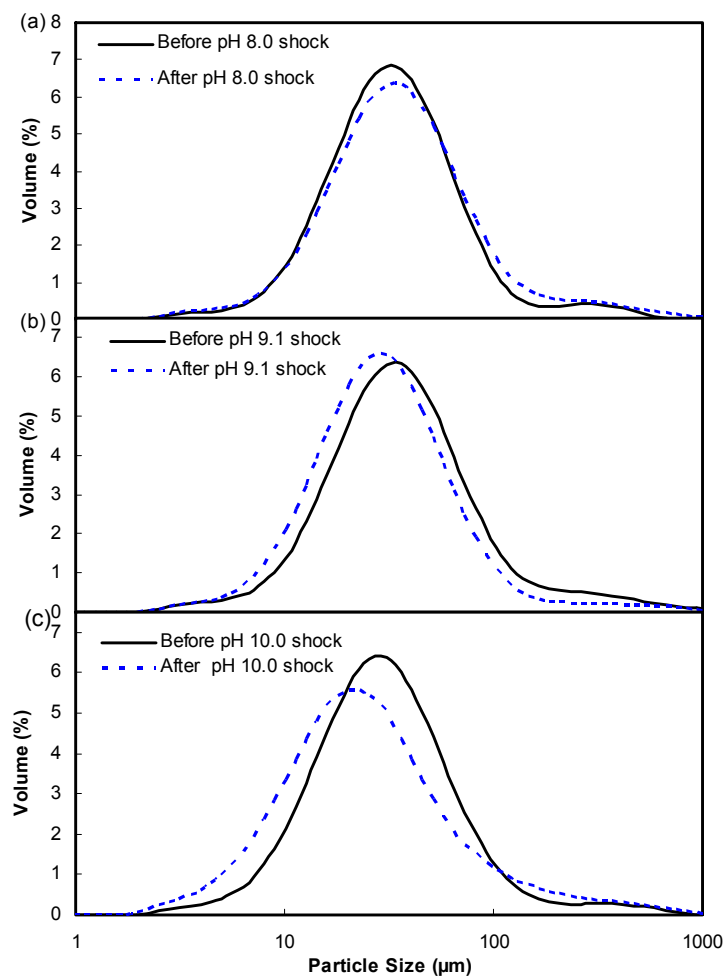


Figure 3-7 Particle size distribution of sludge suspension before and after (a) pH 8.0 shock, (b) pH 9.1 shock and (c) pH 10.0 shock.

Fig. 3-8 shows the variation of the bound EPS (proteins (PN) and polysaccharides (PC)) and PN/PC ratio in EPS with operational time. Proteins were found to be the dominant component in the EPS for all the phases. The variations of PN and PC contents

in EPS were large and no trend could be perceived. In contrast, PN/PC ratio increased from 5.7 to 7.6 in Phase 1 and then remained stable at 7.3 ± 0.2 in Phases 2 and 3. After pH 9.1 shock, PN/PC ratio gradually declined to about 4.5, with a further pH 10.0 shock seeming to have no significant impact on PN/PC ratio.

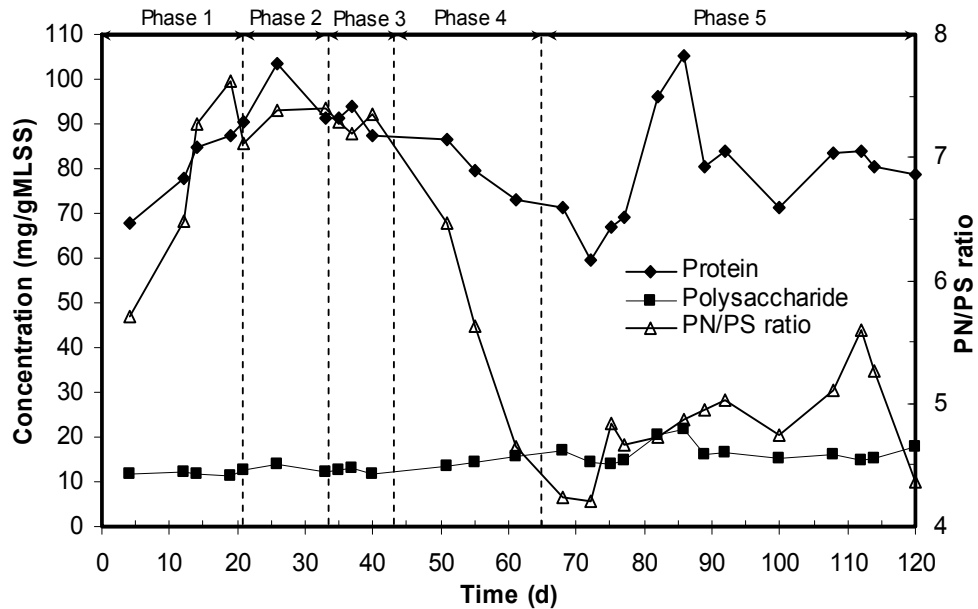


Figure 3-8 Variation of (a) protein, (b) polysaccharide content and (c) PN/PC ratio in EPS with operational time

Statistical analysis shows that PN ($r_p = -0.19$, $p = 0.45$) and PC ($r_p = 0.423$, $p = 0.08$) in EPS and total EPS ($r_p = -0.09$, $p = 0.716$) had no significant correlation with the membrane fouling rate ΔR_{24} ($p > 0.05$, sample number $n = 26$). Lee et al., (2003) also reported that total EPS had no significant impact on membrane fouling resistance. These results could be due to the fact that pH shocks caused the change in EPS content, as well as other biomass characteristics such as SMP and sludge properties. Obviously, EPS is not the sole membrane foulant impacting upon membrane fouling. However, other studies found that an increase in the total EPS content was correlated to an increase in the membrane fouling rate (Khor et al., 2007; Meng and Yang, 2007). The contradictory results in the literature suggest that the role of EPS in membrane fouling rate is complex and depends on the changes in the dominant factors under different conditions.

In contrast, PN/PC ratio was found to have a highly negative correlation ($r_p = -0.852$, $p = 0.00$, sample number $n = 26$) with the membrane fouling rate (ΔR_{24}). The decrease in PN/PC ratio could correlate to the increase of non-flocculating flocs after the pH 9.1 shock in this study. It has been reported that the decrease in the PN/PC ratio coincided with the decrease in the flocs' size with the increased SRT (Massé et al., 2006). It was also reported that a decrease in the PN/PC ratio in EPS led to poorer bioflocculation (Liao et al., 2001). The data obtained from the current investigation, together with other studies in the literature, indicate that the PN/PC ratio is an important factor governing flocs' size in the SAnMBR system, which in turn affects membrane permeability.

3.3.4 Effect on cake layer properties

In this section, attention was focused on properties of cake layers formed on membrane surfaces before and after a pH 10.0 shock since this level of pH shock exerted the most significant impact on sludge properties as well as membrane fouling.

3.3.4.1 FTIR analysis of membrane foulants

The FTIR spectra of membrane foulants, which formed on the membrane surface before and after pH 10.0 shock, are presented in Fig. 3-9. The two curves show similar profiles. There is a broad region of absorption at 3320 cm^{-1} , which is due to the stretching of the O–H bond in hydroxyl groups (Kumar et al., 2006). Peaks in the vicinity of 2916 , 2847 and 1445 cm^{-1} are indicative of the C–H bonds in the alkane class (Kim and Jang, 2006). The asymmetrical stretching peak was noticed at 1726 cm^{-1} , suggesting the presence of carboxyl groups and representing typical characteristics of humic acids (Jarusutthirak et al., 2002). There was a broad peak at 1020 cm^{-1} , which is due to C–O bonds and is associated with polysaccharides (Kimura et al., 2005). There are two peaks at 1636 and 1535 cm^{-1} in the spectrum unique to the protein secondary structure, called amides I and II (Maruyama et al., 2001). The peaks of 1364 and 1244 cm^{-1} imply the presence of amide III (Zhou et al., 2007). The doublet at 2360 and 2343 cm^{-1} is due to carbon dioxide from the atmosphere adsorbed onto the sample surface. By the FTIR

spectra, the major components of the foulants were identified as proteins, polysaccharides and humic acids materials, which are the dominant components typically found in EPS.

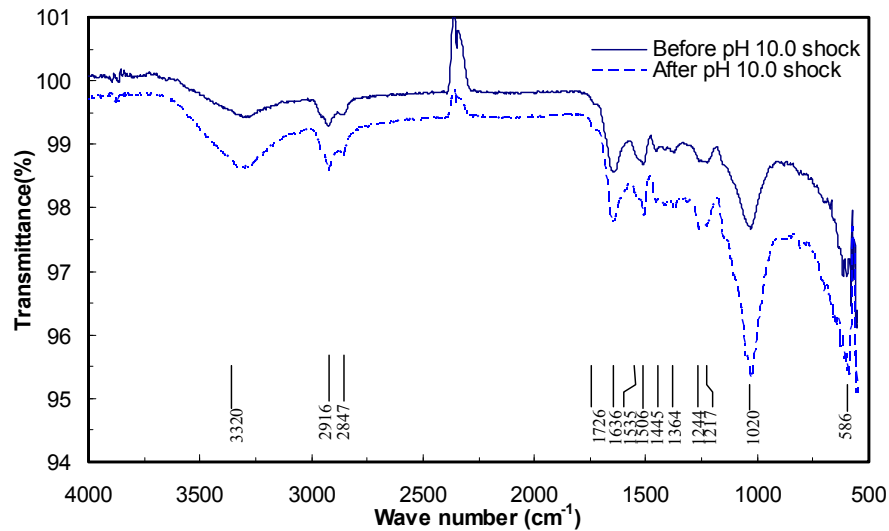


Figure 3-9 FTIR spectra of the membrane foulants in cake layer (cake layer formed after 6 days filtration, 5-8 pieces of membrane with cake layer were used for analysis).

From Fig. 3-9, peaks in the vicinity of 1364, 1244 and 1020 cm^{-1} have a higher intensity for the spectrum after pH 10.0 shock than those of the spectrum before a pH 10.0 shock. The absorption intensity reflected the relative amount of biopolymers in the total foulants (Zhou et al., 2007). In this study, each sample was measured 3 times and a good reproducibility was observed. It is therefore inferred that the relative amount of EPS in the total foulants was increased after a pH 10.0 shock. The increased amount of EPS in the cake layer would certainly contribute to the enhanced membrane filtration resistance.

3.3.4.2 Effect on particle size, porosity and specific resistance

Fig. 3-10 presents the typical PSDs of the cake layer which were measured before and after a pH 10.0 shock, respectively. A bimodal curve was observed after a pH 10.0 shock while cake layer formed before the pH10.0 shock showed a unimodal distribution. This indicates that two populations of aggregates were maintained in the cake layer and formed after pH 10.0 shock - a dispersed one whose size was around 0.1-1.0 μm and a macrofloc population whose mean size was between 10 and 100 μm .

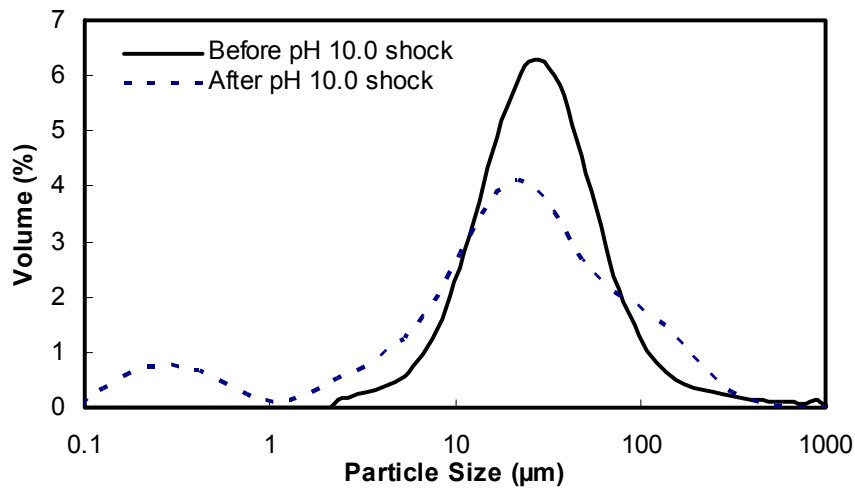


Figure 3-10 Particle size distribution of cake layer before and after pH 10.0 shock (cake layer formed after 6 days filtration, 5-8 pieces of membrane with cake layer were used for analysis).

The lower PSD in the cake layer (Fig. 3-10) after a pH 10.0 shock could be related to the fact that bulk sludge PSD was actually lower as shown in Fig. 3-7(c). Thus, it is not surprising to see that more of the smaller particles were accumulated in the cake layer after pH 10.0 shock, as smaller flocs have lower back transport and consequently trend to preferentially deposit on the membrane surface. In addition, the big difference in PSDs of cake layers formed before and after pH shock might be related to the differences in supernatant COD or BPC (Fig. 3-6). A higher supernatant COD or BPC could facilitate colloidal or small particles deposition on membrane surface. This conclusion is further supported by Li and Elimelech (2006) who reported a synergistic fouling behaviour of colloidal materials and solutes causing a higher flux decline rate during membrane filtration. They attributed the synergistic fouling behaviour to the hindered back diffusion of foulants caused by the interactions between organic and colloidal foulants, which result in faster and more substantial foulants deposition on the membrane surface (Li and Elimelech, 2006).

In previous studies (Bae and Tak, 2005; Liang et al., 2008), it was found that colloids and solutes demonstrated considerable influence on membrane permeability. The

colloids and solutes had a size that was close to or smaller than the size of membrane pores and would penetrate into the membrane pores easily and then block pores (Bae and Tak, 2005). The membranes used in this study have a pore size of about 0.2-0.3 μm , and statistical analysis of PSDs based on number shows that about 90 % of the particles in the cake layer formed after pH 10.0 shocks have a size smaller than 0.3 μm , therefore, pore blocking might make significant contribution to the total membrane fouling after pH 10.0 shock. In comparison, most of the particles in the cake layer formed before pH 10.0 shock have a size larger than 2 μm , and a simple rinse with tap water removed the cake layer coverage from the membrane surface and restored membrane permeability, indicating that sludge cake formation, other than membrane pore clogging, is the predominant cause of fouling. A similar finding was reported by Meng and Yang (2007) who found that the membrane fouling during filtration of deflocculated sludge was dominated by pore blocking resistance and cake resistance.

Fig. 3-11(a) presents the comparison of the average porosity of the cake layer before and after pH 10.0 shock. It can be seen from Fig. 3-11(a), after a pH 10.0 shock, average cake porosity decreased from 12.9 ± 2.0 % to 6.8 ± 1.0 %, indicating that a denser cake layer was formed after the alkaline shock (ANOVA, $p < 0.05$, sample number $n = 4-8$). This is not surprising, considering there were more small particles or colloids in the cake layer and higher solutes in the supernatant after pH 10.0 shock. The colloids and solutes could reduce the cake porosity by filling the void spaces between the sludge flocs in the cake layer (Bae and Tak, 2005).

After the pH 10.0 shock, the cake specific resistance was almost 2 times higher than that before the shock (Fig. 3-11(b)) (ANOVA, $p < 0.05$, sample number $n = 4-8$). According to the Carman-Kozeny equation for cake layer filtration, the specific resistance of the cake layer is significantly influenced by sludge particle size and cake porosity. Therefore, it can be concluded that the smaller particle size and lower porosity resulted in the higher specific resistance of the cake layer formed after a pH 10.0 shock.

Based on the above results, it is evident that the sludge breakup and the enhanced solutes in supernatant was the reason that leads to the deterioration of membrane filtration performance after the pH shock.

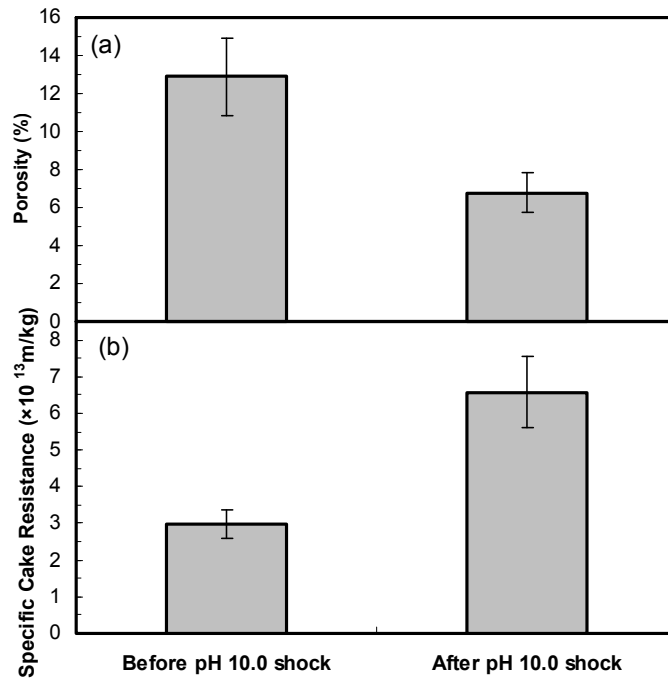


Figure 3-11 (a) Cake porosity, and (b) cake specific resistance before and after pH 10.0 shock (cake layer formed after 6 days filtration, 5-8 pieces of membrane with cake layer were used for analysis).

3.4 Conclusions

This study investigated the effect of elevated pH shocks (pH 8.0, 9.1 and 10.0) on the performance and membrane fouling of an SAnMBR. Based on the results presented in this study, the following conclusions can be drawn:

- The pH 8.0 shock had minor impact, while the pH 9.1 and 10.0 shocks exerted significantly negative impacts on COD removal, biogas production and membrane filtration performance of the SAnMBR. When normal pH (7.0) was resumed, it took approximately 1, 6, and 30 days for the reactor to recover from the pH 8.0, 9.1 and 10.0 shocks, respectively.
- The elevated pH shocks induced breakage of sludge flocs. The small-size particles were closely associated with the severe membrane fouling. Moreover, pH shock resulted in the accumulation of colloids and solutes or biopolymers in the sludge

suspension, and thus deteriorated membrane performance. These substances had significant influence on membrane fouling resistances.

- The bound EPS appeared to be independent of pH shock. However, the EPS composition, in terms of PN/PC ratio was altered, resulting in a lower PN/PC ratio after a pH 9.1 shock, but was not further changed after a 10.0 shock. The PN/PC ratio negatively correlated to the membrane fouling rate.
- The main components of organic matters in the membrane foulants were identified as PN, PS materials and humic acids by the FTIR spectroscopy. The cake layer analysis showed that the higher supernatant COD or BPC after pH shocks facilitated colloidal or small particle deposition on the membrane surface, which caused a denser and more compact cake layer with higher specific resistances.

3.5 References

- Akram, A., Stuckey, D. C., 2008. Flux and performance improvement in a submerged anaerobic membrane bioreactor (SAMBR) using powdered activated carbon (PAC). *Process Biochemistry* 43, 93-102.
- Angelidaki, I., Ellegaard, L., Ahring, B. K., 1993. A mathematical model for dynamic simulation of anaerobic digestion of complex substrates: Focusing on ammonia inhibition. *Biotechnology and Bioengineering* 42, 159-166.
- APHA, 2005. Standard methods for the examination of water and wastewater, 21th ed. American Public Health Association (APHA)/American Water Works Association (AWWA)/Water Environment Federation (WEF), Washington, DC.
- Bae, T.-H., Tak, T.-M., 2005. Interpretation of fouling characteristics of ultrafiltration membranes during the filtration of membrane bioreactor mixed liquor. *Journal of Membrane Science* 264, 151-160.
- Baily, J. E., Ollis, D. F., 1986. *Biochemical engineering fundamentals*, 2nd McGraw-Hill, New York.

- Borja, R., Sánchez, E., Weiland, P., 1996. Influence of ammonia concentration on thermophilic anaerobic digestion of cattle manure in upflow anaerobic sludge blanket (UASB) reactors. *Process Biochemistry* 31, 477-483.
- Cenens, C., Van Beurden, K. P., Jenné, R., Van Impe, J. F., 2002. On the development of a novel image analysis technique to distinguish between flocs and filaments in activated sludge images. *Water Science and Technology*. 46, 381-387.
- Chang, I.-S., Kim, S.-N., 2005. Wastewater treatment using membrane filtration--effect of biosolids concentration on cake resistance. *Process Biochemistry* 40, 1307-1314.
- Dong, B. Z., Chen, Y., Gao, N. Y., Fan, J. C., 2006. Effect of pH on UF membrane fouling. *Desalination* 195, 201-208.
- DuBois, M., Gilles, K. A., Hamilton, J. K., Rebers, P. A., Smith, F., 1956. Colorimetric Method for Determination of Sugars and Related Substances. *Analytical Chemistry* 28, 350-356.
- Frølund, B., Palmgren, R., Keiding, K., Nielsen, P. H., 1996. Extraction of extracellular polymers from activated sludge using a cation exchange resin. *Water Research* 30, 1749-1758.
- Gottschalk, G., 1986. *Bacterial metabolism*, 2nd. Springer-Verlag, New York.
- Han, S.-S., Bae, T.-H., Jang, G.-G., Tak, T.-M., 2005. Influence of sludge retention time on membrane fouling and bioactivities in membrane bioreactor system. *Process Biochemistry* 40, 2393-2400.
- Huang, X., Liu, R., Qian, Y., 2000. Behaviour of soluble microbial products in a membrane bioreactor. *Process Biochemistry* 36, 401-406.
- Jarusutthirak, C., Amy, G., Croué, J.-P., 2002. Fouling characteristics of wastewater effluent organic matter (EfOM) isolates on NF and UF membranes. *Desalination* 145, 247-255.
- Jeison, D., van Lier, J. B., 2007. Cake formation and consolidation: Main factors governing the applicable flux in anaerobic submerged membrane bioreactors (AnSMBR) treating acidified wastewaters. *Separation and Purification Technology* 56, 71-78.

- Khor, S. L., Sun, D. D., Liu, Y., Leckie, J. O., 2007. Biofouling development and rejection enhancement in long SRT MF membrane bioreactor. *Process Biochemistry* 42, 1641-1648.
- Kim, I. S., Jang, N., 2006. The effect of calcium on the membrane biofouling in the membrane bioreactor (MBR). *Water Research* 40, 2756-2764.
- Kimura, K., Yamato, N., Yamamura, H., Watanabe, Y., 2005. Membrane Fouling in Pilot-Scale Membrane Bioreactors (MBRs) Treating Municipal Wastewater. *Environmental science and technology* 39, 6293-6299.
- Kumar, M., Adham, S. S., Pearce, W. R., 2006. Investigation of Seawater Reverse Osmosis Fouling and Its Relationship To Pretreatment Type. *Environmental Science and Technology* 40, 2037-2044.
- Lee, W., Kang, S., Shin, H., 2003. Sludge characteristics and their contribution to microfiltration in submerged membrane bioreactors. *Journal of Membrane Science* 216, 217-227.
- Li, J., Yang, F., Li, Y., Wong, F.-S., Chua, H. C., 2008. Impact of biological constituents and properties of activated sludge on membrane fouling in a novel submerged membrane bioreactor. *Desalination* 225, 356-365.
- Li, Q., Elimelech, M., 2006. Synergistic effects in combined fouling of a loose nanofiltration membrane by colloidal materials and natural organic matter. *Journal of Membrane Science* 278, 72-82.
- Liang, S., Zhao, Y., Liu, C., Song, L., 2008. Effect of solution chemistry on the fouling potential of dissolved organic matter in membrane bioreactor systems. *Journal of Membrane Science* 310, 503-511.
- Liao, B.-Q., Kraemer, J. T., Bagley, D. M., 2006. Anaerobic Membrane Bioreactors: Applications and Research Directions. *Critical Reviews in Environmental Science and Technology* 36, 489 - 530.
- Liao, B. Q., Allen, D. G., Droppo, I. G., Leppard, G. G., Liss, S. N., 2001. Surface properties of sludge and their role in bioflocculation and settleability. *Water Research* 35, 339-350.

- Lin, H. J., Xie, K., Mahendran, B., Bagley, D. M., Leung, K. T., Liss, S. N., Liao, B. Q., 2009. Sludge properties and their effects on membrane fouling in submerged anaerobic membrane bioreactors (SAnMBRs). *Water Research* 43, 3827-3837.
- Lowery, O. H., Rosebrough, N., Farr, A. L., Randall, R. J., 1951. Protein measurement with the folin phenol reagent. *Journal of Biological Chemistry* 193, 265–275.
- Maruyama, T., Katoh, S., Nakajima, M., Nabetani, H., Abbott, T. P., Shono, A., Satoh, K., 2001. FT-IR analysis of BSA fouled on ultrafiltration and microfiltration membranes. *Journal of Membrane Science* 192, 201-207.
- Massé, A., Spérandio, M., Cabassud, C., 2006. Comparison of sludge characteristics and performance of a submerged membrane bioreactor and an activated sludge process at high solids retention time. *Water Research* 40, 2405-2415.
- Meng, F., Yang, F., 2007. Fouling mechanisms of deflocculated sludge, normal sludge, and bulking sludge in membrane bioreactor. *Journal of Membrane Science* 305, 48-56.
- Nanda, D., Tung, K.-L., Li, Y.-L., Lin, N.-J., Chuang, C.-J., 2010. Effect of pH on membrane morphology, fouling potential, and filtration performance of nanofiltration membrane for water softening. *Journal of Membrane Science* 349, 411-420.
- Parker, D. S., Kaufman, W. J., Jenkins, D., 1972. Flocc breakup in turbulent flocculation processes. *Journal of the Sanitary Engineering Division* 98, 79-89.
- Rajganes, B., Sublette, K. L., Camp, C., Richardson, M. R., 1995. Biotreatment of Refinery Spent Sulfidic Caustics. *Biotechnology Progress* 11, 228-230.
- Rao, A. G., Reddy, T. S. K., Prakash, S. S., Vanajakshi, J., Joseph, J., Sarma, P. N., 2007. pH regulation of alkaline wastewater with carbon dioxide: A case study of treatment of brewery wastewater in UASB reactor coupled with absorber. *Bioresource Technology* 98, 2131-2136.
- Ross, W. R., Barnard, J. P., Le JR, D. H., 1990. Application of ultrafiltration membranes for solids-liquids separation in anaerobic digestion systems: The ADUF process. *Water SA* 16, 85-91.

- Sandberg, M.,Ahring, B. K., 1992. Anaerobic treatment of fish meal process waste-water in a UASB reactor at high pH. *Applied Microbiology and Biotechnology* 36, 800-804.
- Sipma, J., Osuna, M. B., Emanuelsson, M. A. E.,Castro, P. M. L., 2010. Biotreatment of Industrial Wastewaters under Transient-State Conditions: Process Stability with Fluctuations of Organic Load, Substrates, Toxicants, and Environmental Parameters *Critical Reviews in Environmental Science and Technology* 40, 147-197.
- Tadkaew, N., Sivakumar, M., Khan, S. J., McDonald, J. A.,Nghiem, L. D., 2010. Effect of mixed liquor pH on the removal of trace organic contaminants in a membrane bioreactor. *Bioresour Technol* 101, 1494-1500.
- Van Tran, A., 2008. Remoal of COD and color loads in bleached kraft pulp efflients by bottom ashes from boilers. *Environmental Technology* 29, 775 - 784.
- Vogelaar, J. C. T., Bouwhuis, E., Klapwijk, A., Spanjers, H.,van Lier, J. B., 2002. Mesophilic and thermophilic activated sludge post-treatment of paper mill process water. *Water Research* 36, 1869-1879.
- Wang, X.-M.,Li, X.-Y., 2008. Accumulation of biopolymer clusters in a submerged membrane bioreactor and its effect on membrane fouling. *Water Research* 42, 855-862.
- Ward, A. J., Hobbs, P. J., Holliman, P. J.,Jones, D. L., 2008. Optimisation of the anaerobic digestion of agricultural resources. *Bioresource Technology* 99, 7928-7940.
- Welander, T., Morin, R.,Nylén, B., 1999. Biological removal of methanol from kraft mill condensate. In: *TAPPI Proceedings International Environmental Conference*,
- Wen, C., Huang, X.,Qian, Y., 1999. Domestic wastewater treatment using an anaerobic bioreactor coupled with membrane filtration. *Process Biochemistry* 35, 335-340.
- Wisniewski, C.,Grasmick, A., 1998. Floc size distribution in a membrane bioreactor and consequences for membrane fouling. *Colloids and Surfaces A: Physicochemical and Engineering Aspects* 138, 403-411.

- Yamamoto, K., Hiasa, M., Mahmood, T., Matsuo, T., 1989. Direct Solid-Liquid Separation Using Hollow Fiber Membrane in an Activated Sludge Aeration Tank. *Water Science and Technology* 21, 43-54.
- Yu, H. Q., Fang, H. H. P., 2003. Acidogenesis of gelatin-rich wastewater in an upflow anaerobic reactor: influence of pH and temperature. *Water Research* 37, 55-66.
- Zhang, T. C., Bishop, P. L., 1994. Density, porosity, and pore structure of biofilms. *Water Research* 28, 2267–2277.
- Zhou, J., Yang, F.-l., Meng, F.-g., An, P., Wang, D., 2007. Comparison of membrane fouling during short-term filtration of aerobic granular sludge and activated sludge. *Journal of Environmental Sciences* 19, 1281-1286.

Chapter 4 Structure of cake layer in a submerged anaerobic membrane bioreactor

Adapted from the publication:

W.J. Gao, H.J. Lin, K.T. Leung, H. Schraft and B.Q. Liao. Structure of Cake Layer in a Submerged Anaerobic Membrane Bioreactor (SAnMBR). *Journal of Membrane Science*, 2011, 347(1-2): 110-120.

Abstract:

A laboratory-scale submerged anaerobic membrane bioreactor (SAnMBR) was used for thermomechanical pulping whitewater treatment. Sludge cake formation on membrane surfaces was identified as the dominant mechanism of membrane fouling. The spatial distribution of physical, chemical and microbiological structure of cake layers was characterized by various analytical techniques, including micro-tome slicing technique, confocal laser scanning microscopy (CLSM), conventional optical microscopy (COM), scanning electron microscopy (SEM)-energy-dispersive X-ray analyzer (EDX), particle size distribution (PSD) analysis, Fourier transform infrared (FTIR) spectroscopy, extraction and chemical analysis of extracellular polymeric substances (EPS), and polymerase chain reaction (PCR)-denaturing gradient gel electrophoresis (DGGE). The results showed that the areal porosity decreased from the top layer to the bottom layer. Smaller flocs had a higher tendency to accumulate on membrane surfaces but the consolidation of cake sludge in the bottom layers resulted in larger flocs as compared to the fresh cake sludge formed on the top layers. There was an increase in the bound EPS density (mg EPS/cm^3 wet sludge) and a decrease in the ratio of proteins to polysaccharides in bound EPS from the top to bottom layers. PCR-DGGE study showed that there were significant differences in microbial community population density along the cake layer depth. Through the CLSM and COM images, cake layer was found to have a loose outer surface when compared with the cake bottom. The results provide a new insight in cake layer structure and suggest that structures change significantly from the top layer to the bottom layer.

4.1 Introduction

Submerged anaerobic membrane bioreactor (SAnMBR) has received considerable attention in recent years. SAnMBR system can not only reduce energy costs and biomass stress associated with recirculation, as compared to side-stream AnMBRs, but also allow for self cleaning of the membrane surface by recirculating the biogas produced (Liao et al., 2006). It offers advantages in terms of low energy requirements, low sludge production, superior quality of treated effluent, net energy production and small footprint (Liao et al., 2006; Hu and Stuckey, 2007; Jeison and van Lier, 2007; Lin et al., 2009). The SAnMBR technology has been used for industrial wastewater treatment in recent years (Kanai et al., 2010). However, membrane fouling and its consequences in terms of the loss of membrane performances, reduced productivity and high costs for cleaning and membrane replacement have been becoming a major obstacle in the application of SAnMBRs (Hu and Stuckey, 2007; Jeison and van Lier, 2007). There are many experimental studies have shown that sludge cake formation on membrane surfaces is the dominant mechanism of membrane fouling in SAnMBRs (Hu and Stuckey, 2007; Jeison and van Lier, 2007; Lin et al., 2009). To effectively optimize the filtration performance of SAnMBRs, an adequate understanding of the dynamic nature and characteristics of cake layers on membrane surfaces is essential.

Cake layers can be defined as porous layers rejected on the membrane surface due to the adsorption, deposition, and accumulation of all kinds of foulants, such as sludge, extracellular polymeric substances (EPS), organic and inorganic particles (Lee et al., 2008). Although cake layer formation is a key factor affecting MBR filtration efficiency (Chu and Li, 2005; Jeison and van Lier, 2007), findings from literature review indicate that optimization of the MBR technology suffers from a lack of detailed fundamental information about cake layer structure (porosity, density, chemical compositions including EPS, microbial populations, and their spatial distribution along cake layer depth). There are only a few studies addressed the cake layer structure in aerobic MBRs. For instance, Meng et al. (2007) characterized some property parameters of cake layer by using series of analytical methods. Furthermore, Wang and Li (2008) found the

accumulation of biopolymer clusters (BPC) in cake layers. However, there is a short of information on spatial distribution of cake layer structure in the literature.

In recent years, confocal laser scanning microscopy (CLSM) has been used to study the spatial distribution of cake layer structure on membrane surfaces (Hwang et al., 2008; Lee et al., 2008) and an improved understanding of the spatial distribution of thin fouling layer properties, such as porosity, has been obtained. However, there is still a limitation of the CLSM system with respect to laser penetration, usually in the range of a few hundred micrometers, which is related to the transparency of the specimen, self-shading, diffraction, etc. Only the information of surface layer can be obtained from solid surfaces. Meanwhile, poor penetration of different fluorescent dyes may cause a rapid decrease in fluorescence as a function of depth, especially for thick cake layers. For thick cake layers, particularly these ones formed in SAnMBRs (Jeison and van Lier, 2007; Lin et al., 2009), the CLSM technique alone is not able to provide comprehensive picture of spatial distribution of cake layer structure. We believe that the use of micro-tome slicing technique, which has been widely used for biofilm structure studies (Zahid and Ganczarczyk, 1994; Zhang and Bishop, 1994), combined with the CLSM and conventional optical microscopy (COM), can provide a more detailed information of spatial distribution of cake layer structure. Quantitative parameters describe the physical structure of different cake layers can be extracted from three-dimensional CLSM and COM images. On the other hand, biopolymers (proteins and polysaccharides materials) and inorganic substances can be determined for different layers. Additionally, microbiology methods can be performed to investigate the spatial distribution of microbial community structures and to identify the bacteria that might be the pioneers of surface colonisation on membranes (Zhang et al., 2006b; Ivnitsky et al., 2007). However, knowledge of the structure of cake layer is still insufficient due to its variability and complexity. Previous studies assumed that the cake layers formed on membrane surfaces are homogeneous (Lee and Clark, 1998; Dufrière et al., 2002). More realistic models that describe sludge cake formation and filtration will require a better understanding of cake layer structures (Di Bella et al., 2008; Zarragoitia-González et al., 2008; Mannina et al., 2010). Understanding the spatial distribution of physical, chemical and

microbiological structure of cake layers formed on membrane surfaces in SAnMBRs is crucial to elucidating the behaviour of cake layers and the filtration performance of the SAnMBR processes.

The objective of this study was to develop an improved fundamental understanding of the spatial distribution of physical, chemical and microbiological structure of cake layer formed on membrane surfaces by using the micro-tome slicing technique, advanced CLSM, COM, scanning electron microscopy (SEM)-energy diffusive x-ray analyzer (EDX), particle size distribution (PSD) analysis, Fourier transform infrared (FTIR) spectroscopy, extraction and chemical analysis of extracellular polymeric substances (EPS), and polymerase chain reaction (PCR)-denaturing gradient gel electrophoresis (DGGE). It is anticipated that this study would provide a new insight with regard to the spatial changes in the inner architecture of cake layer formed on membrane surfaces that are not available in current literature.

4.2 Materials and methods

4.2.1 Experimental system

A schematic representation of the SAnMBR is presented in Xie et al. (2010). It has a working volume of 10L, in which a flat sheet ultrafiltration membrane module (0.015 x 2 = 0.03 m², polyvinylidene fluoride (PVDF), supplied by Shanghai SINAP Membrane Science & Technology Co. Ltd., China) with the molecular weight cut off (MWCO) of 70000 Dalton was immersed. The headspace biogas was recirculated by two gas recycle pumps (Masterflex Console Drive, Model 7520 - 40, Thermo Fisher Scientific, USA) (0.75 x 2 = 1.5 L/min) through two stainless steel tube diffusers (one on each side of the module) at the base of the membrane module to mix the biomass continuously and to control solids deposition over the membrane surface. A pH regulation pump and a pH electrode (Thermo Scientific, Beverly, MA) were used to automatically control the pH value at 7.0 ± 0.2 by using 0.1 M NaOH solution. The temperature was maintained at a mesophilic temperature of 37 ± 1 °C by circulating warm water through the water jacket, the sludge liquor was continuously mixed by a magnetic stirrer (Thermolyne Cimarec, Model no: S47030) located at the bottom of the reactor.

The SAnMBR was operated for over 7 months for treating thermomechanical pulping whitewater collected from a local pulp and paper mill, while this study was conducted from day 85 to day 220 (135 days) to investigate the spatial distribution of physical, chemical and microbiological structure of cake layer formed on membrane surfaces. Some of the influent characteristics are listed in Table 4-1. The reactor was inoculated with seeded sludge developed from a previous study for kraft evaporator condensate treatment (Xie et al., 2010). During the operation of the reactors, no sludge was discharged except for sludge sampling and sludge cake characterization. This corresponded to a sludge age of approximately 280 days. In order to sustain the nutrient concentrations required for biomass growth in an anaerobic environment, nitrogen (NH_4Cl) and phosphorus (KH_2PO_4) were fed as macro-nutrients in a proportion of COD: N: P of 100: 2.6: 0.4 (Vogelaar et al., 2002). Meanwhile, a trace element solution (Welander et al., 1999) was supplemented to the influent to prevent trace metal limitations of the methanogens. The influent was pumped into the bottom of the bioreactor automatically by a feeding pump (Masterflex Model 7520 - 50, Barnant Co., USA) which was controlled by a level sensor (Madison Co., USA) and controller (Flowline, USA). Membrane flux was controlled by adjusting the speed of a peristaltic pump (Masterflex, C/L, Model 77120 - 70, Barnant, Co., USA). Intermittent suction with a cycle of 4-min run and 1-min pause was carried out for permeate production. The trans-membrane pressure (TMP) was measured by a vacuum gauge connecting the bioreactor and the suction pump. The reactor was shut down at different TMP rise stages and new membranes were used in the next run. The cake layer samples were subjected to structure characterization immediately.

When the TMP reached at around 40 kPa, the operation was terminated and the membrane module was taken out for sludge cake characterization. The membrane cleaning procedures were described by Lin et al. (2011). A new membrane was used for a new TMP evolution cycle if the previously fouled membrane was cut in pieces for sludge cake layer characterization.

Table 4-1
Characteristics of influent

pH	4.12 - 4.38
TSS	181.6 - 576.6 mg/L
Total COD	1823 - 3504 mg/L
Soluble COD	1136 - 3189 mg/L
Total Phosphorus	10.17 - 10.85 mg/L
Total Nitrogen	147.9 - 150.5 mg/L
Aluminum	0.123 - 0.136 mg/L
Barium	0.278 - 0.345 mg/L
Calcium	15.60 - 22.59 mg/L
Copper	0.011 - 0.023 mg/L
Iron	0.245 - 0.278 mg/L
Potassium	22.1 - 31.2 mg/L
Magnesium	12.39 - 12.62 mg/L
Manganese	1.331 - 1.334 mg/L
Sodium	32.40 - 72.58 mg/L
Sulfur	27.80 - 50.06 mg/L
Strontium	0.075 - 0.077 mg/L
Zinc	0.207 - 0.275 mg/L

4.2.2 Cake layer cryosectioning and collection

A series of small pieces of cake layer (1 cm×1 cm) were cut from the same piece of membrane with cake layer on its surface. In order to prevent the structure and thickness of cake layer from change, the cake layer was saturated with 0.85 % NaCl aqueous solution (Zhang and Bishop, 1994) and then frozen at -22 °C before being fixed on to a sample stage using optimal cutting temperature (O.T.C) compound (Sakura Finetechnical Co., Ltd. Tokyo, 103, Japan).

As shown in Fig. 4-1, these small pieces of cake layer samples were cut into horizontal slices by using a microtome blade (Feather, S35 type, Japan) from the cake layer surface down to the bottom (membrane surface) at 100 µm intervals with a cryostate microtome (Histostate Microtome, Model: 855, Reichert Scientific Instruments Division of Warner Lambert Technologies Inc., NY, USA), which comprises a microtome and a cooling enclosure to set the temperature at -22 °C while sectioning. The difference in this process for each small piece was that they were cut at different degree. The first piece was kept intact and subjected to top cake layer observation by CLSM. For the

second piece, only 5 or 7 slices were cut from it depending on the thickness of the cake layer. And 7 to 10 slices were cut from the third piece. The rest was done in the same manner until the last piece which was cut from the cake layer surface to the entire depth of the cake layer. These slices were then observed by COM. After removing the cryosectioned slices for COM observation, the rest of the cake layer samples attached to the membrane surface were prepared for CLSM examination to investigate the structure of cake layer and for FTIR spectra at different depths. Meanwhile, cross-section of the corresponding cake layer samples was also cryosectioned. For thick cake layer samples, cake layer thickness was estimated by counting the number of slices and adding them together.

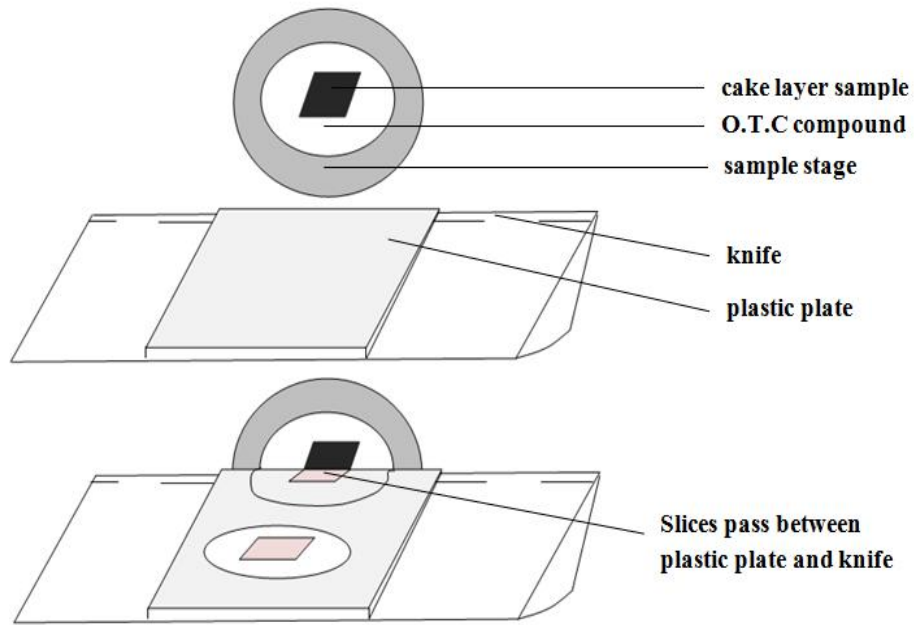


Figure 4-1 Cake layer cryosectioning.

The three layers of cake sludge samples (top cake layer, middle cake layer and bottom cake layer) for some other measurements (density, FTIR, EPS, PSD and microbial community) were obtained by gently scraping off cake layers with care from the membrane surface using a plastic sheet. The thickness of each layer (approximately 200 - 400 μm) was estimated by weighing the scraped sludge from a knowing surface area and a cake layer density measured in this study. This operation was according to

some previous studies (Fan and Zhou, 2007; Wang et al., 2008). The upper layer of the cake was loose and was not obviously compressed, and the middle layer was moderately compressed, which can be felt when use a plastic sheet to scrape it off from the whole cake layer. The rest of the cake layer samples attached to the membrane surface was used as the bottom layer. The separated layers were then subjected to the density, EPS, PSD, and microbial community analyses.

4.2.3 Analytical techniques used for cake characterization

4.2.3.1 Physical structure characterization of cake layer

4.2.3.1.1 COM observation

Cryosectioned slices were observed by conventional optical microscopy (Olympus, Japan) to investigate the physical structure (areal porosity) of sludge cake layers formed on membrane surfaces along the depth. The details for porosity determination from the COM images were given in Gao et al. (2010).

4.2.3.1.2 CLSM observation and image analysis

The cake layer samples from the micro-tome slicing for CLSM observation were stained collectively with Sypro Orange (Invitrogen) to target all the proteins and Concanavalin A, Alexa Flour 633 conjugate (5 mg/L, Invitrogen) to target the polysaccharides (α -Man, α -Glu(polysaccharide)) (Shen et al., 2010) in EPS matrix. The CLSM images were obtained as described in detail by Lin et al. (2009). The purpose of the staining was to investigate the coverage and distribution of EPS matrix along cake depth.

Analysis of the CLSM images was accomplished with the following software packages. The images in three dimensions were reconstructed by Image Structure Analyzer in 3 Dimensions (ISA3D) designed by the Center for Biofilm Engineering at Montana State University to describe biofilm morphology in three dimensions (Beyenal et al., 2004). The substratum coverage of EPS matrix were calculated using the PHLIP

program - a new laser scanning microscope image processing package which was implemented as a MATLAB package running under MATLAB (Xavier et al., 2003).

4.2.3.1.3 Density and water content measurement

The wet density of top, middle and bottom layer was measured by using a 10-mL calibrated cylinder with a known total mass (M_1) and a known pure water volume (V_1) in it (Zahid and Ganczarczyk, 1994). Each layer was put into the cylinder to get a new total mass (M_2) and a volume (V_2). The cake layer density (D) was then calculated by Equation (4-1):

$$D = \frac{M_2 - M_1}{V_2 - V_1} \quad (4-1)$$

The water content of top, middle and bottom cake layer was measured by generally drying the samples in an oven at 105 °C for 24 hours. The samples was dried and weighed again to determine the water content which was expressed in terms of the mass of water per unit mass of the wet samples.

4.2.3.1.4 PSD analysis

Cake layers samples were carefully scraped off from membrane surfaces using a plastic sheet, and were prepared by rinsing sludge samples with distilled water followed by gently shaking to form uniform liquor. The PSDs of and the three layers of cake layers were determined by a Malvern Mastersizer 2000 instrument (Worcestershire, UK) as described by Gao et al. (2010).

4.2.3.2 Chemical structure characterization of cake layer

4.2.3.2.1 EDX analysis and FTIR analysis

The cake layer samples were placed in a dryer at 105 °C for 24 h to obtain dry foulants. A Bruker Ten 37 FTIR Spectrometer (Bruker Co., Ltd.) and the SEM coupled with an energy-diffusive X-ray analyzer (JEOL JSM 5900 LV) were used to determine the major functional groups of the foulants and the chemical components of the cake layer, respectively.

4.2.3.2.2 EPS extraction and measurement

The bound EPS of top, middle and bottom cake layer was extracted according to a cation exchange resin (CER) (Dowex® Marathon® C, Na⁺ form, Sigma-Aldrich, Bellefonte, PA) method (Frølund et al., 1996). The detailed methods for EPS extraction and chemical analysis are described by Lin et al. (2009). For comparison purpose with the CLSM EPS coverage, the EPS content from chemical analysis was calculated as mg EPS/g dried sludge, and then converted into mg EPS/cm³ wet sludge, based on the results of sludge water content and density measured in this study.

Statistical analysis was performed to identify the correlation between extracted EPS content and CLSM image analysis results by means of linear correlations using the Statistical Package for the Social Science (SPSS) V11.0 produced by SPSS Incorporation (America). Pearson's product momentum correlation coefficient (r_p) was used for linear estimations of the strength and direction of linear correlations between every two parameters. The Pearson coefficient ranges between -1 and $+1$, where $r_p = -1$ or $+1$ means a perfect correlation, and 0 means an absence of a relationship (Wang et al., 2006). Correlations were considered statistically significance at a 95% confidence interval ($p < 0.05$).

4.2.3.3 Microbial community

Top cake layer, middle cake layer and bottom cake layer were collected and subjected to DNA extraction respectively by using Fecal DNA isolation kit (MoBio Laboratories, Solana Beach, CA, USA) according to the protocol described by the manufacturer. PCR amplification and DGGE of the PCR products were performed by following the procedures reported by Lin et al. (2011). Two samples were analyzed at different TMPs. Duplicate measurements were conducted for each sample.

4.3 Results and discussion

4.3.1. Process performance

The SAnMBR system was operated for over 7 months in total for thermo-mechanical pulping whitewater treatment. There were some variations in terms of

feed COD, membrane flux, and MLSS, as indicated in the study of Lin et al. (2011). During the sampling period of this study (135 days, from day 85 to day 220), the SAnMBR was loaded at average rates of 1.80 ± 0.14 kg COD/m³·d. The membrane flux was maintained at a value of 4.60 ± 0.25 L/m²·h. The influent COD concentrations fluctuated from 1823 to 3504 mg/L, while permeate COD value changed between 217.5 mg/L and 425.1 mg/L. The steady-state COD removal efficiency was about 87 %. The MLSS concentration was controlled at 8.7 ± 0.4 g/L.

The typical evolution cycle of TMP (from day 100 to day 137) with elapsed time is demonstrated in Fig. 4-2. An obvious three-stage TMP profile was observed with an initially short term rapid TMP rise (lasted for 4 hours from 4 kPa to 22 kPa, stage 1) followed by an extended slow TMP rise period (lasted for 37 days from 22 kPa to 31 kPa, stage 2) and a transition to a rapid TMP rise (lasted for 2 days from 31 kPa to 43.5 kPa, stage 3). At the end of stage 3, physical and chemical cleaning procedure were carried out to remove membrane fouling and to recover the membrane permeability.

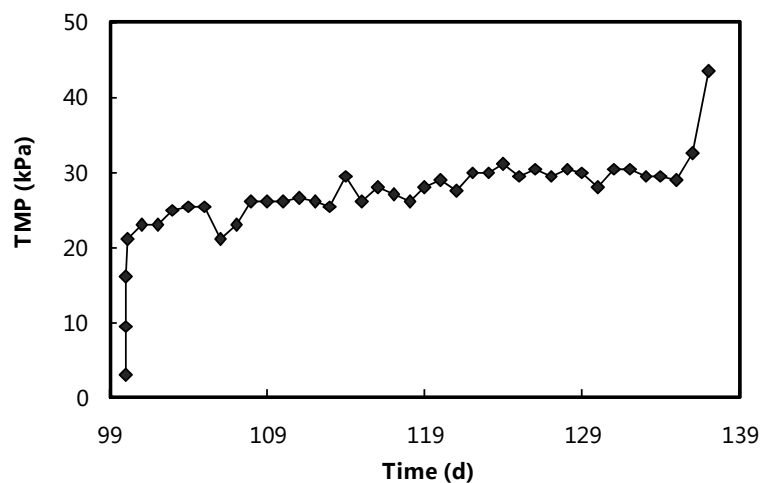


Figure 4-2 Typical TMP profiles plotted with operational time (Flux = 4.57 ± 0.20 L/m²h; MLSS = 8.5 ± 0.20 g/L; biogas sparging rate = 1.5 L/min).

The three-stage TMP profile was frequently observed in SAnMBR systems. Several possible mechanisms for stage 3 TMP rise, such as local flux effect, pore narrowing, pore loss and percolation theory have been proposed, and they were summarised by Zhang et al. (2006a).

4.3.2 Physical structure of cake layer

4.3.2.1 Thickness of cake layer

Microscopic image clearly showed that the cake layer thickness increased with the operation time (Fig. 4-3). The image of the cross-section of the cake layer formed after 5 days (Fig. 4-3b) illustrated three distinct layers along the cake depth. The top layer is composed of both gel like substances and loose sludge depositions, the middle layer is porous and modest compressed, and the bottom layer is dense and compressed, showing an inhomogeneous structure. This structure was also observed in our previous study (Lin et al., 2011). The final cake thickness after TMP jump occurred was measured as 1900 - 2100 μm (image not present). While this thickness was high, it is comparable to those reported by some researchers (Freitas dos Santos and Livingston, 1994; Chu and Li, 2006). Therefore, to better understand the spatial distribution of the structure of a thick cake layer, the use of CLSM and COM, coupled with micro-tome slicing technique is necessary.

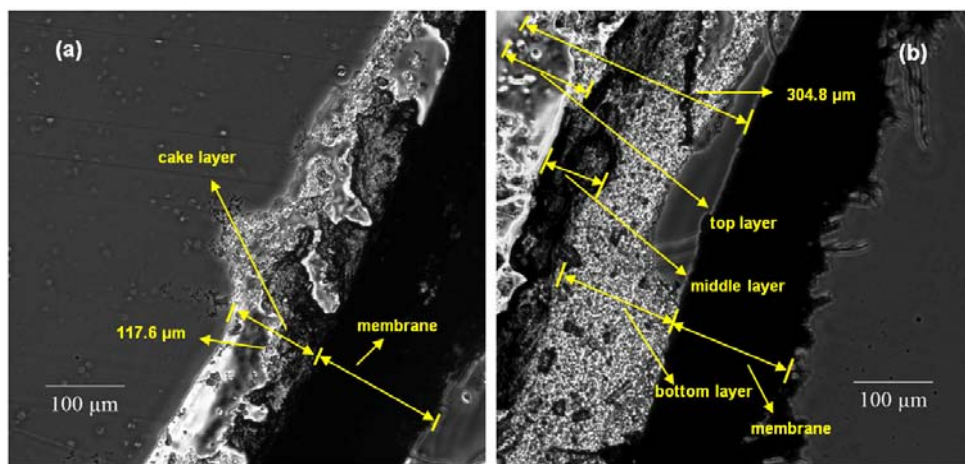


Figure 4-3 Cross section of cake layer observed by COM: (a) after one day of operation, and (b) after 5 days of operation.

The growth of cake layer would certainly increase filtration resistance. However, the thickness of cake layer did not always coincide with the membrane fouling development. For example, during the early period of stage 2, thickness of cake layer increased quickly to about 900 μm , while the average membrane fouling rate was only

9.98×10^{10} m/d, which was over two orders of magnitude lower than the value of 2.38×10^{13} m/d determined for the period where the second TMP jumping occurred. This observation is in agreement with the findings of Hwang et al. (2008) who reported that the average thickness of cake layer could not explain the TMP profile.

4.3.2.2 Porosity

The COM images of cryosectioned slices (Fig. 4-4) show that the cake layer was not of a uniform structure, and the areal porosity decreased from the top layer to the bottom layer. Fig. 4-5 presents cake porosity profiles at different TMPs. It is evident in Figs. 4-4 and 4-5 that areal porosity of cake layer shows a decrease trend from top layer to bottom layer, and a higher TMP corresponds to lower cake layer porosity. The change in areal porosity with a thick cake layer in this study is generally consistent with the observation of CLSM porosity of thin cake layers in aerobic MBRs (Hwang et al., 2008) in that the areal porosity decreased from top to bottom cake layers. The decrease in areal porosity with an increase in TMP (Fig. 4-5) suggests that the areal porosity continuously decreased with experimental time and TMP jump in the 3rd stage might be due to the loss of porosity to a critical value where local flux effect plays an important role (Zhang et al., 2006a). The results from this study suggest that micro-tome technique can be used to study areal porosity of thick cake layers, which is limited for CLSM application.

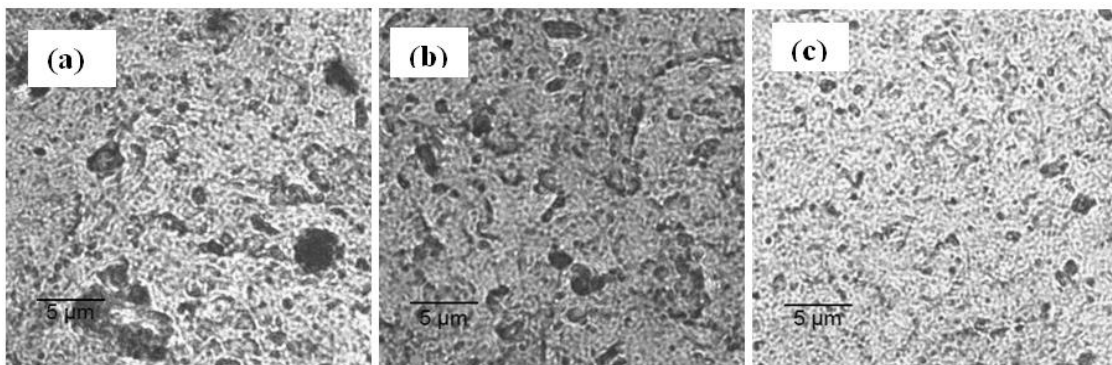


Figure 4-4 COM images of cryosectioned slices of: (a) top cake layer, (b) middle cake layer, (c) bottom cake layer.

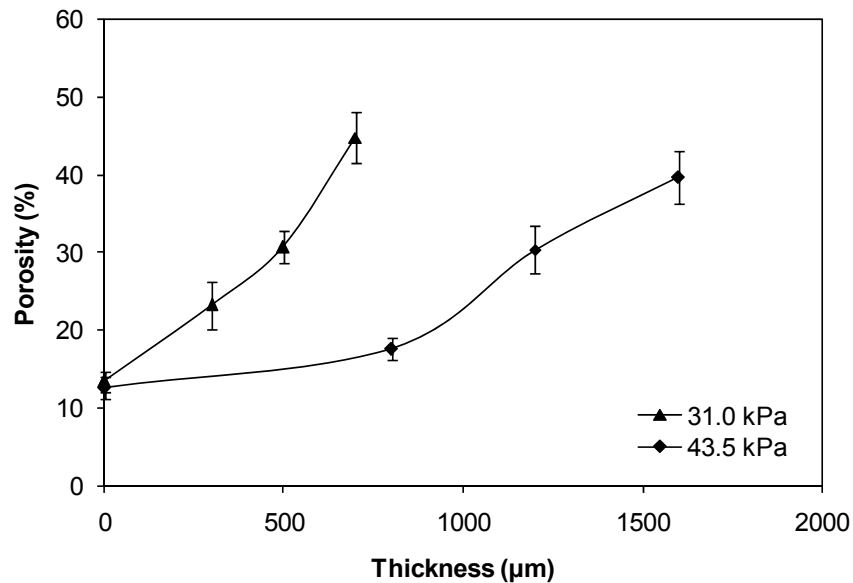


Figure 4-5 Cake layer area porosity distribution with thickness under different TMP.

4.3.2.3 Particle size distribution

The particle size distributions (PSDs) of cake layers (TMP = 43.5 kPa) at different depths are presented in Fig. 4-6. When compared to bulk sludge showed in our previous study (Lin et al., 2011), the top cake layer and middle cake layer had a broader range of PSDs. More importantly, a peak of particles distributed in a size range from 0.1 to 1 μm can only be observed in top cake layer and middle cake layer. The profiles in Fig. 4-6 showed the following order of mean particle size of the three different layers: top cake layer < middle cake layer < bottom cake layer. The larger size of flocs in bottom cake layer was probably due to the effect of the long-term continuous compression (Hong et al., 2007). The small particles portion in the top and middle cake layers indicated that small flocs had a strong tendency to deposit on the membrane surface. This result is in line with the study of Meng et al. (2007) who reported that mean size of the washed liquid of cake layer was much lower than that of bulk sludge. Wang et al. (2008) also observed that gel layer formed on the membrane surface had a smaller PSD compared to bulk sludge.

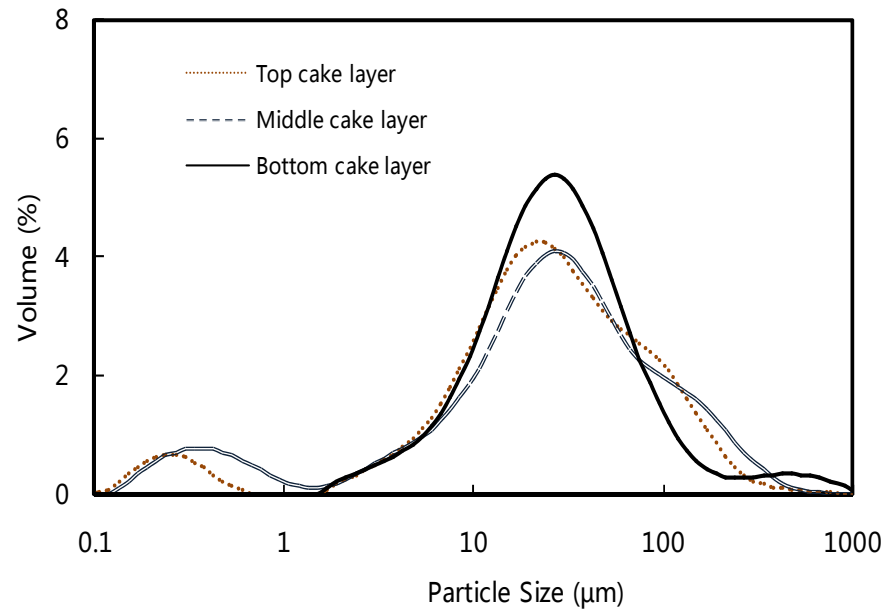


Figure 4-6 Particle size distributions of cake layers at different depths.

The development of membrane fouling was clearly indicated by the continuous TMP increase with time in Fig. 4-2. In general, the cause of membrane fouling is due to initial pore blocking followed by cake formation. Initially, sludge flocs had a size that is close to or smaller than the size of membrane pores would penetrate into and block the membrane pores easily. The number of particles with different sizes reported in Fig. 4-6 shows that about 65 % of the particles in the top cake layer have a size smaller than 0.3 μm , while the membranes used in this study has a pore size of about 0.3 μm . Therefore, pore blocking fouling could be predominant in the initial stage of filtration and responsible for the first jumping in the three-stage TMP profile. The continuous MBR water production brought about continuous sludge deposition on the membrane, which caused cake formation to be the dominant membrane fouling mechanism.

In summary, our findings revealed that the cake layer was not spread uniformly in term of PSD, and small flocs had a stronger tendency to deposit on the membrane surface. A shift of PSD to large size in bottom cake layer was observed, and this could be attributed to the consolidation effect caused by long-term continuous compression.

4.3.2.4 EPS matrix morphology

In the cake layer the bacteria cells are closely packed and embedded in a matrix of EPS (Kim et al., 2001). The EPS matrix determines the living conditions of cells in this microenvironment. Fig. 4-7 presents the spatial distribution of EPS matrix of the stained cake layer at different depths. The images in three dimensions reconstructed by ISA3D visually show that the EPS matrix was not of a uniform structure and the coverage of EPS (white area coverage) increased from top to bottom cake layer.

Meanwhile, substratum coverage of protein and polysaccharides in EPS were calculated from the binary image stacks through automated thresholding of PHLIP. PHLIP calculates the fraction of pixels occupied by protein or polysaccharides for each image and then transforms to percentage (Xavier et al., 2003). Analysis based on CLSM images (Table 4-2) shows that the substratum coverage decreased from the bottom layer to the top layer, which was consistent with the observation from the reconstructed 3D images. Therefore, the EPS matrix was more widespread at the cake layer bottom than on the cake layer outer surface. This could be due to the compression of cake layer at the bottom layer.

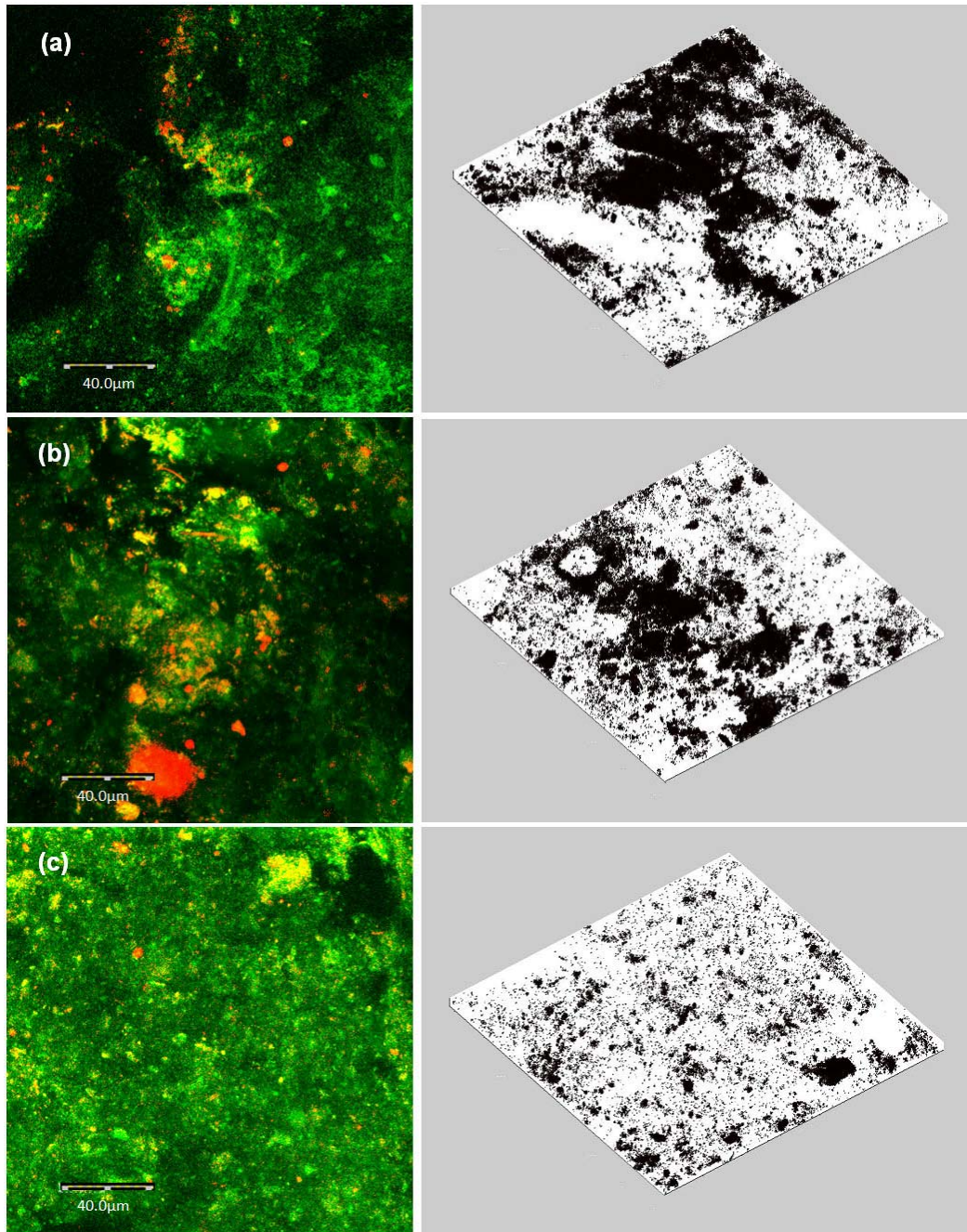


Figure 4-7 CLSM images of cake layer at different depths with 3D reconstruction images on the right accordingly (TMP=43.5kPa): (a) cake layer outer surface; (b) 1200 μm away from the cake outer surface; (c) 1900 μm away from the cake outer surface. Proteins were stained with Sypro Orange (green) and polysaccharides were stained with ConA (red). The white parts of the 3D reconstruction images correspond to the area covered by EPS, and the black parts correspond to other area of the cake layer (area covered by cells and vacancy).

Table 4-2

Structural parameters of the cake layers

TMP (kPa)	Thickness(μm) (From bottom to top)	Substratum coverage (%) of EPS	
		Proteins	Polysaccharides
43.5	0	87.33 ± 1.42	7.10 ± 3.07
	700	76.69 ± 3.29	5.23 ± 2.61
	1500	52.15 ± 4.16	4.10 ± 1.42
	1900	37.72 ± 5.77	1.56 ± 0.25
31.0	0	85.24 ± 1.98	7.51 ± 3.25
	500	71.30 ± 3.82	6.53 ± 0.95
	700	52.15 ± 4.16	3.69 ± 0.60
	900	49.55 ± 3.36	2.32 ± 0.64

4.3.3 Chemical structure

4.3.3.1 FTIR analysis

The FTIR spectrum of cake layers formed at TMP of 43.5 kPa at different depths are presented in Fig. 4-8. The three samples contained proteins as indicated by the peaks at 1647 cm^{-1} (stretching vibration of C=O and C-N amide I) and 1543 cm^{-1} (N-H deformation and C=N stretching amide II), and polysaccharides (3325 cm^{-1} due to stretching of the O-H bonds and 1042 cm^{-1} due to C-O stretching, polysaccharides, aromatics, characteristics for polysaccharides), as well as humic acids as indicated by the peaks at 1740 cm^{-1} (asymmetrical stretching vibration of COO^-) (Jarusutthirak et al., 2002; Kimura et al., 2005; Kim and Jang, 2006). The peak at 1389 cm^{-1} is typical for phenolic OH^- , COO^- and CH_3COO^- . Peaks in the vicinity of 2934, 2891 and 1468 cm^{-1} are indicative of the C-H bonds in the alkanes class (Kim and Jang, 2006). It is evident from above observations that proteins, polysaccharides and humic acids were presented in the sludge cake layers, suggesting a significant organic fouling which mainly stemmed from EPS. The presence of proteins and polysaccharides in the cake layer was also proven by CLSM observation (Fig. 4-7). Bands observed in the ‘‘fingerprint’’ region ($<1000 \text{ cm}^{-1}$) could be attributed to the phosphate and sulfate groups arising from nucleic acids (Guibaud et al., 2003) as well as the feed. This indicates that besides organic fouling, inorganic fouling took some responsibilities for total membrane fouling.

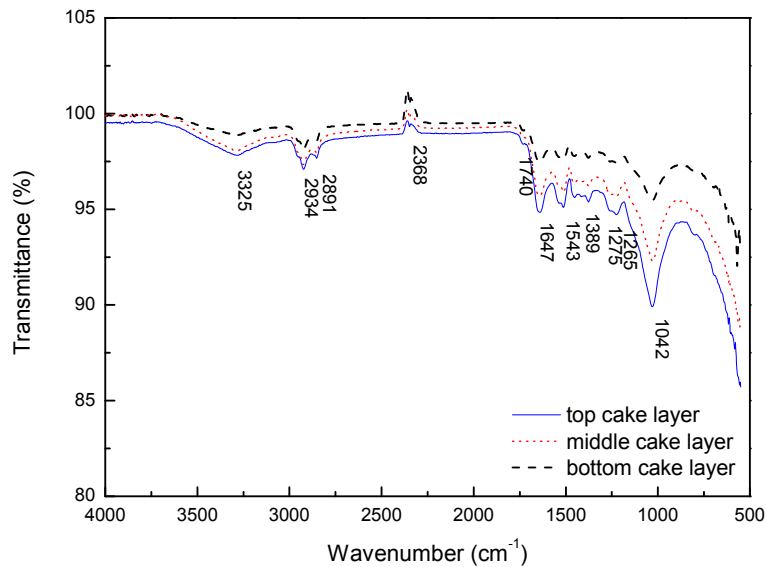


Figure 4-8 FTIR spectrum of top, middle and bottom cake layers.

4.3.3.2 Extracted EPS content

In our previous study, Lin et al. (2011) found that the cake layer had higher EPS content (both proteins and polysaccharides) than that of bulk sludge, indicating significant EPS accumulation in the cake layer. In this study, we mainly focus on the EPS content of the cake layer along its depths. Fig. 4-9(a) presents the extracted EPS content calculated as EPS weight per unit dry weight of the cake layers with different depths. The cake layer samples were collected at TMP values of 43.5, 35.0 and 44.5 kPa on day 137, 176 and 211, respectively. For each layer of the sludge cake, proteins were the predominant component. Furthermore, there were no significant differences in the total EPS content with variations in depth in cake layers, while proteins content in cake layer appeared to decrease and polysaccharides content in cake layer showed an increase tendency from top layer to bottom layer, presenting a decreased ratio of proteins to polysaccharides along its depth from top to bottom layer. The higher proteins content in the top cake layer may be due to the presence of an abundant amount of loose bound EPS which consists mainly of proteins as suggested by Li and Yang (2007). Mikkelsen and Keiding (2002) observed a positive correlation between the protein content (calculated as mg/g dry cake sludge) and the water-holding capacity of EPS protein. Measurement of water content showed that the top cake layer contained 96 % water, much higher than the

value of 91 % and 89 % for the middle and bottom cake layer, respectively. As the thickness of cake layer grows, more bound water, as well as loose bound EPS (mainly proteins) would be lost as a result of cake layer compression at the bottom layer. Polysaccharides are extracellular components synthesized for a specific function (Lee et al., 2003). The stressful micro-environment of the bottom layer might promote the bacteria to synthesize polysaccharides for survive. The developed endogenous environment due to limit of substrate transfer in the bottom layer may also induce cell lysis and release of polysaccharides (Drews et al., 2007). This would be helpful to explain the increased polysaccharides content along cake layer depth. According to Lee et al. (2003) and Massé et al. (2006), the affinity of sludge flocs for proteins could be greater than polysaccharides due to their hydrophobicity and surface charge. Therefore, sludge with a higher ratio of proteins to polysaccharides in EPS, as shown in the top cake layer, is considered to have high stickiness and thus favour the development of cake formation. This argument is consistent with the direct observation of the different cake layers which showed the top cake layer was very slime compared to the middle and bottom cake layers. In a submerged MBR system, because the top cake layer is always exposed to shear force caused mostly by biogas scouring, flocs with higher EPS content, especially higher protein content, are expected to have greater opportunities to attach to form a new protein-rich cake layer.

However, we surprisingly noticed that the extracted EPS protein content (as mg/g dry cake sludge) showed the opposite trend with the substratum coverage results (protein) of CLSM image analysis. This could be due to the changes in sludge water content and density along cake depth and the substratum coverage of EPS from CLSM images is based on volume or measured area. In order to compare the extracted EPS content with the CLSM image analysis results, the EPS content was then converted to EPS weight per unit volume of wet cake sludge according to the water content and the density of top cake layer ($1.0099 \pm 0.0103 \text{ g/cm}^3$), middle cake layer ($1.0617 \pm 0.0133 \text{ g/cm}^3$) and bottom cake layer ($1.1022 \pm 0.0800 \text{ g/cm}^3$). As shown in Fig. 4-9(b), protein, polysaccharides and total EPS in cake layer (as mg/cm^3 wet cake sludge) all showed the same tendency with substratum coverage (Table 4-2): an increase from top layer to bottom layer. There

was no statistically significant correlations between the substratum coverage and extracted EPS content (as mg/g dry cake sludge) ($p > 0.05$), whereas Fig. 4-10 illustrates there were significant correlations between the substratum coverage and extracted EPS content (as mg/cm^3 wet cake sludge) of both protein ($r_p = 0.891$; $p = 0.001$) and polysaccharides ($r_p = 0.950$; $p < 0.001$). The results indicate that CLSM images of EPS matrix are consistent with the findings of chemical extraction and analysis of EPS content. These results further confirmed the heterogeneous spatial distribution of EPS in cake layer from both CLSM images and chemical analysis of EPS matrix.

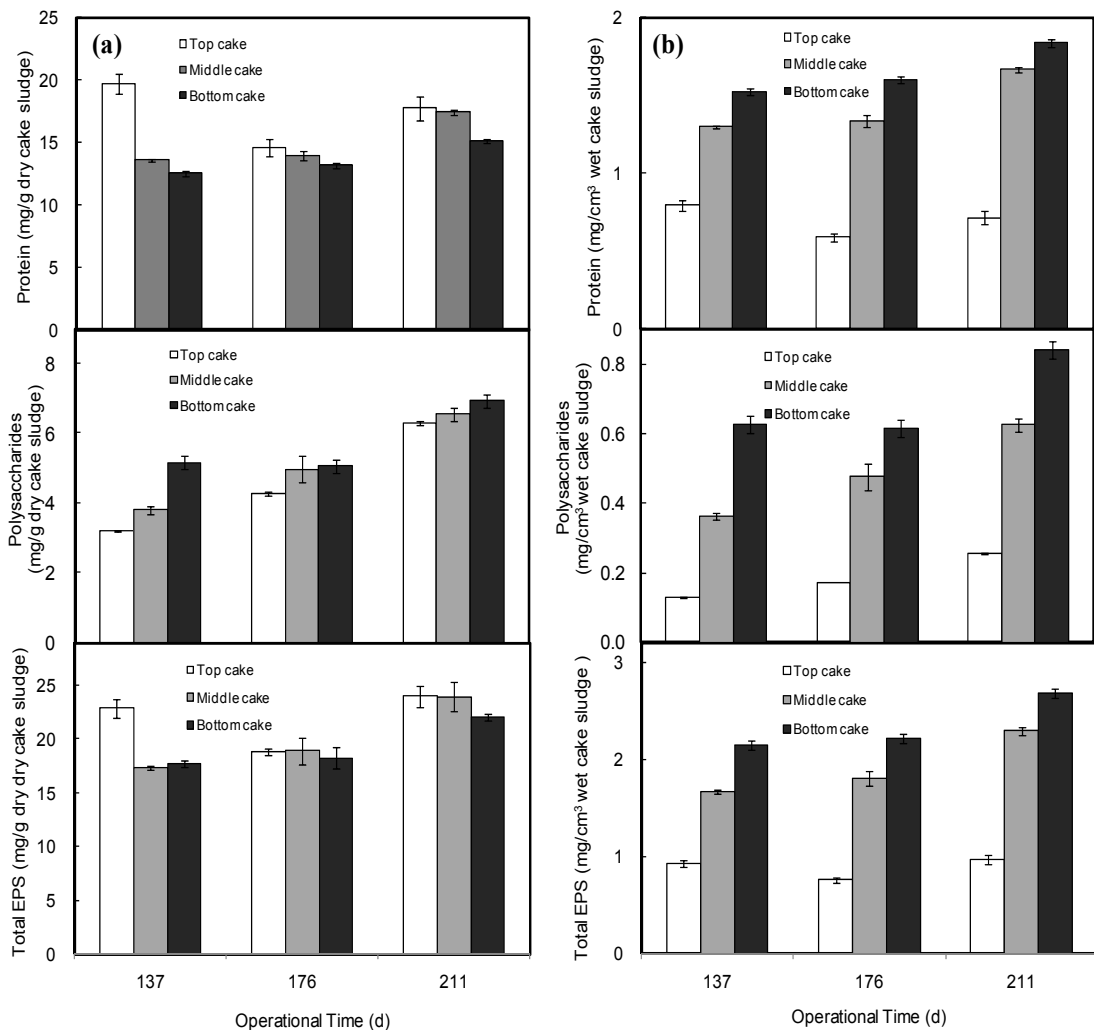


Figure 4-9 Extracted EPS content in the top, middle and bottom cake layers: (a) calculated as EPS weight per unit cake layer dry weight and (b) calculated as EPS weight per unit volume of wet cake layer.

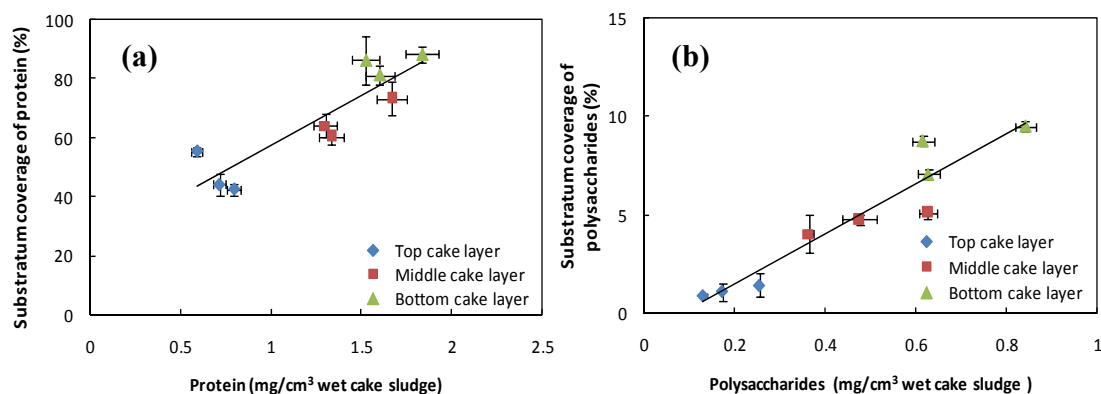


Figure 4-10 The correlation between the content of EPS (calculated as EPS weight per unit wet weight of the cake layers) and the substratum coverage of: (a) protein ($r_p=0.891$; $p=0.001$) and (b) polysaccharides ($r_p=0.950$; $p=0.000$).

4.3.3.3 EDX analysis

Gel layer represents the initial stage of cake layer. Fig. 4-11 presents the comparison of elemental composition of the cake layer and gel layer. Generally, the elements of C, O, Na, Mg, Al, F, Cl, S, Si, P, K, and Ca were detected in both cake layer and gel layer by SEM-EDX system (Fig. 4-11). This is not surprising. During the operation of SAnMBR, a great many of the metal clusters or metal ions presented in influent water, and nutrients would present the origin of inorganic fouling. The inorganic elements may exert significant effects on the formation of cake layer. Through concentration polarization (Sheikholeslami, 1999), charge neutralization (Seidel and Elimelech, 2002) and bridging, metal clusters and metal ions would be caught by the flocs or biopolymers (Hong and Elimelech, 1997). It has been reported that deposition of inorganic foulants played a key role in the formation of the strongly attached cake layer limiting membrane permeability in anaerobic bioreactor (Choo and Lee, 1996). It was also reported that the internal SAnMBR had a severe inorganic fouling problem with calcium addition to the system (You et al., 2006). Therefore, the inorganic precipitation coupled the organic foulants would enhance the formation of cake layer and thus caused the membrane fouling problem in SAnMBR systems.

It can also be seen from Fig. 4-11, more Ca element was detected in the cake layer, indicating a high level of mineralization in cake layer, which certainly enhance membrane fouling potential of cake layer.

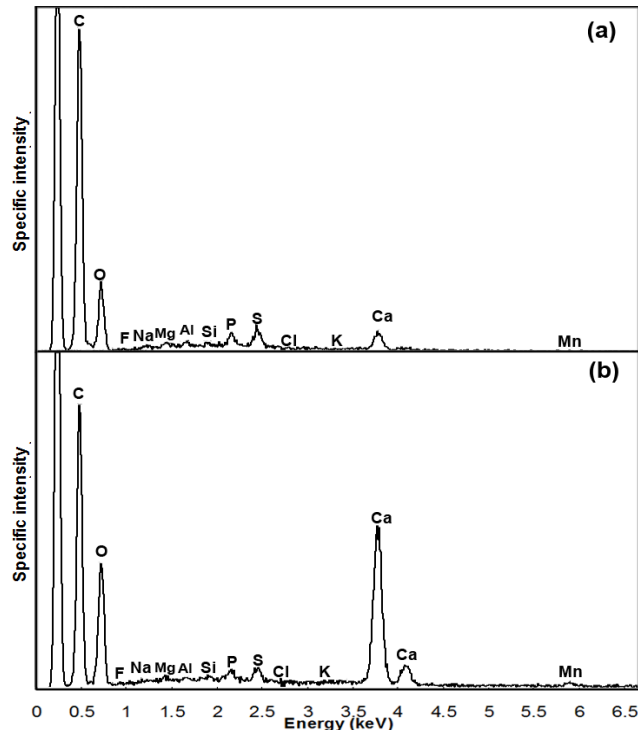


Figure 4-11 EDX analysis for: (a) gel layer and (b) cake layer.

4.3.4 Microbial community

The microbial community in the bulk sludge and the cake layers (TMP = 31.0, 43.5 kPa) at different depths (top, middle and bottom cake layer) was analyzed and compared by PCR-DGGE analysis (Fig. 4-12).

From Fig. 4-12, it is clear that populations represented by bands 1, 3, 6, 10, 11, 14, 15, 16, 18, 19, 20, 21, 22, 24, 25, 26, 27, 28 and 29 were presented in all the four samples. They were the main composition of microbial community in bulk sludge and cake sludge. Generally speaking, there was limited difference in species diversity between bulk sludge and cake sludge. This is consistent with the fact that the bulk sludge was the source of the cake sludge on the membrane surface. The less significant difference in microbial diversity between bulk sludge and cake sludge, as compared to the finding of our previous study (Lin et al., 2011), might be due to the temporal variation of the microbial

community structure (i.e. difference in cake age) in cake layers. The results suggest that a study on potential temporal change in microbial community in bulk and cake sludge is needed. Of particular interest is the microbial community of bulk and cake sludge at the initial stage of cake formation. The results from the present study indicate that there were visible changes in the intensity of some species along the cake layer depth. For example, the intensity of bands 12 and 29 was particularly high in the bottom layer while they were weak in the top and middle layers, populations represented by bands 5, 9, 13 and 23 were more abundant in the bottom layer than in the top and middle layers. In contrast, compared to the top and middle layers, the intensity of bands 4, 6, 20, 21, 24, 25 and 27 was weaker in the bottom layer, indicating the reduced density of these populations in the bottom layer. Among the three layers, DGGE banding patterns of the top and middle cake layers were more similar than that between middle and bottom layers. The results indicate that microbial community changed along cake layer depth. The diversities and their changes can be attributed to the different micro-environment due to the differences in the substrate transfer.

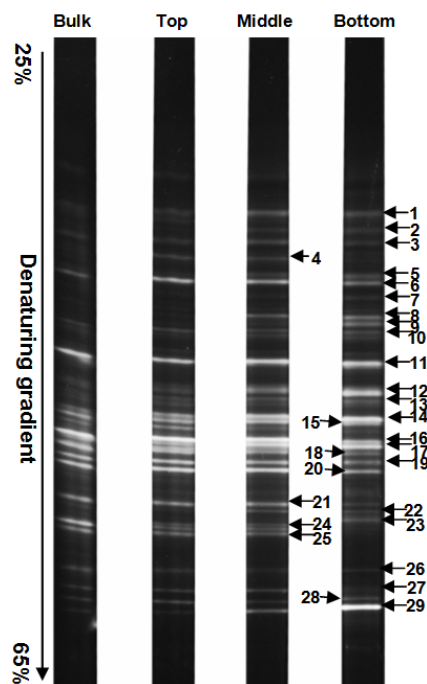


Figure 4-12 PCR-DGGE fingerprints of 16S rDNA gene fragments amplified from DNA extracted from bulk sludge and cake sludge at different depths.

All of the previous mechanisms of three-stage TMP rise seemed to miss taking into account the changes of microbial community of the sludge cake during MBR operation. Microbial community may exert significant effects on membrane fouling. It was suggested that some bacteria, like *Acinetobacter* sp. tends to be sticky, and caused the most severe fouling in MBR under the relatively static condition (Choi et al., 2006). Since some changes in microbial community were found in cake layers, the effect of microbial characteristics on membrane fouling should not be overlooked.

4.3.5 Relation to membrane fouling

The structure of cake layer appears to be a key factor that regulates the development of membrane fouling. TMP was correlated to some extent with cake layer porosity. Fig. 4-5 clearly shows that TMP increased as cake layer porosity decreased. The formed cake layer (Fig. 4-3) would function as a secondary membrane, and cake porosity seems to govern TMP evolution. For constant flux operation, the local flux would increase as cake porosity decreases. Previous studies (Cho and Fane, 2002; Wang et al., 2008) have shown that sub-critical flux conditions could prevent a rapid TMP increase while operation above critical flux would cause dramatic TMP increase. According to the inhomogeneous area loss model (Cho and Fane, 2002), the local flux would reach values where $dTMP/dt$ was rising rapidly leading to acceleration of TMP typical of stage 3 due to the decrease in cake porosity. It is hypothesized that cake layer porosity decreases continuously with time due to consolidation, as shown in Fig. 4-5, and when the porosity decreases to a critical point that the applied membrane flux is larger than the critical flux, a second TMP jump is anticipated.

The exact cause for the significant change in cake porosity needs to be identified. Obviously, filtration compression is the direct cause of the change in cake porosity. As discussed above, the amount of EPS content in cake layer played a critical role in the cake layer development. However, analysis of data in Fig. 4-5 and Fig. 4-9(a) shows that there is a lack of correlation of cake porosity with the total EPS content (as mg/g dry cake sludge). This suggests that the total EPS content is not the cause of change of cake porosity along cake layer depth. From another point of view, the spatial distribution of EPS density (Fig. 4-7, Table 4-2 and Fig. 4-9 (b)) and cake layer porosity (Fig. 4-5) show

that from the top to the bottom cake layer, the more widespread EPS matrix is, the less porous cake layer is. Therefore, the spatial distribution of EPS matrix plays a role to determine the cake porosity. Microbial community analysis revealed that there were significant changes in population densities along the different cake layers (Fig. 4-12), and these findings will need to be correlated to cake porosity and membrane fouling in further work.

4.4 Conclusions

The experimental analysis in this study was based only on the cake layer investigation and parameter variations with cake depth. The spatial distribution of physical, chemical and microbiological structure of cake layer from an SAnMBR was characterized using various analytical tools. The results provide a new insight in cake layer structure and suggest that structures change significantly from the top layer to the bottom layer. The main conclusions are summarized below.

- Micro-tome slicing technique can be effectively used for cake layer structure spatial distribution characterization, when combined with other techniques. The porosity of cake layer decreased from top layer to bottom layer.
- Particle size distribution of cake layer changes from the top layer to bottom layer. Smaller flocs had a higher tendency to accumulate on membrane surfaces but the consolidation of cake sludge in the bottom layers resulted in larger flocs as compared to the fresh cake sludge formed on the top layers.
- The relative concentration of EPS density and composition changed along the cake depth. The results of both the CLSM images and chemical analysis of EPS matrix suggest that EPS density (mg EPS/cm^3 wet sludge) in cake layer increased from top to bottom cake layer and the ratio of proteins to polysaccharides in EPS decreased from the top to bottom layers. The EPS results suggest a heterogeneous structure of EPS along cake layer depth and not only the EPS content but also the spatial distribution of EPS matrix would affect cake layer formation.
- PCR-DGGE study showed that there were significant differences in microbial community population density along the cake layer depth.

- Through the CLSM and COM images, cake layer was found to have a loose outer surface when compared with the bottom cake layer. The water content of cake layers decreased from top to bottom cake layers.

4.5 References

- Beyenal, H., Donovan, C., Lewandowski, Z., Harkin, G., 2004. Three-dimensional biofilm structure quantification. *Journal of Microbiological Methods* 59, 395-413.
- Cho, B. D., Fane, A. G., 2002. Fouling transients in nominally sub-critical flux operation of a membrane bioreactor. *Journal of Membrane Science* 209, 391-403.
- Choi, H., Zhang, K., Dionysiou, D. D., Oerther, D. B., Sorial, G. A., 2006. Effect of activated sludge properties and membrane operation conditions on fouling characteristics in membrane bioreactors. *Chemosphere* 63, 1699-1708.
- Choo, K.-H., Lee, C.-H., 1996. Membrane fouling mechanisms in the membrane-coupled anaerobic bioreactor. *Water Research* 30, 1771-1780.
- Chu, H. P., Li, X. Y., 2005. Membrane fouling in a membrane bioreactor (MBR): sludge cake formation and fouling characteristics. *Biotechnology and Bioengineering* 90, 323-331.
- Chu, L., Li, S., 2006. Filtration capability and operational characteristics of dynamic membrane bioreactor for municipal wastewater treatment. *Separation and Purification Technology* 51, 173-179.
- Di Bella, G., Mannina, G., Viviani, G., 2008. An integrated model for physical-biological wastewater organic removal in a submerged membrane bioreactor: Model development and parameter estimation. *Journal of Membrane Science* 322, 1-12.
- Drews, A., Mante, J., Iversen, V., Vocks, M., Lesjean, B., Kraume, M., 2007. Impact of ambient conditions on SMP elimination and rejection in MBRs. *Water Research* 41, 3850-3858.
- Duffrèche, J., Prat, M., Schmitz, P., 2002. Effective hydraulic resistance of the first cake layers at the membrane surface in microfiltration. *Desalination* 145, 129-131.

- Fan, F., Zhou, H., 2007. Interrelated Effects of Aeration and Mixed Liquor Fractions on Membrane Fouling for Submerged Membrane Bioreactor Processes in Wastewater Treatment. *Environmental Science & Technology* 41, 2523-2528.
- Freitas dos Santos, L. M., Livingston, A. G., 1994. Extraction and biodegradation of a toxic volatile organic compound (1,2-dichloroethane) from waste-water in a membrane bioreactor. *Applied Microbiology and Biotechnology* 42, 421-431.
- Frølund, B., Palmgren, R., Keiding, K., Nielsen, P. H., 1996. Extraction of extracellular polymers from activated sludge using a cation exchange resin. *Water Research* 30, 1749-1758.
- Gao, W. J. J., Lin, H. J., Leung, K. T., Liao, B. Q., 2010. Influence of elevated pH shocks on the performance of a submerged anaerobic membrane bioreactor. *Process Biochemistry* 45, 1279-1287.
- Guibaud, G., Tixier, N., Bouju, A., Baudu, M., 2003. Relation between extracellular polymers' composition and its ability to complex Cd, Cu and Pb. *Chemosphere* 52, 1701-1710.
- Hong, S.-H., Lee, W.-N., Oh, H.-S., Yeon, K.-M., Hwang, B.-K., Lee, C.-H., Chang, I.-S., Lee, S., 2007. The Effects of Intermittent Aeration on the Characteristics of Bio-Cake Layers in a Membrane Bioreactor. *Environmental science and technology* 41, 6270-6276.
- Hong, S., Elimelech, M., 1997. Chemical and physical aspects of natural organic matter (NOM) fouling of nanofiltration membranes. *Journal of Membrane Science* 132, 159-181.
- Hu, A. Y., Stuckey, D. C., 2007. Activated Carbon Addition to a Submerged Anaerobic Membrane Bioreactor: Effect on Performance, Transmembrane Pressure, and Flux. *Journal of Environmental Engineering* 133, 73-80.
- Hwang, B.-K., Lee, W.-N., Yeon, K.-M., Park, P.-K., Lee, C.-H., Chang, i.-S., Drews, A., Kraume, M., 2008. Correlating TMP Increases with Microbial Characteristics in the Bio-Cake on the Membrane Surface in a Membrane Bioreactor. *Environmental Science and Technology*. 42, 3963-3968.

- Ivnitsky, H., Katz, I., Minz, D., Volvovic, G., Shimoni, E., Kesselman, E., Semiat, R., Dosoretz, C. G., 2007. Bacterial community composition and structure of biofilms developing on nanofiltration membranes applied to wastewater treatment. *Water Research* 41, 3924-3935.
- Jarusutthirak, C., Amy, G., Croué, J.-P., 2002. Fouling characteristics of wastewater effluent organic matter (EfOM) isolates on NF and UF membranes. *Desalination* 145, 247-255.
- Jeison, D., van Lier, J. B., 2007. Cake formation and consolidation: Main factors governing the applicable flux in anaerobic submerged membrane bioreactors (AnSMBR) treating acidified wastewaters. *Separation and Purification Technology* 56, 71-78.
- Kanai, M., Ferre, V., Wakahara, S., Yamamoto, T., Moro, M., 2010. A novel combination of methane fermentation and MBR -- Kubota Submerged Anaerobic Membrane Bioreactor process. *Desalination* 250, 964-967.
- Kim, I. S., Jang, N., 2006. The effect of calcium on the membrane biofouling in the membrane bioreactor (MBR). *Water Research* 40, 2756-2764.
- Kim, J.-S., Lee, C.-H., Chang, I.-S., 2001. Effect of pump shear on the performance of a crossflow membrane bioreactor. *Water Research* 35, 2137-2144.
- Kimura, K., Yamato, N., Yamamura, H., Watanabe, Y., 2005. Membrane Fouling in Pilot-Scale Membrane Bioreactors (MBRs) Treating Municipal Wastewater. *Environmental science and technology* 39, 6293-6299.
- Lee, C. H., Park, P. K., Lee, W. N., Hwang, B. K., Hong, S. H., Yeon, K. M., Oh, H. S., Chang, I. S., 2008. Correlation of biofouling with the bio-cake architecture in an MBR. *Desalination* 231, 115-123.
- Lee, W., Kang, S., Shin, H., 2003. Sludge characteristics and their contribution to microfiltration in submerged membrane bioreactors. *Journal of Membrane Science* 216, 217-227.
- Lee, Y., Clark, M. M., 1998. Modeling of flux decline during crossflow ultrafiltration of colloidal suspensions. *Journal of Membrane Science* 149, 181-202.

- Li, X. Y., Yang, S. F., 2007. Influence of loosely bound extracellular polymeric substances (EPS) on the flocculation, sedimentation and dewaterability of activated sludge. *Water Research* 41, 1022-1030.
- Liao, B.-Q., Kraemer, J. T., Bagley, D. M., 2006. Anaerobic Membrane Bioreactors: Applications and Research Directions. *Critical Reviews in Environmental Science and Technology* 36, 489 - 530.
- Lin, H., Liao, B.-Q., Chen, J., Gao, W., Wang, L., Wang, F., Lu, X., 2011. New insights into membrane fouling in a submerged anaerobic membrane bioreactor based on characterization of cake sludge and bulk sludge. *Bioresource Technology* 102, 2373-2379.
- Lin, H. J., Xie, K., Mahendran, B., Bagley, D. M., Leung, K. T., Liss, S. N., Liao, B. Q., 2009. Sludge properties and their effects on membrane fouling in submerged anaerobic membrane bioreactors (SAnMBRs). *Water Research* 43, 3827-3837.
- Mannina, G., Di Bella, G., Viviani, G., 2010. Uncertainty assessment of a membrane bioreactor model using the GLUE methodology. *Biochemical Engineering Journal* 52, 263-275.
- Massé, A., Spérandio, M., Cabassud, C., 2006. Comparison of sludge characteristics and performance of a submerged membrane bioreactor and an activated sludge process at high solids retention time. *Water Research* 40, 2405-2415.
- Meng, F., Zhang, H., Yang, F., Liu, L., 2007. Characterization of Cake Layer in Submerged Membrane Bioreactor. *Environmental Science and Technology* 41, 4065-4070.
- Mikkelsen, L. H., Keiding, K., 2002. Physico-chemical characteristics of full scale sewage sludges with implications to dewatering. *Water Research* 36, 2451-2462.
- Seidel, A., Elimelech, M., 2002. Coupling between chemical and physical interactions in natural organic matter (NOM) fouling of nanofiltration membranes: implications for fouling control. *Journal of Membrane Science* 203, 245-255.
- Sheikholeslami, R., 1999. Composite fouling - inorganic and biological: A review. *Environmental Progress* 18, 113-122.

- Shen, L., Zhou, Y., Mahendran, B., Bagley, D. M., Liss, S. N., 2010. Membrane fouling in a fermentative hydrogen producing membrane bioreactor at different organic loading rates. *Journal of Membrane Science* 360, 226-233.
- Vogelaar, J. C. T., Bouwhuis, E., Klapwijk, A., Spanjers, H., van Lier, J. B., 2002. Mesophilic and thermophilic activated sludge post-treatment of paper mill process water. *Water Research* 36, 1869-1879.
- Wang, X.-M., Li, X.-Y., 2008. Accumulation of biopolymer clusters in a submerged membrane bioreactor and its effect on membrane fouling. *Water Research* 42, 855-862.
- Wang, Z., Wu, Z., Yin, X., Tian, L., 2008. Membrane fouling in a submerged membrane bioreactor (MBR) under sub-critical flux operation: Membrane foulant and gel layer characterization. *Journal of Membrane Science* 325, 238-244.
- Wang, Z., Wu, Z., Yu, G., Liu, J., Zhou, Z., 2006. Relationship between sludge characteristics and membrane flux determination in submerged membrane bioreactors. *Journal of Membrane Science* 284, 87-94.
- Welander, T., Morin, R., Nylén, B., 1999. Biological removal of methanol from kraft mill condensate. In: TAPPI Proceedings International Environmental Conference,
- Xavier, J. B., White, D. C., Almeida, J. S., 2003. Automated biofilm morphology quantification from confocal laser scanning microscopy imaging. *Water Science and Technology* 47, 31-37.
- Xie, K., Lin, H. J., Mahendran, B., Bagley, D. M., Leung, K. T., Liss, S. N., Liao, B. Q., 2010. Performance and fouling characteristics of a submerged anaerobic membrane bioreactor for kraft evaporator condensate treatment. *Environ Technol* 31, 511-521.
- You, H. S., Huang, C. P., Pan, J. R., Chang, S. C., 2006. Behavior of Membrane Scaling During Crossflow Filtration in the Anaerobic MBR System. *Separation Science and Technology* 41, 1265 - 1278.
- Zahid, W. M., Ganczarczyk, J. J., 1994. Structure of RBC biofilms. *Water Environment Research* 66, 100-106.

- Zarragoitia-González, A., Schetrite, S., Alliet, M., Jáuregui-Haza, U., Albasi, C., 2008. Modelling of submerged membrane bioreactor: Conceptual study about link between activated sludge biokinetics, aeration and fouling process. *Journal of Membrane Science* 325, 612-624.
- Zhang, J., Chua, H. C., Zhou, J., Fane, A. G., 2006a. Factors affecting the membrane performance in submerged membrane bioreactors. *Journal of Membrane Science* 284, 54-66.
- Zhang, K., Choi, H., Dionysiou, D. D., Sorial, G. A., Oerther, D. B., 2006b. Identifying pioneer bacterial species responsible for biofouling membrane bioreactors. *Environmental Microbiology* 8, 433-440.
- Zhang, T. C., Bishop, P. L., 1994. Density, porosity, and pore structure of biofilms. *Water Research* 28, 2267-2277.

Chapter 5 Effects of temperature and temperature shock on the performance and microbial community structure of a submerged anaerobic membrane bioreactor

Adapted from the accepted manuscript:

W.J. Gao, K.T. Leung, W. S. Qin, and B.Q. Liao. Effects of temperature and temperature shock on the performance and microbial community structure of a submerged anaerobic membrane bioreactor. *Bioresource Technology* 102, 8733-8740.

Abstract:

Effects of temperature and temperature shock on the performance and microbial community structure of a submerged anaerobic membrane bioreactor (SAnMBR) treating thermomechanical pulping pressate were studied for 416 days. The results showed that the SAnMBR system were highly resilient to temperature variations in terms of chemical oxygen demand (COD) removal. The residual COD in treated effluent was slightly higher at 55 °C than that at 37 °C and 45 °C. There were no significant changes in biogas production rate and biogas composition. However, temperature shocks resulted in an increase in biogas production temporarily. The SAnMBR could tolerate the 5 and 10 °C temperatures shocks at 37 °C and the temperature variations from 37 to 45 °C. The temperature shock of 5 °C and 10 °C at 45 °C led to slight and significant disturbance of the performance, respectively. Temperature affected the richness and diversity of microbial populations.

5.1 Introduction

Submerged anaerobic membrane bioreactor (SAnMBR) has attracted much interest due to its high-treatment efficiency, high biomass concentrations, low sludge production, excellent effluent quality, small footprint and net energy production (Liao et al., 2006). It has been successfully studied for a wide range of wastewater treatment in

recent years, such as domestic wastewater, pulp and paper wastewaters (Xie et al., 2010), saline effluent, municipal solid waste leachate, and so on. However, the stability and efficiency of anaerobic treatment processes is greatly influenced by many factors (Chen et al., 2008), including wastewater specificity, hydraulic retention time (HRT), solid retention time (SRT), organic loading rate (OLR) (Wijekoon et al., 2011), pH (Gao et al., 2010), temperature (Choorit and Wisarnwan, 2007) and nutrient availability, etc. Among these factors, temperature is commonly believed to play a significant role in the biological wastewater treatment performance and stability.

Anaerobic digestion can be conducted in psychrophilic (< 25 °C), mesophilic (25 - 40 °C), and thermophilic (> 45 °C) temperature ranges (El-Mashad et al., 2004). Earlier studies investigating effect of temperature on the anaerobic digestion process have mainly focused on the comparison of the steady state performance at two or more fixed operating temperatures (Kim et al., 2002; Ndegwa et al., 2008; Yilmaz et al., 2008). The effect of temperature fluctuations on anaerobic treatment efficiency at certain temperature ranges has been also studied. A temporary decrease in the temperature (between 10 and 20 °C) of psychrophilic anaerobic reactors treating swine manure only have temporary effects on the performance and stability of the process (Massé et al., 2003). The effects of digestion temperature and temperature shock on the biogas yields, temperature shocks of the mesophilic anaerobic digestion were recently studied (Chae et al., 2008). Some of the studies were only conducted in the thermophilic range because thermophilic process is characterized to be more susceptible to the environmental and operational conditions than mesophilic process (Ahring et al., 2001; Iranpour et al., 2005). El-Mashad et al. (2004) found that the imposed daily upward temperature fluctuation affected the maximum specific methanogenesis activity more severely than daily downward temperature fluctuations in completely stirred tank reactors (CSTRs).

There are also a few reports of the influence of temperature variation from mesophilic to the thermophilic temperature ranges. Both temperature increases and temperature drops will affect the performance of the anaerobic digestion (Ahn and Forster, 2002). Bouskova et al. (2005) found that one-step temperature increase (from 37

to 55 °C) is better than step-wise increase in changing from mesophilic to thermophilic operation in anaerobic digestion.

The effects of temperature variations have been linked with poor sludge settling that brings high effluent suspended solids, effluent turbidity and biomass washout (Ahn and Forster, 2002). However, these problems caused by temperature variation can be alleviated in an SAnMBR with the incorporation of the membrane filtration technology. The employment of membrane in the anaerobic process can achieve complete solid-liquid separation, so that biomass can be fully retained in the reactor. Obviously, SAnMBR is more resistant to temperature variation than conventional anaerobic digestions do. To our knowledge, the effect of temperature variation and temperature shock on the performance and microbial community of an SAnMBR has not been investigated. Thus, the effect deserves to be investigated in detail.

Some causes of temperature variations can be controlled (operational conditions) or predicted (environmental conditions in a region) so that the system can be adjusted to accommodate to the new conditions, whereas sudden transient changes can lead to deterioration of the reactor's performance. In the pulp and paper industry, wastewaters are discharged at high strength and wide temperature (20 – 70 °C) range (Jahren and Rintala, 1997; Morgan-Sagastume and Allen, 2003). In this case, temperature variations can be caused by frequent temperature transits of wastewater streams or the accordant junction of them. Failure to control temperature (unexpected cooling and heating problems) will also introduce temperature fluctuations. It is important for a system to deal with these situations in industrial applications. The treatments of several types of pulp and paper effluents have been successfully achieved by mesophilic and thermophilic SAnMBRs in our previous studies (Gao et al., 2010; Xie et al., 2010). However, little is known about the tolerance of an SAnMBR to changes of operating temperature and temperature shocks. In addition, temperature has primary impact on microbial activity and community composition in a wastewater treatment reactor. Although microbial community has been analyzed in both anaerobic and aerobic membrane bioreactors (Calderón et al., 2011; Chang et al. 2011), there is insufficient understanding concerning

the effect of temperature variations (from mesophilic to thermophilic temperatures ranges) and temperature shocks on microbial community structures in an SAnMBR.

Consequently, the purpose of this study was to investigate the feasibility of using an SAnMBR for thermomechanical pulping pressate treatment and to assess the influence of temperature and temperature shocks on the performance of the SAnMBR with respect to process stability, process recovery and microbial community in the reactor.

5.2 Materials and methods

5.2.1 Experimental set up

The lab-scale SAnMBR (10 L) used in this study was schematically presented by Xie et al. (2010). The system was equipped with a 0.03 m² of flat sheet ultrafiltration membrane module (Shanghai SINAP Membrane Science & Technology Co. Ltd., China). Nominal molecular weight cut off (MWCO) and material of the membrane were 70000 Daltons and polyvinylidene fluoride (PVDF), respectively. The physical configuration of the SAnMBR was described previously (Xie et al., 2010), although the biogas sparging rate was increased from 0.75 to 1.5 L/min to mix the biomass continuously and to control solid deposition over the membrane surface. The SAnMBR was inoculated with seeded sludge developed from a previous study for kraft evaporator condensate treatment (Xie et al., 2010). During the operation of the reactor, no sludge was discharged except for sludge sampling. This corresponded to a sludge age of approximately 350 days. The pH value was maintained at 7.0 ± 0.2 by an automatic pH regulation pump and a pH electrode (Thermo Scientific, Beverly, MA).

Thermomechanical pulping pressate collected from a local pulp and paper mill (Abitibi-Bowater Inc., Canada) was automatically fed into the reactor by a feeding pump which was controlled by a level sensor (Madison Co., USA) and controller (Flowline, USA). The characteristics of the thermomechanical pulping pressate are listed as follows: pH: 3.89 - 4.43; total suspended solids (TSS): 170 - 400 mg/L; total COD: 2120 - 3600 mg/L; soluble COD: 1220 - 2000 mg/L; total phosphorus: 0.82 – 1.28 mg/L; total nitrogen: < 0.03 mg/L; aluminium: 0.363 - 0.450 mg/L; Arsenic: 0.021 – 0.024 mg/L; barium: 0.489 - 0.577 mg/L; calcium: 33.67 – 34.18 mg/L; chromium: 0.003 - 0.004

mg/L; copper: 0.014 - 0.030 mg/L; iron: 0.304 - 0.384 mg/L; potassium: 31.8 – 34.2 mg/L; magnesium: 6.15 – 6.51 mg/L; manganese: 2.223 – 2.424 mg/L; sodium: 53.91 – 56.04 mg/L; lead: < 0.015 mg/L; total sulphur: 59.03 – 61.29 mg/L; strontium: 0.127 – 0.134 mg/L; titanium: 0.010 – 0.014 mg/L; zinc: 0.302 - 0.367 mg/L. A trace element solution (Xie et al., 2010) was supplemented to the influent to prevent trace metal limitations of the methanogens. In order to sustain the nutrient concentrations required for biomass growth in an anaerobic environment, nitrogen (NH₄Cl) and phosphorus (KH₂PO₄) were fed as macro-nutrients in a proportion of COD: N: P of 100: 2.6: 0.4 (Xie et al., 2010). The trans-membrane pressure (TMP) was measured by a vacuum gauge connecting the bioreactor and the suction pump. Membrane flux was controlled by adjusting the speed of a peristaltic pump with intermittent suction of a 4-min run and 1-min pause cycle. Before starting the reactor, nitrogen (99.998 %) was bubbled for 5 min to remove air in the system. The biogas production was monitored with a water displacement gas collector at ambient temperature (23-25 °C). The biogas yield values were corrected to standard conditions (1 atm, 0 °C).

5.2.2 Temperature variations

The operating temperature was controlled by circulating water through the water jacket. The main temperature variations were described as follows (Fig. 6-1).

In phase 1, the wastewater was initially treated at a mesophilic temperature of 37 ± 1 °C. The SAnMBR was then subjected to periodic temperature shocks: 5 °C shocks (from 37 to 42 °C) and 10 °C shocks (from 37 to 47 °C). Three temperature shocks were conducted at each temperature fluctuation. The temperature shocks were simulated by increasing suddenly from 37 to 42 or 47 °C and lasted approximately 12 hours from the point at which the temperature started to rise until the point at which the temperature began to drop. It was adjusted back to the normal operating temperature quickly (within 1 hour) right after the shock. The next shock started after the system stayed at 37 °C for 36 hours.

In phase 2, the operating temperature of the SAnMBR was increased slowly from 37 to 45 °C (0.5 - 1 °C /day) over a 10-day interval. Similarly, the SAnMBR was subjected to 5 °C shocks (from 45 to 50 °C) and 10 °C shocks (from 45 to 55 °C) after

steady-state operation was achieved at 45 °C. Finally, the temperature was gradually increased to a thermophilic temperature of 55 °C (0.5 - 1 °C /day) over a period of 13 days (phase 3). Each operating temperature and temperature shock was delayed until the system performed as well as it was prior to the temperature change, except in phase 3. Two new pieces of membrane (one on each side of the module) were used for each operating temperature.

Samples of influent, effluent and mixed liquor were taken from the system every 2-3 days during the steady state of each operating temperature, while specific samples were collected right before and after the temperature shocks were imposed.

5.2.3 Particle size distribution

The particle size distribution (PSD) of mixed liquor was measured by a Malvern Mastersizer 2000 instrument (Worcestershire, UK) with a detection range of 0.02–2000 µm. The scattered light is detected by means of a detector that converts the signal to a size distribution based on volume or number. Each sample was measured 3 times. The PSD measurements were conducted routinely 2–3 times every week.

5.2.4 Analytical methods

The mixed liquor samples were centrifuged at 18700 times of gravitational acceleration for 15 minutes to obtain supernatant for chemical oxygen demand (COD) measurement. COD and mixed liquor suspended solids (MLSS) were determined in duplicate according to standard methods (APHA, 2005).

Biogas samples were taken from the headspace of the reactor by a syringe. Composition of biogas (methane, nitrogen, and carbon dioxide) was measured by gas chromatography (Shimazu, GC-2014) equipped with a thermal conductivity detector and a silica gel packed column. Helium was used as the carrier gas at a flow rate of 30 mL/min.

5.2.5 Microbial community analysis

For microbial community analysis, duplicate samples of each mixed liquor sample were collect at the steady state of three operating temperatures. The mixed liquor

samples before and after the temperature shocks were also collected. Genomic deoxyribonucleic acid (DNA) was extracted in duplicates from 0.25 g of mixed liquor samples respectively with a Fecal DNA isolation kit (MoBio Laboratories, Solana Beach, CA, USA) according to the manufacturer's instructions.

Polymerase chain reaction (PCR) amplification was performed in 50 µl reaction volume on a Hybaid Thermocycler (Thermo Electron Corp., USA). The primer set, 341f-GC (5'-GC-clamp-CCTAGGGAGGCAGCAG-3') and 534r (5'-ATTACCGCGGCTGCTGG-3') were used. PCR cycling was consisted of an initial denaturation at 94 °C for 5 min followed by 35 cycles consisting of denaturation at 94 °C for 1 min, primer annealing at 56°C for 1 min, and DNA extension at 72 °C for 1 min. A final extension step was conducted at 72 °C for 5 min prior to cooling at 4 °C. PCR products were purified using a DNA purification kit (Fermentas Life Sciences, Burlington, ON, Canada) in accordance with the manufacturer's recommendations prior to use in denaturing gradient gel electrophoresis (DGGE) analysis. Polyacrylamide gels (10 % polyacrylamide, 25–65 %) were cast using a gradient maker (Bio-Rad, USA). The gels were run at 30 V for 18 h at 60 °C. After electrophoresis, the polyacrylamide gel was stained in 150 mL TAE buffer containing 15 µL 10000× concentrated SYBR Green I stain (Fermentas Life Sciences) for 1 h, and then photographed with a CCD camera (SynGene a division of Synoptics Ltd, UK) to acquire the DGGE band image. Duplicate measurements were performed for each sample.

Cluster analysis of the DGGE band patterns was performed with Fingerprinting II Informatix Software Program v.3.00 (Bio-Rad, USA) by using the Jaccard coefficient and the unweighted-pair group method with arithmetic mean (UPGMA). A position tolerance of 1.00 % was used.

5.3 Results and discussion

5.3.1 Effect on COD removal

Throughout the 416 days of operation, the pH, OLR, membrane flux and gas sparging rate were controlled approximately constant to separate the influences of the temperature variation on system performance from other factors. MLSS concentration

was maintained at 10.9 ± 0.5 g/L (Fig. 5-1). Although the growth/decay rates are different at different temperatures, MLSS concentration was not correlated to the temperature variations, which will be discussed in later part. The SANMBR was operated at an average OLR of 2.59 ± 0.53 kg COD/m³day (Fig. 5-1). The influent COD concentrations fluctuated from 2120 to 3600 mg/L. The first 28 days were considered to be the initial start-up period during which the permeate COD value fell from 1220 mg/L to 470 mg/L to allow the acclimation of the biomass (Fig. 5-2).

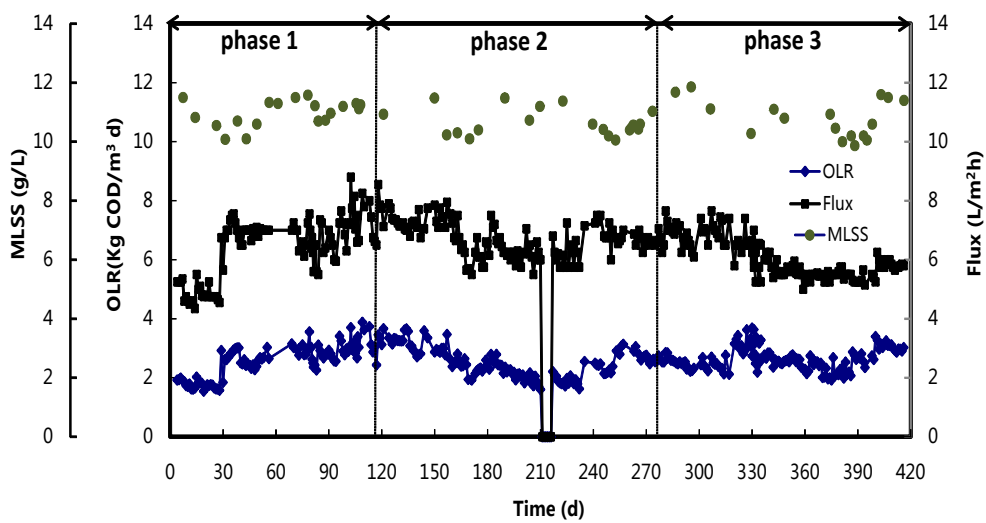


Figure 5-1 Variation of organic loading rate and membrane flux during operation.

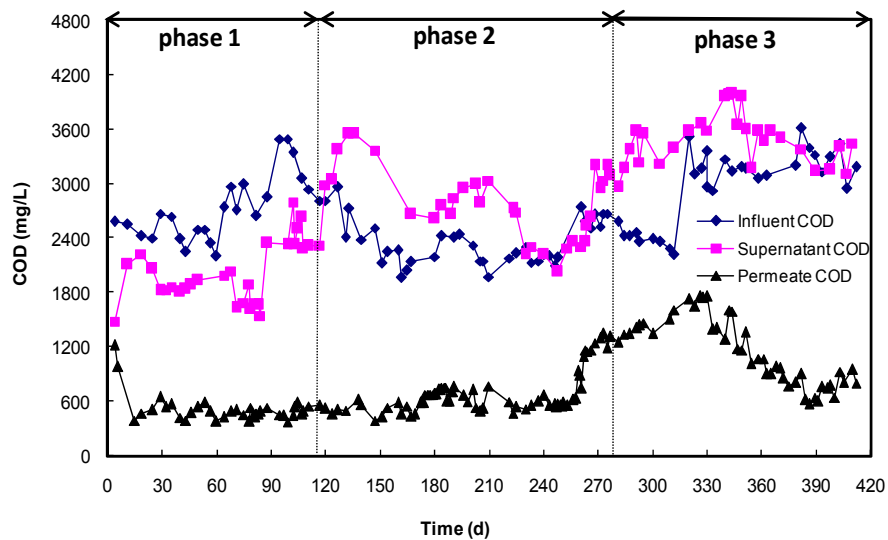


Figure 5-2 Variation of the influent, supernatant and permeate COD (5 °C shocks at 37 °C (day 78 - 83), 10 °C shocks at 37 °C (day 102 - 107), 5 °C shocks at 45 °C (day 245 - 250), 10 °C shocks at 45 °C (day 259 - 264)).

The membrane flux was first maintained at 6.89 ± 0.56 L/m²h. After the operating temperature rose to 55 °C, the flux dropped to 5.68 ± 0.43 L/m²h (Fig. 5-1). It is known that PVDF is a hydrophobic and chemically inert fluoropolymer which has a very low glass transition temperature (T_g) of -40 °C and a relatively low melting point of around 177 °C, making it quite flexible for membrane application and tolerate with a wide temperature range (-30 and 140 °C) (Nunes and Peinemann, 2006). In spite of this, the properties of the PVDF membrane may change with increasing temperature. The temperature usually enhances flux as the sludge viscosity becomes lower and the membrane pore size may increase at a higher temperature. However, no such influence was observed with increasing temperature. Instead, it is noted that a higher temperature (55 °C) resulted in a lower membrane flux in this study. The impact of temperature on membrane flux was considered to be largely offset by a significant increase in membrane fouling extent. Potential impact of temperature on membrane properties needs to be further studied in future studies.

The stability and efficiency of the reactor is usually evaluated in terms of the COD removal, gas production and methane content. At phase 1, the permeate COD value changed between 380 mg/L and 530 mg/L during the steady state at 37 °C. The 5 °C and 10 °C temperature shocks were conducted as described above at day 78-83 and day 102-107, respectively. As shown in Fig. 5-2, there is no changes in permeate COD value during and after the temperature shocks. Although the higher COD value in the supernatant during the 10 °C shocks period can be observed, it decreased as soon as the temperature was restored to normal condition. These results indicated that the system can tolerate the 5 and 10 °C shocks at the operating temperature of 37 °C.

The reactor processes were reasonably stable while slowly increasing the temperature from 37 °C to 45 °C at phase 2. It even remained stable after short period (day 211 to 216) of shut down for repair. The permeate COD value remained between 500 mg/L and 720 mg/L until the 10 °C shock at 45 °C resulting in a deteriorating COD removal efficiency (from 80.6 % to 53.3 %). Meanwhile, the supernatant COD value went higher than the influent COD from then on probably because of improved dissolution of organic compounds and increased cell lysis at higher temperatures (Fig.

5-2). The SAnMBR seemed not to be affected by 5 °C temperature shocks (day 245-250), while the 10 °C temperature shocks (day 259-264) exerted significantly negative impacts on COD removal. This is supported by experiments on temperature shifts (Bouskova et al., 2005; Choorit and Wisarnwan, 2007) showed a loss of stability and change in the performance of the reactor when an operating temperature was raised over 45 °C. Because 45 °C is at the edge between mesophilic and thermophilic temperature ranges, the SAnMBR was more sensitive to the temperature shocks when operated at 45 °C than at 37 °C.

At phase 3, starting from day 278, the operating temperature gradually shifted from 45 °C to 55 °C. The permeate COD value subsequently went up to 1760 mg/L. It took approximately 94 days for the COD removal efficiency to restore to steady values exceeding 75 %. The average level of permeate COD at 55°C steady state was around 600-810 mg/L. The SAnMBR produced lower quality effluent during the 55 °C steady state compared with that during the 37 and 45 °C steady state in some sort. These results are consistent with previous findings (Harris and Dague, 1993; Song et al., 2004) that the mesophilic anaerobic digestion was superior in effluent quality to the thermophilic digestion. The poorer performances at thermophilic conditions and the above mentioned MLSS observations could be caused by the combined action of the temperature and the substrate limitation. In a thermophilic aerobic process, Abeynayaka and Visvanathan (2011) observed that although the reaction rates as well as the growth/decay rates are higher at thermophilic conditions than that at mesophilic conditions, achievement of maximum growth rate was simultaneously affected by the substrate available in the reactor. Limited substrate could enhance decay rate and thus induce low net biomass production. The by product of cell lysis and decay may cause COD increment both in supernatant and permeate. The poorer performances at 55 °C might also be attributed to that the community are less adept at utilizing the same range of substrates at a thermophilic temperature, which was found by LaPara et al. (2000) during an aerobic process. The high COD value of supernatant might indicate the presence of a great many of colloidal particle, soluble microbial products (SMPs), and volatile fatty acids in sludge suspension due to high temperature. Konopka et al. (1999) found that in aerobic

biological wastewater treatment systems, thermophilic microbes might have more difficulty in maintaining cell integrity than mesophilic microbes. The release of cell lysate and other microbial products might be responsible for the high COD values in the supernatant. Further studies regarding the high supernatant COD value are needed.

5.3.2 Effect on gas production

Fig. 5-3A shows the biogas production rate converted to standard values (1 atm, 0 °C) during the whole operating time. At 37 °C, 45 °C and 55 °C steady state, the biogas production rates were 0.21 ± 0.03 , 0.20 ± 0.03 and 0.21 ± 0.02 L/g COD removed, respectively, indicating a similar biogas production rate at three operating temperatures. It may attribute to the similar species of microorganisms developed in the same reactor all along. The short period of shut down did not affect the biogas production which rose back to the previous level within 24 hours. The observed biogas production rate in this study could be less (up to 10 %) than the theoretical values because of the loss of a small part of CO₂ in the water displacement arrangement by the dissolution of CO₂ in water.

An increase in biogas production rate was observed during each temperature shocks. Increasing temperature is known to lead to an increase in the maximum specific growth and substrate utilization rates (Chen and Hashimoto, 1980). Therefore, the temperature shock could temporarily result in much faster chemical and biological reactions (Ratkowsky et al., 1982). Both 5 °C and 10 °C shocks at 37 °C did not show any detrimental effect on biogas production rate and composition (Fig. 5-3B) after the shocks. Minor instabilities of the process were observed after the 5 °C shocks at 45 °C, although steady-state conditions were re-established within 24 hours. However, temperature shocks of 10 °C at 45 °C gave a serious drop in the treatment efficiency. It took 16 days for the SAnMBR system to reproduce methane after the temperature variation from 45 °C to 55 °C in phase 3. The growth and activity rates of microorganisms as a function of temperature are considered to increase in certain temperature ranges. Further increases in temperature cause a decline in these rates until zero. Therefore, the extent of influences was determined by the magnitude of temperature shocks and the tolerance of the microorganisms in the sludge liquor, which is in agreement with El-Mashad et al. (2004). Barr et al. (1996) also found that in an activated

sludge system, transient upsets in treatment efficiency were proportional to the magnitude of the rapid temperature decreases.

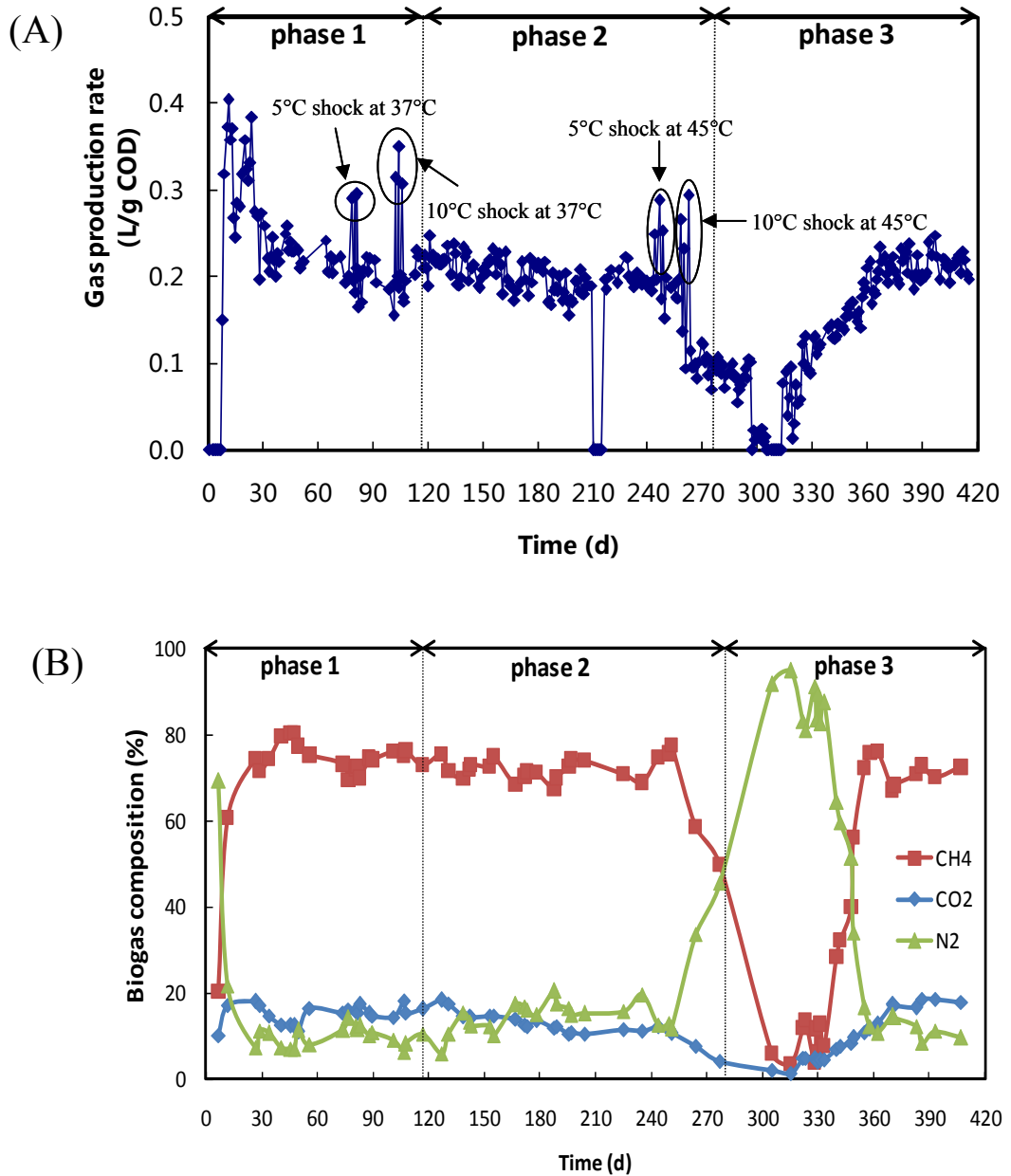


Figure 5-3 Biogas production. (A) variation of biogas production rate (B) biogas composition and concentration.

The first indication of a loss of stability of the process was biogas production rate. It occurred right after the 10 °C shocks (at 45 °C) were imposed, indicating a significant change in the balance among the microbial groups involved in the system as the various groups of bacteria respond the change in a different manner (Peck et al., 1986). For a complex anaerobic microbial community, the biogas production depends on the activities of various groups of bacteria during the four steps (hydrolysis, fermentation, acetogenesis and methanogenesis) of the anaerobic digestion. When the system reached a steady state at certain operating temperature, these groups of bacteria were compatible. When the temperature was beyond the durability of bacteria, their death rate would exceed growth rate and consequently result in a loss of the performance of the SAnMBR in terms of the removal efficiency and biogas production (Visser et al., 1993). Slower yield of methanogens due to high temperature (Kim et al., 2002) may be responsible for the long recovery period. Although the anaerobic microorganisms in the SAnMBR could not quickly adapt to the imposed high temperature variation, they finally thrived at the new living condition and had a tolerance for a fairly wide range of temperatures.

5.3.3 Effect on particle size distributions

Fig. 5-4 shows the comparison of particle size distributions (PSDs) before and after each temperature shocks. Fig. 5-4A shows that the large flocs shrank after the 5 °C shocks at 37 °C. Floc strength has been reported to decrease with increasing temperature (Jarvis et al., 2005), so higher temperature during the shocks induced the breakage of large flocs. There is no obvious difference between the two curves in Fig. 5-4B-D indicating 10 °C shocks at 37 °C, 5 °C and 10 °C shocks at 45 °C had no significant impact on PSDs.

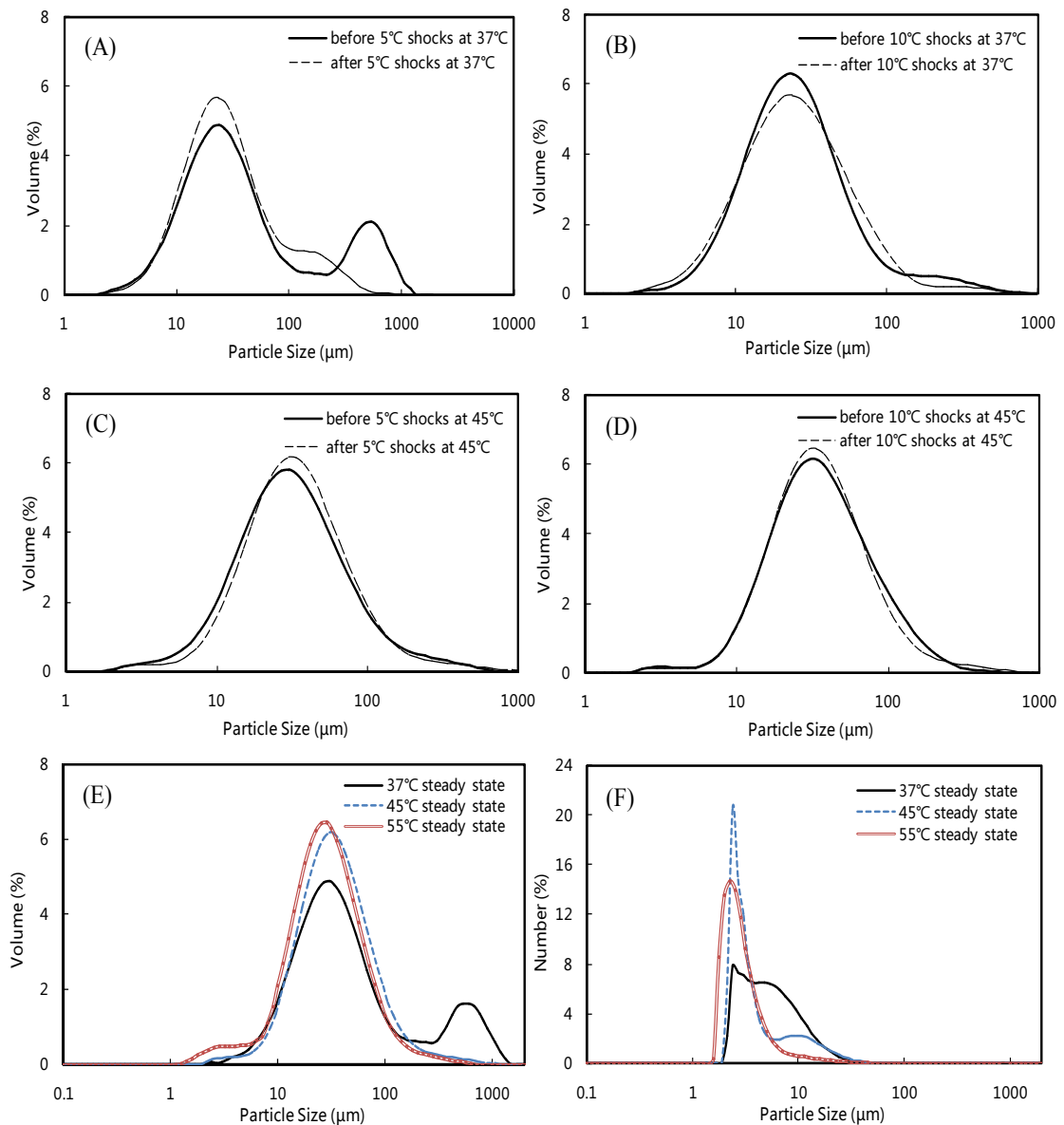


Figure 5-4 Particle size distribution of sludge suspension (A) before and after 5 °C shocks at 37 °C (B) before and after 10 °C shocks at 37 °C (C) before and after 5 °C shocks at 45 °C (D) before and after 10 °C shocks at 45 °C (E) at 37 °C, 45 °C and 55 °C steady state based on volume (F) at 37 °C, 45 °C and 55 °C steady state based on number.

The PSDs of sludge suspension in the SANMBR at steady state of three operating temperatures are presented in Fig. 5-4. Two distinct peaks of the PSD of 37 °C steady state ranging from 2 to 1500 μm are showed in Fig. 5-4E. One is in the range of 2-200

μm with a mean size of 28.25- 35.56 μm , and the other is in the range of 200-1400 μm with a mean size of 563.67-632.45 μm . Although the mean sizes of sludge flocs at 45 °C and 55 °C steady state are similar, we can see a small portion in the range of 1.5 -2 μm at 55 °C. Much larger differences can be noticed in the PSD based on number (Fig. 5-4F). At the 55 °C steady state, 92.2 % of sludge flocs were smaller than 5 μm . This percentage decreased by 75.8 % when the operating temperature was 45 °C. Only 48.5 % of flocs were in that size range during 37 °C steady state, and there were a large part of flocs in the range of 5-20 μm . The results suggest that operating temperature had a significant impact on the floc size in the SAnMBR. Long-term exposure at high temperatures can induce the deflocculation of the sludge flocs with large sizes (Morgan-Sagastume and Grant Allen, 2005). In spite of this, the MLSS and the effluent quality were not affected by the deflocculation because of the efficient separation by membrane filtration, demonstrating that SAnMBR have the ability to alleviate the effect of temperature variations on the performance of the system in some extent.

5.3.4 Microbial community

The DGGE fingerprints of mixed liquor samples collected at three operating temperatures and after the temperature shocks were presented in Fig. 5-5A. It was evident that not only the diversity but also the species richness of the microbial populations was affected by temperature variations.

It appears that sudden temperature increases had little impact on this microbial community. Temperature shocks at 37 °C did not affect the microbial community, except that there was a missing of band 1 after 10 °C shocks at 37 °C. For temperature shocks at 45 °C, only some changes in intensity of band 14, 15, 16, 17 and 18 were observed. The dendrogram generated by cluster analysis also reflects similarities of DGGE band patterns between the temperature shocks and steady states accordingly (Fig. 5-5B). There are 3 major clusters with similarity at approximately 70 %. In addition, the 5 °C and 10 °C shocks at 37 °C and 37 °C steady state were located in one cluster, and so were the 5 °C and 10 °C shocks at 45 °C and 45 °C steady state. These results further confirmed the results of the performance of the SAnMBR that temperature shocks didn't affect the COD removal ability of the reactor.

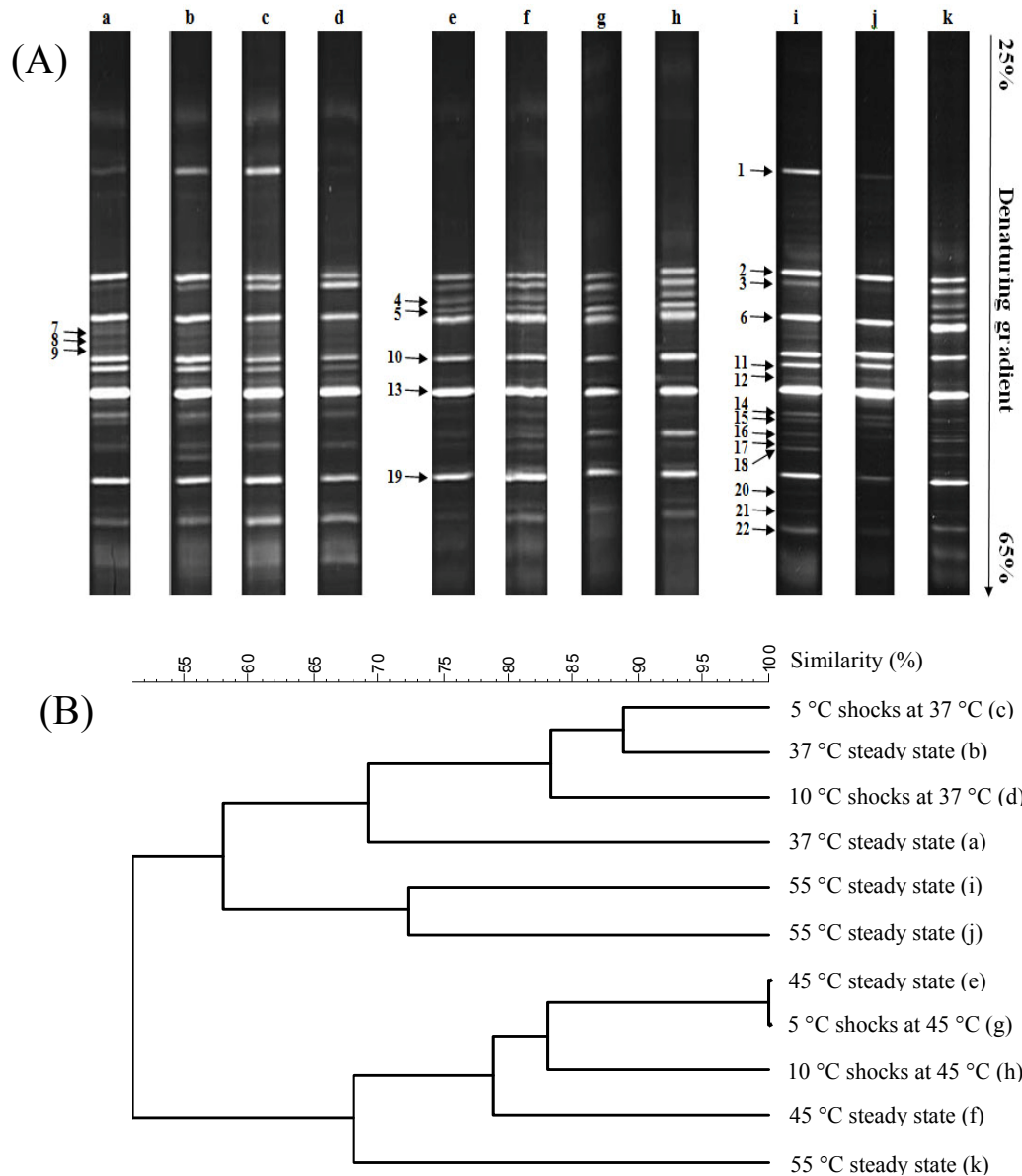


Figure 5-5 PCR-DGGE fingerprints of 16S rDNA gene fragments amplified from DNA extracted from bulk sludge (A) and cluster analysis of the DGGE band patterns (B). (a) 37 °C steady state (day 53); (b) 37 °C steady state (day 68); (c) 5 °C shock at 37 °C; (d) 10 °C shock at 37 °C; (e) 45 °C steady state (day 207); (f) 45 °C steady state (day 245); (g) 5 °C shock at 45 °C; (h) 10 °C shock at 45 °C; (i) 55 °C steady state (day 400); (j) 55 °C steady state (day 412); (k) 55 °C steady state (day 416).

Comparing the DGGE patterns of the mixed liquor samples at 37 °C, 45 °C and 55 °C steady state, it is clear that there are some differences in species diversity among the three operating temperatures. For example, band 11 which appeared both at 37 °C and 55 °C steady state were missing at 45 °C. Band 4 and 5 were detected at 45 °C steady state while they were not detectable at 37 °C steady state. Moreover, in the dendrogram (Fig. 5-5B), three main clusters clearly separated the patterns of the three operating temperatures except that lane k was more close to lane f. On the other hand, there were populations (bands 2, 6, 10, 13, 19) presented in all the samples. These species may be highly temperature tolerant and play a significant role in maintaining the stability of the SAnMBR. This might be the reason of the similar biogas production rate at 37 °C, 45 °C and 55 °C steady state. The similarity of the microbial community at three operating temperatures may be due to the development of thermotolerant mesophiles rather than true thermophiles when the temperature was raised from the mesophilic range to the thermophilic range (Iranpour et al., 2002).

Some temporal changes in the DGGE patterns at 55 °C steady state within 16 days of operation can be noticed (Fig. 5-5A, lanes i, j, k). Cluster analysis also illustrates that similarity of microbial community between 55 °C steady state was the lowest among that between the steady states of three operating temperatures, and k seems to be more like the 45 °C than the other two 55 °C populations (Fig. 5-5B). After the temperature was lifted from the mesophilic range to the thermophilic range, some microorganisms adapted to the new living conditions quickly. In contrast, some other populations which could not acclimatize themselves to the new condition decreased sharply or even disappeared in the system, while a minor part of them got the chance to live because of their high temperature tolerance. This part of microorganisms would grow up and become abundant again.

5.4 Conclusions

It is feasible to treat thermomechanical pulping pressate by using an SAnMBR at the operating temperatures of 37, 45 and 55 °C and achieve a COD removal efficiency of 76-83%. Temperature shocks led to a temporary increase in biogas production rate. Larger magnitudes (10 °C) of temperature shock had more severe impact on the

performance of the SAnMBR. Increasing the operating temperature caused the deflocculation of the large sludge flocs. Temperature shocks had little impact on the microbial community structure, while the diversity and species richness would be affected by temperature variations.

5.5 References

- Abeynayaka, A., Visvanathan, C., 2011. Mesophilic and thermophilic aerobic batch biodegradation, utilization of carbon and nitrogen sources in high-strength wastewater. *Bioresource Technology* 102, 2358-2366.
- Ahn, J. H., Forster, C. F., 2002. The effect of temperature variations on the performance of mesophilic and thermophilic anaerobic filters treating a simulated papermill wastewater. *Process Biochemistry*. 37, 589-594.
- Ahring, B. K., Ibrahim, A. A., Mladenovska, Z., 2001. Effect of temperature increase from 55 to 65 °C on performance and microbial population dynamics of an anaerobic reactor treating cattle manure. *Water Research*. 35, 2446-2452.
- APHA, 2005. Standard methods for the examination of water and wastewater, 21th ed. American Public Health Association (APHA)/American Water Works Association (AWWA)/Water Environment Federation (WEF), Washington, DC.
- Barr, T. A., Taylor, J. M., Duff, S. J. B., 1996. Effect of HRT, SRT and temperature on the performance of activated sludge reactors treating bleached kraft mill effluent. *Water Research*. 30, 799-810.
- Bouskova, A., Dohanyos, M., Schmidt, J. E., Angelidaki, I., 2005. Strategies for changing temperature from mesophilic to thermophilic conditions in anaerobic CSTR reactors treating sewage sludge. *Water Research*. 39, 1481-1488.
- Calderón, K., Rodelas, B., Cabirol, N., González-López, J., Noyola, A., 2011. Analysis of microbial communities developed on the fouling layers of a membrane-coupled anaerobic bioreactor applied to wastewater treatment. *Bioresource Technology* 102, 4618-4627.
- Chae, K. J., Jang, A., Yim, S. K., Kim, I. S., 2008. The effects of digestion temperature and temperature shock on the biogas yields from the mesophilic anaerobic digestion of swine manure. *Bioresource Technology* 99, 1-6.

- Chang, C.-Y., Tanong, K., Xu, J., Shon, H., 2011. Microbial community analysis of an aerobic nitrifying-denitrifying MBR treating ABS resin wastewater. *Bioresource Technology* 102, 5337-5344.
- Chen, Y., Cheng, J. J., Creamer, K. S., 2008. Inhibition of anaerobic digestion process: A review. *Bioresource Technology* 99, 4044-4064.
- Chen, Y. R., Hashimoto, A. G., 1980. Substrate utilization kinetic model for biological treatment process. *Biotechnology and Bioengineering*. 22, 2081-2095.
- Choorit, W., Wisarnwan, P., 2007. Effect of temperature on the anaerobic digestion of palm oil mill effluent. *Electronic Journal of Biotechnology* 10, 376 - 385.
- El-Mashad, H. M., Zeeman, G., van Loon, W. K., Bot, G. P., Lettinga, G., 2004. Effect of temperature and temperature fluctuation on thermophilic anaerobic digestion of cattle manure. *Bioresource Technology* 95, 191-201.
- Gao, W. J. J., Lin, H. J., Leung, K. T., Liao, B. Q., 2010. Influence of elevated pH shocks on the performance of a submerged anaerobic membrane bioreactor. *Process Biochemistry* 45, 1279-1287.
- Harris, W. L., Dague, R. R., 1993. Comparative performance of anaerobic filters at mesophilic and thermophilic temperatures. *Water Environment Research* 65, 764-771.
- Iranpour, R., Alatrisme-Mondragon, F., Cox, H. H., Haug, R. T., 2005. Effects of transient temperature increases on odor production from thermophilic anaerobic digestion. *Water Science and Technology* 52, 229-235.
- Iranpour, R., Oh, S., Cox, H. H. J., Shao, Y. J., Moghaddam, O., Kearney, R. J., Deshusses, M. A., Stenstrom, M. K., Ahring, B. K., 2002. Changing mesophilic wastewater sludge digestion into thermophilic operation at terminal island treatment plant. *Water Environment Research* 74, 494-507.
- Jahren, S. J., Rintala, J. A., 1997. The closure of water circuits by internal thermophilic (55 and 70 °C) anaerobic treatment in the thermomechanical pulping process. *Water Science and Technology* 35, 49-56.
- Jarvis, P., Jefferson, B., Gregory, J., Parsons, S. A., 2005. A review of floc strength and breakage. *Water Research* 39, 3121-3137.

- Kim, M., Ahn, Y.-H., Speece, R. E., 2002. Comparative process stability and efficiency of anaerobic digestion; mesophilic vs. thermophilic. *Water Research* 36, 4369-4385.
- Konopka, A., Zakharova, T., LaPara, T. M., 1999. Bacterial function and community structure in reactors treating biopolymers and surfactants at mesophilic and thermophilic temperatures. *Journal of Industrial Microbiology and Biotechnology* 23, 127-132.
- LaPara, T. M., Konopka, A., Nakatsu, C. H., Alleman, J. E., 2000. Effects of elevated temperature on bacterial community structure and function in bioreactors treating a synthetic wastewater. *Journal of Industrial Microbiology and Biotechnology* 24, 140-145.
- Liao, B.-Q., Kraemer, J. T., Bagley, D. M., 2006. Anaerobic membrane bioreactors: applications and research directions. *Critical Reviews in Environmental Science and Technology* 36, 489 - 530.
- Massé, D. I., Masse, L., Croteau, F., 2003. The effect of temperature fluctuations on psychrophilic anaerobic sequencing batch reactors treating swine manure. *Bioresource Technology* 89, 57-62.
- Morgan-Sagastume, F., Allen, D. G., 2003. Effects of temperature transient conditions on aerobic biological treatment of wastewater. *Water Research* 37, 3590-3601.
- Morgan-Sagastume, F., Grant Allen, D., 2005. Activated sludge deflocculation under temperature upshifts from 30 to 45 °C. *Water Research* 39, 1061-1074.
- Ndegwa, P. M., Hamilton, D. W., Lalman, J. A., Cumba, H. J., 2008. Effects of cycle-frequency and temperature on the performance of anaerobic sequencing batch reactors (ASBRs) treating swine waste. *Bioresource Technology* 99, 1972-1980.
- Nunes, S. P., Peinemann, K. V., 2006. *Membrane technology in the chemical industry*, second ed. Weinheim, Germany.
- Peck, M. W., Skilton, J. M., Hawkes, F. R., Hawkes, D. L., 1986. Effects of temperature shock treatments on the stability of anaerobic digesters operated on separated cattle slurry. *Water Research* 20, 453-462.

- Ratkowsky, D. A., Olley, J., McMeekin, T. A., Ball, A., 1982. Relationship between temperature and growth rate of bacterial cultures. *Journal of Bacteriology* 149, 1-5.
- Song, Y.-C., Kwon, S.-J., Woo, J.-H., 2004. Mesophilic and thermophilic temperature co-phase anaerobic digestion compared with single-stage mesophilic- and thermophilic digestion of sewage sludge. *Water Research* 38, 1653-1662.
- Visser, A., Gao, Y., Lettinga, G., 1993. Effects of short-term temperature increases on the mesophilic anaerobic breakdown of sulfate containing synthetic wastewater. *Water Research* 27, 541-550.
- Wijekoon, K. C., Visvanathan, C., Abeynayaka, A., 2011. Effect of organic loading rate on VFA production, organic matter removal and microbial activity of a two-stage thermophilic anaerobic membrane bioreactor. *Bioresource Technology* 102, 5353-5360.
- Xie, K., Lin, H. J., Mahendran, B., Bagley, D. M., Leung, K. T., Liss, S. N., Liao, B. Q., 2010. Performance and fouling characteristics of a submerged anaerobic membrane bioreactor for kraft evaporator condensate treatment. *Environmental Technology* 31, 511-521.
- Yilmaz, T., Yuceer, A., Basibuyuk, M., 2008. A comparison of the performance of mesophilic and thermophilic anaerobic filters treating papermill wastewater. *Bioresource Technology* 99, 156-163.

Chapter 6 Effects of extracellular polymeric substances and soluble microbial products on membrane fouling in a submerged anaerobic membrane bioreactor

Abstract:

Effects of temperature (37, 45 and 55 °C) and temperature shock (5 and 10 °C) on the production of extracellular polymeric substances (EPS) and soluble microbial products (SMP) and their role in membrane fouling were studied using a laboratory-scale submerged anaerobic membrane bioreactor (SAnMBR) for thermomechanical pulping pressate treatment for 416 days. The results showed that the bound EPS, soluble SMP, and colloidal particles contents and membrane filtration resistances increased with an increase in operating temperature (ANOVA, $p < 0.05$). Temperature shocks promoted the production of bound EPS, while the concentration of the soluble polysaccharides was reduced after the shocks. Statistical analyses show that total bound EPS, bound carbohydrates, and bound proteins, soluble total SMP, soluble carbohydrates, soluble proteins, and colloidal particle content in supernatant positively correlated to the membrane filtration resistance, implying the importance of bound EPS, soluble SMPs, and colloidal particles in supernatant in membrane fouling. The results suggest that, from membrane fouling control point of view, operation of the SAnMBR in the mesophilic temperature range is more attractive than that in a thermophilic temperature.

6.1 Introduction

A submerged membrane bioreactor (SMBR), in which biomass is completely retained in the reactor by the employment of an immersed membrane filtration unit, are able to enrich the bacterial groups including those slow-growing anaerobic microorganisms inside the reactor. Meanwhile, the SMBR system retains a variety of sludge constituents such as suspended solids, cell debris, extracellular polymeric substances (EPS), soluble microbial products (SMP), colloids, feed components and other

metabolites (Liao et al., 2004). Despite superior COD removals and high organic loading rates, SBR systems suffer from reduced performances due to membrane fouling. In an SBR system, membrane fouling is a result of the interaction between the membrane material and all the components of the bulk sludge influenced by various factors (system design (Sofia et al., 2004), hydrodynamic conditions (Meng et al., 2007), operational conditions (Kimura et al., 2009), etc.). Therefore, these sludge constituents, especially EPS and SMP, have been proposed to play a significant role in membrane fouling.

Based on size, the mixed liquor is fractionated into three main groups: suspended solids, colloids and solutes. Each of the fractions has been investigated by many researchers to identify their role in membrane fouling. Mixed liquor suspended solids (MLSS) concentrations were found not to be responsible for membrane fouling (Hong et al., 2002; Fan and Zhou, 2007), while some authors reported that high MLSS concentrations can accelerate membrane fouling (Rosenberger et al., 2005; Trussell et al., 2007). Wisniewski and Grasmick (1998) reported that half of the total resistance could be due to the soluble fraction. Colloidal particles, which mainly consist of the inorganic precipitates and organic constituents, exhibited intermediate characteristics between suspended solids and solutes (Bae and Tak, 2005). The relative contributions of suspended solids, colloids, and solutes to the fouling resistance were found to be 65 %, 30 % and 5 %, respectively (Defrance et al., 2000).

EPS, widely recognized as a group of compounds responsible for membrane fouling, is of key interest to researchers. EPS refers to a complex mixture of polysaccharides, proteins, lipids and nucleic acids excreted by microorganisms (Drews et al., 2006). These compounds can be divided into bound EPS (organic matter bound to the cell) and soluble EPS. SMP is defined as part of the metabolic products or soluble cellular components that are released during cell lysis and then diffuse into the liquid phase (Laspidou and Rittmann, 2002). According to the unified theory for EPS, SMP, and biomass proposed by Laspidou and Rittmann (2002), SMP are the same as soluble EPS. Some authors identified EPS as the main component contributing to fouling resistance (Chang and Lee, 1998; Chang et al., 2002), and more serious membrane fouling correlated with greater bound EPS amount (Fonseca et al., 2007; Wu et al., 2011).

On the contrary, Rosenberger and Kraume (2003) found no impact of extractable EPS concentration on the sludge filterability. Similar situation can be seen in the literature for SMP. No correlation between SMP and membrane fouling was observed by Drews et al. (2008), whereas the SMP was reported to provide a substantial barrier to filtration (Harada et al., 1994; Rosenberger et al., 2006).

Overall, the relationship of EPS and SMP with membrane fouling is still controversial and needs to be deeply investigated. Although considerable efforts have been made to demonstrate the role of EPS and SMP in membrane fouling, there is a lack of information on the effect of temperature and temperature shocks on EPS production. It appears that the studies regarding the effect of temperature variations have been mainly focused on the performance of the systems (Ndegwa et al., 2008; Wilson et al., 2008). The possible influence of temperature on EPS and SMP is of interest. Moreover, submerged anaerobic membrane bioreactor (SAnMBR) is a new technology for sustainable wastewater treatment. Membrane fouling phenomena in SAnMBR systems has not been well studied, as compared to aerobic SAnMBR.

The purpose of this study was to investigate the potential variation and of EPS and SMP at different temperatures (37, 45 and 55 °C) and temperature shocks (5 and 10 °C) at tested temperatures (37 and 45 °C), as well as their role in membrane fouling in an SAnMBR.

6.2 Materials and methods

6.2.1 Experimental set up

A 10L SAnMBR as shown in Xie et al. (2010) was used to conduct this study. The system was fitted with a flat sheet polyvinylidene fluoride (PVDF) ultrafiltration membrane module (Shanghai SINAP Membrane Science & Technology Co. Ltd., China) with a nominal molecular weight cut off (MWCO) of 70,000 Daltons. The membrane module had a membrane area of 0.03 m². At the base of the membrane module, two stainless steel tube diffusers were located (one on each side) and headspace biogas was recirculated by two gas recycle pumps (Masterflex Console Drive, Model 7520-40, Thermo Fisher Scientific, USA). Gas sparging was maintained at 1.5 L/min to provide

mixing and surface shear on the membrane surface. The reactor was inoculated with anaerobic sludge that was previously acclimated to mesophilic conditions for kraft evaporator condensate treatment (Xie et al., 2010). The pH value was automatically maintained at 7.0 ± 0.2 by an automatic pH regulation pump and a pH electrode (Thermo Scientific, Beverly, MA). The operating temperature was controlled by circulating water through the water jacket.

The SAnMBR was fed with thermo-mechanical pulping pressate collected from a local pulp and paper mill. The influent pump (Masterflex Model 7520-50, Barnant Co., USA) was controlled by a level sensor (Madison Co., USA) and controller (Flowline, USA) to maintain a constant water level in the bioreactor. A trace element solution (Welander et al., 1999) was supplemented to the influent to prevent trace metal limitations of the methanogens. In order to sustain the nutrient concentrations required for biomass growth in an anaerobic environment, nitrogen (NH_4Cl) and phosphorus (KH_2PO_4) were fed as macro-nutrients in a proportion of COD: N: P of 100: 2.6: 0.4 (Vogelaar et al., 2002). Permeate was collected by means of a peristaltic pump (Masterflex, C/L, Model 77120-70, Barnant, Co., USA) with a suction cycle of a 4 min followed by 1 min relaxation (no suction). The trans-membrane pressure (TMP) was measured by a vacuum gauge located in the permeate line connecting the bioreactor and the suction pump.

6.2.2 Operating conditions

The organic loading rate of the lab-scale SAnMBR was kept constant at average rates of 2.69 ± 0.47 kg COD/m³·d throughout the 416 days of operation. The mixed liquor suspended solids (MLSS) concentration was controlled at 10.9 ± 0.5 g/L. During the operation of the reactors, no sludge was discharged except for sludge sampling. This corresponded to a sludge age of approximately 350 days.

The main temperature variations are illustrated in Fig. 6-1. In phase 1, the SAnMBR was initially operated at 37 ± 1 °C. The 5 °C shocks (from 37 to 42 °C) and 10°C shocks (from 37 to 47 °C) were conducted at day 78 - 83 and day 102 - 107, respectively. As shown in Fig. 6-1 (b), three temperature shocks were conducted in each temperature fluctuation. The temperature shocks were simulated by increasing suddenly

from 37 to 42 °C / 47 °C in a few hours and lasted approximately 12 hours from the point at which the temperature started to rise until the point at which the temperature began to drop. It was adjusted back to the normal operating temperature quickly (within 1 hour) right after a shock. The next shock started after the system stayed at 37 °C for 36 hours.

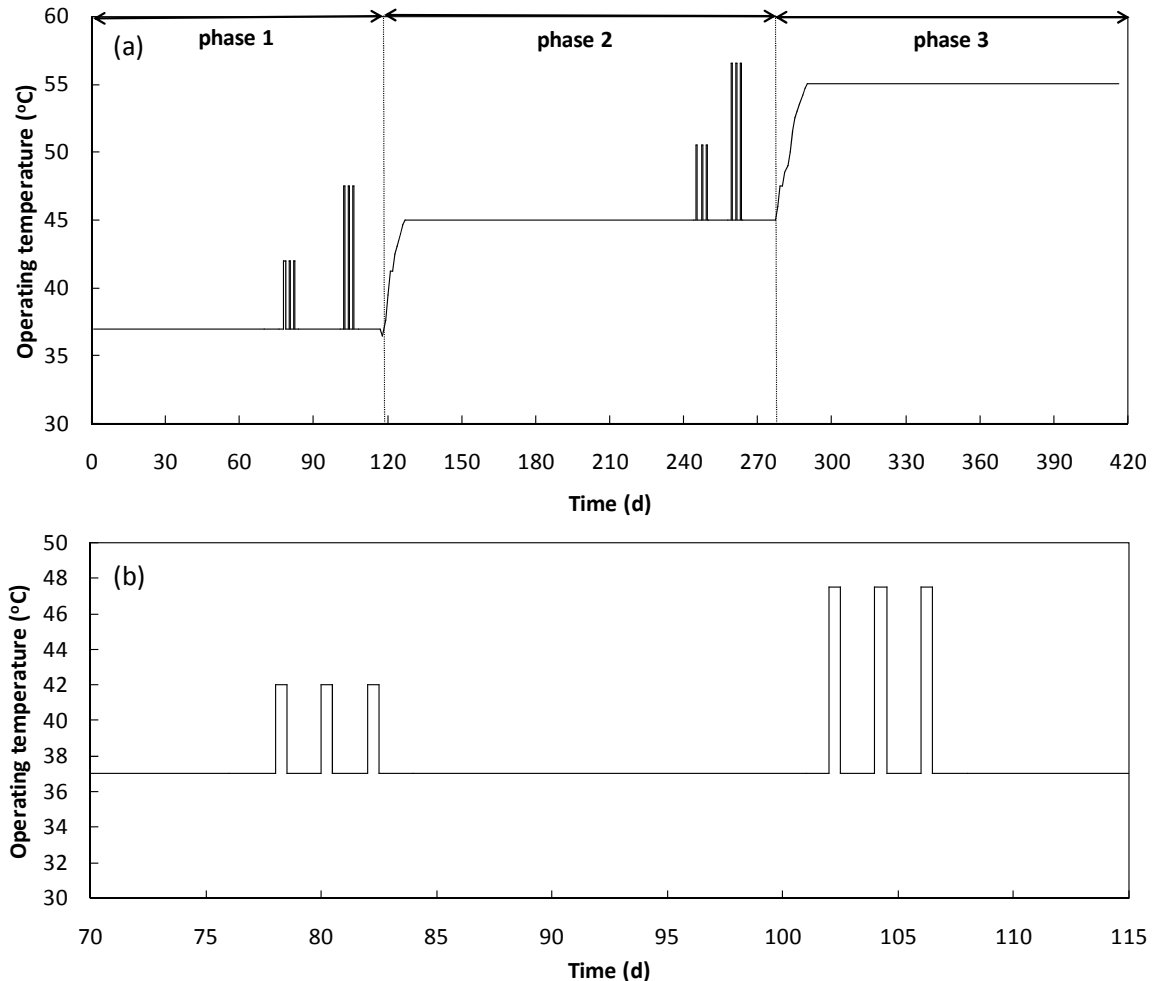


Figure 6-1 Temperature variations (a) three phases throughout the operating time (b) detailed temperature rises during the shocks at 37°C.

In phase 2, the operating temperature of the SAnMBR was then increased slowly from 37 to 45 °C (0.5 – 1 °C /day) during 10 days. Similarly, the SAnMBR was subjected to 5 °C shocks (from 45 to 50.5 °C) and 10 °C shocks (from 45 to 55 °C) after steady-state operation was achieved at 45 °C. At last, the temperature was gradually increased to a thermophilic temperature of 55 °C (0.5 – 1 °C /day) over a period of 13

days (phase 3). Each operating temperature and temperature shock was delayed until the system performed as well as it had prior to the temperature change except phase 3. A new membrane was used before each temperature variation.

Samples of influent, effluent and mixed liquor were taken from the system every 2 - 3 days during the steady state of each operating temperature, while specific samples were collected right before and after the temperature shocks were imposed.

6.2.3 Total fouling resistance

The total fouling resistance (R_t) can be used to evaluate the extent of fouling using the Darcy's Law (Yamato et al., 2006):

$$R_t = R_m + R_f = \frac{\Delta P}{J \cdot \eta_T} \quad (6-1)$$

where R_t is the total resistance (m^{-1}), R_m is the membrane resistance (m^{-1}), R_f is the total fouling resistance due to cake layer formation and pore blocking (m^{-1}), J is the permeate flux (m^3/m^2s), ΔP is the transmembrane pressure difference (Pa), and η_T is the permeate dynamic viscosity (Pa s).

R_t was evaluated by the final flux of biomass filtration. In order to compare the extent of fouling at different temperatures applied, R_t was calculated with the temperature correction to 20 °C to compensate the dependence of viscosity on temperature.

$$\eta_T = \eta_{20^\circ C} \cdot e^{-0.0239 (T-20)} \quad (6-2)$$

R_m was estimated by measuring the water flux of de-ionized water. R_f was obtained by R_t and R_m according to equation 6-1.

6.2.4 Mixed liquor fractions sampling

The mixed liquor samples at different operating temperatures were collected during the steady state at each phase. The steady state period is a period when the COD concentration of influent and effluent, the biomass concentration, and the biogas production rate are constant and stable for at least 10 days. The mixed liquor was sampled right before and after each temperature rise during each temperature shock.

The supernatant containing soluble and colloidal substances was obtained from the mixed liquor by centrifugation ($18700 \times g$, 15 min) to separate the suspended solids. The supernatant was then filtered by 0.45 μm membrane filters (Millipore) which are often used to classify the particulates from the colloidal particles and solutes (Wang, 1994; Henze et al., 1999; Yamato et al., 2006; Elmitwalli et al., 2007). The filtrate obtained was subjected to SMP analyzes. The membrane filters were weighed before the filtrations. After filtration the membrane filters were generally dried in an oven at 105 °C for 24 hours and weighed again to measure the concentration of colloidal particles in the supernatant which was expressed in terms of the mass of colloidal particles per litre of the supernatant. There is no standard definition for the size of and colloidal particles and solutes. The SMP is defined here as the soluble compound with size less than 0.45 μm .

6.2.5 Analytical methods

Chemical oxygen demand (COD) was determined colorimetrically using test vials (Bioscience, Inc.) in the range of 20 - 900 mg/L. The MLSS concentrations were analysed according to standard methods (APHA, 2005).

The bound EPS was extracted using the cation exchange resin (DOWEX) according to Frølund et al. (1996) after reaching the steady state for each operating temperature. The extracted solution was analysed for proteins and polysaccharides that are the dominant components typically found in SMP and EPS (Reid et al., 2008). Polysaccharide concentrations in the SMP and in the bound EPS were measured according to the widely used anthrone method proposed by DuBois et al. (1956) which yields results in glucose equivalents. Protein concentrations were measured with bovine serum albumin as a reference according to Lowery et al. (1951). The sum of the concentrations of bound polysaccharides and proteins represented the total bound EPS. The total SMP was summed by adding the concentrations of soluble polysaccharides and soluble proteins. Additionally, SMP was estimated by COD measurement.

6.2.6 Statistical analysis

Statistical analysis was performed to identify the correlations between EPS/SMP and membrane fouling by means of linear correlations using the Statistical Package for

the Social Science (SPSS) V11.0 produced by SPSS Incorporation (America). Pearson's product momentum correlation coefficient (r_p) was used for linear estimations of the strength and direction of linear correlations between every two parameters. The Pearson coefficient ranges between -1 and $+1$, where $r_p = -1$ or $+1$ means a perfect correlation, and 0 means an absence of a relationship. Correlations were considered statistically significant at a 95 % confidence interval ($p < 0.05$). Additionally, the one-way analysis of variance (ANOVA) was used to determine whether there are any significant differences in EPS and SMP among different operating temperatures.

6.3 Results and discussion

6.3.1 Total fouling resistance

A laboratory-scale SAnMBR was operated for thermo-mechanical pulping pressate treatment for 416 days at different temperatures (37, 45 and 55 °C) and temperature shocks (5 and 10 °C) at tested temperatures (37 and 45 °C). The performance of the SAnMBR was reported in Chapter 5. The sustainable membrane flux was first maintained at 6.89 ± 0.56 L/m²•h. After the operating temperature rose to 55 °C, the sustainable membrane flux dropped to 5.68 ± 0.43 L/m²•h. The steady-state COD removal efficiency varied from 68 to 85 % under the conditions tested. Biogas production rate was 0.21 L/g COD removed.

Fig. 6-2 displays the development of total fouling resistance for 26 days at different temperatures when the SAnMBR achieved steady state. The three fouling resistance profiles in Fig. 6-2 show the similar trends: an abrupt initial rise followed by a slow increase in R_f . A turning point at which sudden changes in R_f occurred was clearly observed for the operating temperature of 55 °C. According to equation 6-1, a three-stage TMP profile, frequently observed in SMBR systems (Zhang et al., 2006a), will lead to a similar trend of filtration resistance during a constant flux operation mode.

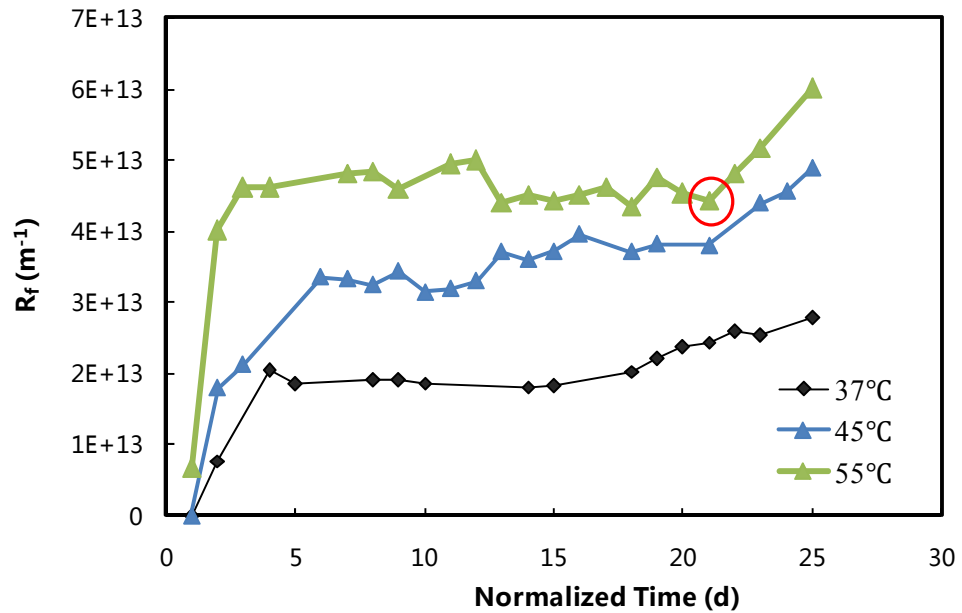


Figure 6-2 Development of total fouling resistance at different temperatures (steady state) (Flux = 6.65 ± 0.44 L/m²•h (37 °C); Flux = 6.46 ± 0.33 L/m²•h (45 °C); Flux = 5.49 ± 0.26 L/m²•h (55 °C)).

Furthermore, the higher the operating temperature, the greater fouling resistance was reached. The total fouling resistance relatively stabilized after an initial rise in this study, rather than continuously increasing over time as reported by Rosenberger et al. (2006). In this case, it is hard to determine the fouling rate according to the slope of filtration resistance. The variation of fouling resistance directly shows the degree of membrane fouling. Therefore, over the same operation period, the membrane fouling degree increased with an increase in the operating temperature.

Neither MLSS nor OLR could be accounted for the fouling behaviour at different operating temperatures, as these parameters were kept constant during the operation. Thus, the following study was based on an investigation of the mixed liquor fractions and their relationship with fouling resistance.

6.3.2 Effect of operating temperatures on bound EPS and SMP

The bound EPS contents at 37, 45 and 55 °C were analyzed (Fig. 6-3). Total bound EPS at 37, 45 and 55 °C were 26.76 ± 1.75 mg/gMLSS, 30.47 ± 1.41 mg/gMLSS and 37.59 ± 3.25 mg/gMLSS, respectively. Both proteins (PN) and polysaccharides (PC) concentration increased with an increase in the operating temperature. There were significant differences in the bound EPS contents when the temperature increased from 37 to 55 °C (ANOVA, $p < 0.05$). The PN/PC value was comparable for 37 and 45 °C (ANOVA, $p = 0.901$), whereas a slightly reduced PN/PC value was observed at 55 °C (ANOVA, $p < 0.05$) (Fig. 6-3(b)). The PN/PC value is related with the hydrophobicity of bound EPS. It is reported that the hydrophobic EPS fractions mainly comprise proteins, while the hydrophilic fraction mainly consisted of polysaccharides (Jorand et al., 1998). A higher ratio of proteins to polysaccharides in bound EPS is connected with greater affinity between proteins and sludge flocs, and thus favors the formation of sludge flocs (Liu and Fang, 2003). Therefore, the lower PN/PC value at high operating temperature further explain the deflocculation observed in our previous study (section 5.3.3).

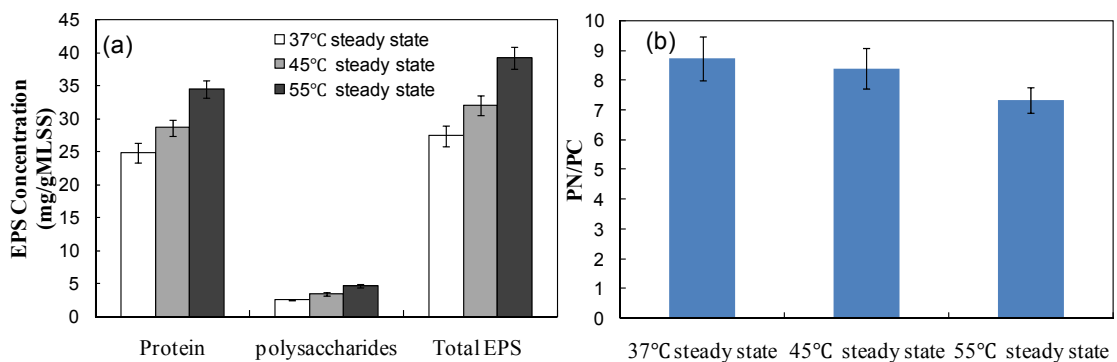


Figure 6-3 Bound EPS contents at different operating temperatures (steady state).

The total SMP and soluble protein concentrations at three operating temperatures (Fig. 6-4) show the same trend as the bound EPS (ANOVA, $p < 0.05$). Although there were no significant differences in the soluble polysaccharides concentrations between 37 and 45 °C (ANOVA, $p = 0.130$) or between 45 and 55 °C (ANOVA, $p = 0.149$), there were significant differences between 37 and 55 °C (ANOVA, $p < 0.05$). The PN/PC values were relatively steady (ANOVA, $p > 0.05$) (data not shown). Meanwhile, an

increase in the concentration of colloidal particles existed in the supernatant due to the increase in the operating temperature (Fig. 6-5). The presence of a greater amount of colloidal particle and soluble microbial products (SMPs) in sludge suspension at high temperatures (45 and 55 °C) than that at 37 °C could be the causes of the high supernatant COD in phase 2 and phase 3 as reported in Chapter 5.

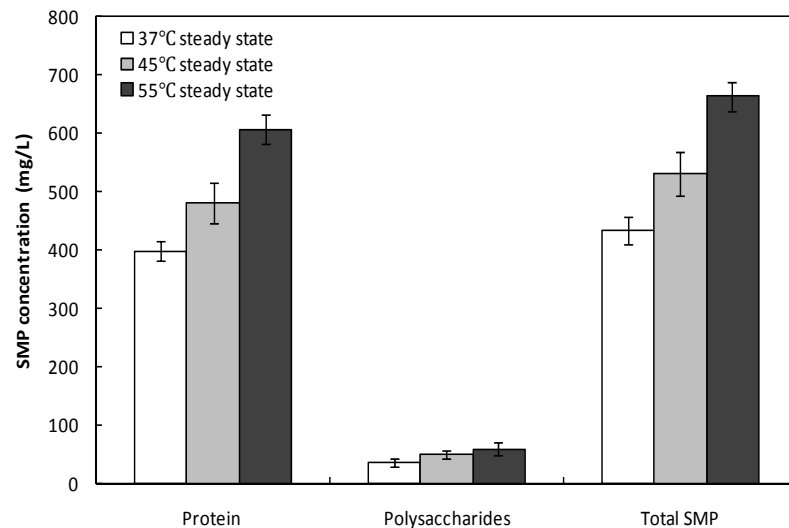


Figure 6-4 SMP concentrations at different operating temperatures (steady state).

The effect of temperature on EPS production is highly variable and is dependent on the microbial community and the experimental conditions. Theoretically, the increase in temperature will improve dissolution of organic compounds and accelerate the metabolic activity of microbes including the secretion of EPS (Grobben et al., 1995; Zhang et al., 2006b). Comte et al. (2006b) also reported that the heating method for EPS extraction at high temperature can create disruption of flocs facilitating the detachment of bound EPS from cells. According to our study in Chapter 5, the high operating temperatures and temperature shocks induced breakage of large sludge flocs. Floc breakage exposes the EPS present inside the floc structure as well as increasing the SMP level in the bulk sludge (Chang et al., 2002). On the other hand, we found some differences of species diversity and richness in the microbial community developed at the three operating temperatures (see section 5.3.4). When the temperature rose from 37 to 45 °C, the stressful micro-environment at the edge of the mesophilic range may promote the bacteria to synthesize more EPS to survive. As the temperature further rose to 55 °C, it

took almost 96 days for the SAnMBR to restore system performance. The mesophilic microorganisms had to acclimate to the high temperature, or those populations best suitable for the specific temperature would be growing in the microbial community. The high EPS production at 45 and 55 °C may also be attributed to the gradual shifts in species and the number of bacterial population as the temperature increased (LaPara et al., 2001).

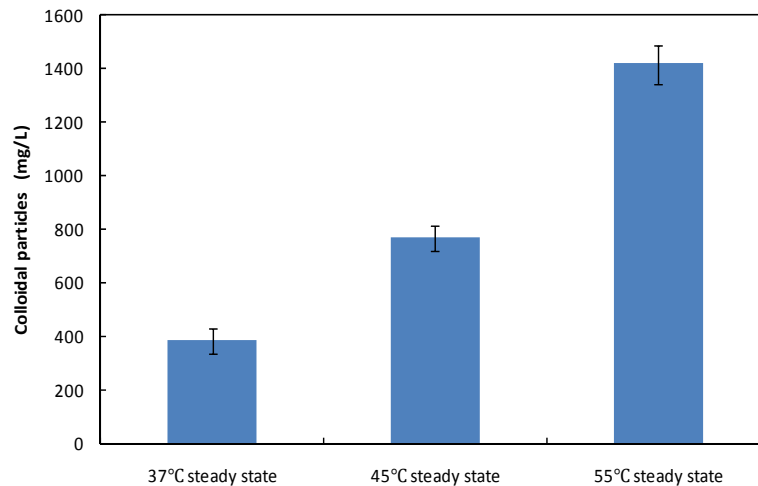


Figure 6-5 Colloidal particles contents at different operating temperatures (ANOVA, $p < 0.05$).

6.3.3 Effect of temperature shocks on bound EPS and SMP

Bound EPS was extracted before and after the temperature shocks. No significant difference was found in polysaccharides (ANOVA, $p > 0.05$) for the 5 and 10 °C shocks at 37 °C. Increased bound protein amount was only detected after the 10 °C shock at 37 °C (Fig. 6-6 (a)), and the total bound EPS and PN/PC were higher compared with those during 37 °C steady state operation. For the 5 °C and 10 °C shocks at 45 °C, it is evident that both the proteins and the polysaccharides were higher after the temperature shocks than that at 45 °C steady state, resulting in a concomitant reduction in PN/PC value (Fig. 6-6 (b)). Therefore, the bacteria could tolerate the 5 °C temperature shocks at 37 °C. The 5 and 10 °C shocks at 45 °C exerted greater impacts on microbial activities than temperature shocks at 37 °C did. It is well known that an increase in temperature will lead to an increase in the maximum specific growth and substrate utilization rates. The production of bound EPS is growth-associated and in direct proportion to substrate

utilization (Laspidou and Rittmann, 2002), so that more bound EPS was produced during the temperature shocks. Also, bacteria tend to produce more EPS under unfavorable conditions (Sheng et al., 2010).

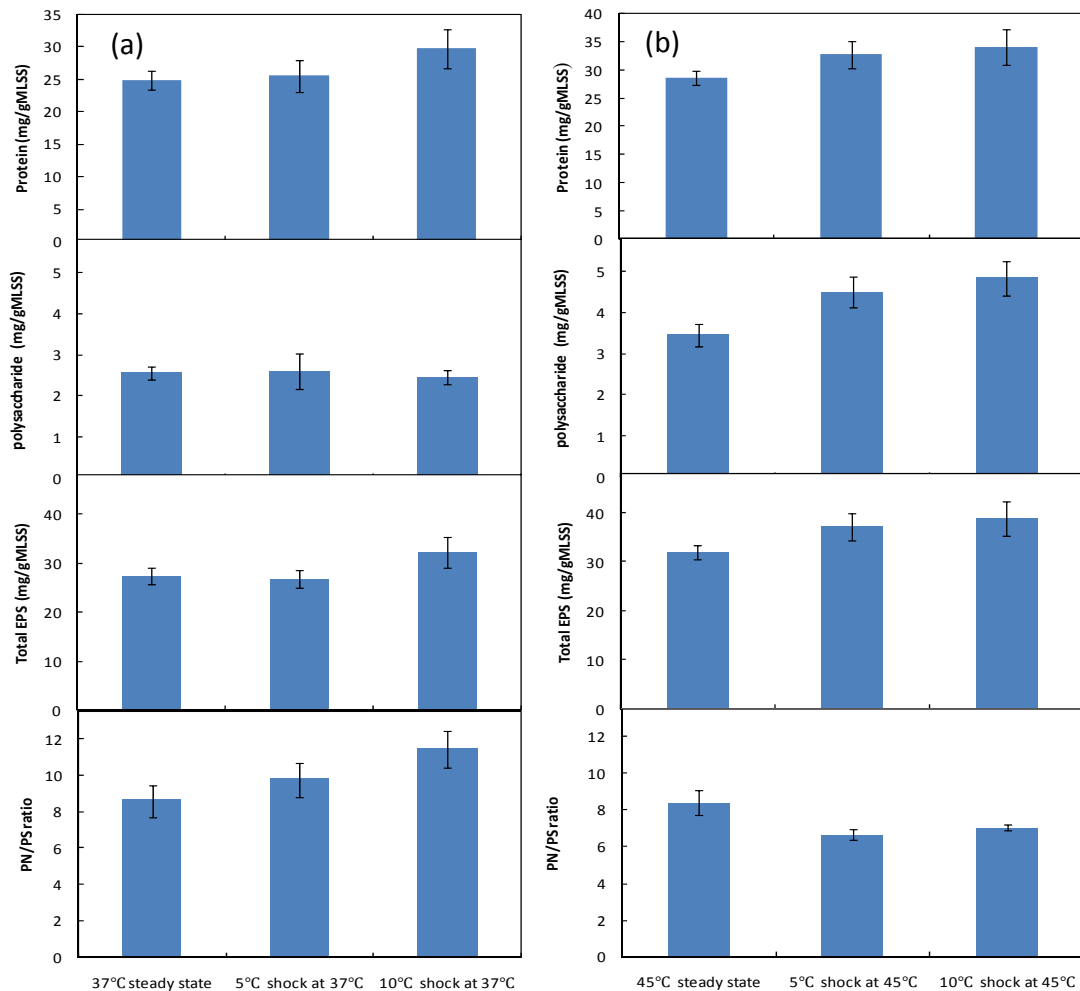


Figure 6-6 Bound EPS contents: (a) 5 and 10 °C shocks at 37 °C; (b) 5 and 10 °C shocks at 45 °C.

Figure 6-7 presents the SMP concentrations examined before and after the temperature shocks, showing reduced polysaccharide concentrations after the shocks. There was no influence of 5 °C shocks at 37 °C on soluble protein production (ANOVA, $p = 0.462$), while a slightly increased concentration of proteins was found after 10 °C shocks at 37 °C (ANOVA, $p < 0.05$) (Fig. 6-7 (a)). For temperature shocks at 45 °C, both

5 and 10 °C shocks caused increased soluble proteins in the supernatant, and the higher temperature rises corresponded to a higher concentration (ANOVA, $p < 0.05$).

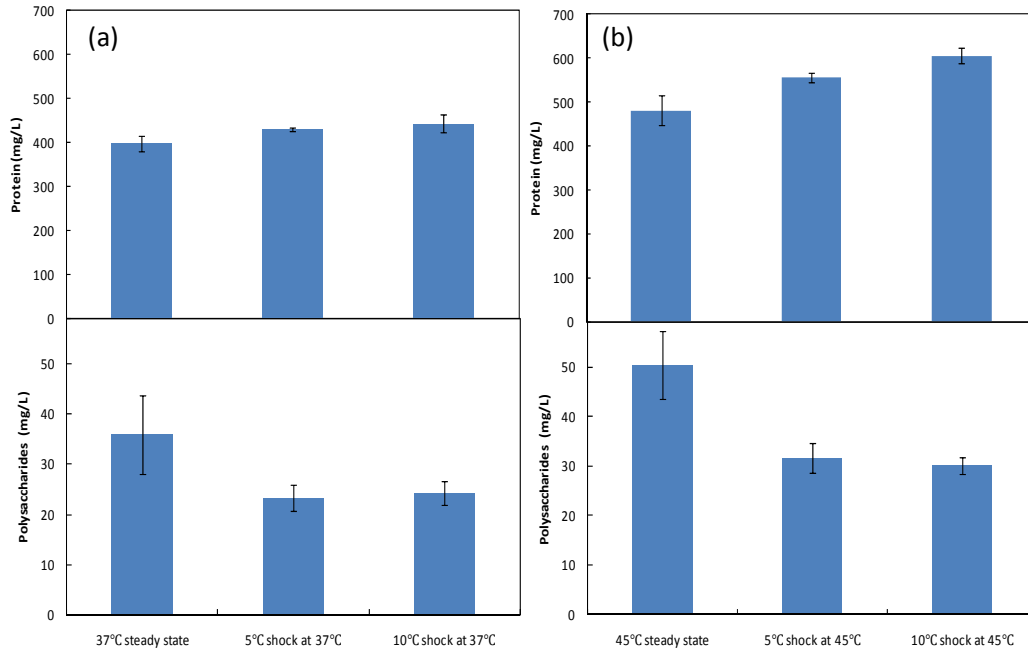


Figure 6-7 SMP concentrations: (a) 5 and 10 °C shocks at 37 °C; (b) 5 and 10 °C shocks at 45 °C.

SMP include organic molecules released by cell lysis and products of the dissolution or hydrolysis of bound EPS (Comte et al., 2006a). Parts of SMP, which are biodegradable, can be utilized as recycled substrate by cells (Laspidou and Rittmann, 2002), and the polysaccharides could be utilized faster than proteins (Zhang and Bishop, 2003). Polysaccharide is believed to be the only one of the bound EPS components that is synthesized for a specific function. Bacteria tend to synthesize extracellular polysaccharides to survive stressful environments (Tay, 2004; Wang and Zhang, 2010). Consequently, when the temperature shocks were imposed, sudden exposure at a high temperature might stimulate the bacteria to produce extracellular polysaccharides as a protective/adaptive response by utilizing the soluble polysaccharides as substrate.

6.3.4 Relationships of bound EPS to membrane fouling

Fig. 6-8 plots the total fouling resistance as a function of EPS concentrations for all the sludge samples tested under steady states at three operating temperatures. A

negative relationship exists between the PN/PC ratio and fouling resistance ($r_p = -0.668$; $p < 0.001$). Correlations between protein in bound EPS and fouling resistance ($r_p = 0.911$; $p < 0.001$), polysaccharides in bound EPS and fouling resistance ($r_p = 0.875$; $p < 0.001$), and total bound EPS and fouling resistance are statistically significant ($r_p = 0.896$; $p < 0.001$), meaning that the more bound EPS is present, the higher the extent of fouling. The higher fouling resistance at higher operating temperature was not only caused by a lower PN/PC ratio but also by higher EPS concentration.

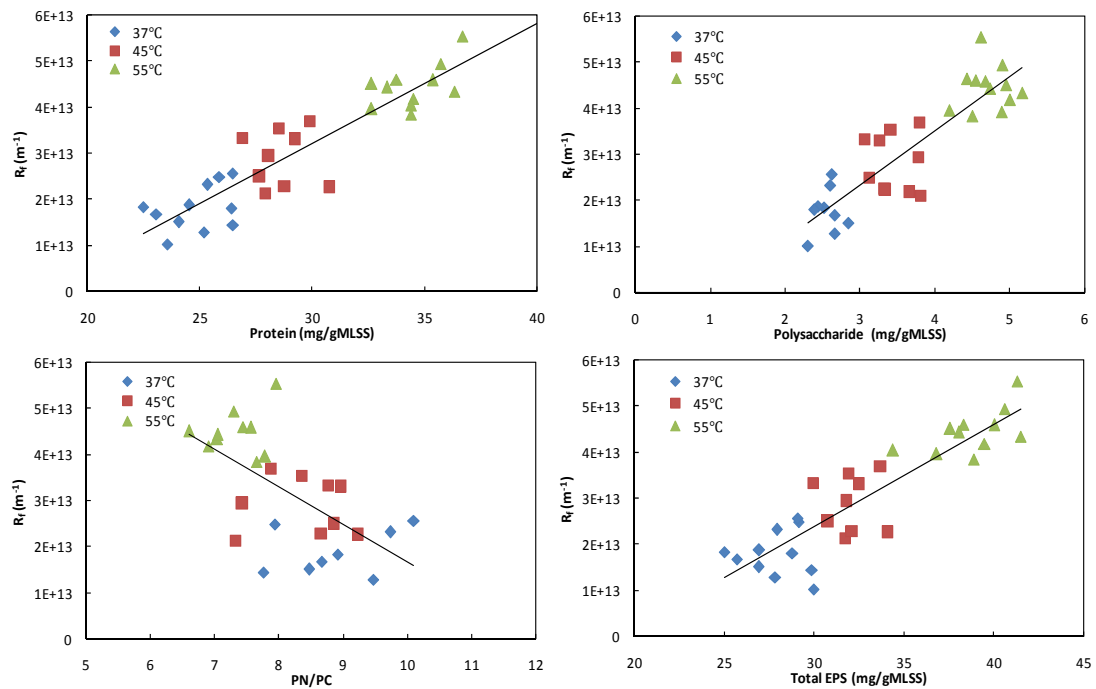


Figure 6-8 Correlation between total fouling resistance and bound EPS.

It is out of question that bound EPS concentrations have great effects on sludge characteristics such as flocculation ability, surface charge and viscosity that can affect membrane fouling (Meng et al., 2009). As mentioned earlier, some contradictory results have been published regarding the role of bound EPS on membrane fouling. The difference between this study and other studies was that the changes in bound EPS concentration were induced by temperature variation rather than other operational conditions (e.g. SRT). Considering that many factors can affect membrane fouling (Meng

et al., 2009), the contradictory results may be determined by the changes in the dominant causes of membrane fouling under different conditions.

6.3.5 Relationships of mixed liquor fractions to membrane fouling

In order to discuss the relationship between each mixed liquor fraction and membrane fouling, the total fouling resistance was plotted as a function of their concentrations measured at the steady state of 37, 45 and 55 °C (Fig. 6-9). As shown in Fig. 6-9 (a), there was a strong correlation between fouling resistance and supernatant COD ($r_p = 0.913$; $p < 0.001$), demonstrating a tendency for increasing fouling extent with increasing COD in the mixed liquor.

With further study of specific fractions, good correlations to fouling resistance were observed for both colloid particles ($r_p = 0.906$; $p < 0.001$) (Fig. 6-9 (c)) and soluble COD ($r_p=0.859$; $p < 0.001$) (Fig. 6-9 (b)), indicating that colloidal content was responsible for the fouling behaviour. Although plots of fouling resistance as a function of soluble polysaccharides concentration were scattered ($r_p = 0.525$; $p = 0.025$) (Fig. 6-9 (e)), the concentration of soluble protein gave a good correlation with fouling resistance ($r_p = 0.907$; $p < 0.001$) (Fig. 6-9 (d)), resulting in a positive linear relationship between fouling resistance and total SMP ($r_p = 0.880$; $p < 0.001$) (Fig. 6-9 (f)). A linear relationship between the fouling rate and the polysaccharides concentration in the sludge water phase was demonstrated by Lesjean et al. (2005). Rosenberger et al. (2006) also found that organic colloids, soluble proteins and polysaccharides impacted fouling. These results suggest that colloidal particles and SMP (especially soluble protein) play a significant role in membrane fouling.

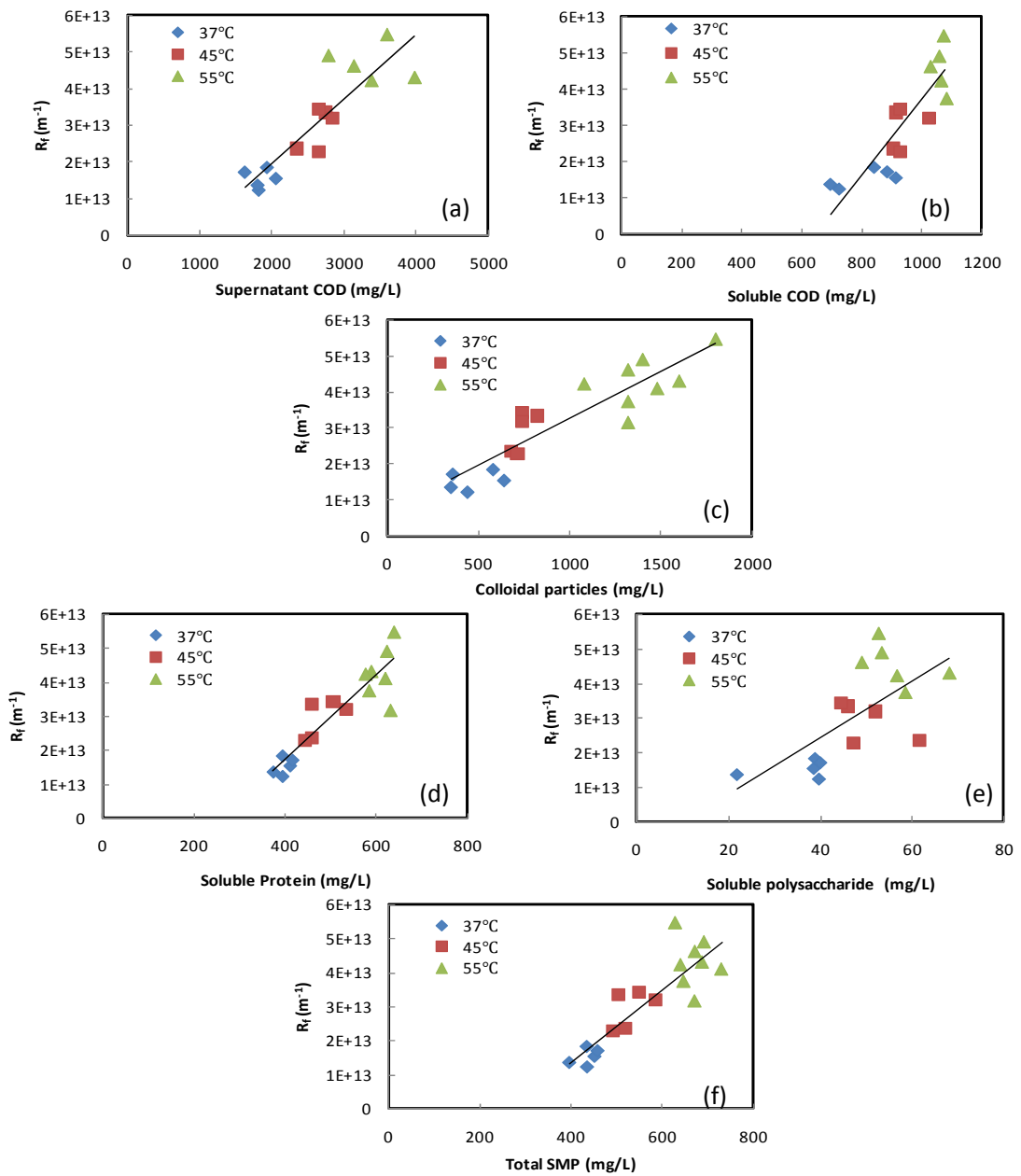


Figure 6-9 Correlation between total fouling resistance and SMP.

Membrane fouling was reported to occur due to the continuous deposition of sludge flocs accompanied by adsorption of small mixed liquor constituents (colloids and solutes) onto the membrane surface (Meng et al., 2009). Colloidal particles and solutes could even penetrate into pores of membrane or secondary membrane (known as cake

layer formed by all kinds of foulants) because of their sizes that are similar or smaller than those membrane pore sizes. When their concentrations increased with the operating temperature, it can be assumed that more colloidal particles and solutes would accumulate within/on the membrane surface or cake layer at higher temperatures. As a result, although fouling resistance can be determined by many factors (i.e. particle size of sludge flocs, cake layer structure), colloidal particles and solutes made significant contributions to the fouling resistance at three operating temperatures (Fig. 6-2) and the following sequence was observed: 55 °C > 45 °C > 37 °C (Fig. 6-2).

6.4 Conclusions

An investigation on the effects of temperature and temperature shock on EPS and SMP production and their role in membrane fouling was carried out under different operating temperatures (37, 45 and 55 °C) and temperature shocks (5/10 °C at 37/45 °C) to establish correlations between EPS/SMP and membrane fouling in a SAnMBR. For the same operation period, the extent of membrane fouling increased with an increase in the operating temperature. The bound EPS, soluble SMP, and colloidal particles contents increased with an increase in operating temperature. Temperature shocks promoted the production of bound EPS, while concentrations of the soluble polysaccharides were reduced after the shocks. Statistical analyses show that total bound EPS, bound polysaccharides, and bound proteins, soluble total SMP, soluble polysaccharides, soluble proteins, and colloidal particle content in supernatant positively correlated to the fouling resistance, indicating that bound EPS, SMPs, and colloidal particles have significant contribution to membrane fouling. Operation of the SAnMBR in the mesophilic temperature range is more attractive than that in a thermophilic temperature, from a membrane fouling control point of view.

6.5 References

APHA, 2005. Standard methods for the examination of water and wastewater, 21th ed. American Public Health Association (APHA)/American Water Works Association (AWWA)/Water Environment Federation (WEF), Washington, DC.

- Bae, T.-H., Tak, T.-M., 2005. Interpretation of fouling characteristics of ultrafiltration membranes during the filtration of membrane bioreactor mixed liquor. *Journal of Membrane Science* 264, 151-160.
- Chang, I.-S., Le Clech, P., Jefferson, B., Judd, S., 2002. Membrane Fouling in Membrane Bioreactors for Wastewater Treatment. *Journal of Environmental Engineering* 128, 1018.
- Chang, I.-S., Lee, C.-H., 1998. Membrane filtration characteristics in membrane-coupled activated sludge system -- the effect of physiological states of activated sludge on membrane fouling. *Desalination* 120, 221-233.
- Comte, S., Guibaud, G., Baudu, M., 2006a. Biosorption properties of extracellular polymeric substances (EPS) resulting from activated sludge according to their type: Soluble or bound. *Process Biochemistry* 41, 815-823.
- Comte, S., Guibaud, G., Baudu, M., 2006b. Relations between extraction protocols for activated sludge extracellular polymeric substances (EPS) and EPS complexation properties: Part I. Comparison of the efficiency of eight EPS extraction methods. *Enzyme and Microbial Technology* 38, 237-245.
- Defrance, L., Jaffrin, M. Y., Gupta, B., Paullier, P., Geaugey, V., 2000. Contribution of various constituents of activated sludge to membrane bioreactor fouling. *Bioresource Technology* 73, 105-112.
- Drews, A., Lee, C.-H., Kraume, M., 2006. Membrane fouling - a review on the role of EPS. *Desalination* 200, 186-188.
- Drews, A., Vocks, M., Bracklow, U., Iversen, V., Kraume, M., 2008. Does fouling in MBRs depend on SMP? *Desalination* 231, 141-149.
- DuBois, M., Gilles, K. A., Hamilton, J. K., Rebers, P. A., Smith, F., 1956. Colorimetric Method for Determination of Sugars and Related Substances. *Analytical Chemistry* 28, 350-356.
- Elmitwalli, T. A., Shalabi, M., Wendland, C., Otterpohl, R., 2007. Grey water treatment in UASB reactor at ambient temperature. *Water Science & Technology* 55, 173-180.

- Fan, F., Zhou, H., 2007. Interrelated Effects of Aeration and Mixed Liquor Fractions on Membrane Fouling for Submerged Membrane Bioreactor Processes in Wastewater Treatment. *Environmental Science & Technology* 41, 2523-2528.
- Fonseca, A. C., Summers, R. S., Greenberg, A. R., Hernandez, M. T., 2007. Extra-Cellular Polysaccharides, Soluble Microbial Products, and Natural Organic Matter Impact on Nanofiltration Membranes Flux Decline. *Environmental Science & Technology* 41, 2491-2497.
- Frølund, B., Palmgren, R., Keiding, K., Nielsen, P. H., 1996. Extraction of extracellular polymers from activated sludge using a cation exchange resin. *Water Research* 30, 1749-1758.
- Grobben, G. J., Sikkema, J., Smith, M. R., Bont, J. A. M. D., 1995. Production of extracellular polysaccharides by *Lactobacillus delbrueckii* spp. *bulgaricus* NCFB 2772 grown in a chemically defined medium. *Journal of Applied Bacteriology* 79, 103-107.
- Harada, H., Momonoi, K., Yamazaki, S., Takizawa, S., 1994. Application of anaerobic UF membrane reactor for treatment of a wastewater containing high strength particulate organics. *Water Science and Technology* 30, 307-319.
- Henze, M., Gujer, W., Mino, T., Matsuo, T., Wentzel, M. C., Marais, G. v. R., Van Loosdrecht, M. C. M., 1999. Activated Sludge Model No.2d, ASM2d. *Water Science and Technology* 39, 165-182.
- Hong, S. P., Bae, T. H., Tak, T. M., Hong, S., Randall, A., 2002. Fouling control in activated sludge submerged hollow fiber membrane bioreactors. *Desalination* 143, 219-228.
- Jorand, F., Boué-Bigne, F., Block, J. C., Urbain, V., 1998. Hydrophobic/hydrophilic properties of activated sludge exopolymeric substances. *Water Science and Technology* 37, 307-315.
- Kimura, K., Naruse, T., Watanabe, Y., 2009. Changes in characteristics of soluble microbial products in membrane bioreactors associated with different solid retention times: Relation to membrane fouling. *Water Research* 43, 1033-1039.

- LaPara, T. M., Nakatsu, C. H., Pantea, L. M., Alleman, J. E., 2001. Aerobic Biological Treatment of a Pharmaceutical Wastewater: Effect of Temperature on COD Removal and Bacterial Community Development. *Water Research* 35, 4417-4425.
- Laspidou, C. S., Rittmann, B. E., 2002. A unified theory for extracellular polymeric substances, soluble microbial products, and active and inert biomass. *Water Research* 36, 2711-2720.
- Lesjean, B., Rosenberger, S., Laabs, C., Jekel, M., Gnirss, R., Amy, G., 2005. Correlation between membrane fouling and soluble/colloidal organic substances in membrane bioreactors for municipal wastewater treatment. *Water Science and Technology* 51, 1-8.
- Liao, B. Q., Bagley, D. M., Kraemer, H. E., Leppard, G. G., Liss, S. N., 2004. A review of biofouling and its control in membrane separation bioreactors. *Water Environment Research* 76, 425-436.
- Liu, Y., Fang, H. H. P., 2003. Influences of Extracellular Polymeric Substances (EPS) on Flocculation, Settling, and Dewatering of Activated Sludge. *Critical Reviews in Environmental Science and Technology* 33, 237-273.
- Lowery, O. H., Rosebrough, N., Farr, A. L., Randall, R. J., 1951. Protein measurement with the folin phenol reagent. *Journal of Biological Chemistry* 193, 265-275.
- Meng, F., Chae, S.-R., Drews, A., Kraume, M., Shin, H.-S., Yang, F., 2009. Recent advances in membrane bioreactors (MBRs): Membrane fouling and membrane material. *Water Research* 43, 1489-1512.
- Meng, F., Shi, B., Yang, F., Zhang, H., 2007. Effect of hydraulic retention time on membrane fouling and biomass characteristics in submerged membrane bioreactors. *Bioprocess and Biosystems Engineering* 30, 359-367.
- Ndegwa, P. M., Hamilton, D. W., Lalman, J. A., Cumba, H. J., 2008. Effects of cycle-frequency and temperature on the performance of anaerobic sequencing batch reactors (ASBRs) treating swine waste. *Bioresource Technology* 99, 1972-1980.

- Reid, E., Liu, X., Judd, S. J., 2008. Sludge characteristics and membrane fouling in full-scale submerged membrane bioreactors. *Desalination* 219, 240-249.
- Rosenberger, S., Evenblij, H., te Poele, S., Wintgens, T., Laabs, C., 2005. The importance of liquid phase analyses to understand fouling in membrane assisted activated sludge processes--six case studies of different European research groups. *Journal of Membrane Science* 263, 113-126.
- Rosenberger, S., Kraume, M., 2003. Filterability of activated sludge in membrane bioreactors. *Desalination* 151, 195-200.
- Rosenberger, S., Laabs, C., Lesjean, B., Gnirss, R., Amy, G., Jekel, M., Schrotter, J. C., 2006. Impact of colloidal and soluble organic material on membrane performance in membrane bioreactors for municipal wastewater treatment. *Water Research* 40, 710-720.
- Sheng, G.-P., Yu, H.-Q., Li, X.-Y., 2010. Extracellular polymeric substances (EPS) of microbial aggregates in biological wastewater treatment systems: A review. *Biotechnology Advances* 28, 882-894.
- Sofia, A., Ng, W. J., Ong, S. L., 2004. Engineering design approaches for minimum fouling in submerged MBR. *Desalination* 160, 67-74.
- Tay, Y.-Q. L. Y. L. J.-H., 2004. The effects of extracellular polymeric substances on the formation and stability of biogranules. *Appl Microbiol Biotechnol* 65, 143-148.
- Trussell, R. S., Merlo, R. P., Hermanowicz, S. W., Jenkins, D., 2007. Influence of mixed liquor properties and aeration intensity on membrane fouling in a submerged membrane bioreactor at high mixed liquor suspended solids concentrations. *Water Research* 41, 947-958.
- Vogelaar, J. C. T., Bouwhuis, E., Klapwijk, A., Spanjers, H., van Lier, J. B., 2002. Mesophilic and thermophilic activated sludge post-treatment of paper mill process water. *Water Research* 36, 1869-1879.
- Wang, K. (1994). Integrated anaerobic and aerobic treatment of sewage. Wageningen, The Netherlands, Wageningen University. Ph.D.
- Wang, Z.-P., Zhang, T., 2010. Characterization of soluble microbial products (SMP) under stressful conditions. *Water Research* 44, 5499-5509.

- Welander, T., Morin, R., Nylén, B., 1999. Biological removal of methanol from kraft mill condensate. In: TAPPI Proceedings International Environmental Conference,
- Wilson, C. A., Murthy, S. M., Fang, Y., Novak, J. T., 2008. The effect of temperature on the performance and stability of thermophilic anaerobic digestion. *Water Science and Technology* 57, 297-304.
- Wisniewski, C., Grasmick, A., 1998. Floc size distribution in a membrane bioreactor and consequences for membrane fouling. *Colloids and Surfaces A: Physicochemical and Engineering Aspects* 138, 403-411.
- Wu, B., Yi, S., Fane, A. G., 2011. Microbial behaviors involved in cake fouling in membrane bioreactors under different solids retention times. *Bioresource Technology* 102, 2511-2516.
- Xie, K., Lin, H. J., Mahendran, B., Bagley, D. M., Leung, K. T., Liss, S. N., Liao, B. Q., 2010. Performance and fouling characteristics of a submerged anaerobic membrane bioreactor for kraft evaporator condensate treatment. *Environmental Technology* 31, 511-521.
- Yamato, N., Kimura, K., Miyoshi, T., Watanabe, Y., 2006. Difference in membrane fouling in membrane bioreactors (MBRs) caused by membrane polymer materials. *Journal of Membrane Science* 280, 911-919.
- Zhang, J., Chua, H. C., Zhou, J., Fane, A. G., 2006a. Factors affecting the membrane performance in submerged membrane bioreactors. *Journal of Membrane Science* 284, 54-66.
- Zhang, S., Yang, F., Liu, Y., Zhang, X., Yamada, Y., Furukawa, K., 2006b. Performance of a metallic membrane bioreactor treating simulated distillery wastewater at temperatures of 30 to 45 °C. *Desalination* 194, 146-155.
- Zhang, X., Bishop, P. L., 2003. Biodegradability of biofilm extracellular polymeric substances. *Chemosphere* 50, 63-69.

Chapter 7 Influence of temperature and temperature shock on cake layer structure and membrane fouling from a submerged anaerobic membrane bioreactor

Abstract:

A laboratory-scale submerged anaerobic membrane bioreactor (SAnMBR) treating thermomechanical pulping pressate was used to study cake layer structure and membrane fouling at different operating temperatures (37, 45 and 55 °C) and under different magnitudes (5 and 10 °C) of temperature shocks. Various analytic techniques, including micro-tome slicing technique, conventional optical microscopy (COM), extraction and chemical analysis of extracellular polymeric substances (EPS), particle size analysis, and polymerase chain reaction (PCR)-denaturing gradient gel electrophoresis (DGGE), were used to characterize the cake layer structure and membrane fouling. The results showed that the thickness and particle size of the cake layers decreased with an increase in operating temperature, while both the protein and carbohydrate concentrations of bound extracellular polymeric substances (EPS) in the cake layer decreased with an increase in operating temperature. PCR-DGGE analysis indicated that there are some differences in species diversity and richness among different operating temperatures in cake sludge. At 55 °C steady state, the freshly formed cake layers (2 days) were thinner, higher in EPS concentration, higher in porosity, much lower in particle size distributions (PSDs), and significantly different in microbial community, as compared to the cake layers of 12 and 25 days.

7.1 Introduction

In recent years, considerable attention has been paid on the development of submerged anaerobic membrane bioreactor (SAnMBR) for sustainable wastewater treatment. Its potential for wastewater treatment lies on some of the principal advantages of SAnMBR systems, such as high quality effluent, complete solid-liquid separation, high

loading rate, low energy consumption, low sludge production, net energy production and small footprint (Liao et al., 2006). But in practice, membrane fouling, which leads to membrane performance decline and operating costs increase, has restricted the wide application of the SAnMBRs. Cake layer formation on membrane surfaces was identified as the dominant and inevitable contributor to the total membrane fouling (Chu and Li, 2005; Jeison and van Lier, 2008).

The high hydraulic resistance of the cake layer is of great interest because it accounts for 95–98% of the total filtration resistances (Ramesh et al., 2007). A number of techniques (backwashing, gas sparging, intermittent suction, membrane fouling reducer, etc.) have been applied to mitigate cake layer formation. Apparently, cake sludge originates from the bulk sludge in the membrane bioreactor system. It consists of a variety of components, including sludge, microorganisms, extracellular polymeric substances (EPS), organic and inorganic particles (Meng et al., 2009). Thus, many previous investigations have been carried out with the analysis of different fouling components in various fractions of mixed liquor (Defrance et al., 2000; Fan and Zhou, 2007). However, limited attention has been paid to the cake layer structure.

To effectively optimize the filtration performance of SAnMBRs, an adequate understanding of the dynamic characteristics of cake layers is essential. However, most studies have focused on the surface morphology of the cake layer, and limited information is available with regard to cake layer characterization. Hwang et al. (2007) reported the effect of membrane fouling reducer on 3D architecture and its quantitative analysis of the cake layer in MBR. The major components of cake layer were systematically investigated by Meng et al. (2007). The spatial distribution of physical, chemical and microbiological structure along cake layer depth from an SAnMBR was characterized using various analytical tools in our previous study (Gao et al., 2011). On the other hand, investigations of microbial community structure on the membrane surface involved in cake layer formation has brought great attention to researchers in recently years (Jinhua et al., 2006; Zhang et al., 2006) for identifying fouling-causing bacteria.

The temperature of industrial wastewaters is usually fluctuant due to the operational conditions, the seasonal variations, and conjunction of wastewater streams

(Sipma et al., 2010). Thus, it is highly desirable to understand the effects of temperature variation and temperature shocks on the performance of biological systems for industrial wastewater treatment. Temperature is considered to be a key factor to affect the stability and efficiency of biological treatment processes (Lishman et al., 2000; LaPara et al., 2001), especially for anaerobic treatment processes (Mahmoud et al., 2004; Bouskova et al., 2005), in terms of sludge properties, effluent quality and microbial community, etc. For a membrane bioreactor, it can be anticipated that the temperature will also affect cake layer formation. Although several studies have been dedicated to examinations of cake layer structure (Hwang et al., 2007; Meng et al., 2007; Gao et al., 2011), the effect of temperature and temperature shocks on cake layer structure and membrane fouling in SAnMBRs has not previously been investigated. In this study, a laboratory-scale SAnMBR treating thermomechanical pulping pressate was operated for 416 days to assess the influence of temperature and temperature shocks on characteristics of cake layer structure and their role in membrane fouling.

7.2 Materials and methods

7.2.1 Laboratory-scale SAnMBR

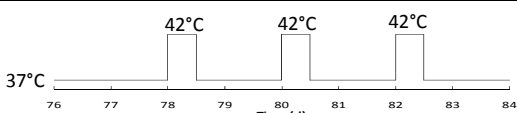
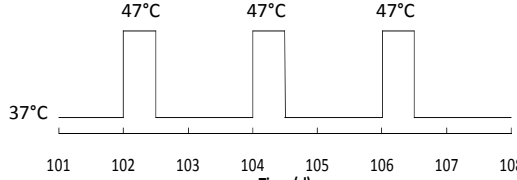
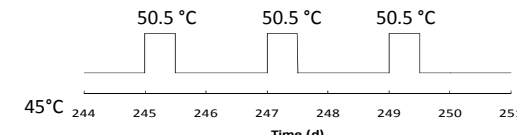
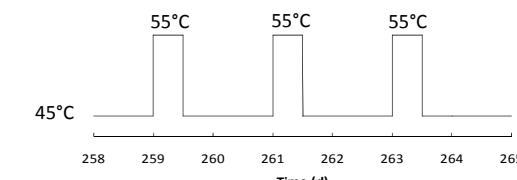
The SAnMBR has a working volume of 10 L, in which a flat sheet microfiltration membrane module (normal pore size of 0.3 μm , total area of 0.03 m^2 , polyvinylidene fluoride (PVDF)) was immersed in the top zone (6.5 L). The headspace biogas was recirculated at a flow rate of 1.5 L/min to control sludge deposition on membrane surfaces. The details of the SAnMBR system were described in Gao et al. (2010). Thermo-mechanical pulping pressate collected from a local pulp and paper mill was used as the influent, which was enriched with NH_4Cl and KH_2PO_4 to provide a proportion of COD:N:P of 100:2.6:0.4, and trace element nutrients, as described by Gao et al. (2010), to prevent trace metal limitations of the methanogens.

7.2.2 Experimental plan

The operating temperature was controlled by circulating water through the water jacket. The main temperature variations are illustrated in Table 7-1. In phase 1, the

wastewater was initially treated at a mesophilic temperature of 37 ± 1 °C. The SAnMBR was then subjected to periodic temperature shocks: 5°C shocks (from 37 °C to 42 °C) and 10 °C shocks (from 37 to 47 °C). As described in Table 6-1, three temperature shocks were conducted at each temperature fluctuation. The temperature shocks were simulated by suddenly increasing the temperature from 37 to 42 °C or 47 °C and lasted approximately 12 hours from the point at which the temperature started to rise until the point at which the temperature began to drop. It was adjusted back to the normal operating temperature quickly (within 1 hour) right after the shock. The next shock started after the system stayed at 37 °C for 36 hours.

Table 7-1
Temperature variations in detail

Time	Operating temperature	
Phase 1 (day 1 - 117)	day 78 - 83 (5°C shocks at 37°C) 	
	day 102 - 107 (10°C shocks at 37°C) 	
	Other days during phase 1	37°C
Phase 2 (day 118 - 277)	day 245 - 250 (5°C shocks at 45°C) 	
	day 259 - 264 (10°C shocks at 45°C) 	
	Other days during phase 2	45°C
Phase 3 (day 278 - 416)	day 278 - 416	55°C

In phase 2, the operating temperature of the SAnMBR was slowly increased from 37 to 45 °C (0.5-1 °C /day) over a 10-day interval. Similarly, the SAnMBR was subjected

to 5 °C shocks (from 45 to 50.5 °C) and 10 °C shocks (from 45 to 55 °C) after steady-state operation was achieved at 45 °C. Finally, the temperature was gradually increased to a thermophilic temperature of 55 °C (0.5-1 °C /day) over a period of 13 days (phase 3). Temperature shock experiments (5 and 10 °C) at 37 and 45 °C were conducted in sequences after steady state operation was achieved prior to temperature shock. A new membrane was used for each new condition (before and after temperature shock and different temperatures).

7.2.3 Fouling resistance

The total fouling resistance (R_f) can be used to evaluate the extent of membrane fouling using the Darcy's Law [19]:

$$R_t = R_m + R_f = \frac{\Delta P}{J \cdot \eta_T} \quad (7-1)$$

where R_t is the total resistance (m^{-1}), R_m is the membrane resistance (m^{-1}), R_f is the total fouling resistance (m^{-1}), J is the permeate flux (m^3/m^2s), ΔP is the transmembrane pressure difference (Pa), and η_T is the permeate dynamic viscosity (Pa s).

R_m was estimated by measuring the water flux of de-ionized water. R_t was evaluated by the final flux of sludge wastewater filtration. R_f was obtained by subtracting the R_m from the R_t according to equation 1. In order to compare the extent of fouling at different temperatures applied, R_t was calculated with the temperature correction to 20 °C to compensate the dependence of viscosity on temperature:

$$\eta_T = \eta_{20^\circ C} \cdot e^{-0.0239 (T-20)} \quad (7-2)$$

$$R_f = R_c + R_i + R_p \quad (7-3)$$

where R_c the fouling resistance caused by the cake sludge deposited over the membrane surface which can be easily removed by physical cleaning. The fouling caused by adsorption or pore blockage of solutes and/or colloidal within the membrane was classified into irremovable fouling (R_i) that needs chemical cleaning to be eliminated and permanent fouling (R_p) which cannot be removed by any approaches. The experimental procedure to determine R_i and R_p was as follows: (1) the membrane surface was flushed with tap water and cleaned with a sponge to remove the cake layer; (2) as shown in Fig.

7-1, the de-ionized water was measured in a 180 mL stirred filtration cell (Amicon, USA) at a constant pressure of 30 kPa to obtain the resistance of $R_m + R_i + R_p$; (3) chemical cleaning was then performed by immersing the membrane in 200 ppm NaOCl for 2 hours. After that, the de-ionized water was measured again to get the resistance of $R_m + R_p$. From steps (1)-(3), R_i and R_p were calculated.

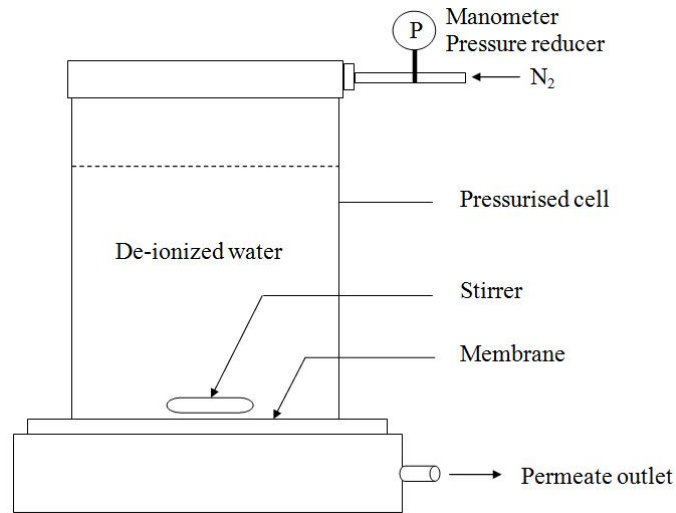


Figure 7-1 Schematic diagram of a stirred filtration cell.

7.2.4 Cake layer sampling

The cake layer samples were collected under steady state operation of different operating temperatures (37, 45 and 55 °C) and temperature shocks (5 and 10 °C) with the same operation time (i. e., cake age).

A series of small pieces of cake layer (1 cm × 1 cm) were cut from the same piece of membrane with cake layer on its surface. In order to prevent the structure and thickness of cake layer from changing, the cake layer was saturated with 0.85 % NaCl (Zhang and Bishop, 1994) aqueous solution and then frozen at -22 °C before being fixed onto a sample stage using optimal cutting temperature compound (O.T.C) (Sakura Finetechnical Co., Ltd. Tokyo, 103, Japan). Part of these cake layer samples were cryosectioned from the cake layer surface down to the bottom (membrane surface) at 100 µm intervals or cut into cross-sections by using a microtome blade (Feather, S35 type, Japan) with a cryostate microtome (Histostate Microtome, Model: 855, Reichert

Scientific Instruments Division of Warner Lambert Technologies Inc., NY, USA), which comprises a microtome and a cooling enclosure to set the temperature at -22 °C while sectioning. These slices were then observed by a conventional optical microscope (COM).

The cake sludge samples attached to the membrane surface were gently scraped off with care from the membrane surface using a plastic sheet (Wang et al., 2008) and were weighed to get the cake mass (M). These samples were then subjected to EPS, particle size distribution (PSD) and microbial community analyses.

7.2.5 Analytical methods for cake layer characterization

7.2.5.1 Cake porosity

The specific cake resistance (α) is the cake resistance normalized to the mass of cake sludge deposited per unit of membrane surface area as the following equation (Jin et al., 2006):

$$R_c = \frac{\alpha M}{A_m} \quad (7-4)$$

where α is the specific cake resistance (m/kg), M is the mass of cake sludge (kg), A_m is the membrane area (m²).

The specific cake resistance can also be determined by the Carman-Kozeny equation:

$$\alpha = \frac{180(1 - \varepsilon)}{\rho_p d_p^2 \varepsilon^3} \quad (7-5)$$

where ε is the porosity of the cake layer, ρ_p is the density of particles (kg/m³) and d_p is the particles diameter (m). Putting α obtained by equation (7-4) into equation (7-5), the cake porosity can be determined with knowing particle size and density. The density of cake layer was assumed to be 1.015 g/mL.

7.2.5.2 Particle size distribution analysis

The cake layers scraped off the membrane surface were prepared by rinsing sludge samples with distilled water followed by gently shaking to form uniform liquor.

The particle size distributions (PSD) of bulk sludge and cake layers were determined by a Malvern Mastersizer 2000 instrument (Worcestershire, UK) with a detection range of 0.02-2000 μm .

7.2.5.3 EPS extraction and measurement

The extraction of EPS was based on a cation exchange resin (Dowex® Marathon® C, Na⁺ form, Sigma-Aldrich, Bellefonte, PA) method (Frølund et al., 1996). The resin-to-biomass ratio was maintained at 80 g/g MLSS, and extraction was performed for 2 h at 4 °C. The EPS was normalized as the sum of carbohydrates and proteins, which were determined according to DuBois et al. (1956) and Lowery et al. (1951), respectively.

7.2.5.4 Microbial community

DNA was extracted from 0.2 g of cake sludge samples respectively with a Fecal DNA isolation kit (MoBio Laboratories, Solana Beach, CA, USA) as described in the manufacturer's instructions. Polymerase chain reaction (PCR) amplification was performed in a total volume of 50 μl on a Hybaid Thermocycler (Thermo Electron Corp., USA). The primer set, 341f-GC (5'-GC-clamp-CCTAGGGAGGCAGCAG-3') and 534r (5'-ATTACCGCGGCTGCTGG-3') were used. PCR cycling consisted of an initial denaturation at 94 °C for 5 min followed by 35 cycles consisting of denaturation at 94 °C for 1 min, primer annealing at 56 °C for 1 min, and primer extension at 72 °C for 1 min. A final extension step was conducted at 72 °C for 5 min prior to cooling at 4 °C. PCR products were purified using a DNA purification kit (Fermentas Life Sciences, Canada) in accordance with the manufacturer's recommendations prior to use in DGGE analysis. Polyacrylamide gels (10 % polyacrylamide, 25–65 %) were poured using a gradient maker (Bio-Rad, USA). The gels were run at 30 V for 18 h at 60 °C. After electrophoresis, the polyacrylamide gel was stained in 150 mL TAE buffer containing 15 μL 10 000 \times concentrated SYBR Green I stain (Fermentas Life Sciences, Canada) for 1 h, and then photographed with a digital camera (SynGene a division of Synoptics Ltd, UK) to acquire the denaturing gradient gel electrophoresis (DGGE) band image. Duplicate measurements were performed for each cake layer sample.

Cluster analysis of the DGGE band patterns was performed with Fingerprinting II Informatix v.3.00 by using the Jaccard coefficient and the unweighted-pair group method with arithmetic mean (UPGMA).

7.3 Results and discussion

7.3.1 Performance of the SAnMBR

Effects of temperature (37, 45 and 55 °C) and temperature shock (5 and 10 °C magnitude) on the performance and microbial community of a submerged anaerobic membrane bioreactor (SAnMBR) were studied for thermomechanical pulping pressate treatment for 416 days as reported in Chapter 5. The performance results showed that SAnMBR is a promising technology for thermomechanical pulping wastewater treatment with a sustainable membrane flux of 5-8 L/m²•h, a chemical oxygen demand (COD) removal efficiency of 76-82 %, and a biogas production rate of 0.21 L/g COD removed with the methane content above 70 % (Chapter 5).

For a SAnMBR, the temperature shocks could affect not only the system performances, but also the development of membrane fouling. To compare the membrane fouling extent of steady state operation with rapid temperature increases, short-term experiments at steady state and 5 °C /10 °C shocks at 37 °C /45 °C were conducted. Each shock comprised three temperature rises. The fouling resistance was calculated right before and after each temperature rise. As indicated by black circles in Fig. 7-2, the fouling resistance was mitigated during the 12 hours of almost all the temperature rises. Temperature shocks resulted in a temporary decrease in fouling resistance, except for the first or second 5 °C shocks. This could be attributed to the combined effect of deflocculation and reduction in viscosity in the first and/or second 5 °C shock and temporarily decreased mixed liquor viscosity in later temperature shocks (5 and 10 °C). Deflocculation due to temperature shock would negatively affect membrane fouling, while an increase in temperature decreases the viscosity of the mixed liquor, and consequently decreases the hydraulic shearing force on the membrane surface. No significant deflocculation was observed in later temperature shocks after the first or second 5 °C shocks (Chapter 5). Viscosity was found to have positive effects on

membrane fouling (Wu et al., 2007) and negative effects on flux (Trzcinski and Stuckey, 2010). Also, the 5 °C shock at 37°C caused a greater fouling resistance than the steady state, while a sudden rise in R_f was observed after the third temperature rise of the 10 °C shock at 37 °C (Fig. 7-2 (a)). On the other hand, temperature shocks at 45 °C resulted in lower fouling resistances than the corresponding steady state, and the larger temperature shocks (10 °C shock at 45 °C) correlated to the lowest R_f (Fig. 7-2 (b)). The causes of changes in fouling resistances were related to the changes in cake porosity, which is discussed in later sections.

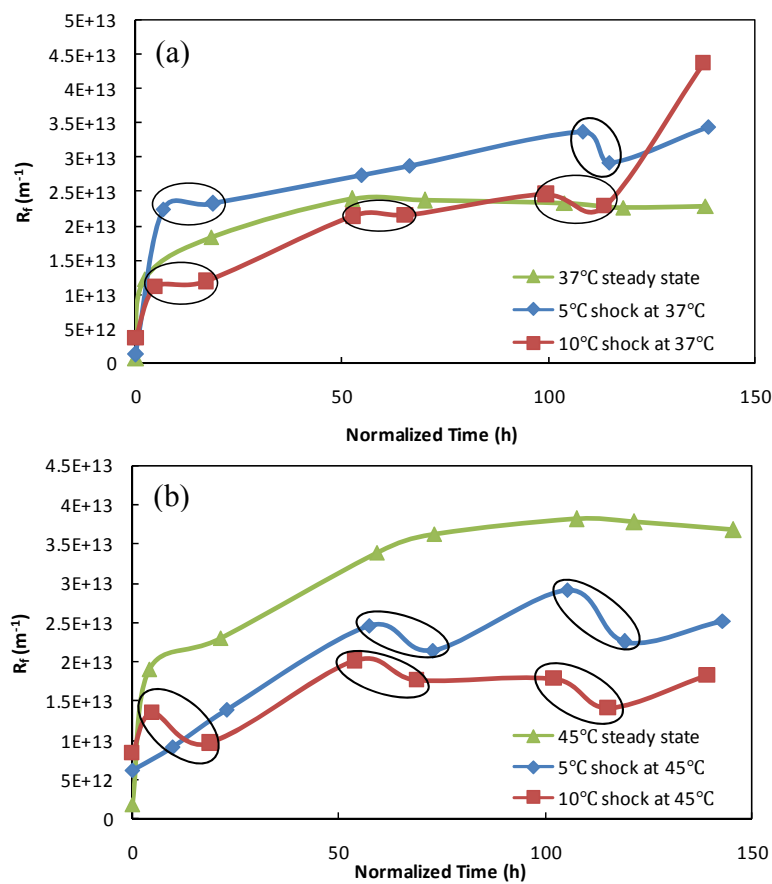


Figure 7-2 Comparison of total fouling resistance between steady state and temperature shocks: (a) 5 °C and 10 °C shocks at 37 °C; (b) 5 °C and 10 °C shocks at 45 °C. (In each black cycle, the 1st and 2nd data point indicates the fouling resistance just before and after temperature shock, respectively).

The irremovable fouling resistance R_i and permanent fouling resistance R_p were measured in a 180 mL stirred filtration cell (Fig. 7-3) at 37, 45, and 55 °C steady state

operation with filtration periods of 6, 6, and 12 days, respectively. R_i and R_p only accounted for less than 1 % of the total fouling resistance, again indicating that cake layer formation is the major contributor to membrane fouling. More importantly, although the membranes used at 55 °C had a longer operation period, their tested R_i and R_p were lower than that at 37 °C and 45 °C, showing that the irremovable fouling and permanent fouling were lighter at 55 °C.

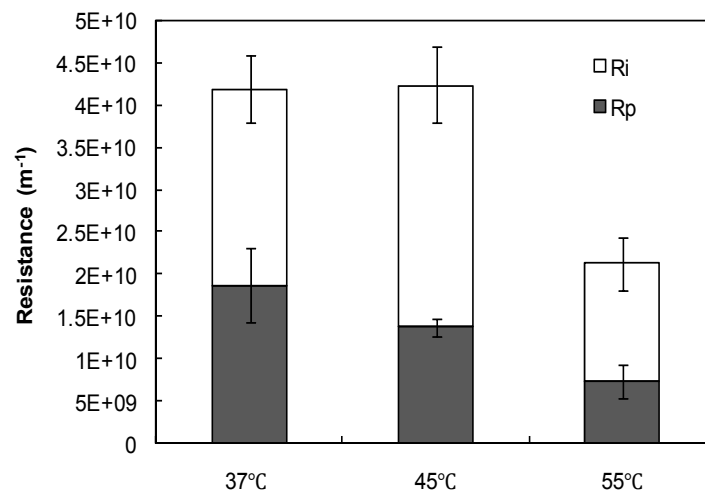


Figure 7-3 R_i and R_p at 37 °C (6d), 45 °C (6d) and 55 °C (12d) steady state.

7.3.2 Cake layer thickness

Because the cake layers could not be absolutely even, at least 10 pieces of cake layer samples located on different sites of the membrane surface were subjected to cryosectioning to get the cross sections. Microscopic imaging clearly showed that the thickness of the cake layers obtained after the same operation period (25 days) decreased with an increase in operating temperature (Fig. 4(a-c)). At 55 °C, the cake layer formed after 25 days operation was thicker and more compressed (Fig.4(c)), and the cake layer formed after 2 days operation was more loose and transparent (Fig. 4(d)).

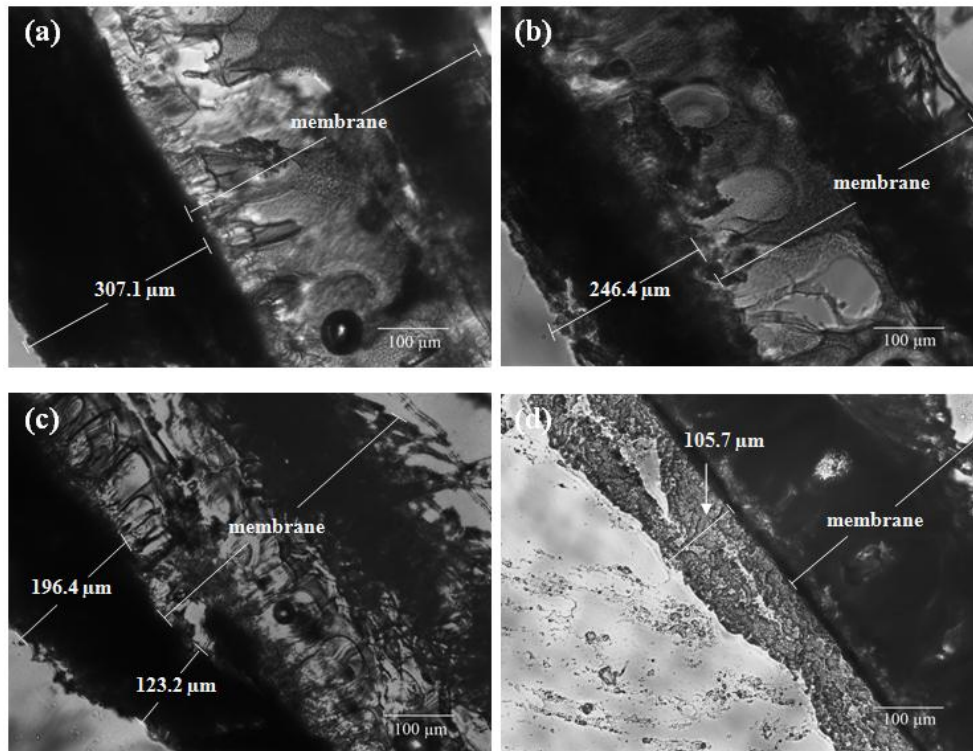


Figure 7-4 Cross sections of cake layers observed by COM: (a) at 37 °C steady state (cake layer age, 25d) (b) at 45 °C steady state (cake layer age, 25d) (c) at 55 °C steady state (cake layer age, 25d) (d) at 55 °C steady state (cake layer age, 2 d).

7.3.3 Effect on PSDs

PSDs of the cake sludge at 37, 45 and 55 °C steady state, as shown in Fig. 7-5 (a), indicate that the cake sludge had a broader range of PSDs with a group of small particles in a size range from 0.1 to 1 μm when compared to the bulk sludge (Chapter 5). The mean particle sizes of the cake sludge at different operating temperatures are in descending order as follows: 37 °C > 45 °C > 55 °C. The cake sludge particle sizes shifted to a smaller size range with an increase in operating temperature (Fig. 7-5 (a)). This tendency was the same as the bulk sludge (Chapter 5) due to the deflocculation of the large sludge flocs at higher temperatures. Moreover, at 55 °C steady state, there were more cake sludge flocs (volume percentage) with smaller particle sizes attached on the membrane surface within 2 days than those obtained after 25 days of operation (Fig. 7-5 (b)). This result suggests that freshly formed cake layers would have smaller particle

sizes and aged cake layers might lead to larger particles, due to cake layer compression (Wu et al., 2007).

The effect of temperature shocks on PSDs of cake sludge is shown in Fig. 7-5 (c) and (d). The smaller particles increased after 5 °C shocks at 37 °C. A shift in PSDs to smaller particles was also observed after 10 °C shocks at 37 °C, while the fraction of particles from 0.1 to 1 μm disappeared (Fig. 7-5 (c)). High temperature caused not only deflocculation of the large sludge flocs (Chapter 5) but also high solubility of small particles (e.g., colloids). Thus, sudden increases in temperature may result in the dissolution of particles from 0.1 to 1 μm in the mixed sludge suspension instead of accumulating onto the membrane surface. On the other hand, a shift of PSDs of cake sludge to larger size was observed after 5 and 10 °C shocks at 45 °C (Fig. 7-5 (d)), which may be due to the effect of compression.

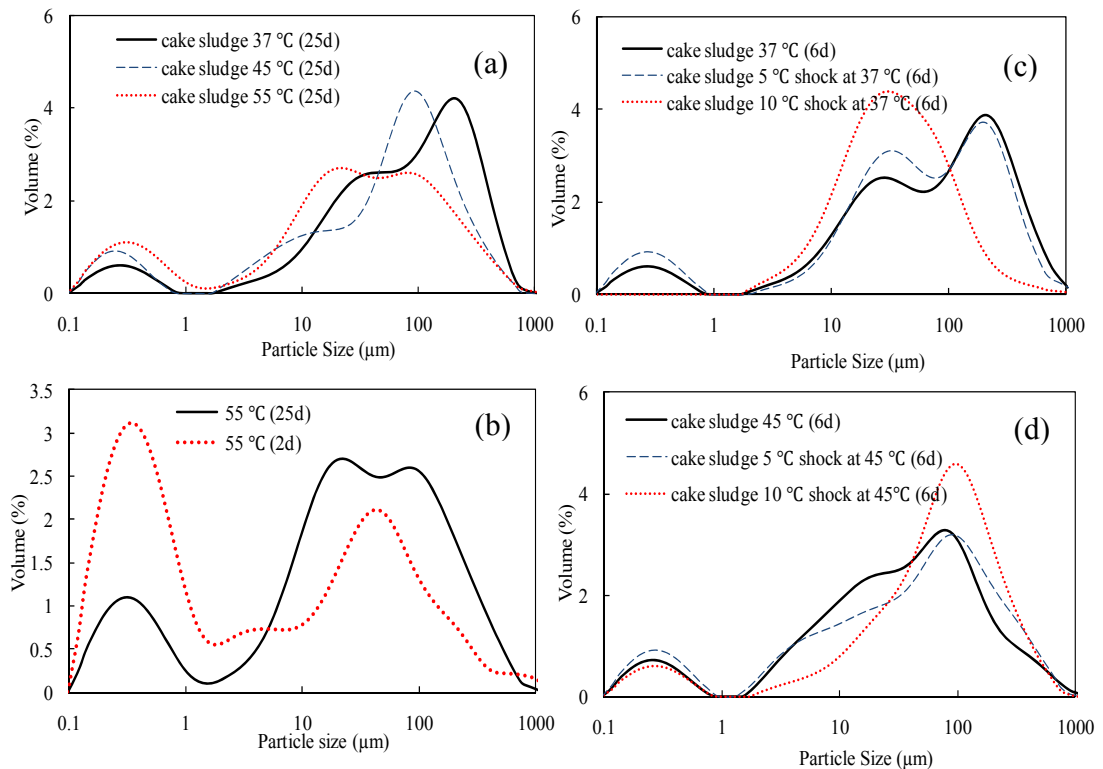


Figure 7-5 Particle size distributions of (a) cake layers at 37, 45 and 55 °C steady state (cake layer age, 25d) (b) cake layers at 55 °C steady state with different cake layer ages (c) 5 and 10 °C shocks at 37 °C (cake layer age, 6d) (d) 5 and 10 °C shocks at 45 °C (cake layer age, 6d).

7.3.4 Effect on cake layer porosity

The calculated cake layer porosities under different operation temperature conditions are presented in Table 7-2. During each phase, the cake layers with longer operation periods had lower cake porosity than those with shorter operation periods. This may be attributed to the long-term continuous compression of cake layers. As the TMP slowly increased, a higher TMP corresponded to lower cake porosity, which was consistent with our previous study (Gao et al., 2011).

Table 7-2
Cake layer porosity

	d_p (μm) ^a	Average porosity (%)
37 °C steady state (25d)	2.12	8.83
37 °C steady state (6d)	1.42	10.55
5 °C shock at 37 °C (6d)	1.34	9.04
10 °C shock at 37 °C (6d)	1.42	8.55
45 °C steady state (25d)	1.68	7.88
45 °C steady state (6d)	1.42	8.73
5 °C shock at 45 °C (6d)	1.42	10.25
10 °C shock at 45 °C (6d)	1.26	12.71
55 °C steady state (25d)	1.12	9.05
55 °C steady state (12d)	1.26	9.34
55 °C steady state (2d)	0.94	10.12

^a The particle sizes (d_p) used in the calculation were provided by $d(0.5)$ in PSDs results of cake sludge based on the number distributions. $D(0.5)$ is the diameter where 50% of the number distribution is below this value.

As shown in Table 7-2, in terms of cake layer porosity with the same operation period (6 days), the following sequence is observed in phase 1: 37 °C steady state > 5 °C shock at 37 °C > 10 °C shock at 37 °C. In phase 2, the sequence went to the opposite way: 45 °C steady state < 5 °C shock at 45 °C < 10 °C shock at 45 °C. Returning to Fig. 7-2 and the Carman-Kozeny equation (equation 7-5), we can find that cake porosity is inversely related to the filtration resistance. At the end of each cycle (Fig. 7-2), lower cake porosity and smaller PSDs after 5 or 10 °C shocks at 37 °C resulted in the higher filtration resistance, and higher porosity and larger PSDs after 5 or 10 °C shocks at 45 °C led to a lower filtration resistance.

Under steady-state operation (25 days and 6 days cake age), the cake porosity at 45 °C was lower than that at 37 °C, which explains the higher total fouling resistance at 45 °C. In our previous work (Chapter 6), the total fouling resistance was found to increase with an increase in operating temperature for the same operation period. However, the cake porosity was the highest at 55 °C (Table 7-2), which seemed incompatible with the results observed in Chapter 6. According to Equations (7-4) and (7-5), after the temperature correction, the high fouling resistance of the cake layer depends on not only the cake porosity, but also on the amount of cake sludge and floc size. The PSDs of bulk sludge (Chapter 5) or cake sludge all decreased as the operating temperature increased. The combined effect of these factors (cake porosity, floc size, and cake sludge quantity) implied that floc size would be the dominant factor to control fouling resistance at 55 °C (Chu and Li, 2005).

7.3.5 Effect on EPS content in cake layer

Fig. 7-6 shows the bound EPS of cake layers extracted before and after temperature shocks. The 5 °C shocks at 37 °C had no effect on EPS production in the cake layer, while 10 °C temperature shocks at 37 °C led to a significant increase in protein content of bound EPS. Similar results were observed in bulk sludge (Chapter 6). More bound EPS was synthesized during the temperature shocks (5 and 10 °C) at 45 °C, as compared to that at 45 °C steady state, because they are growth-associated and in direct proportion to high substrate utilization rate at a high temperature (Laspidou and Rittmann, 2002). No significant difference was found in carbohydrates of bound EPS (ANOVA, $p > 0.05$, data not shown) for the 5 °C /10 °C shocks at 37 °C/45 °C.

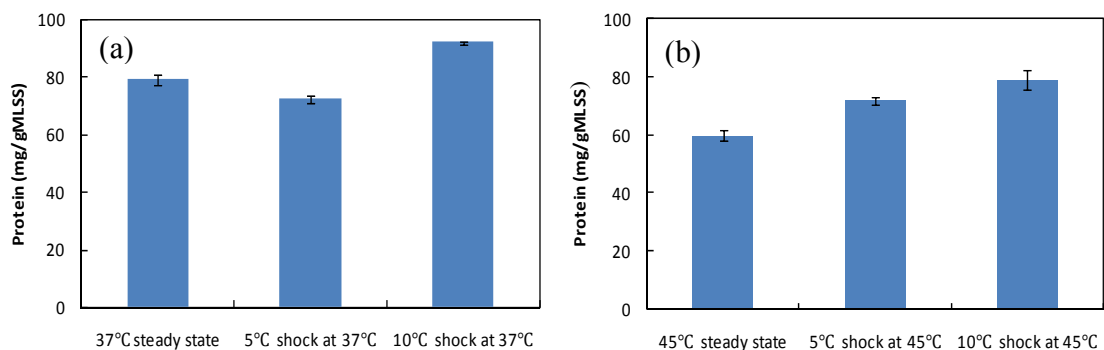


Figure 7-6 Protein concentrations in bound EPS of cake layers (6d): (a) 5 and 10 °C shocks at 37 °C; (b) 5 and 10 °C shocks at 45 °C.

Fig. 7-7 presents the results of bound EPS content in the cake sludge with different cake ages at 37, 45 and 55 °C steady state. During the 55 °C steady state, the EPS content (both proteins and carbohydrates) in cake sludge decreased with an increase in cake age (Fig. 7-7). The cake layer samples obtained within 2 days at 55 °C were freshly formed by small particles (Fig. 7-5 (b)). Small flocs were believed to have higher bound EPS compared to large flocs and bulk sludge (Lin et al., 2011b). They probably result from the clustering agglomeration of SMP polymers and colloidal substances, which were considered to be rich in proteins and carbohydrates. A similar trend for proteins was observed at 37 °C steady state, while no significant change in proteins and carbohydrates was observed at 45 °C steady state. These results demonstrate that the EPS content in cake layers tends to stabilize within 6 days at 37 and 45 °C. For 55 °C, the stabilization period is presumably less than 12 days.

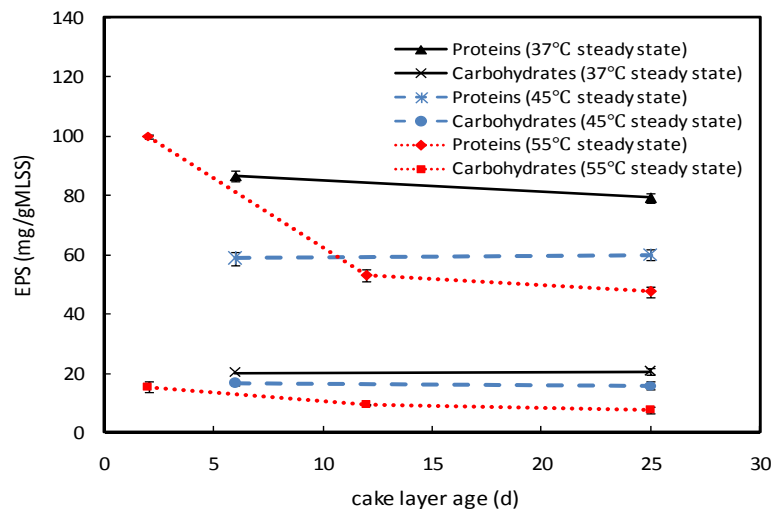


Figure 7-7 EPS content in the cake sludge at 37, 45 and 55 °C steady state with different cake ages.

It is also interesting to note that both the protein and carbohydrate concentrations of bound EPS in cake layers (25d and 6d cake age) decreased with an increase in

operating temperature (Fig. 7-7), while the EPS content increased with operating temperature in bulk sludge (Chapter 6). Despite all that, the EPS content in cake sludge was always higher than that in bulk sludge at all the three temperatures, and the difference between them was narrowing as the temperature was increased. For instance, for cake layers after 25 days of operation, the protein concentration in cake sludge was 55 mg/gMLSS higher than that in bulk sludge at 37 °C, while this difference was reduced to only 15 mg/gMLSS at 55 °C. As for carbohydrate, the same trend was observed.

This may be related to changes in operating temperature. The increase in temperature will not only accelerate the metabolic activity of microbes, including the secretion of EPS, but also lead to increased EPS thermal extraction and cell lysis rate. More importantly, the hydrolysis rate of EPS is much higher in the thermophilic temperature range than that in the mesophilic temperature range (Veeken and Hamelers, 1999; Bouallagui et al., 2004), causing the degradation of more organic matter with high molecular weight (Mw) into low Mw substances. A proposed filtration process with the cake layer formed on membrane surfaces is demonstrated in Fig. 7-8. The sludge flocs, especially small flocs with higher EPS, in the bulk sludge will deposit onto the cake layer. Meanwhile, soluble microbial products (SMP), which can be adsorbed as part of bound EPS, can be entrapped in the cake layer. Moreover, changes in microbial community would also contribute to the differences in EPS content between bulk sludge and cake sludge. These are the three possible reasons for the higher EPS content in cake layers proposed by Lin et al. (2011a). As a filtration setting, the membrane module acts as a sieve retaining anything beyond a certain size depending on the properties of the membrane used. Mainly the EPS and SMP fractions with high Mw are liable to accumulate in the cake layer. At 37 °C, continuous rejection of sludge flocs and entrapment of high Mw fractions in SMP/EPS caused the highest EPS content in the cake sludge. However, at higher operating temperatures (45 and 55 °C), substantial EPS and SMP may release into the permeate because of the existence of more low Mw fractions caused by the higher hydrolysis rates of EPS. This hypothesis was supported by the observed increase in COD value (Chapter 5) and SMP concentration in permeate with an increase in operating temperature. By analysis as the sum of carbohydrates and proteins,

the SMP concentration in permeates of 37, 45, and 55 °C steady state was 365.91 ± 38.44 mg/L, 415.08 ± 7.90 mg/L, and 582.17 ± 36.69 mg/L, respectively. Of course, the enlarged membrane pore size, thermal extraction of EPS, and enhanced resolvability at high temperatures could also contribute to this trend. Therefore, all these reasons may lead to less EPS left in the cake layer at 45 and 55 °C.

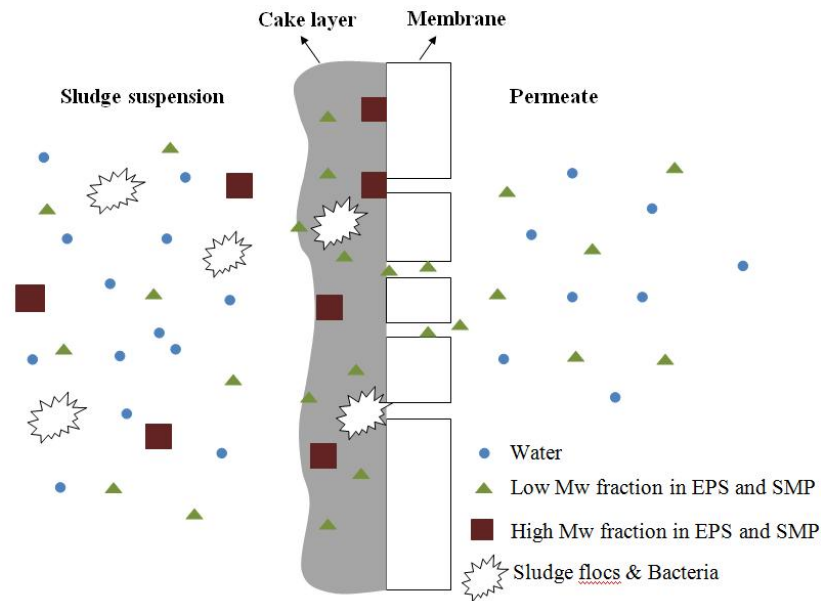


Figure 7-8 Profile of EPS and SMP transporting through cake layer and membrane

In addition, the change in cake layer thickness at different operating temperatures may also be partially responsible for the change in EPS content. The thinner cake layer would favour the mass transfer during the filtration process. The thicker cake layer formed at 37 °C would lead to insufficient substrate transfer and stressful micro-environment in the bottom cake layer, inducing cell lysis to release microbial products and promoting the production of EPS by bacteria for survival (Drews et al., 2007). Moreover, the change in microbial community structure might also contribute to the decrease in cake layer EPS content with an increase in operating temperature, as discussed in later sections.

7.3.6 Microbial community

In this study, cake sludge and the bulk sludge samples were collected at the same time for microbial community analysis. PCR-DGGE analysis of these samples was performed to examine the microbial community composition exposed to different operating temperatures and temperature shocks. Fig. 7-9 presents PCR-DGGE patterns of cake sludge samples, and the DGGE profiles of the bulk sludge samples were reported in Chapter 5. The corresponding lanes were named after the same letter. The cluster analysis using the PCR-DGGE patterns of all the bulk sludge and cake sludge samples divided them into three clusters, designated I, II and III (Fig. 7-10). With the exception of k and k', all the samples at 55 °C were located in cluster II. Samples collected at 37 °C steady state and 5 °C/10 °C shocks at 37°C appeared in cluster I, and samples collected at 45 °C steady state and 5 °C/10 °C shocks at 45 °C were located in cluster III. Cluster I and III were composed of a more diverse microbial community, indicating the microbial community had shifted in response to the temperature shocks during phase 1 and phase 2.

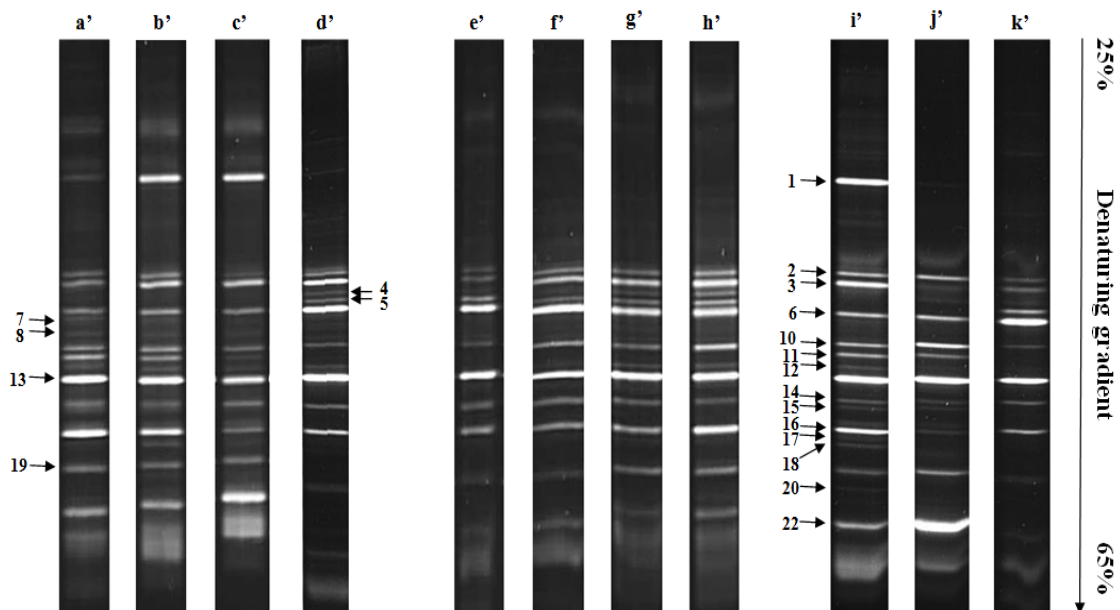


Figure 7-9 PCR-DGGE fingerprints of 16S rDNA gene fragments amplified from DNA extracted from cake sludge. (a') 37 °C steady state (day 53, cake layer age: 25d); (b') 37 °C steady state (day 68, cake layer age: 6d); (c') 5 °C shock at 37 °C (day 83, cake layer age: 6d); (d') 10 °C shock at 37 °C (day 107, cake layer age: 6d); (e') 45 °C steady state (day 207, cake layer age: 25d); (f') 45 °C steady state (day 245, cake layer age: 6d); (g')

5 °C shock at 45 °C (day 250, cake layer age: 6d); (h')10 °C shock at 45 °C (day 264, cake layer age: 6d); (i') 55 °C steady state (day 400, cake layer age: 25d); (j') 55 °C steady state (day 412, cake layer age: 12d); (k') 55 °C steady state (day 416, cake layer age: 2d).

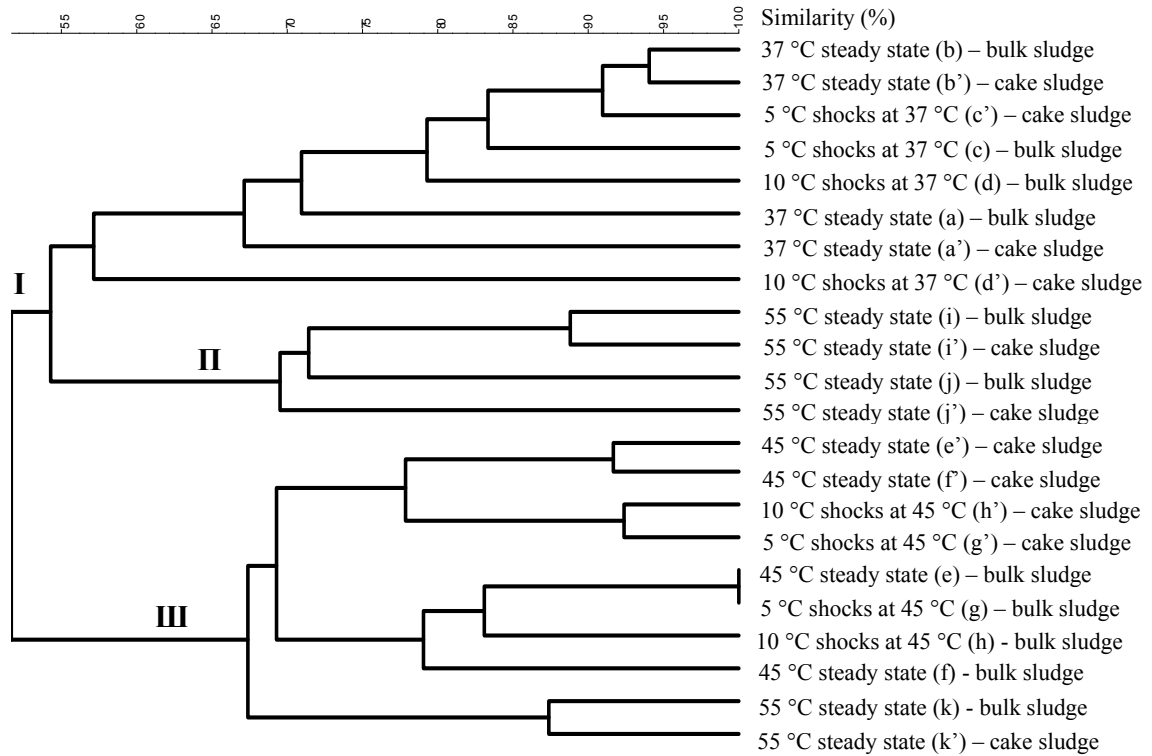


Figure 7-10 Cluster analysis of the DGGE band patterns.

Comparing the DGGE patterns between bulk sludge (lanes a, b, c, and d (Chapter5, Fig. 5-5)) and cake sludge (lanes a', b', c', and d'(Fig. 7-9)) at 37 °C, the similarity of about 57 % was the lowest for the sample group of 10 °C shocks at 37 °C. A series of changes in band presence (bands 4 and 5) or absence (bands 11, 19, and 21) accompanied by some changes in band intensity (bands 2, 10, and 16) were observed in lane d' when compared to lane d. It seemed that 10 °C shocks at 37 °C significantly influenced the microbial behaviour in selective attachment to the membrane surface. The similarity was the highest (up to 94 %) for lanes b and b', and it is about 71-77 % for the other two groups mainly due to the changes in the intensity of some bands. For the bulk sludge (lanes e, f, g, and h) and cake sludge (lanes e', f', g', and h') at 45 °C, the similarity between each group of the DGGE patterns (from about 68 to 81 %) was mainly

caused by differences in population density. For example, populations represented by bands 2, 3, 4, 10 and 19 were more abundant in bulk sludge (lane f (Chapter5, Fig. 5-5)) than in cake sludge (lane f' (Fig. 7-9)) at 45 °C steady state, while bands 14 and 16 showed up more clearly in lane f' than in lane f. At 55 °C, the microbial community in cake sludge represented by lanes i', j', and k' had similarities of about 88 %, 75 % and 87 %, respectively, when compared to the microbial community in their corresponding bulk sludge.

In addition, band 19 was dominant in the microbial community of almost all the bulk sludge samples except lane j, while the intensity of this band was very weak in all the cake sludge samples. On the other hand, a number of bacterial species represented by bands 2, 6, 10, 13 and 19 were present in the microbial communities of all the bulk and cake sludge samples, indicating that they may not only be the highly temperature tolerant species, stable in the SAnMBR, but also be responsible for sludge attachment on the membrane surface. A recent study revealed that some specific microbial species were selectively accumulated on the membrane surface and may not be dominant in the bulk sludge (Wu et al., 2011).

From the perspective of cake sludge at different operating temperatures, the DGGE profiles (Fig. 7-9) revealed that the cake sludge samples were colonized by complex bacterial communities and there are some differences in species diversity and richness at 37 °C, 45 °C and 55 °C steady state. For example, bands 7, 8, 11 and 12 were present at 37 °C steady state, whereas they disappeared at 45 °C steady state. The faint and smearing DNA bands (bands 11, 16 and 19) at 45 °C steady state are relatively major DNA bands at 37 °C steady state. According to the cluster analysis, the similarity of the microbial communities between 37 °C (a') and 45 °C (e'), 45 °C (e') and 55 °C (i'), 37 °C (a') and 55 °C (i') were about 45 %, 50 %, and 61 %, respectively. It indicated that the developed microbial communities not only in the bulk sludge but also in the cake sludge at the steady state of different operating temperatures were significantly different from each other. These significant differences may influence the modes of synthesizing EPS, which may also help to explain the decreasing EPS content in cake layers with increase in operating temperature.

The 5 °C shocks at 37 °C exerted little impact on the microbial community in cake sludge samples, as the similarity between the fingerprints of lane c' and b' was as high as 93 % showing some changes in band intensity (i.e. bands 10, 11 and 16 in lane b' and c') after temperature shocks. Distinctively, lane d' only had a similarity of 62 % with lane b', demonstrating that 10 °C shocks at 37 °C significantly affected the microbial community in the cake sludge. Lane g' and h' shared a similarity of about 77 % with lane f' (Fig. 7-10), and thus 5 °C and 10 °C shocks at 45 °C exerted mild impact on the microbial community

With respect to cake layer age, at 55 °C, the cake layer of 2 days had a lower similarity (63 %) in microbial community structure with the cake layer of 25 days than the cake layer of 12 days did (75 %). Although there were no similar comparisons obtained at 37 °C and 45 °C, the cake layer of 6 days and 25 days still exhibited a low similarity of about 68 % for the steady state of both operating temperatures. These results indicated that other than the shift in microbial communities in bulk sludge (Chapter 5), cake layer age also could cause the differences in the microbial communities during cake layer formation. The significant difference in microbial community structure between bulk sludge (lane k (Chapter 5, Fig. 5-5)) and cake sludge (k') at the initial stage of membrane fouling indicates that some pioneering bacteria might be responsible for the initial development of membrane fouling.

7.3.7 Development of membrane fouling at the initial stage of filtration

The SAnMBR was found to gain most of the fouling resistance during the first two days of each new run. Therefore, the analysis of cake layer structure was carried out at 55 °C right after this stage (on the second day of a new run).

Our previous study showed that at 55 °C steady state, the fouling resistance reached $3.9 \times 10^{13} \text{ m}^{-1}$ on the second day of operation. Then the fouling resistance was maintained at $4.0 \times 10^{13} \text{ m}^{-1}$ to $4.8 \times 10^{13} \text{ m}^{-1}$ for more than 20 days operation until a sudden increase occurred at a certain point as indicated by a red circle in Fig. 6-2. As shown in Figure 7-11, the mass of cake sludge increased by approximately 40.6 % on the twelfth day of operation, as compared to that of 2 days operation, but the fouling resistance remained on the same level. On the contrary, there was only a rise of 13.3 % in the mass

of cake sludge from the 12th day to the 25th day, while the fouling resistance on the 25th day jumped to $6.0 \times 10^{13} \text{ m}^{-1}$. These results indicate that the fouling resistance does not necessarily increase linearly with the quantity of the cake sludge accumulated on the membrane surface. The continuous change in cake porosity with operating time might be related to the 3rd transmembrane pressure (TMP) jump or fouling resistance jump. It is hypothesized that the 3rd TMP jump was related to the reduction of cake layer porosity. When the cake layer porosity decreased to a critical point, where the operating membrane flux exceeded the critical membrane flux, the 3rd TMP jump occurred.

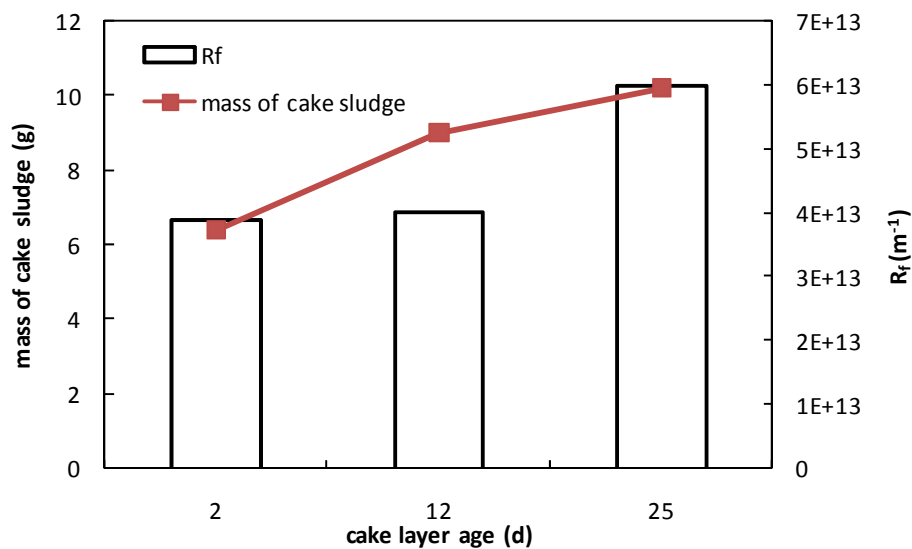


Figure 7-11 Relation between fouling resistance and cake layer quantity (55 °C).

As shown in Fig. 7-12, the surface of fresh cake layers (2 days cake age) was as compact as the cake layer bottom of 25 days cake age. Compared to the cake layer samples obtained after 25 days of operation, the freshly formed cake layers were thinner, higher in EPS concentration, and much lower in PSDs. Besides, the difference in microbial community between cake age of 2 days and 25 days was larger than that of the cake age of 12 days and 25 days at 55 °C. These results illustrate that at the initial stage of filtration smaller particles with higher EPS content tend to deposit onto the membrane surface as discussed in Lin et al. (2011b). Although the porosity of these fresh cake layers (2 days) was higher than that of cake layers with longer operation periods (25 days), they

still generated high fouling resistance, further confirming that the smaller particles in the fresh cake layers could make key contributions to fouling resistance.

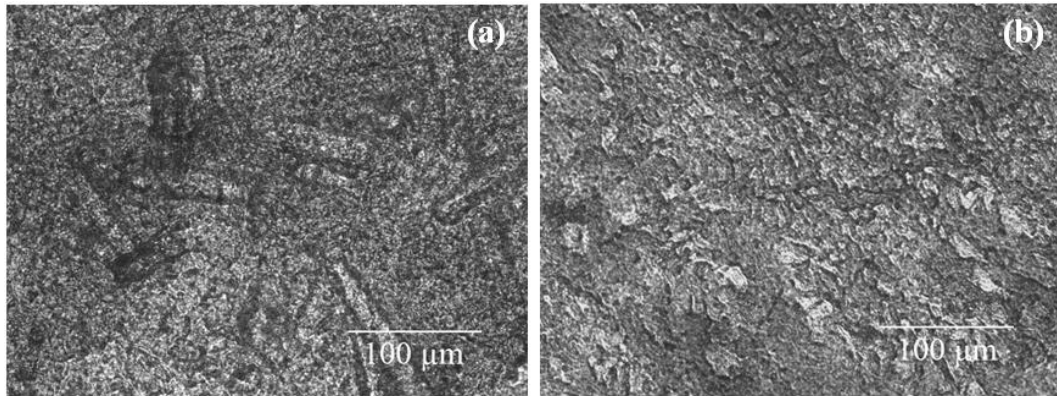


Figure 7-12 Cake layers observed by COM: (a) at 55 °C steady state after 25 days of operation (bottom layer) (b) at 55 °C steady state after 2 days of operation (surface).

The dominant fouling mechanism in the earlier stage of filtration was attributed to adsorption of solutes/colloids or pore plugging, leading to fast TMP rise or flux decline (Meng et al., 2009). Afterwards, the dominant mechanism may be cake layer build-up, leading to slower TMP increase due to the appearance of a stationary cake layer whose structure changes very slowly (Huisman et al., 2000). In this case, the more soluble microbial product (SMP) and EPS contained in the mixed liquor, the more severe organic adsorption or pore plugging will be. However, in this study, although the SMP and bound EPS increased with the increase in operating temperature (Chapter 6), the tested R_i and R_p at 55 °C were lower than those at 37 and 45 °C. Protein, as a crucial component in SMP and EPS, was found to cause irreversible membrane fouling during filtration processes by protein - membrane interaction to deposit on the upper membrane surface or in its pores (Marshall et al., 1993; Huisman et al., 2000). Furthermore, the rate of protein denaturation i.e., aggregation and polymerization, increased with temperature (Meireles et al., 1991). When the protein concentration is increased at higher temperature as observed in Chapter 6, denatured proteins tend to aggregate and form either a precipitate or a gel (Meireles et al., 1991). Therefore, at the initial stage of filtration at a higher temperature, large protein aggregates or even gels physically deposit on the membrane surface instead of adsorption or pore plugging within the membrane pores, leading to

lower R_i and R_p . In the later stages of filtration, cake layer started to be built as a secondary membrane preventing further mixed liquor - membrane interaction. The PN/PC ratio in the cake layers was found to be lower at 55 °C than at 37 °C, indicating a lower protein – membrane interaction which may also result in less irremovable and permanent fouling.

7.4 Conclusions:

The influence of temperature variations and temperature shocks on cake layer structure and membrane fouling was studied in a SAnMBR treating thermomechanical pulping pressate. The following conclusions could be drawn.

- Temperature shocks can either increase or decrease fouling resistance, as compared to steady-state operation, depending operating temperature. This is the result of the combined effect of changes in sludge properties (floc size) and water viscosity. The fouling resistance had a close relationship with the cake layer porosity, while it could be influenced by the combined effect of all the factors, such as the amount of cake sludge, cake pore size and floc size.
- The thickness and the floc size of cake layers with the same operation period decreased with an increase in operating temperature.
- Both protein and carbohydrate concentration of bound EPS in cake layers decreased with an increase in operating temperature.
- The protein and carbohydrate concentration of bound EPS in cake layers at younger cake age could be higher or at least at the same level of that at an older age.
- PCR-DGGE analysis demonstrated that the microbial community of the cake sludge was different from that of the bulk sludge. There are some differences in species diversity and richness among different operating temperatures in cake sludge. During cake layer formation, the change in the microbial community in the cake layer can be caused by the cake layer age and the shift in microbial communities in the bulk sludge. Pioneering bacteria of membrane fouling were observed at the initial stage of membrane fouling.

- The fouling resistance does not necessarily increase with the quantity of the cake sludge accumulated on the membrane surface. Smaller particles in both bulk sludge and cake layers could act as a key factor to generate high fouling resistance.

7.5 References

- Bouallagui, H., Haouari, O., Touhami, Y., Ben Cheikh, R., Marouani, L., Hamdi, M., 2004. Effect of temperature on the performance of an anaerobic tubular reactor treating fruit and vegetable waste. *Process Biochemistry* 39, 2143-2148.
- Bouskova, A., Dohanyos, M., Schmidt, J. E., Angelidaki, I., 2005. Strategies for changing temperature from mesophilic to thermophilic conditions in anaerobic CSTR reactors treating sewage sludge. *Water Research* 39, 1481-1488.
- Chu, H. P., Li, X. Y., 2005. Membrane fouling in a membrane bioreactor (MBR): sludge cake formation and fouling characteristics. *Biotechnology and Bioengineering* 90, 323-331.
- Defrance, L., Jaffrin, M. Y., Gupta, B., Paullier, P., Geaugey, V., 2000. Contribution of various constituents of activated sludge to membrane bioreactor fouling. *Bioresource Technology* 73, 105-112.
- Drews, A., Mante, J., Iversen, V., Vocks, M., Lesjean, B., Kraume, M., 2007. Impact of ambient conditions on SMP elimination and rejection in MBRs. *Water Research* 41, 3850-3858.
- DuBois, M., Gilles, K. A., Hamilton, J. K., Rebers, P. A., Smith, F., 1956. Colorimetric Method for Determination of Sugars and Related Substances. *Analytical Chemistry* 28, 350-356.
- Fan, F., Zhou, H., 2007. Interrelated Effects of Aeration and Mixed Liquor Fractions on Membrane Fouling for Submerged Membrane Bioreactor Processes in Wastewater Treatment. *Environmental Science & Technology* 41, 2523-2528.
- Frølund, B., Palmgren, R., Keiding, K., Nielsen, P. H., 1996. Extraction of extracellular polymers from activated sludge using a cation exchange resin. *Water Research* 30, 1749-1758.

- Gao, W. J., Lin, H. J., Leung, K. T., Schraft, H., Liao, B. Q., 2011. Structure of cake layer in a submerged anaerobic membrane bioreactor. *Journal of Membrane Science* 374, 110-120.
- Gao, W. J. J., Lin, H. J., Leung, K. T., Liao, B. Q., 2010. Influence of elevated pH shocks on the performance of a submerged anaerobic membrane bioreactor. *Process Biochemistry* 45, 1279-1287.
- Huisman, I. H., Prádanos, P., Hernández, A., 2000. The effect of protein-protein and protein-membrane interactions on membrane fouling in ultrafiltration. *Journal of Membrane Science* 179, 79-90.
- Hwang, B.-K., Lee, W.-N., Park, P.-K., Lee, C.-H., Chang, I.-S., 2007. Effect of membrane fouling reducer on cake structure and membrane permeability in membrane bioreactor. *Journal of Membrane Science* 288, 149-156.
- Jeison, D., van Lier, J. B., 2008. Anaerobic wastewater treatment and membrane filtration: a one night stand or a sustainable relationship? *Water Science and Technology* 57, 527-532.
- Jin, Y.-L., Lee, W.-N., Lee, C.-H., Chang, I.-S., Huang, X., Swaminathan, T., 2006. Effect of DO concentration on biofilm structure and membrane filterability in submerged membrane bioreactor. *Water Research* 40, 2829-2836.
- Jinhua, P., Fukushi, K., Yamamoto, K., 2006. Bacterial Community Structure on Membrane Surface and Characteristics of Strains Isolated from Membrane Surface in Submerged Membrane Bioreactor. *Separation Science and Technology* 41, 1527 - 1549.
- LaPara, T. M., Nakatsu, C. H., Pantea, L. M., Alleman, J. E., 2001. Aerobic Biological Treatment of a Pharmaceutical Wastewater: : Effect of Temperature on COD Removal and Bacterial Community Development. *Water Research* 35, 4417-4425.
- Lapidou, C. S., Rittmann, B. E., 2002. A unified theory for extracellular polymeric substances, soluble microbial products, and active and inert biomass. *Water Research* 36, 2711-2720.

- Liao, B.-Q., Kraemer, J. T., Bagley, D. M., 2006. Anaerobic Membrane Bioreactors: Applications and Research Directions. *Critical Reviews in Environmental Science and Technology* 36, 489 - 530.
- Lin, H., Liao, B.-Q., Chen, J., Gao, W., Wang, L., Wang, F., Lu, X., 2011a. New insights into membrane fouling in a submerged anaerobic membrane bioreactor based on characterization of cake sludge and bulk sludge. *Bioresource Technology* 102, 2373-2379.
- Lin, H. J., Gao, W. J., Leung, K. T., Liao, B. Q., 2011b. Characteristics of different fractions of microbial flocs and their role in membrane fouling. *Water Science and Technology* 63, 262-269.
- Lishman, L. A., Legge, R. L., Farquhar, G. J., 2000. Temperature effects on wastewater treatment under aerobic and anoxic conditions. *Water Research* 34, 2263-2276.
- Lowery, O. H., Rosebrough, N., Farr, A. L., Randall, R. J., 1951. Protein measurement with the folin phenol reagent. *Journal of Biological Chemistry* 193, 265-275.
- Mahmoud, N., Zeeman, G., Gijzen, H., Lettinga, G., 2004. Anaerobic stabilisation and conversion of biopolymers in primary sludge-effect of temperature and sludge retention time. *Water Research* 38, 983-991.
- Marshall, A. D., Munro, P. A., Trägårdh, G., 1993. The effect of protein fouling in microfiltration and ultrafiltration on permeate flux, protein retention and selectivity: A literature review. *Desalination* 91, 65-108.
- Meireles, M., Aimar, P., Sanchez, V., 1991. Albumin denaturation during ultrafiltration: Effects of operating conditions and consequences on membrane fouling. *Biotechnology and Bioengineering* 38, 528-534.
- Meng, F., Chae, S.-R., Drews, A., Kraume, M., Shin, H.-S., Yang, F., 2009. Recent advances in membrane bioreactors (MBRs): Membrane fouling and membrane material. *Water Research* 43, 1489-1512.
- Meng, F., Zhang, H., Yang, F., Liu, L., 2007. Characterization of Cake Layer in Submerged Membrane Bioreactor. *Environmental Science and Technology* 41, 4065-4070.

- Ramesh, A., Lee, D. J., Lai, J. Y., 2007. Membrane biofouling by extracellular polymeric substances or soluble microbial products from membrane bioreactor sludge. *Applied Microbiology and Biotechnology* 74, 699-707.
- Sipma, J., Osuna, M. B., Emanuelsson, M. A. E., Castro, P. M. L., 2010. Biotreatment of Industrial Wastewaters under Transient-State Conditions: Process Stability with Fluctuations of Organic Load, Substrates, Toxicants, and Environmental Parameters *Critical Reviews in Environmental Science and Technology* 40, 147-197.
- Trzcinski, A. P., Stuckey, D. C., 2010. Treatment of municipal solid waste leachate using a submerged anaerobic membrane bioreactor at mesophilic and psychrophilic temperatures: Analysis of recalcitrants in the permeate using GC-MS. *Water Research* 44, 671-680.
- Veeken, A., Hamelers, B., 1999. Effect of temperature on hydrolysis rates of selected biowaste components. *Bioresource Technology* 69, 249-254.
- Wang, Z., Wu, Z., Yin, X., Tian, L., 2008. Membrane fouling in a submerged membrane bioreactor (MBR) under sub-critical flux operation: Membrane foulant and gel layer characterization. *Journal of Membrane Science* 325, 238-244.
- Wu, B., Yi, S., Fane, A. G., 2011. Microbial behaviors involved in cake fouling in membrane bioreactors under different solids retention times. *Bioresource Technology* 102, 2511-2516.
- Wu, Z., Wang, Z., Zhou, Z., Yu, G., Gu, G., 2007. Sludge rheological and physiological characteristics in a pilot-scale submerged membrane bioreactor. *Desalination* 212, 152-164.
- Zhang, K., Choi, H., Dionysiou, D. D., Sorial, G. A., Oerther, D. B., 2006. Identifying pioneer bacterial species responsible for biofouling membrane bioreactors. *Environmental Microbiology* 8, 433-440.
- Zhang, T. C., Bishop, P. L., 1994. Density, porosity, and pore structure of biofilms. *Water Research* 28, 2267-2277.

Chapter 8 Conclusions and recommendations

The pulp and paper industry is the third largest industrial polluter in North America. Currently, most of pulp and paper mill effluents are treated in a secondary biological wastewater treatment system. Aerobic biological wastewater treatment is the dominant technology used in the mills, although anaerobic digestion has been used in some mills. The aerobic biological treatment has suffered from a high energy cost, due to the low oxygen utilization rate and sludge bulking is common in biomass separation. The conventional anaerobic digestion of pulp and paper wastewater has the advantages of recovering energy (biogas) from wastewater and thus significantly reduces the energy cost in anaerobic digestion, but faces the challenges of low treated effluent quality, which requires the further polishing of anaerobically treated effluent. Therefore, there is an incentive to develop better treatment technologies with advantages that are not achievable with current treatment technologies.

A promising approach is to incorporate membrane separation technology into conventional anaerobic digestion. The submerged anaerobic membrane bioreactor (SAnMBR) employs membranes submerged in the bulk solution to achieve a better effluent quality, eliminate biomass separation problems, and increase bioreactor productivity. To the best of my knowledge, studies appear to be very limited in this area. In addition, membrane fouling is a big challenge for the use of SAnMBRs. A better understanding of the structure of membrane fouling layers and approaches to control membrane fouling will improve the applicability of SAnMBRs in wastewater treatment.

Laboratory-scale SAnMBRs were constructed for this study. Real pulp and paper wastewaters (TMP whitewater and pressate) from a local pulp and paper mill were used to test the efficiency of SAnMBRs for pollutant removal and biogas production, and to understand and control of membrane fouling. The impact of transient conditions in terms of pH shock, temperature variation and temperature shocks on the performance of SAnMBRs and membrane fouling were systematically studied. Advanced analytical tools,

including microtome section technique, confocal laser scanning microscopy (CLSM), and conventional optical technique, molecular staining technique, scanning electron microscopy (SEM)-energy-dispersive X-ray analyzer (EDX), particle size distribution (PSD) analysis, Fourier transform infrared (FTIR) spectroscopy, extraction and chemical analysis of extracellular polymeric substances (EPS), and polymerase chain reaction (PCR)-denaturing gradient gel electrophoresis (DGGE), were used to study membrane fouling and the structure of sludge cake layers formed on membrane surfaces. Based on the findings of this work, the following specific conclusions can be drawn.

8.1 Conclusions

8.1.1 Feasibility of SAnMBR system for treatment of thermomechanical pulping whitewater / pressate

The SAnMBR system was operated for over 7 months for thermomechanical pulping whitewater treatment, as described in Chapter 3 and 4. The organic loading rate was a little higher during the first 4 months of operation (2.4 ± 0.4 kgCOD/m³d) than that during the later 3 months of operation (1.80 ± 0.14 kgCOD/m³ d). The biogas production rates were 0.41 ± 0.04 and 0.397 ± 0.053 L/g COD removed, respectively, with 62–75% methane and 22–30% carbon dioxide in the biogas. In spite of the fluctuating influent COD concentration and MLSS concentration caused by pH shocks, the steady-state COD removal efficiency was maintained at about 90%. Therefore, a SAnMBR system is competent for the treatment of thermo-mechanical pulping whitewater.

For thermo-mechanical pulping pressate treatment, it is feasible to use a SAnMBR at the operating temperatures of 37°C, 45°C and 55°C throughout the 416 days of operation. The COD removal efficiencies were around 82.9%, 78.9% and 76.1% on average, respectively. The biogas production was maintained around 0.21 L/g COD removed with the methane content above 70%.

8.1.2 Cake layer investigation and parameter variations with cake depth

The structure of cake layer changes from the top to the bottom layer. From a physical point of view, the cake layer is composed of a loose outer surface, a modestly

compressed middle layer, and a dense and compressed bottom layer, showing an inhomogeneous structure. When compared with the bottom cake layer, the top cake layer was found to be composed of smaller flocs. The small-size particles had a higher tendency to accumulate on membrane surfaces and were closely associated with severe membrane fouling. More importantly, the porosity of cake layer decreased from top to bottom layer.

From a chemical perspective, the main components of organic matters in the membrane foulants were identified as proteins (PN), polysaccharides (PC) materials and humic acids by FTIR spectroscopy. Among the elements of C, O, Na, Mg, Al, F, Cl, S, Si, P, K, and Ca in the cake layer, more Ca was detected which was related to a high level of mineralization in the cake layer, and this certainly enhanced the membrane fouling potential of the cake layer. The wet density of EPS changed along the cake depth, suggesting a heterogeneous structure of EPS along cake layer depth and not only the EPS content, but also the spatial distribution of EPS matrix would affect cake layer formation.

From a microbiological perspective, there were significant differences in microbial community population density along the cake layer depth.

8.1.3 Impact of transient conditions on the performance of the SAnMBR and membrane fouling

8.1.3.1 pH shock

The SAnMBR system was tolerant of moderate alkali pH conditions (pH 8.0 and pH 9.1 shocks). The performance of the system was largely deteriorated by the elevated pH shocks in terms of COD removal, biogas production and membrane filtration performance. When normal pH (7.0) was resumed, it took approximately 1, 6, and 30 days for the reactor to recover from the pH 8.0, 9.1 and 10.0 shocks, respectively.

The pH 8.0 shock had a minor effect on the membrane fouling rate. However, the pH 9.1 and 10.0 shocks significantly increased the membrane fouling rate. The elevated pH shocks resulted in the breakage of sludge flocs, the accumulation of colloids and solutes or biopolymers in the sludge suspension, as well as a denser and more compact cake layer with higher specific resistances. The higher supernatant COD or BPC

facilitated colloidal or small particle deposition on the membrane surface, and thus deteriorated membrane performance. The bound EPS appeared to be independent of pH shock. However, the PN/PC ratio negatively correlated to the membrane fouling rate.

8.1.3.2 Temperature

The SAnMBR was more tolerant to temperature variations and the temperature shocks at the operating temperature of 37 °C than that of 45 °C which is at the edge of the mesophilic temperature range. The SAnMBR could tolerate the 5 °C /10 °C temperatures shocks at 37 °C and the temperature variations from 37 °C to 45 °C. The 5 °C shocks at 45 °C had minor impact, while the 10 °C shocks at 45 °C and the temperature variation from 45 °C to 55 °C exerted significantly negative impacts on membrane flux, COD removal and biogas production of the SAnMBR. Larger magnitudes of temperature shock had more severe impacts on the performance of the SAnMBR.

Increasing the operating temperature caused the deflocculation of the flocs, which resulted in smaller sizes in bulk sludge as well as in the corresponding cake sludge without affecting the MLSS and permeate COD value. The employment of membrane filtration can mitigate the effect of temperature variation and enhance the temperature tolerance of the process.

For the same operation period (25 days), the extent of membrane fouling increased with the operating temperature. The temperature shocks at 37 °C caused increases in fouling resistance compared to 37 °C steady state, while temperature shocks at 45 °C resulted in decreases in fouling resistance compared to the corresponding steady state. This is related to the changes in cake layer porosity. From the viewpoint of constituents in the bulk sludge, total bound EPS, bound polysaccharides, and bound proteins, soluble total SMP, soluble polysaccharides, soluble proteins, and colloidal particle content in the supernatant positively correlated to the fouling resistance, indicating that bound EPS, SMPs, and colloidal particles have significant contribution to membrane fouling. From the viewpoint of cake layer structure, the fouling resistance had a close relationship with the cake layer porosity, while it could be influenced by combined effects of all the factors, such as the amount of cake sludge, cake pore size and floc size.

Both the protein and polysaccharide concentrations in the cake layers decreased with increasing operating temperature and cake layer age. The thickness and the PSDs of the cake layers with the same operation period decreased with an increase in operating temperature. At the initial stage of filtration, the freshly formed cake layers were found thinner, higher in EPS concentration, and much lower in PSDs than that the older cake layers.

PCR-DGGE analysis demonstrated that the microbial community of the cake sludge was different from that of the bulk sludge. Temperature shocks had limited impact on the microbial community of bulk sludge, while there were some differences in species diversity and richness among different operating temperatures in both bulk sludge and cake sludge. During cake layer formation, the change in microbial community can be caused by the cake layer age and the shift in microbial communities in the bulk sludge.

8.2 Recommendations for future research

The SAnMBR technology is an option for sustainable treatment for industrial wastewater owing to several appealing benefits compared to the conventional anaerobic technologies, such as excellent effluent quality, low excess sludge production, high-treatment efficiency, small footprint, and net energy production. However, research is still required with the intention of enhancing its commercial feasibility. There are three ways to achieve this purpose: (1) To extend the applicable range (i.e., type of wastewater, operating conditions, and reactor design); (2) To improve the treatment efficiency and stability; (3) To reduce the operating and maintenance costs.

Currently, only a few types of wastewaters have been tested by SAnMBRs, and further research is needed to access other potential applications. In this thesis, several types of wastewater, including thermo-mechanical pulping whitewater and pressate, have been successfully treated by SAnMBR in our group. Each wastewater type results in distinct treatment efficiency and membrane fouling behaviour. Further research is needed to reveal the impact of influent characteristics on membrane fouling and the performance of SAnMBR technology for wastewater treatment.

More studies on long-term MBR fouling are needed to fully understand the full-scale membrane fouling and enhance filtration performance. Except for pH and

operating temperature, the occurrence and effects of other transient conditions encountered in industrial wastewater treatment, such as organic loading rate, salinity, toxic compound load need to be investigated for SAnMBRs.

Even though a flux of 6.89 ± 0.56 L/m²h was successfully maintained for 25 days without any cleaning (Chapter 5), higher flux without deteriorating wastewater treatment efficiency implies high productivity accompanied by low unit cost. Thus, pursuance of flux enhancement is always crucial for the broad application of SAnMBR in the future. Better and more detailed understanding of membrane fouling processes and mechanisms will help to develop better fouling control and cleaning strategies.

Although many MBR publications deal with fouling, it still is a non-resolved problem requiring special attention. Small particle size was identified as the key factor to generate great fouling resistance (Chapter 4 and 7). The addition of flocculants may be helpful to control particle size. On the other hand, Chapter 6 showed that sludge constituents are strongly correlated with membrane fouling. Consequently, further research needs to be conducted on the modification of the suspension by the use of flocculants or adsorbents that may also be effective to reduce the concentrations of those sludge suspension contents and mitigate membrane fouling.

Cake layer formation and fouling evolution (three-stage TMP profile) in a SAnMBR, especially the initial stage and TMP jump, were observed and discussed in this thesis (Chapter 4 and 7). The structure of cake layer appears to be a key factor that regulates the development of membrane fouling. The TMP jump was correlated to some extent with cake layer porosity. However, the initial fouling stage and TMP jump remain not well explained. It is necessary that future research evaluates this aspect to achieve a full understanding of membrane fouling mechanisms.

The dynamic microbial communities in the cake layer and in the mixed liquor at different operating temperatures were investigated in Chapter 5 and 7. It was revealed that there were significant changes in population densities along the cake layer depth (Chapter 4). Also, pioneering bacteria of membrane fouling were observed at the initial stage of membrane fouling (Chapter 7). Additional research is required with regard to the identification of pioneering bacteria that are prone to attach onto the membrane surface.

Existing mathematical models allow prediction of membrane fouling based on a number of fouling factors (e.g., operating parameters, membrane properties, sludge properties, and reactor design). Membrane fouling can be better simulated with the consideration of the inhomogeneous structure of cake layer found in Chapter 4. Modified fouling models should be developed to examine and predict membrane fouling based on this new insight.

Nomenclature and abbreviations

Nomenclature

A_m	membrane area
C_b	bulk MLSS concentration
D	cake layer density
J	permeate flux
M	mass
R_c	cake resistance
R_i	irremovable fouling
R_m	membrane resistance
R_p	permanent fouling
R_t	total resistance
R_f	total fouling resistance due to cake layer formation and pore blocking
R_0	the R values (m^{-1}) at starting time
R_{24}	the R values (m^{-1}) after a 24-hour filtration
r_p	pearson's product momentum correlation coefficient
U_G	superficial gas velocity
V	permeate volume per unit area
α	specific cake resistance
η / η_T	dynamic viscosity
ΔR	membrane fouling rate
ΔR_{24}	the change rate of R within 24 h of filtration
$\Delta P / \Delta p_T$	trans-membrane pressure
Δt	filtration time
ε	porosity
ρ_p	density of particles
d_p	particles diameter

Abbreviations

AnMBR	anaerobic membrane bioreactor
AFM	atomic force microscopy
ANOVA	analysis of variance
AOX	absorbable organic halides
AS	activated sludge
BAP	biomass-associated products
BOD	biochemical oxygen demand
BPC	biopolymer clusters
BSA	Bovine serum albumin
CAS	conventional activated sludge
CER	cation exchange resin
CLSM	confocal laser scanning microscopy
COD	chemical oxygen demand
COM	conventional optical microscopy
CSTR	continuously stirred tank reactor
CTMP	chemi-thermomechanical pulping
DNA	Deoxyribonucleic acid
EDTA	Ethylenediaminetetraacetic acid
EDX	energy-dispersive X-ray spectroscopy
EEM	three-dimensional excitation-emission matrix fluorescence spectroscopy
EPS	extracellular polymeric substances
FA	free form of ammonia
FTIR	Fourier transform infrared spectroscopy
FISH	Fluorescence In Situ Hybridization
GAC	granular activated carbon
HRT	hydraulic retention time
ICP	inductively coupled plasma
LB-EPS	loosely bound EPS

MBR	membrane bioreactor
MF	microfiltration
MFE	membrane flux enhancer
MFR	membrane fouling reducer
MLSS	mixed liquor suspended solids
M _w	molecular weight
MWCO	molecular weight cut-off
NF	nanofiltration
NMR	¹³ C-nuclear magnetic resonance spectroscopy
OLR	organic loading rate
O.T.C	optimal cutting temperature compound
PAC	powdered activated carbon
PCR-DGGE	polymerase chain reaction-denaturing gradient gel electrophoresis
PE	polyethylene
PES	polyethersulfone
PN	proteins
PN/PC	proteins to carbohydrates (polysaccharides) ratio
PSD	particle size distribution
PVC	polyvinyl chloride
PVDF	polyvinylidene fluoride
PC	polysaccharides/carbonhydrate
RIS	resistance-in-series model
RO	reverse osmosis
rRNA	ribosomal ribonucleic acid
SAnMBR	submerged anaerobic membrane bioreactor
SBR	sequencing batch reactor
SEC	size exclusion chromatography
SEM	scanning electron microscopy
SMBR	submerged membrane bioreactor
SMP	soluble microbial products

SRT	solids retention time
TB-EPS	tightly bound EPS
TMP	trans-membrane pressure
TOC	total organic carbon
TSS	total suspended solids
UAP	substrate-utilisation-associated products
UASB	upflow anaerobic sludge blanket
UF	ultrafiltration
VOCs	volatile organic compounds
VFA	volatile fatty acids
XPS	X-ray photoelectron spectroscopy

Publication list

Peer-reviewed Journals:

- [1] **W.J. Gao**, H.J. Lin, K.T. Leung, H. Schraft and B.Q. Liao. Structure of Cake Layer in a Submerged Anaerobic Membrane Bioreactor (SAnMBR). *Journal of Membrane Science*, 2011, 347(1-2): 110-120.
- [2] **W.J. Gao**, H.J. Lin, K.T. Leung and B.Q. Liao. Influence of elevated pH shocks on the performance of a submerged anaerobic membrane bioreactor. *Process Biochemistry*, 2010, 45(8):1279-1287.
- [3] **W.J. Gao**, K.T. Leung, W. S. Qin, and B.Q. Liao. Effects of temperature and temperature shock on the performance and microbial community structure of a submerged anaerobic membrane bioreactor. *Bioresource Technology* 102, 8733-8740.
- [4] H.J. Lin, **W.J. Gao**, F.G. Meng, B.Q. Liao, K.T. Leung, et al. Membrane Bioreactors for Industrial Wastewater Treatment: A Critical Review. *Critical Reviews in Environmental Science and Technology*, Accepted.
- [5] H.J. Lin, **W.J. Gao**, K.T. Leung and B.Q. Liao. Characteristics of different fractions of microbial flocs and their role in membrane fouling. *Water Science and Technology*, 2011. 63(2): 262-269.
- [6] B.Q. Liao, H.J. Lin, S.P. Langevin, **W.J. Gao** and G.G. Leppard. Effects of temperature and dissolved oxygen on sludge properties and their role in bioflocculation and settling. *Water Research*, 2011. 45(2): 509-520.
- [7] H. J. Lin, B. Q. Liao, J. R. Chen, **W. J. Gao**, L. M. Wang, F. Y. Wang, X. F. Lu. New insights into membrane fouling in a submerged anaerobic membrane bioreactor based on characterization of cake and bulk sludge. *Bioresource Technology*, 2011, 102(3), 2373-2379.
- [8] **W.J. Gao**, X. Qu, A. Chen, K.T. Leung, and B.Q. Liao, Effects of Extracellular Polymeric Substances and Soluble Microbial Products on Membrane Fouling in a Submerged Anaerobic Membrane Bioreactor. *Separation and Purification Technology* (under review)
- [9] **W.J. Gao**, K.T. Leung, and B.Q. Liao, Effects of temperature and temperature shocks on cake layer structure and membrane fouling in a submerged anaerobic membrane bioreactor. (under preparation)

